University of Reading

Exploring the role of vector trait in the incidence of vector-borne disease

Doctor of Philosophy

School of Biological Sciences

Dominic Brass

September 2022

Abstract

Climate change and ecological disturbances are having profound effects on species survival. Predicting how populations will adapt to these changes relies on our understanding of how environment affects species' life-histories, how this feeds back into abundance, and vice versa. In general, current modelling frameworks over-simplify these relationships, giving spurious predictions. Here, I derive a novel general mathematical modelling framework that links environmentally induced trait variation to population level responses. Applying the framework to classical Nicholson's blowfly experiments I demonstrate how predictions of population's responses to environmental change made directly from environment-trait relationships do not always hold. I demonstrate the framework's accuracy, and how cryptic population dynamics can emerge from mechanisms of environmentally driven trait variation.

The framework is then applied to the globally invasive dengue mosquito vector, *Aedes albopictus*. Developing predictions at a global scale is difficult as environmental variation acts on the vector-pathogen-host triad in complex and non-linear ways. I show how the species population and trait dynamics explain the location, magnitude, and timing of historical dengue outbreaks. By representing the effect of mechanisms of variation on epidemiologically important traits expressed by vectors, I show that the competence of vector populations to transmit disease changes according to their current and historic experience of the environment. Long-lived individuals that developed under favourable environmental conditions can persist within the population long after the environmental conditions that created them have passed and may consequently have

a disproportionate effect on pathogen transmission. Importantly, this cannot be accounted for by current modelling approaches that assume all vectors express the same average trait value. This demonstrates that the representation of mechanisms of trait variation is required to produce predictions that account for the underlying complexity inherent in population responses to environmental change, which is required for accurate predictions to inform risk assessment and mitigation strategies.

Declaration of original authorship

Declaration: I confirm that this is my own work and the use of all material from other sources has been properly and fully acknowledged.

Dominic Brass

Acknowledgements

I would like to thank my supervisors Dr. Steven White, Professor Christina Cobbold, Dr. Bethan Purse, Dr. David Ewing, and Professor Amanda Callaghan for their support and encouragement throughout my PhD. I am grateful to UKCEH, my host institution, and the student community there who were always there when I needed coffee and a chat. Finally, thank you to my family and friends for supporting me through it all.

Contents

List of Figures

List of Tables

Chapter 1

Introduction

1.1 Aims of the thesis

In this thesis I aim to:

- Develop a general modelling framework to represent the effect of environmentally induced mechanisms of variation on population's responses to change.
- Use this framework to predict the population dynamics of the invasive dengue vector *Ae. albopictus* and explore how vector trait variation alters the risk of vector-borne disease.

1.2 The role of environmental variation in producing dengue outbreaks

1.2.1 Vector-borne disease

An organism that transmits infectious pathogens between other organisms is called a vector, and the World Health Organisation estimates that vector-borne viral diseases currently account for 17% of all disease globally (World Health Organisation, 2017). The incidence of vector-borne disease is on the rise, representing a significant threat to public health and global economies

(Jones et al., 2008). Driving this rapid change are anthropogenic factors, such as land use change, climate change, and increased global connectivity through trade and travel (Norris, 2004; Soriano-Panõs et al., 2020; De La Rocque et al., 2011; Rocklöv, Dubrow, 2020). The consequences of these disturbances are already evident in the concurrent trends of increasing of disease burdens in endemic countries and the expansion of diseases to new areas (Kilpatrick, Randolph, 2012). Implementing effective public health strategies, that will remain robust to the evolving challenges of an uncertain future, requires a thorough understanding of how the drivers of vector-borne disease determine the location and intensity of disease outbreaks.

The risk of vector-borne disease in a region is inherently linked to vector ecology. Vectors encompass a diverse range of taxa and transmit pathogens through a wide range of mechanisms. Schistosomiasis is a parasitic disease caused by worms and is vectored by aquatic snails through the release of infectious larvae into fresh-water (McManus et al., 2018). Rats and bats vector leptospirosis through their urine, a bacterial infection that in its severe form is known as Weil's disease (Samrot et al., 2021). However, by far the most prevalent vector-borne diseases are arboviruses, viruses transmitted through the bites of blood-sucking arthropods (Gubler, 1998). Vectorial flies, ticks, fleas, midges, and mosquitoes transmit diseases while taking blood meals from host species. The two most prevalent vector-borne diseases, malaria and dengue, are both vectored by mosquitoes *via* this transmission route. While the prevalence of malaria is currently decreasing thanks to sustained control efforts, it is estimated that the years of lost life to dengue increased over the period between $2007 - 2017$ despite widespread and sustained control efforts and this is of great concern to global health authorities (Roth et al., 2018).

1.2.2 Dengue

Dengue fever is a viral vector-borne disease that in 2017 was responsible for $40,467$ deaths and an estimated $2,922,630$ disability-adjusted life years (Zeng et al., 2021). Dengue incidence has rapidly increased since the mid 20^{th} century (Figure 1.1), and as of 2019 there was evidence

of dengue transmission in 204 countries or territories with up to 3.97 billion people living in regions classified as "at risk" making dengue a truly global threat. It is estimated that 75% of dengue cases are sub-clinical and are either asymptomatic or only mildly symptomatic (Duong et al., 2015). Of the 25% of cases that present with more severe clinical manifestations, infection begins with a mild illness referred to as dengue fever which may then progress to the more severe dengue haemorrhagic fever (Guzman et al., 2013). DENV has multiple distinct serotypes, DENV-I, DENV-2, DENV-3, and DENV-4, and infection by one serotype provides life-long protection from further infection by viruses of that same serotype (Gibbons et al., 2007). However, secondary infection by other serotypes is both possible and antibody-dependent enhancement of infection increases the chances of developing more severe forms of dengue when this occurs (Guzman et al., 2013).

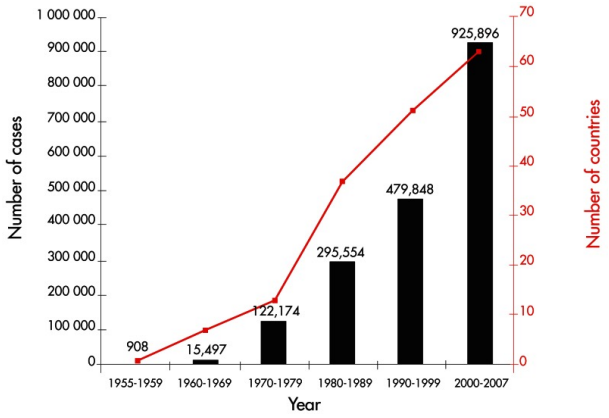

Figure 1.1: The number of countries reporting dengue and the average number of dengue fever and dengue haemorrhagic fever cases reported to the WHO between 1955 – 2007. (Geneva: World Health Organization;, 2009).

Dengue viruses have two primary transmission cycles, a sylvatic cycle between mosquito vectors and non-human primates hosts, and an urban cycle between *Aedes* mosquitoes and human hosts. Sylvatic transmission cycles are thought to be important for the emergence of new strains of dengue, but have only been confirmed in limited rural regions of Asia and Africa (Althouse et al., 2015; Valentine et al., 2019). However, unlike arboviruses such as yellow fever virus, dengue does not rely on the sylvatic cycle and can be maintained solely through

the urban transmission cycle (Gubler, 2002). Autochthonous instances of dengue transmission now occur worldwide (Figure 1.2A), but different patterns of disease transmission are observed across regions that currently experience regular dengue outbreaks. In tropical regions the urban transmission cycle can be maintained at low levels all year round, with larger outbreaks generally occurring around once every $3-6$ years (for example, the outbreak of dengue on La Réunion reproduced in Figure 1.2B) (Lin et al., 2020). By contrast, in temperate regions the transmission cycle is interrupted during the cold winter months as conditions become unfavourable for both virus replication and vector activity (for example, the outbreak of dengue in Tokyo reproduced in Figure 1.2C) (Watts et al., 1987; Brady et al., 2012). This divides regions where dengue outbreaks occur into source regions, where the virus is endemic, and sink regions where the virus must be newly imported each year (Li et al., 2021a).

For an outbreak of dengue to be maintained environmental conditions need to be favourable both virus and vector, with sufficient contact between vector and host to maintain the infection within both populations. As mosquitoes are ectotherms, temperature is an important factor in determining whether a region is at risk of a disease outbreak due to its direct effect on vector competence and on viral replication rates (Liu et al., 2017). The transmission cycle (Figure 1.3) begins when an uninfected female mosquito bites an infected human and takes a bloodmeal, and both the frequency at which mosquitoes bite and the probability of infection are temperature dependent (Mordecai et al., 2017). Once the mosquito becomes infected the virus begins replicating in the midgut and once this infection disseminates to the salivary glands the mosquito becomes infective (Bosio et al., 2000). The time this process takes is called the extrinsic incubation period (EIP) and the duration of the EIP is also temperature dependent (Xiao et al., 2014). Finally, the mosquito with a disseminated infection must find and bite an uninfected host and transmit the infection to complete the pathogen transmission cycle.

By considering the relationship between temperature and each component of the transmission cycle an understanding can be built of the current patterns of dengue incidence that are observed around the globe. For example, whenever the temperature is lower than the thermal minimum

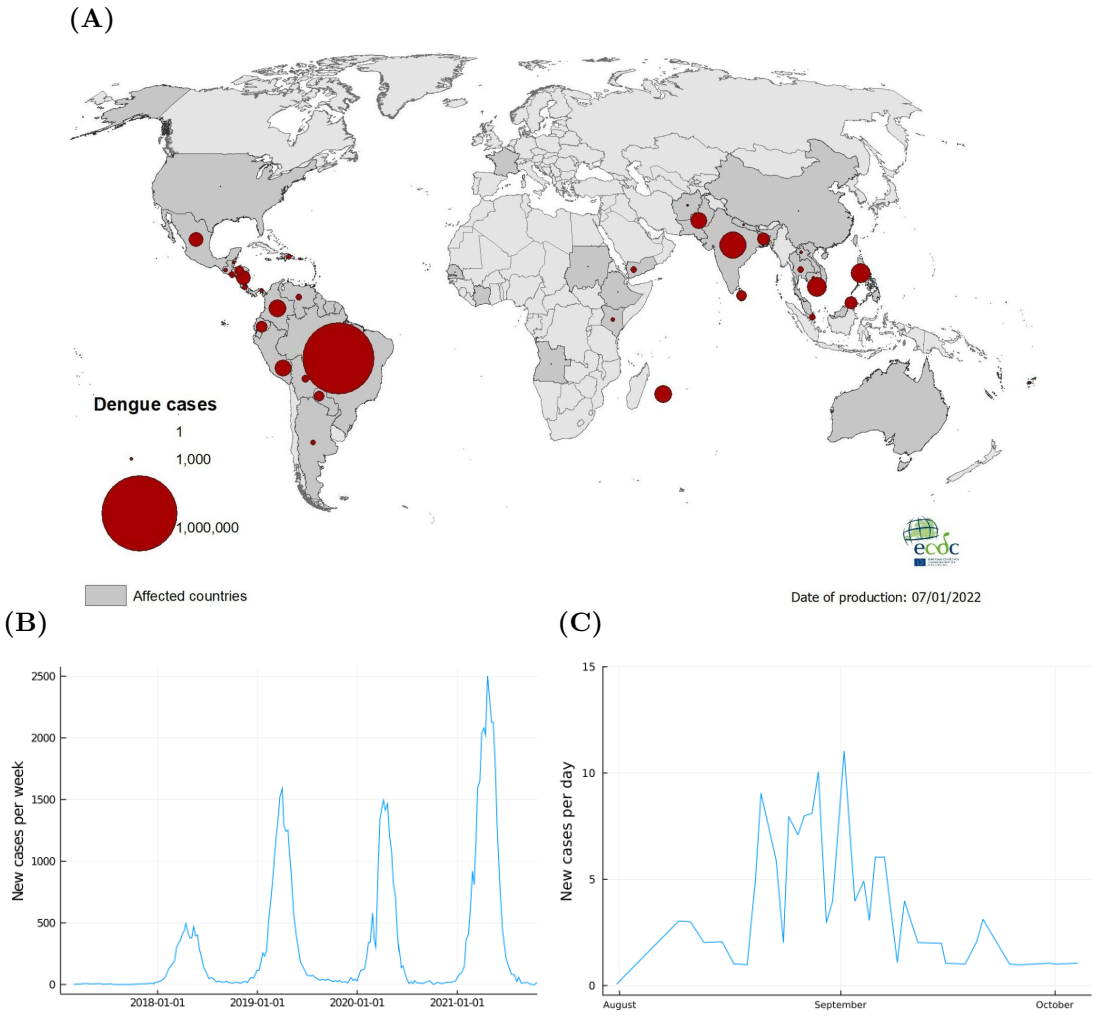

Figure 1.2: **(A)** The geographical distribution of dengue cases in 2021 taken from the ECDC (ECDC, 2022a). **(B)** The 2017 – 2020 outbreak of dengue on La Réunion, data from (Santé publique France, 2022). **(C)** The number of dengue cases reported in the 2014 outbreak of dengue in Tokyo, data from (Yuan et al., 2019).

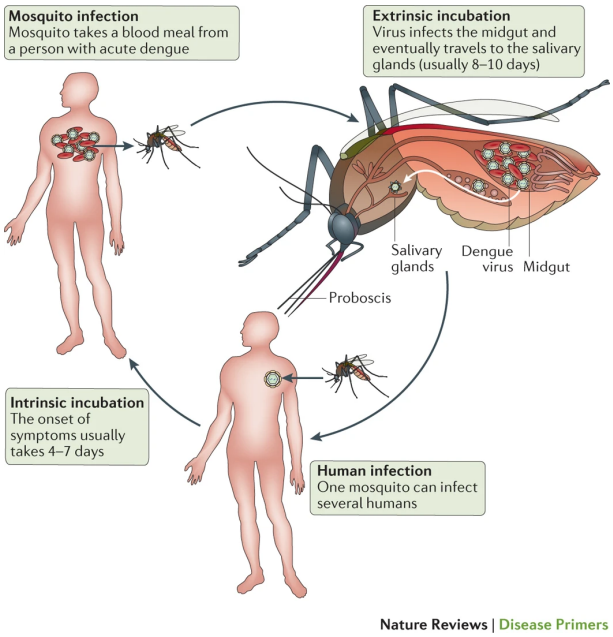

Figure 1.3: A diagram showing the urban dengue transmission cycle, taken from Guzman et al. (2016). Mosquitoes become may become infected after taking a bloodmeal from an infected human. After becoming infected the dengue virus must disseminate from the mosquito's midgut to the salivary glands, after which the mosquito can transmit the infection after biting a susceptible human. Once infected a human will enter the viremic phase after a short delay of $4 - 7$ days and can then infect uninfected mosquitoes.

or above the thermal maximum required for transmission, the risk of a dengue outbreak is clearly low. Similarly, regions with temperatures unsuitable for the development and survival of the mosquito vectors will also not be at risk (Petrić et al., 2021). However, for populations of mosquitoes in seasonal environments it is unclear how long the temperature would need to be above the thermal minimum to facilitate an outbreak, nor how disease risk can be compared between regions using such an approach making this intuition alone inadequate. The presence of a competent vector alone has not proved sufficient to predict the occurrence of dengue outbreaks, and in much of *Aedes albopictus'* invasive range there is yet to be any evidence of autochthonous transmission of dengue (Messina et al., 2019). For example, populations of *Ae. albopictus* are now widely established throughout Europe, yet despite the wide-spread presence of established vector populations and regular introductions of dengue into the region, outbreaks are currently limited to a small geographical range (Schaffner, Mathis, 2014; Gossner et al., 2022). To guide vector control efforts it will be critical to understand the reasons why some regions with vector populations experience regular outbreaks and others do not.

1.2.3 Aedes albopictus

Ae. albopictus is a tree hole mosquito originating from South East Asia and is generally considered to be the secondary vector of dengue (Waldock et al., 2013). The range of *Ae. albopictus* is currently at its widest extent and this range is projected to increase in the coming years (Kraemer et al., 2019). Populations of *Ae. albopictus* have now spread to temperate regions that *Ae. aegypti* has previously been unable to colonise and in this invaded range sporadic outbreaks of dengue now occur (Brady et al., 2012). Like all mosquitoes *Ae. albopictus* undergoes complete metamorphosis over the course of its lifespan moving through four distinct developmental stages (Abd, 2020). Adult female mosquitoes take blood meals from available hosts to develop eggs, with an evidenced preference for human hosts but also feeding on a wide variety of other mammals, and a smaller selection of birds (Richards et al., 2006b). Juvenile mosquitoes require aquatic habitats to complete development, and oviposition sites are selected according to

a broad range of criteria, including container size, physical chemical properties of the water, the presence of conspecific and heterospecific mosquito larvae, resource availability, and the presence of predators (Shragai et al., 2019; Gunathilaka et al., 2018a; Wasserberg et al., 2013).

Ae. albopictus is known to utilise a range of both natural and artificial containers, requiring minimal space and resources to complete development and eclose to the aerial adult stage (Li et al., 2014). The habitats that *Ae. albopictus* prefers are small and ephemeral and species has several adaptations that allow for population persistence in the face of these temporary habitats drying out (Vitek, Livdahl, 2009). Adult mosquitoes engage in skip oviposition behaviour, distributing their eggs across many containers in a hedge-betting strategy that provides redundancy in the eventuality that the water in the container habitat completely evaporates (Reinbold-Wasson, Reiskind, 2021). If the habitat an egg is placed in does dry out, the eggs of *Aedes* mosquito species are desiccation resistant and can remain viable through long periods of time out of the water (Diniz et al., 2017). This allows for the swift colonisation of bodies of water immediately after rainfall, and for the persistence of populations through extended periods of drought. By colonising habitats before other species can become established *Ae. albopictus* both evades predators and escapes competition from other mosquito species (Binckley, 2017). However, when sharing a developmental habitat with other mosquito species *Ae. albopictus* can be an aggressive competitor and has been known to displace populations of the primary dengue vector *Ae. aegypti* (Juliano et al., 2004). After finishing development eggs hatch into larvae which compete for organic matter within the aquatic developmental habitat progressing through four instars before beginning pupating and subsequently emerging as adults (Abd, 2020).

Ae. albopictus can complete its life-cycle over a broad range of temperatures contributing to the extraordinary latitudinal gradient over which populations of *Ae. albopictus* are now established (Kraemer et al., 2019). Throughout the life-cycle of *Ae. albopictus* temperature alters vital rates and this can greatly change the population dynamics that are observed across the species range (Haramboure et al., 2020; Marini et al., 2017). For example, the time taken for eggs to complete embryonation has been observed to vary from 2 days at 36°C to 42 days at 15°C (Waldock

et al., 2013). In some populations of *Ae. albopictus* the lower thermal limit on development is extended as under conditions of falling temperatures and photoperiod the production of cold-resistant diapausing eggs can be triggered (Lacour et al., 2015). Diapausing eggs can remain viable and dormant over winter until conditions are suitable for larval development in the spring, allowing populations of *Ae. albopictus* to persist in temperate regions with cold winters. Larvae and pupae are similarly sensitive to temperature and both development times and mortality rates throughout both stages are strongly temperature dependent (Delatte et al., 2009). For adult mosquitoes temperature alters the expression of traits that determine vector competence in addition to population dynamics such as adult mortality and biting rates (Mordecai et al., 2017).

The same mechanisms that allow *Ae. albopictus* to exploit its environmental niche have also facilitated its global invasion through international trade routes (Swan et al., 2022) (Figure 1.4). For long distance dispersal events *Ae. albopictus* relies on passive dispersal routes, and its desiccation and cold resistant eggs have proved capable of remaining viable for extended periods of time through international shipping routes. The used tire trade was identified as the mode of introduction to the United States and South Africa and the trade in ornamental plants, specifically "lucky bamboo" has led to the establishment of a colony of *Ae. albopictus* in greenhouses in the Netherlands within which the species is now established (Reiter, 1998; Hofhuis et al., 2009). Despite the ability of the species to utilise long-range dispersal methods it has been shown that the global invasion of *Ae. albopictus* global can be best be described as a dispersal front, and there are a range of short distance dispersal routes that species has been shown to use (Kraemer et al., 2019). The primary mode of dispersal over short-distances appears to be through vehicles, which have been implicated in the reintroduction of the species in parts Spain after successful control efforts (Eritja et al., 2017; Goiri et al., 2020). Contrary to previous evidence *Ae. albopictus* is not a weak flier and has been observed to fly a distance of $1km$ from release sites in mark-recapture experiments and so is capable of actively dispersing (Vavassori et al., 2019).

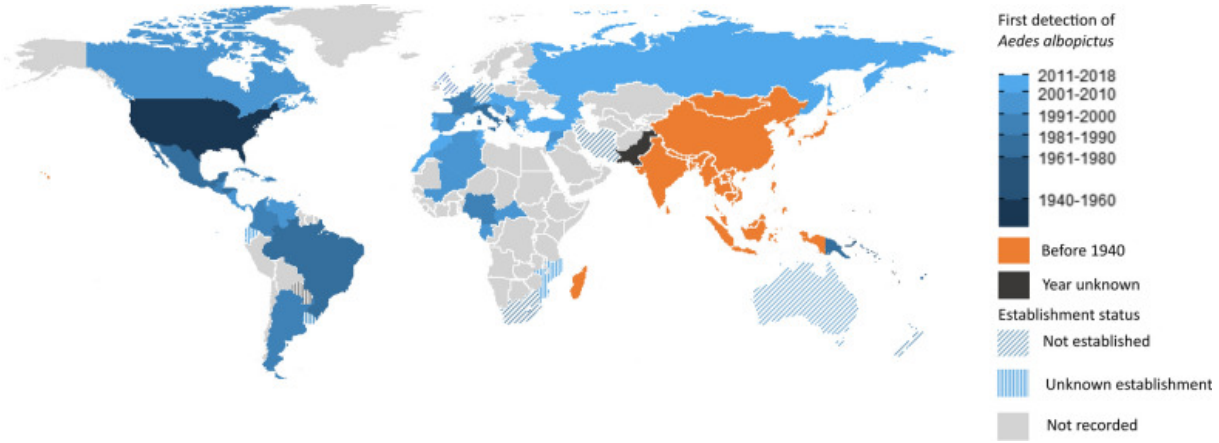

Figure 1.4: A map of the known distribution *Ae. albopictus* as of 2022, taken from Swan et al. (2022). The year the species was first recorded in each country is indicated by the colour, and whether the species became established is indicated by the type of fill."

1.3 Predicting dengue risk

There are a range of modelling approaches that are commonly used to predict the risk of mosquito-borne disease. These approaches can be broadly classified as either correlative, mechanistic, or a hybrid of both (Kearney et al., 2010; Johnston et al., 2019). Correlative approaches use statistical associations between information about the population of interest and other data to identify trends and have been widely used to predict dengue incidence on regional and global scales (Withanage et al., 2018; Carvajal et al., 2018; Xu et al., 2014; Rogers et al., 2014; Bhatt et al., 2013). However, the environmental variables that are predicted by correlative approaches to be associated with dengue incidence are not consistent between locations (Morin et al., 2013). For example, in some regions it has been shown that precipitation is positively correlated with dengue incidence, but in others precipitation is either non-significant or negatively associated (Pinto et al., 2011; Benedum et al., 2018; Su, 2008).

The changing role of environmental variables in driving dengue incidence between regions can be in part understood by considering how these variables alter the vector processes that underpin disease transmission. For example, it is suggested in regions where there is a positive

association between precipitation and dengue incidence, increased precipitation creates larval habitats, increasing vector abundance and so disease risk (Su, 2008). However, in regions such as Singapore, where there is a negative association between precipitation and dengue incidence it instead thought that larval habitats are plentiful (Benedum et al., 2018). In these regions intense precipitation events can cause the small containers that the species prefers to overflow, flushing out larvae and decreasing vector abundance and so explaining the negative association between precipitation and dengue that is observed (Dieng et al., 2012). Producing generalisable predictions of dengue risk therefore requires the ability to account for how the role of environment in driving disease transmission cycles changes between regions.

To achieve increased generality one could consider a model that considered the risk of dengue over a global range. However, predictions made by models predicting the global risk of dengue incidence also differ. Bhatt et al. (2013) used a Boosted Regression Tree approach to predict the probability that a dengue outbreak could occur in year 2010. This model considered a range of environmental, socio-economical, and land-use variables in addition to data relating to the occurrence and absence of dengue. This approach was subsequently built upon in Messina et al. (2019) to produce predictions of dengue incidence for the year 2015. These models predict a limited risk of dengue throughout temperate regions, in contrast to the predictions of the model by Rogers et al. (2014) who predicted high suitability throughout locations further north. While these global models may capture the risk of current outbreak, they do not reliably inform us about how this risk might change in novel environments. This is of concern as the lack of generality that was observed in regional models of dengue risk is still applies to global models, and Medley (2010) that found that the predictions made by species distribution models trained on data from populations of *Ae. albopictus* over its native range did not generalise to predict the distribution observed in invaded range and *vice versa*.

1.3.1 The basic reproduction number

To predict the intensity of transmission mechanistic models are often used, using expert knowledge of the system they represent to predict population responses from verifiable mechanisms. By representing the processes underlying the phenomena they aim to estimate mechanistic models are able to generalise to novel scenarios but are also vulnerable to overlooking important aspects of the system being represented. Mechanistic models can only account for processes that are explicitly included within them, and so to use a mechanistic approach to predict the incidence of vector-borne disease it is important to carefully consider and represent the biological processes underlying the transmission cycle.

The most widely recognised mechanistic model that predicts the risk of vector-borne disease is the Ross-MacDonald model for the transmission of malaria (MacDonald, 1952). Although there are now many formulations of this theory applied to a wide-range of systems, in its most fundamental form this approach uses mathematical equations to describe how an infection moves between host and vector populations (Jin et al., 2020; Auger et al., 2008; Smith et al., 2012). Using these equations it is possible to predict the conditions under which an infection introduced into a population will propagate to cause an outbreak. To summarise the behaviour of this system the basic reproduction number, R_0, is defined to describe the number of new infections caused by the introduction of single infectious individual into a completely susceptible population. This quantity is easy to calculate and interpret making R_0 approaches appealing to policy makers and applicable beyond vector-borne disease (Smith et al., 2012). The equation as defined by MacDonald has since been reformulated to resolve various issues regarding dimensionality and to better reflect the times-scale over which disease transmission occurs. A commonly used formulation of R_0 is

$$R_0(T) = \left(\frac{b(T)^2 v_h(T) h_v(T) e^{(-\delta_A(T)\tau_{EIP}(T))} M(T)}{H_T r \delta_A(T)} \right)^{1/2} \tag{1.1}$$

which has been used to predict the transmission of dengue over broad environmental gradients (Dietz, 1993; Mordecai et al., 2017; Liu-Helmersson et al., 2016).

Equation 1.1 is composed of functions and constants that describe how components of the transmission cycle respond to temperature, combining parameters relating to vector, host, and disease in a way prescribed by the underlying population model. In this case $b(T)$ is biting rate of which mosquitoes held at temperature T, $v_h(T)$ the proportion of bites by infected mosquitoes that will transmit the infection from the vector to the host, $h_v(T)$ is the proportion of bites from infected hosts that transmit the infection to the vector, μ is the mortality rate of adult mosquitoes, τ_{EIP} is the time taken for an mosquito infected by biting an infected human to become infective (otherwise known as the extrinsic incubation period (EIP)), $M(T)$ is the density of adult mosquitoes, H_T is the density of humans, and r is the rate at which humans recover from the infection. This equation formalises the earlier intuition that environmental variation should alter transmission risk, in a way that is interpretable and generalisable. This approach is able to produce predictions of relative disease risk that can be compared through time and between regions from meteorological data (see Figure 1.5 for an example of a prediction of dengue risk using this approach over Europe).

Although this formulation of R_0 can be calculate directly from climatic variables it inherits the assumptions made in the underlying transmission model which could have a profound impact on the predicts of disease risk that are made. For example, in Equation 1.1 R_0 is dependent on the density of adult mosquitoes, but because of the difficulty of estimating this parameter is it common to assume that adult density depends solely on the current temperature or to use a constant host-to-vector ratio (Liu-Helmersson et al., 2016; Mordecai et al., 2017). Although convenient these assumptions overlook the complex factors that determine vector abundance which can vary seasonally, with land-use type, and is known to respond in a delayed manner to a range of environmental variables (Valentine et al., 2020; Beck-Johnson et al., 2017). By making simplifying assumptions about how vector density responds to environmental variation the risk of outbreak may be mis-estimated especially in seasonal environments where vector

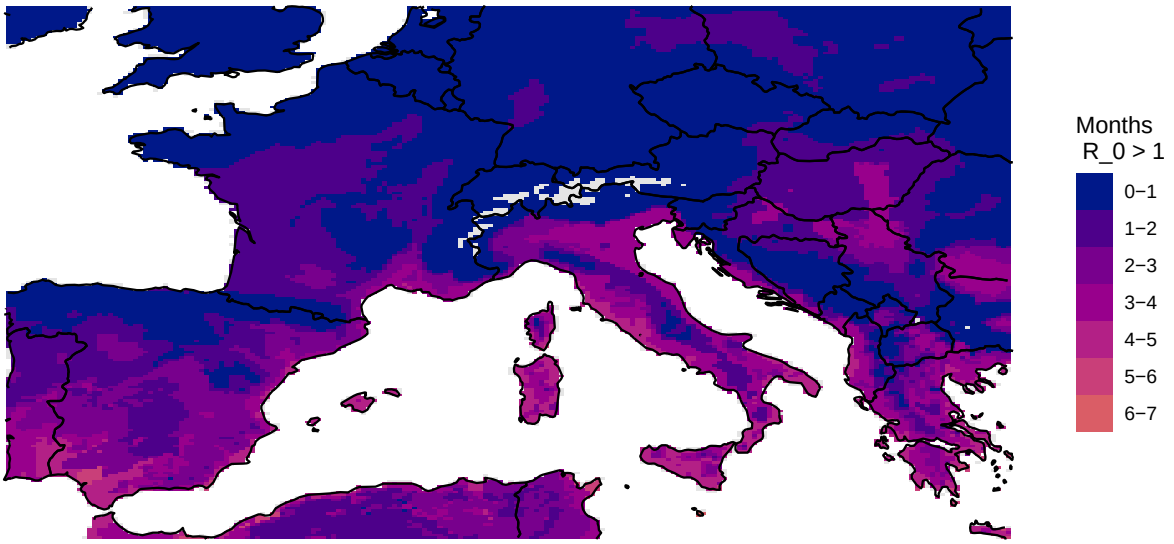

Figure 1.5: A map of the predicted period over which dengue transmission is predicted to be possible in Europe by the equation defined in Mordecai et al. (2017). The equation is applied over Europe over the years $2016 - 2020$ and the average number of consecutive months per year for which $R_0 > 1$ at each grid cell is reported.

abundances vary through time.

Another assumption often made in this formulation of R_0 is that vector trait only varies instantaneously in response to the current environment. For some traits such as human-to-vector transmission efficacy this assumption seems appropriate but for others, such as adult mortality, this is a substantial simplification of a complex biological process. The mortality rate of adult mosquitoes, $\delta_A(T)$, is known to vary with the instantaneous temperature adults experience, but also is known to depend on other environmental variables such as humidity, and also the adult's historical experience of temperature and intraspecific competition throughout development (Brady et al., 2013; Schmidt et al., 2018; Ezeakacha, Yee, 2019). The traits expressed by adult mosquitoes are therefore inherently linked population dynamics, meaning that by assuming that adult mortality can be adequately estimated from instantaneous relationships that were validated in individuals a mismatch in scales is introduced (Lord et al., 2014). These simplifying assumptions are of concern as Equation 1.1 is highly sensitive to this parameter. However, to

incorporate a more complete description of how vector trait responds to environmental variation it is necessary to account for the outcome of a series of historical environmental and population states. To achieve this generality in a formulation of R_0 it will be necessary to formulate an underlying model of vector dynamics that can account for the relationship between vector population and trait dynamics.

1.3.2 Using differential equations to model vector population dynamics

In this thesis I develop mechanistic models that use differential equations to describe how the population dynamics of vector populations alter the ability of those populations to transmit disease with a special focus on representing the interaction between demographic processes and trait expression. The central idea behind such models is that by defining equations that numerically describe a population's demographic processes, such as the rate of births or deaths, the evolution of that population through time can be predicted.

The Nisbet and Gurney framework for stage-structured models with variable delay

Over the course of a mosquito's life-cycle it undergoes complete metamorphosis, and the environmental stressors and biological processes that are important to determining population dynamics change throughout the course of development (Rolff et al., 2019). Stage-structured models are a form of population model widely used in mathematical biology to represent the population dynamics of species with multiple distinct life-stages (Murdoch et al., 2003). In a stage-structured model a species' life-history is categorised into distinct developmental stages, each of which is then represented in the model by a separate equation that represents stage-specific processes. These equations are linked, allowing individuals to move through the stage structure as they develop. Stage-structured models have been previously used to predict the population dynamics of mosquito species, design vector control campaigns, and to predict the efficacy of vaccination drives (Ewing et al., 2016; Oliva et al., 2021; Ferguson et al., 2016).

Existing stage-structured models of mosquito population dynamics vary in complexity from systems of ordinary differential equations to more complex systems of delay-differential equations or partial differential equations (Erickson et al., 2010; Huang et al., 2020; Pasquali et al., 2020). The biological processes included in these models and consequently the assumptions made by them vary depending on their stated goals, the scale at which they operate, and the data available when they were parametrised. Although these previous models are often applied over a wide range of locations they are rarely validated against multiple datasets across the species global range. There is now widely available data from field populations of *Ae. albopictus* from around the globe, often with simultaneous observations of multiple life-stages. For a models predictions to be considered generalisable across climates the validation of that model should include a demonstration of an ability to independently predict the dynamics of field populations from across the species full range.

In the work that follows I develop stage-structured models that build upon the Nisbet and Gurney for formulating well-posed stage-structured systems of delay-differential equations with variable delays to predict population dynamics (Nisbet, Gurney, 1983). Models that use this approach have been previously used to predict the population dynamics of various species including mosquitoes (Ewing et al., 2016). What follows is intended to provide an intuitive understanding of how models formulated using this framework function with the rigorous mathematical details deferred to Chapter 2 where I make similar arguments in full detail.

Assume that there is a population divided into n developmental stages with the number of individuals in developmental stage i at time t denoted $N_i(t)$. For a given developmental stage i, individuals are assumed to enter the stage through recruitment, denoted $R_i(t)$, and leave through either maturation or death, denoted $M_i(t)$ and $D_i(t)$ respectively. Individuals enter the system at life-stage $i = 1$ through birth and cease development at life-stage n. The assumption that individuals are born into life-stage 1 means that this recruitment term takes a special form which can be expressed

$$R_1(t) = \sum_{i=1}^{n} \beta_i(t) N_i(t)$$

where $\beta_i(t)$ is the *per capita* rate of production of offspring for individuals in life-stage i. Note that production of offspring is both stage-specific and variable, allowing the representation of stage-specific differences in reproductive output. For example if individuals in life-stage 1 are eggs I am free to choose $\beta_1(t) = 0$ so that individuals in the eggs stage produce no offspring and so contribute no new individuals to the sum. That the fecundity of individuals is permitted to vary with time means that I can represent the effect of biotic and abiotic environmental variables on the traits of individuals in different stages. For example, for a species where the *per capita* rate of production of offspring by individuals in life-stage n depends linearly on the current temperature this could be expressed as $\beta_n(t) = aT(t) + b$, where $T(t)$ is the temperature at time t, with a, b constants.

After recruitment into life-stage i individuals begin to develop until leaving the stage either through maturation into life-stage $i + 1$ or through death. The time it takes for an individual to develop from recruitment into the stage to maturation out of the stage is referred to as the stage duration and is denoted $\tau_i(t)$. Stage-duration is permitted to vary, and this can be used to represent environmentally induced changes in development rates. To describe how the stage duration, $\tau_i(t)$, evolves through time it is now necessary to account for the cumulative effect of variation in the stage-specific rate of development, $g_i(t)$, and it can be shown that this can be expressed using the equation

$$\frac{d\tau_i(t)}{dt} = 1 - \frac{g_i(t)}{g_i(t - \tau_i(t))}, \text{ for } i \in \quad 1, ..., n.$$

To understand how this equation functions consider the scenario where after a long period of remaining constant, the development rate, $g_i(t)$, which for simplicity is assumed here to be continuous, bounded, monotone, and to achieve its bounds, very slowly tends to its minimal value

from some non-zero value (additionally requiring that the length of the delay is substantially smaller than the length of time over which this change takes place). In this situation $g_i(t) \leq g_i(t-\tau_i(t))$ and so $1 - \frac{g_i(t)}{g_i t - \tau_i(t)} \geq 0$. Therefore the stage-duration, $\tau_i(t)$, will slowly increase until the minimum development rate is reached and eventually (after a delay of $\tau_i(t)$) will also stop increasing, reaching its maximal value, as at this point $g_i(t) = g_i(t-\tau_i(t))$ and therefore $\frac{d\tau_i(t)}{dt} = 0$. Consider now that the scenario where after a sufficient period of time the direction of the change of $g_i(t)$ were to be reversed. As the development rate is slowly increased, such that $g_i(t) \geq g_{i-1}(t)$, then $1 - \frac{g_i(t)}{g_i t - \tau_i(t)} \leq 0$ and so the stage-duration slowly decreases towards its minimum. In either case the rate at which the stage-duration changes at time t depends on the "steepness" of the function $g_i(t)$ in the locality of t, as the faster $g_i(t)$ changes the greater the difference between its value at time t and time $t - \tau_i(t)$ and so the greater the instantaneous rate of change of the stage-duration is.

After being recruited into life-stage i, and having survived for the stage-duration of the stage, individuals mature into life-stage $i+1$. At time t the number of individuals maturing into life-stage $i+1$ from life-stage i is necessarily equal to the number of individuals that were recruited into the life-stage i at time $t - \tau_i(t)$ and survived. To be able to describe this relationship an expression that describes the proportion of individuals that survive through the stage is required. By definition in life-stage i, the number of individuals that die per unit time is denoted $D_i(t)$, and this function is assumed to take the form $D_i(t) = \delta_i(t) N_i(t)$, where $\delta_i(t)$ is the mortality rate of individuals in stage i. As under this formulation it is possible that both the duration of the life-stage and the stage-specific mortality rates are variable the expression for the number of individuals that survive for the duration of life-stage i reflects this. The through-stage survival of individuals that were recruited into life-stage i at time $t - \tau_i(t)$ and mature out of life-stage i at time t is denoted $P_i(t)$ and is defined

$$\frac{dP_i(t)}{dt} = P_i(t)\left(\frac{g_i(t)\delta_i(t-\tau_i(t))}{g_i(t-\tau_i(t))} - \delta_i(t)\right), \text{for } i \in \quad 1, ..., n.$$

To understand the behaviour of this equation assume both $g_i(t)$ and $\delta_i(t)$ take simple forms (specifically assume they are continuous, bounded, monotone, and achieve their bounds) and also assume they take non-zero values. If once again the rate of development slowly tends to its minimal value, then $g_i(t) \leq g_i(t - \tau_i(t)$ and $\frac{g_i(t)}{g_i(t-\tau_i(t))} < 1$. In the bracket the contribution of $\delta_i(t - \tau_i(t))$ to the total value of the derivative is reduced as compared to $\delta_i(t)$, and depending on the behaviour of $\delta_i(t)$ this can have different consequences on the value of $P_i(t)$. If $\delta_i(t) = \delta_i(t - \tau_i(t))$ then the term in the bracket becomes negative and so the probability of surviving through the stage decreases, representing that as the stage-duration increases individuals must survive for a longer period of time before leaving the stage and so fewer individuals successfully mature out of the stage. This behaviour continues until $g_i(t) = g_i(t - \tau_i(t))$ is reached where $\frac{dP_i(t)}{dt} = 0$ and the through-stage survival stops changing. If now, as before, $g_i(t)$ is slowly increased to is maximal value the opposite behaviour would be observed as through stage survival increases as stage-duration decreases. One can make similar arguments to see how when $g_i(t)$ is fixed and the mortality rate $\delta_i(t)$ is slowly varied that the proportion of individuals surviving through the developmental stage increases or decreases as expected. In a variable environment where both $g_i(t)$ and $\delta_i(t)$ are permitted simultaneously co-vary the probability of surviving through the stage is therefore represented appropriately by this equation.

The number of individuals maturing out of life-stage i and into life-stage $i + 1$ can be expressed in terms of the number of individuals that were recruited into life-stage i at $t - \tau_i(t)$ units of time in the past and have completed development by time t by

$$M_i(t) = \frac{g_i(t)}{g_i(t - \tau_i(t))} R_i(t - \tau_i(t)) P_i(t) \;\; i \in \quad 1, ..., n.$$

Further, as the number of individuals being recruited into life-stage $i + 1$ must be equal to the number of individuals maturing out of life-stage i, then $R_{i+1}(t) = M_i(t)$. Thus from the expression for $R_1(t)$ I can recursively define all other $R_i(t)$ and $M_i(t)$ for $i \neq 1$.

The final components necessary to fully specify the model are the initial conditions that describe

the state of the system at $t = 0$, the initial history that defines what the state of the system was at $t < 0$ such that the delay terms are always well-defined, and an initial impulse to begin the dynamics. The impulse function represents the introduction of individuals into the system from time $t = 0$ to time $t = T$. Denote this function $I(t)$ which and define it such that

$$I(t) = J, \quad \text{for} \quad 0 < t \leq T, \tag{1.2}$$

$$= 0, \quad otherwise. \tag{1.3}$$

Therefore the population dynamics of a species with n developmental stages of variable duration can be described using the following system of equations

$$\frac{dN_i}{dt} = R_i(t) - M_i(t) - D_i(t), \tag{1.4}$$

$$\frac{dP_i(t)}{dt} = P_i(t)\left(\frac{g_i(t)\delta_i(t-\tau_i(t))}{g_i(t-\tau_i(t))} - \delta_i(t)\right), \tag{1.5}$$

$$\frac{d\tau_i(t)}{dt} = 1 - \frac{g_i(t)}{g_i(t-\tau_i(t))}. \tag{1.6}$$

for $i \in 1, ..., n$ and $t > 0$ with recruitment terms defined,

$$R_i(t) = \begin{cases} \frac{g_i(t)}{g_i(t-\tau_i(t))} R_i(t-\tau_i(t))P_i(t), & \text{for } i \neq 1 \\ \sum_{i=1}^{n} \beta_i N_i(t), & \text{for } i = 1. \end{cases} \tag{1.7}$$

with initial conditions $\tau_i(0) = \tau_{i0}$, $P_i(0) = \exp -\delta_{i0}\tau_{i0}$, and initial history such that for $t \leq 0$, $N_i(t) = 0$, and $R_i(t) = 0$.

Susceptible-Infected-Resistant models of disease dynamics

To incorporate models of mosquito population dynamics into a prediction of disease risk it is also necessary to describe both host and disease dynamics. Susceptible-Infected-Resistant models are a form of compartmental model used to represent the progression of a disease through a population structured by infection status rather than developmental progress. SIR models are extensively used to predict the transmission dynamics of dengue vectored by *Aedes* mosquitoes and to design intervention campaigns. Although there are many variations upon SIR models the fundamental idea is to divide the population into classes based upon their current experience of infection. Usually individuals are classified as either susceptible to the disease, infected with the disease, or recovered from the disease. The susceptible class consists of individuals that do not currently have the disease and either have never had the disease or had the disease at a sufficiently distant point in the past that any acquired specific immunity is no longer present. After contracting the disease individuals in the susceptible class progress to the infected class which contains individuals that currently have the infection and are competent to transmit it through whatever specific mechanism this is achieved. After ceasing to be infectious individuals proceed to the recovered class, which contains individuals that are no longer susceptible to the disease due to some form of specific immunity gained from contracting the disease. Depending on the disease being modelled and the time-frame being considered, individuals in the recovered class may eventually progress back through to the susceptible class as their immunity fades. For a vector-borne disease the infection moves through both vector host populations, and so in addition to modelling the infection status of the host population, the infection status of the vector population must also be accounted for.

SIR models of dengue transmission vary in complexity and make a broad range of assumptions about depending on their stated goals. To represent how variation in vector density alters transmission risk it is common to use a previously derived model to predict vector dynamics. However, not all models choose to explicitly represent the vector population and may instead

implicitly represent vector dynamics in transmission terms. Comparisons between models of dengue transmission with explicit and implicit vector populations indicate that over short periods and in a location where there is little seasonal variation in mosquito abundance implicit approaches can perform well (Pandey et al., 2013). Vector traits are often represented either through constants or through functions that assume they vary instantaneously with the current temperature. As described when discussing R_0 approaches this is a simplification of complex biological processes and is problematic as the predictions made by SIR models are often particularly sensitive to traits such as the adult mortality rate (Barbazan et al., 2010; Luz et al., 2003). However, more fully representing the mechanisms by which vector trait varies in response to environmental variation is not trivial and requires a substantial increase in model complexity.

Incorporating mechanisms of trait variation into predictions of disease risk

The collection of traits an individual expresses is called its phenotype, and all inter-individual variation can be described through changes in this phenotype. Mechanisms of variation can be broadly categorised as either genotypic variation, phenotypic plasticity, or epigenetic effects. Genotypic variation is the ability of individuals expressing different genotypes to express different traits (Sultan, 2017). Phenotypic plasticity is the ability of individuals expressing the same genotype to express different phenotypes when exposed to different environmental conditions (Fusco, Minelli, 2010). Epigenetic variation is the ability of the environmental experience of an individual to cause changes in the expression of genes in offspring.

Genotypic variation between populations of *Ae. albopictus* is widely observed and has been a significant factor in the species' global invasion. *Ae. albopictus* has recently evolved a photoperiodic diapause response, whereby cold-resistant eggs are produced in response to falling temperatures and lowering photoperiod. This response allows populations of *Ae. albopictus* to become established in temperate regions but is absent from populations in tropical climates where adult activity can be maintained all year round (Urbanski et al., 2012). In temperate zones there is

evidence of latitudinal variation in the critical photoperiod, providing evidence that this trait remains under strong selection (Hawley et al., 1987). Genotypic variation can also alter the risk posed by populations of *Ae. albopictus* indirectly through changes in the genotype of the disease being vectored. For example, a change in the genotype of the Chikungunya virus, increased the replication rate of the virus in *Ae. albopictus* and facilitated the global re-emergence of this disease (Sam et al., 2012; Carrieri et al., 2011).

The role that phenotypic plasticity plays in producing population responses to environmental change is less well understood and is currently under vigorous debate (Fusco, Minelli, 2010; Hulme, 2008). There is plethora of seemingly contradictory evidence from experimental systems demonstrating how phenotypic plasticity can both help and hinder how populations adapt to change. For example in 1965 it was hypothesised that species expressing high degrees of phenotypic plasticity would make more successful invasive species than species that did not display strong plastic responses (Baker, Stebbins, 1965). This hypothesis is still debated and meta-analyses reaching contradictory conclusions were published in the same year (Davidson et al., 2011; Godoy et al., 2011). Similarly opposing evidence has been found in the role of phenotypic plasticity in determining populations responses to climate change (Anderson et al., 2012; Chevin et al., 2010; Henn et al., 2018; Acasuso-Rivero et al., 2019; Valladares et al., 2014; Oostra et al., 2018). To resolve these and reconcile the role of phenotypic plasticity in population ecology will require a more complete understanding of how mechanisms of individual variation generalise to population responses to environmental change (Violle et al., 2012).

Phenotypic plasticity alters the population dynamics of *Ae. albopictus* throughout the species life-cycle altering the expression of traits through both instantaneous responses to the current environment and delayed responses to historic environments (Delatte et al., 2009; Ezeakacha, Yee, 2019). Instantaneous responses to the current environment such as temperature induced variation in development and mortality rates, are well represented in models of disease transmission (Ewing et al., 2021; Mordecai et al., 2017). However, the effects of environmental variation on trait expression can also be delayed, and the effect of delayed environmental variation on the

trait structure of vector populations is rarely considered in models of disease risk (Beckerman et al., 2002; Cator et al., 2020).

The ability to represent multiple instances of phenotypic plasticity both in response to both current and historical environmental conditions will be a necessary component of any modelling approach that hopes to understand how environmental variation alters disease risk. However, there are currently few modelling tools that allow this sort of flexibility. When a population has distinct generations integral projection models (IPMs) can be used to represent within population trait variation (Childs et al., 2003; Kuss et al., 2008). Models formulated using this method define distributions describing how trait is expected to change between time steps and use these to predict how a populations trait distribution will change through time. However, to represent the population and trait dynamics of *Ae. albopictus* a modelling approach that can also represent detailed intra-generational dynamics will be required and for this physiologically structured population models (PSPMs) could be considered (De Roos, Persson, 2001). PSPMs use partial differential equations to link deterministic variation in an individual's size to population response and resource dynamics. However, for a species such as *Ae. albopictus*, where resource dynamics are relatively unexplored and there are stage-specific gaps in the knowledge of its life-history, such a complete approach cannot be fully utilised and so an alternative modelling method is needed (Bolnick et al., 2011; Violle et al., 2012; Lipowsky et al., 2015; Johnston et al., 2019; Sgrò et al., 2016; Hendry, 2016; Turcotte, Levine, 2016; Lloyd-Smith et al., 2005; Lion, 2018).

1.4 Summary of work

In this thesis I develop a novel mathematical modelling framework to represent the effects of phenotypic plasticity on population dynamics. This framework is applied to two organisms initially to Nicholson's blowflies, a well-studied model system and then to the invasive dengue vector *Ae. albopictus*. In each case I explore the effect of environmentally driven trait varia-

tion on population dynamical processes and demonstrate their importance in determining how population-level processes respond to change.

In Chapter 2 I justify the need for and derive a novel mathematical modelling framework to represent the effect of phenotypic plasticity on population dynamics. I argue that environmentally driven trait variation is currently poorly represented in mathematical modelling frameworks. I then derive a mathematically rigorous framework that is able is able to represent trait-environmental feedbacks, using systems of stage-phenotypically structured delay-differential equations. This framework is then applied to Nicholson's blowflies, where it is able to predict cryptic population dynamical behaviour. This demonstrates that predictions made directly from environment-trait relationships do not necessarily generalise to population response. This example demonstrates both the efficacy of the model framework and the need to fully account for the effects of phenotypic plasticity on population dynamics.

In Chapter 3 I then apply the framework derived in Chapter 2 to predict the population and trait dynamics of the invasive mosquito species *Ae. albopictus* on a global range. To do this I identify the ecological and environmental processes important to mosquito population dynamics and formulate a model to represent this. The model is parametrised and statistically fitted using laboratory data. I then validate the model against data from field populations of *Ae. albopictus* across the species global range, considering populations from 14 countries and territories across 4 continents. The model produces excellent predictions of the population and trait dynamics of the species that are completely independently of the populations I validate against. This reveals that there are distinct differences in the trait dynamics of mosquito populations in temperate and tropical climates driven by environment-trait interactions.

In Chapter 4 the model derived in Chapter 3 is extended to include a Susceptible-Infected-Resistant model for dengue fever. Following the same process for validation as in the previous chapter the model is able to predict the timing, magnitude, and locations of dengue outbreaks. This approach is compared to previous methods and is found to be considerably more specific

in its predictions and to simultaneously better match real-world dengue transmission. I predict lower dengue risk throughout Europe and North America than previous approaches, regions that have not experienced large scale dengue outbreaks vectored by *Ae. albopictus*. Predictions for where transmission is possible in these regions align with verified instances of autochthonous transmission. By contrast I predict that eastern and southern China, a region that experiences regular, large, outbreaks of dengue vectored by *Ae. albopictus*, highly suitable for transmission. It is demonstrated that these highly generalisable results are achieved due to the full representation of mechanisms of phenotypic plasticity that drive variation in vector trait. Further, in regions where large outbreaks occurred I find that the majority of vectors were competent to maintain the dengue transmission cycle, but in regions where small outbreaks occur only a small subset of vectors expressing high trait values could maintain the pathogen transmission cycle. This shows the need to consider mechanisms of variation when predicting disease risk between regions.

Chapter 5 is a general discussion of the work presented in the thesis, reviewing the implications of the work undertaken in the previous chapters and suggest avenues for future research.

Chapter 2

Deriving a stage-phenotypically structured model and application to Nicholson's Blowflies

The work presented in this Chapter forms the basis of a published paper (Brass et al., 2021).

2.1 Abstract

Predicting complex species-environment interactions is crucial for guiding conservation and mitigation strategies in a dynamically changing world. Phenotypic plasticity is a mechanism of trait variation that determines how individuals and populations adapt to changing and novel environments. For individuals, the effects of phenotypic plasticity can be quantified by measuring environment–trait relationships, but it is often difficult to predict how phenotypic plasticity affects populations. The assumption that environment–trait relationships validated for individuals indicate how populations respond to environmental change is commonly made without sufficient justification. Here we derive a novel general mathematical framework linking trait variation due to phenotypic plasticity to population dynamics. Applying the framework to the classical example of Nicholson's blowflies, we show how seemingly sensible predictions made from

environment–trait relationships do not generalise to population responses. As a consequence, trait-based analyses that do not incorporate population feedbacks risk mischaracterising the effect of environmental change on populations. This framework is used in Chapters 3 and 4 to predict how phenotypic plasticity in a transmission critical trait alters the ability of populations of the invasive mosquito *Aedes albopictus* to maintain dengue transmission cycles across its global range.

2.2 Introduction

Understanding how mechanisms of individual variation act upon populations is key to predicting how changes in the biotic and abiotic environment alter population processes. Phenotypic plasticity has been shown to be a mechanism by which species respond to climate change (Seebacher et al., 2015; Crozier, Hutchings, 2014; Stoks et al., 2014; Boutin, Lane, 2014). There is evidence that species exhibiting high levels of phenotypic plasticity are more successful at spreading across environmental gradients (Szabó et al., 2018; Hahn et al., 2012), and it is predicted that phenotypic plasticity contributes to determining the outcome of interspecific competition (Palkovacs, Post, 2009; Buskirk, Mccollum, 2016). Quantifying phenotypic plasticity in individuals is generally straightforward, but it is often more difficult to measure the effects on populations (Merilä, Hendry, 2014; Valladares et al., 2006). It is theorised that phenotypic plasticity contributes to the occurrence of seemingly paradoxical population dynamical behaviours such as the paradox of enrichment, whereby an increase in available resources causes a destabilisation of population's dynamics (Miner et al., 2005), and the hydra effect where an increase in per capita mortality results in increased population density (Cameron, Benton, 2004). Disentangling the complex network of inter-dependent individual and population processes necessary to demonstrate how phenotypic plasticity contributes to species responses to environmental change is inherently difficult using existing model frameworks (Forsman, 2015). In particular, the population dynamic consequences of phenotypic plasticity often manifest as delayed-density dependence (Beckerman

et al., 2002) which is known to cause cryptic dynamical behaviours (Pedraza-Garcia, Cubillos, 2008; Lima et al., 1999).

Despite the potentially complex relationship between individual variation and population response, environment-trait relationships observed in individuals are routinely employed to predict the outcome of population processes (Figure 2.1). For example, in epidemiology environmental-trait relationships are used in parameter-based approaches for calculating the basic reproduction number, R_0 (Mordecai et al., 2017; Brand et al., 2016; Parham, Michael, 2010). This implicitly assumes that variation observed in a population's trait distribution is independent of environmental stressors and population dynamics, such that an averaged trait value suitably represents the population at any given time and location (Liu-Helmersson et al., 2016). This is the mean-field approach and there is an increasing body of evidence that this approach under-represents the importance of variation between individuals and community structure in population ecology (Violle et al., 2012; McGill et al., 2006; Cator et al., 2019; Fox, Kendall, 2002). Consideration of purely stochastic forms of variation has demonstrated that the outcome of population processes such as species persistence do not always follow mean-field predictions (Hart et al., 2016; Morozov et al., 2013). In contrast to environmental or demographic noise, individual variation caused by phenotypic plasticity has a strong mechanistic component, and so can and should be suitably accounted for when predicting how population's respond to changes in their environment (Nylin, Gotthard, 2002).

To describe the effect phenotypic plasticity has on population dynamics it is key to link trait and effect mechanistically combining empirically derived relationships with theoretical methods. Here, I propose a novel general mathematical framework that links experimentally derived environment-trait relationships to well-parametrised stage-structured population models that allow trait distributions to emerge from population-trait-environment interactions (Figure 2.1). I utilise a continuous time stage-structured modelling approach, widely used to model organisms with multiple distinct life stages (Murdoch et al., 2003), adapted to represent the persistent and delayed effects of phenotypic plasticity across multiple developmental stages. By using this

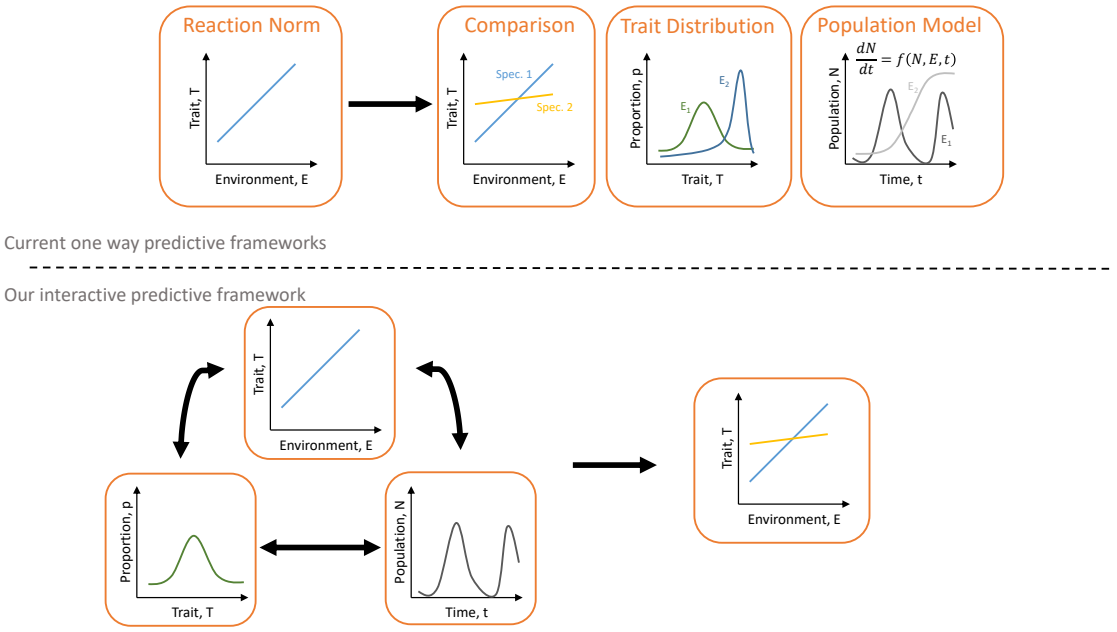

Figure 2.1: Current predictive frameworks typically use environment-trait relationships, such as reaction norms, to predict population responses without consideration of how population processes may alter the traits individuals express. This framework incorporates environment-trait relationships that interact with population dynamics and trait distributions. This allows the framework to account for the effect of interaction between environment, trait, and population as experienced by many organisms in predictions of population processes.

framework to represent mechanisms of individual variation in response to environmental change, it is shown that even simple forms of phenotypic plasticity can lead to complex population dynamical responses that previous approaches overlook. This is demonstrated by an application of the framework to a classical population ecology study, Nicholson's blowflies (Nicholson, 1957), where it has been hypothesised that previously unexplained population dynamics can be attributed to phenotypic plasticity. This application reveals a rich set of counter-intuitive population-dynamical behaviours caused by the interaction between phenotypic plasticity and population dynamics.

2.3 Methods

2.3.1 Framework overview

I present a modelling framework that dynamically links the expression of phenotypic plasticity in individuals to population dynamics. This consists of a continuous time stage-structured population model in the form described in Gurney et al. (1983) (as described in Chapter 1 and shown in Figure 2.2A), widely used to predict the population dynamics of interacting life-stages (e.g. Gurney et al. (1980)), combined with a set of empirically-derived reaction norms. Models created using the framework are systems of stage-phenotypically structured delay-differential equations, within which, cohorts of individuals are tracked based on their cumulative environmental experience. Each cohort is then associated with a unique phenotype (Figure 2.2B). Within the framework an individual's phenotype may consist of multiple traits varying in response to multiple environmental factors, both current and historic. By tracking this experience across all individuals a dynamic phenotypic structure is defined allowing multiple phenotypes to be represented within a population simultaneously. The distribution of traits expressed within a population is not assumed, as it is in an integral projection matrix (IPM) (Merow et al., 2014), but instead emerges as a feature of empirically verified mechanistic processes. This links

individual level variation in life-history traits to population level response and so represents the effects of phenotypic plasticity on populations. Models derived using the framework are able to represent both intra- and inter-generational forms of phenotypic plasticity, in response to both instantaneous and delayed environmental conditions. Moreover, the framework can account for the effects of multiple environmental cues on single or multiple traits, giving rise to a highly flexible modelling framework.

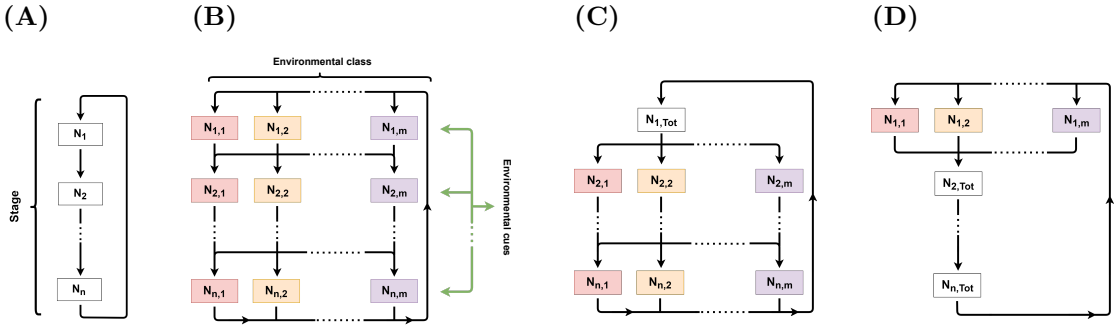

Figure 2.2: Schematics of the ways phenotypic plasticity in stage-structured populations can be described by the new model framework. The population being considered in all cases is stage-structured with n life-stages. The number of individuals in life-stage i, expressing phenotype j is denoted $N_{i,j}$. **(A),** The Gurney et al. (Gurney et al., 1983) framework for stage-structured populations that is used as a basis for the novel framework. This framework represents a continuous age structure by a discrete number of developmental classes e.g. eggs, larvae, pupae, and adults. **(B),** The most general form of the novel framework, where an individual's experience of the environmental cues in each developmental stage determines the phenotype it expresses as partitioned by the environmental classes. **(C),** The new framework adapted to represent developmental plasticity in life-stage 2. It is assumed that individuals experience an environmental cue in life-stage 1 that does not affect individuals in life-stage 1 but results in the expression of phenotypic plasticity in subsequent life-stages. This allows the reduction of the phenotypic structure in life-stage 1 to just a single class, $N_{1,\mathrm{Tot}} = \sum_{j=1}^{m} N_{1,j}$. **(D),** The new framework adapted to represent a maternal effect in response to an environmental cue experienced by parents in life-stage n that manifests as phenotypic plasticity in life-stage 1 which is then assumed to have no effect on subsequent life-stages.

2.3.2 Incorporating phenotypic plasticity into stage-structured models

Variation caused by phenotypic plasticity is often expressed in terms of a reaction norm, a function that describes how an individual's environmental experience alters the phenotype they

express (Nylin, Gotthard, 1998) (e.g. food consumed as a juvenile predicts adult body mass). It is assumed that organisms with similar experiences of their environment express the same phenotype as determined via reaction norms and to represent this multiple linked copies of the Gurney et al. framework are created (as in Figure 2.2B). Each copy corresponds to a unique set of environmental conditions and individuals then move through this structure on a path determined by their current and historical experience of the environment. This allows cohorts of individuals that share the same environmental history to be tracked and so represents the effects of phenotypic plasticity on populations.

I consider a stage-structured population with n life-stages where phenotypic plasticity is expressed according to d reaction norms $r_1(\boldsymbol{\alpha}), ..., r_d(\boldsymbol{\alpha})$ in response to z environmental cues $\boldsymbol{\alpha}(t) = (\alpha_1(t), ..., \alpha_z(t))$. For computational tractability, each environmental cue is discretised, $\alpha_j(t)$, into m_j subintervals and I denote by α_{jp} the midpoint of the p^{th} subinterval of the discretisation of $\alpha_j(t)$. Define an *environmental class* to be a vector of length z with entries that consist of one midpoint from each discretised environmental cue, i.e.

$$(\alpha_{1l_1}, \alpha_{2l_2}, \alpha_{3l_3}, ..., \alpha_{zl_z}),$$

where $l_j \in \{1, ..., m_j\}$. Define $g : \mathbb{R}^z \to \Omega_{\boldsymbol{\alpha}}$ such that

$$g(\boldsymbol{\alpha}(t)) = (\alpha_{1l_1}, \alpha_{2l_2}, \alpha_{3l_3}, ..., \alpha_{zl_z}),$$

if $\alpha_j(t)$ takes values within the ${l_j}^{th}$ subinterval of $\alpha_j(t)$. The function g defines a mapping of $\boldsymbol{\alpha}$ onto the discretisation of $\boldsymbol{\alpha}$. The number of environmental classes is given by

$$m = \prod_{h=1}^{z} m_h,$$

and the set of all such vectors (environmental classes) is denoted by $\Omega_{\boldsymbol{\alpha}}$. Assign an ordering

to the m elements of the set of environmental classes $\Omega_{\boldsymbol{\alpha}}$ and let $\boldsymbol{\alpha}^k$ denote the k^{th} element of the ordered set, i.e. the k^{th} environmental class. Thus, $g(\boldsymbol{\alpha}) = \boldsymbol{\alpha}^k$ if $g(\boldsymbol{\alpha})$ is the k^{th} element of the ordered set $\Omega_{\boldsymbol{\alpha}}$. Environmental classes define cohorts of individuals that have experienced a shared environmental history.

For example, suppose there are 2 environmental cues $\boldsymbol{\alpha}(t) = (\alpha_1(t), \alpha_2(t))$ which are discretised such that $\alpha_1(t)$ is divided into 3 subintervals ($m_1 = 3$) and $\alpha_2(t)$ into 2 subintervals ($m_2 = 2$). In this case an environmental class is a vector of the form

$$(\alpha_{1l_1}, \alpha_{2l_2}), \text{ where } l_1 \in \{1, 2, 3\} \text{ and } l_2 \in \{1, 2\}.$$

The set of all possible vectors of this type is Ω_α. So for example, if $\alpha_1(t)$ represents temperature and $\alpha_2(t)$ represents food availability, say, then $\boldsymbol{\alpha}(t)$ may be approximated by an element from Ω_α. To order the elements of the set Ω_α an ordering needs to be defined. One common ordering of such a set is called lexicographic ordering which gives

$$\begin{aligned}(\Omega_\alpha, \preceq) &= \{(\alpha_{11}, \alpha_{21}), (\alpha_{11}, \alpha_{22}), (\alpha_{12}, \alpha_{21}), (\alpha_{12}, \alpha_{22}), (\alpha_{13}, \alpha_{21}), (\alpha_{13}, \alpha_{22})\} \\ &= \{\boldsymbol{\alpha}^1, \boldsymbol{\alpha}^2, \boldsymbol{\alpha}^3, \boldsymbol{\alpha}^4, \boldsymbol{\alpha}^5, \boldsymbol{\alpha}^6\}.\end{aligned}$$

So if $g(\boldsymbol{\alpha}(t)) = \boldsymbol{\alpha}^4$ at time t the environment is in state 4 and the temperature is within α_{12} and food availability is within α_{22}.

It is assumed that an individual's current and historic experience of the environment completely determines the phenotype an individual acquires when it matures from life stage i to $i+1$ or is born into stage life stage 1 at time t. This permits the effects of environmental variation to be deferred to future developmental stages or generations. As the environmental cues are discretised

this means there are a discrete number of phenotypes that can arise in the framework. The traits that these phenotypes express are calculated using the reaction norms according to, $r_k(g(\boldsymbol{\alpha}))$. This process pre-defines both the traits individuals express and the range of environmental conditions that give rise to those individuals.

2.3.3 The general framework for representing phenotypic plasticity in stage-structured population models

Denote the number of individuals in life-stage i and environmental class j at time t by $N_{i,j}(t)$. Denote by $R_{i,j}(t)$ the rate of recruitment of individuals into life-stage i and environmental class j, $M_{i,j}(t)$ the rate of maturation out of life-stage i and environmental class j, and $D_{i,j}(t)$ the death rate in life-stage i and environmental class j. The population is described by the system of equations

$$\frac{dN_{i,j}(t)}{dt} = R_{i,j}(t) - M_{i,j}(t) - D_{i,j}(t) \tag{2.1}$$

for $i \in 1, ..., n$, and $j \in 1, ..., m$. The death rate is $D_{i,j}(t) = \delta_{i,j}(t)N_{i,j}(t)$ where $\delta_{i,j}(t)$ is the mortality rate of individuals in life-stage i and environmental class j. The recruitment term in Equation 2.1 when $i = 1$ is given by

$$R_{1,j}(t) = \sum_{k=1}^{m} \left(w_{kj}(\boldsymbol{\alpha}(t)) \sum_{v=1}^{n} \beta_{v,k}(t)N_{v,k}(t) \right) \tag{2.2}$$

for $j = 1, ..., m$ where $w_{kj}(\boldsymbol{\alpha}(t))$ denotes the proportion of individuals from environmental class k that transition to environmental class j at time t and $\beta_{v,k}(t)$ is the birth rate of individuals in life-stage v and environmental class k. The transition functions, $w_{kj}(\boldsymbol{\alpha}(t))$, are the mechanism

through which the environment acts to express phenotypic plasticity within the model. Equation 2.2 represents the birth of new individuals into the first life-stage and environmental class j by parents from across all environmental classes and life-stages. The birth term, $\beta_{v,k}(t)N_{v,k}(t)$ describes the number of new individuals produced by parents in life-stage v and environmental class k, and is summed across all life-stages and environmental-classes to account for all new individuals entering the population. The transition functions $w_{kj}(\boldsymbol{\alpha}(t))$ then determine the proportion of the new births that are assigned to environmental class j dependent on the environmental state.

The number of individuals recruited into life-stage i and environmental class j is equal to the number of individuals maturing out of life-stage $i-1$ that are assigned to environmental class j. Hence, for $i = 2, ..., n$ and $j = 1, ..., m$, $R_{i,j}(t) = \sum_{k=1}^{m} w_{kj}(\boldsymbol{\alpha}(t))M_{i-1,k}(t)$. Further, the number of individuals maturing out of life-stage i and environmental class j is equal to the number of individuals recruited into life-stage i and environmental class j one developmental period ago that survived. Denote the duration of life-stage i for individuals in environmental class j by $\tau_{i,j}$. Thus, $M_{i,j}(t) = R_{i,j}(t - \tau_{i,j})S_{i,j}(t)$ where $S_{i,j}(t)$ is the probability an individual in life-stage i and environmental class j survives to life-stage $i + 1$. Hence,

$$R_{i,j}(t) = \sum_{k=1}^{m} w_{kj}(\boldsymbol{\alpha}(t))R_{i-1,k}(t - \tau_{i-1,k})S_{i-1,k}(t) \tag{2.3}$$

for $i = 2, ..., n$ and $j = 1, ..., m$ where $S_{i,j}(t) = \exp\left\{-\int_{t-\tau_{i,j}}^{t} \delta_{i,j}(t')dt'\right\}$. Although in this formulation of the framework the stage duration $\tau_{i,j}$ is kept constant an extension to variable stage duration is also possible (Nisbet, Gurney, 1983; Ewing et al., 2016).

The exact form of the transition functions, $w_{kj}(\boldsymbol{\alpha}(t))$, is left unspecified as the way individuals transition from one environmental class and life-stage to the next is case specific. However, the choice of $w_{kj}(\boldsymbol{\alpha}(t))$ is subject to the constraints $0 \leq w_{kj}(\boldsymbol{\alpha}(t)) \leq 1$, $\forall j, k \in 1, ..., m$ and

$\sum_{j=1}^{m} w_{kj}(\boldsymbol{\alpha}(t)) = 1$. Although the transition functions are stage-independent, the environmental vector $\boldsymbol{\alpha}(t)$ is able to refer the state of each environmental cue independently and so can consider the sequence of past environments that an individual has encountered. A rigorous derivation of this framework from first principals is provided in Appendix A.

2.3.4 Some common simplifications

In some circumstances the complexity of the model can be decreased by reducing the number of environmental classes for developmental stages that do not express plasticity in response to environmental conditions. This is analogous to grouping technically distinct but functionally similar stages in a purely stage-structured model. Denote by $N_{i,\mathrm{Tot}}$ the total number of individuals in life-stage i over all environmental classes. Similarly define $R_{i,\mathrm{Tot}}(t),\ M_{i,\mathrm{Tot}}(t),\ D_{i,\mathrm{Tot}}(t)$ as the rates of recruitment, maturation, and death in life stage i respectively across all environmental classes. Assuming that the first instance of a cue inducing the expression of plasticity occurs in life-stage c there is no need to differentiate individuals prior to stage c. From stage c onwards individuals are differentiated by phenotype. It is then sufficient to describe the population dynamics as

$$\frac{dN_{i,\mathrm{Tot}}(t)}{dt} = R_{i,\mathrm{Tot}}(t) - M_{i,\mathrm{Tot}}(t) - D_{i,\mathrm{Tot}}(t) \qquad \text{for} \quad i < c \tag{2.4a}$$

$$\frac{dN_{i,j}(t)}{dt} = R_{i,j}(t) - M_{i,j}(t) - D_{i,j}(t) \qquad \text{for} \quad i \geq c \ \ j = 1, ..., m. \tag{2.4b}$$

Similarly, in the case that the expression of phenotypic plasticity ceases in life-stage c, as depicted in Figure 2.2D, the following formulation is appropriate

$$\frac{dN_{i,j}(t)}{dt} = R_{i,j}(t) - M_{i,j}(t) - D_{i,j}(t) \qquad \text{for } i \leq c, \;\; j = 1, ..., m \tag{2.5a}$$

$$\frac{dN_{i,\mathrm{Tot}}(t)}{dt} = R_{i,\mathrm{Tot}}(t) - M_{i,\mathrm{Tot}}(t) - D_{i,\mathrm{Tot}}(t) \qquad \text{for } i > c. \tag{2.5b}$$

These reduced forms of the model can be substantially less computationally demanding than the general model in the case that the reductions are appropriate.

2.4 Results

2.4.1 Nicholson's blowflies

To demonstrate the insights that can be gained from this framework it is applied to Nicholson's classical blowfly study (Nicholson, 1957), which aimed to describe how populations adjust in response to changes in their abiotic environment. In this study, the population dynamics of *Lucilia cuprina* (Wiedemann, 1830) were examined under different competitive conditions. In each culture, food was supplied separately to larvae and adults and both food supplies were replenished daily. Cultures were maintained for over two years and the number of adults and eggs present was recorded every two days. The results of Nicholson's study have been extensively discussed in theoretical ecology (Gurney et al., 1983; May, 1986; Bakker, 1963; Wood, 2010; Glyzin, 2018).

In Nicholson's experiment, blowflies experienced competition for food in their larval and adult stages. Competition for food between adult blowflies reduces fecundity if individuals cannot acquire enough protein to mature all their eggs (Vogt et al., 1985). Larval competition for food reduces adult body size and the probability of survival through the pupal stage (Jannicke Moe et al., 2002). For blowflies, body size is linearly related to the number of ovarioles an adult has (Vogt et al., 1985) which determines the maximum number of eggs the adult can

produce (Jannicke Moe et al., 2002), and so larval competition alters the maximum potential fecundity of adults. Using the terminology I have previously developed the intensity of larval competition for food resources can be considered as an environmental cue, altering maximum potential adult fecundity and through pupal stage survival through developmental plasticity. It is important to note that maximum potential adult fecundity is distinct from observed adult fecundity, the former representing the maximum number of eggs an individual could produce under ideal environmental conditions and the latter representing the actual number of eggs an individual produces under the environmental conditions that individual experiences.

In Nicholson's culture (reproduced in Figure 2.4A here), the daily larval food supply was kept constant, but the amount of adult food supplied was reduced from an "unlimited" amount to a more limiting 1000mg after around 600 days. The reduction of adult food resulted in an increased average adult population density, and the stabilisation of the previously regular population cycles. This is somewhat counter-intuitive, since a decrease in available resource substantially increased the average number of individuals and stabilised the previously regular oscillations - an example of the paradox of enrichment (Roy, Chattopadhyay, 2007).

Nicholson hypothesises that the population dynamics observed in the blowfly culture can be explained by phenotypic plasticity induced by larval competition. Adults in the period of unlimited adult food were observed to produce many eggs. When these eggs hatched into larvae, they experienced high levels of competition for larval food. This caused very few larvae to gain sufficient mass to pupate successfully, resulting in increased pupal mortality and low adult numbers in the next generation. When adult food was limited, an increase in adult competition resulted in fewer eggs being produced. The lower number of eggs resulted in fewer larvae and a larger amount of food being available per larva, subsequently reducing larval competition and juvenile mortality causing an increase in average adult population density. I evaluate evidence for Nicholson's hypothesis and heuristic arguments using the modelling framework derived here to represent phenotypic plasticity induced by resource competition in blowfly populations.

2.4.2 Application of model framework to represent phenotypic plasticity in Nicholson's blowflies

To formulate a model that represents phenotypic plasticity in blowfly populations I extend a previously derived mean-field model from Gurney et al. 1983, that considered only the instantaneous effects of adult competition on blowfly population dynamics which is described in Appendix B. Gurney's model is adapted to introduce reaction norms relating through pupal-stage survival (Jannicke Moe et al., 2002) and maximum potential fecundity (maximum number of eggs an individual could produce in conditions of excess adult food) (Webber, 1954), to the availability of larval food. As this is an example of developmental plasticity the model takes the form of Figure 2.2C.

Eggs are laid into a single egg class, within which all individuals express the same phenotype (i.e. there are no maternal effects). After a fixed developmental period, eggs hatch into a single larval class where again all individuals express the same phenotype. When a larva matures into a pupa, the amount of food that it obtained in the larval stage is determined by dividing the total food provided over the larval period by the number of individuals present in the culture over that period assuming scramble competition. The food obtained by an individual in the larval period is subsequently used to determine the traits that individual expresses as a pupa and as an adult.

For this model the previously introduced $N_{i,j}$ notation is abbreviated, dropping the i and replacing the N by a more descriptive letter reflecting the life-stage, for example, L is used for larvae and A for adults. Similarly, as adults are the only explicitly modelled life-stage that expresses phenotypic plasticity (pupae are implicitly modelled due to a lack of density dependence (Gurney et al., 1983)) the j subscript is dropped completely for terms relating to larvae. As only a single environmental cue is considered (larval food) the set of environmental classes, $\mathbf{\Omega_\alpha}$, consists only of the midpoints of $\alpha(t)$.

Denote by $L(t)$ the number of larvae at time t and by $A_j(t)$ the number of adults at time t in environmental class j. Associated with each environmental class are the maximum fecundity of

adults q_j, and survival through the pupal and juvenile stages S_{J_j}. Recruitment into the larval stage is denoted $R_L(t)$ and recruitment of larvae to adults in environmental class j is denoted $R_{A_j}(t)$. The environmental classes are parametrised by discretising an adapted reaction norm for through pupal-stage survival (Jannicke Moe et al., 2002) and a reaction norm for maximum adult fecundity is approximated from various sources (Webber, 1954).

As a proxy for the environmental cue, total protein obtained per larvae over the course of the larval period, I use the average protein available per larvae per day over the course of the larval period. Assume larvae divide the available food equally allowing the cue to be expressed as

$$\alpha(t) = \frac{K_L \tau_L}{\int_{t-\tau_L}^{t} L(s)ds}. \tag{2.6}$$

where K_L is the amount of larval food supplied daily, and τ_L is the duration of the larval stage. This is converted into a derivative for ease of computation, noting that in general the derivative of $f(v)^{-1}$ with respect to v is $-f'(v)/f(v)^2$ provided that $f(v)^{-1}$ satisfies the usual requirements. Hence by the Leibniz rule

$$\frac{d\alpha(t)}{dt} = \frac{-K_L \tau_L (L(t) - L(t-\tau_L))}{\left(\int_{t-\tau_L}^{t} L(s)ds\right)^2}.$$

This can then be simplified using the definition of $\alpha(t)$ such that

$$\frac{d\alpha(t)}{dt} = \frac{-\alpha^2(t)(L(t) - L(t-\tau_L))}{K_L \tau_L}.$$

The model can therefore be described through the equations

$$\frac{dL(t)}{dt} = R_L(t) - R_L(t-\tau_L)S_L - \delta_L L(t) \tag{2.7a}$$

$$\frac{dA_j(t)}{dt} = R_{A_j}(t) - \delta_A A_j(t) \quad \text{for } j \in 1, ..., m \tag{2.7b}$$

$$\frac{d\alpha(t)}{dt} = \frac{-\alpha^2(t)(L(t) - L(t-\tau_L))}{K_L \tau_L}. \tag{2.7c}$$

Recruitment terms are given by

$$R_L(t) = \left[\sum_{j=1}^{m} q_j A_j(t-\tau_E) e^{-A_{\text{Tot}}(t-\tau_E)/K_A} + I(t-\tau_E) \right] S_E \tag{2.8}$$

$$R_{A_j}(t) = \sum_{j=1}^{m} w_j(\alpha(t-\tau_P-\tau_J)) R_L(t-\tau_L-\tau_P-\tau_J) S_L S_{J_j} \tag{2.9}$$

for $j \in 1, ..., m$ where $I(t-\tau_E)$ is an inoculation term that begins the dynamics (Kot, 2001), and represents the introduction of larvae into the system at $t = 0$, and q_j and S_{J_j} are determined by the reaction norms. It is assumed that adults compete equally for the total available food regardless of phenotype, and so the instantaneous effects of adult competition are represented by $e^{-A_{\text{Tot}}(t-\tau_E)/K_A}$ where $A_{\text{Tot}} = \sum_{j=1}^{m} A_j$ indicates competition across all phenotypes. The transition function $w_j(\alpha(t))$, determines the fraction of individuals entering environmental class $A_j(t)$ at time t, and is defined

$$w_j(\alpha(t)) = \begin{cases} 1, & \text{if } g(\alpha(t)) = \alpha^j \\ 0, & \text{otherwise,} \end{cases} \tag{2.10}$$

for $j \in 1, ..., m$. This choice of $w_j(\alpha(t))$ restricts recruitment of individuals into a single environmental class based on that individual's experience of previous larval competition and indicates

that maximum adult fecundity is uniquely determined by past experience of larval competition. This restriction is appropriate, as due to the assumption that all food is split equally, larvae being recruited at time t will have identical experiences of larval competition over the duration of the larval period, and so will express the same traits. Further, I assume that this developmental plasticity is irreversible. Although this choice of $w_j(\alpha(t))$ precludes microenvironmental variation this could be incorporated through a different choice of transition function.

The system is initialised with 9500 larvae at $t = 0$ with history for $t \leq 0$ given by $L(t) = 9500$, $\alpha(t) = K_L/9500$, $A_j(t) = 0 \ \forall j \in \{1, ..., m\}$. Steady-state analysis for this system is provided in Appendix C. The model was simulated in R (R Core Team, 2022) using the package PBSddesolve (Couture-Beil et al., 2019). The code used produce the results that follow can be found at the following repository, `https://zenodo.org/record/5078430#.ZCsj8HbMKUk`.

2.4.3 Model parametrisation

To parametrise the environmental classes empirically derived reaction norms are selected for both q, and S_J. The through pupal stage survival, S_J, is calculated using an adapted version of the functional response parametrised in Moe et al. (2002). This functional response represents the survival rate through the pupal stage when there were x individuals at the beginning of the larval stage provided with $20,000$ mg of larval diet every two days. This is presented as a logistic quadratic regression of the form

$$G(x) = \ln\left(\frac{S_J(x)}{1 - S_J(x)}\right) = v_1 + v_2 \ln(x) + v_3 \ln(x)^2 \tag{2.11}$$

where v_1, v_2, and v_3 are fitted coefficients the values of which can be found in Table 1. This can equivalently be expressed as

$$S_J(x) = \frac{e^{G(x)}}{1 + e^{G(x)}}. \tag{2.12}$$

In the Nicholson culture, food was supplied daily, but in the Jannicke Moe et al. (2002) culture food was supplied every two days. It is assumed that the $20,000$ mg of food every two days provided in the Moe et al. culture is approximately equivalent to a supply of $10,000$ mg of food every day. Further, the amount of larval food supplied in the Nicholson culture accounts only for protein supplied in the form of ground liver. In the Nicholson experiment this was the only limited resource with other necessities such as water being "provided in excess". The experiment by Moe et al. also provided an excess of non-protein resources, limiting only the protein supplied to larvae. However, the food supply reported in Moe et al. accounts for both protein and non-protein resources. The diet provided for the larvae was a mix of 800 ml of water, 50 g of yeast, 20 g of agar, and 200 ml of horse blood per kg of diet. In this diet the main source of protein is the 200 ml of horse blood, which is proportionally around 19% of the diet. Thus, of the allotted daily diet only around $2,000$ mg was a source of protein.

The functional response presented in the Moe et al. experiment is in terms of initial larval density when provided with a set amount of food. As the environmental cue, $\alpha(t)$, is average protein available per larvae per day, this must be converted to a larval density as if the larvae had been provided with the Moe et al. diet. After these alterations the functional response becomes

$$S_J(\alpha(t)) = \frac{e^{G\left(\frac{K_L}{5\alpha(t)}\right)}}{1 + e^{G\left(\frac{K_L}{5\alpha(t)}\right)}}. \tag{2.13}$$

The form of this reaction norm is shown in Figure 2.3A for different fixed values of $\alpha(t)$.

The plastic trait maximum fecundity of adults, $q(\alpha(t))$, depends on the average protein available per larvae per day, the same environmental cue as S_J. The values $q(\alpha(t))$ takes are calculated

from the study Webber (1954) and is defined as

$$q(\alpha(t)) = h_1(h_2 \ln(\alpha(t)) - h_3)^{h_4} \tag{2.14}$$

where h_1, h_2, h_3, and h_4 are fitted coefficients the values of which can be found in Table 1.The form of this reaction norm is shown in Figure 2.3B for different fixed values of $\alpha(t)$.

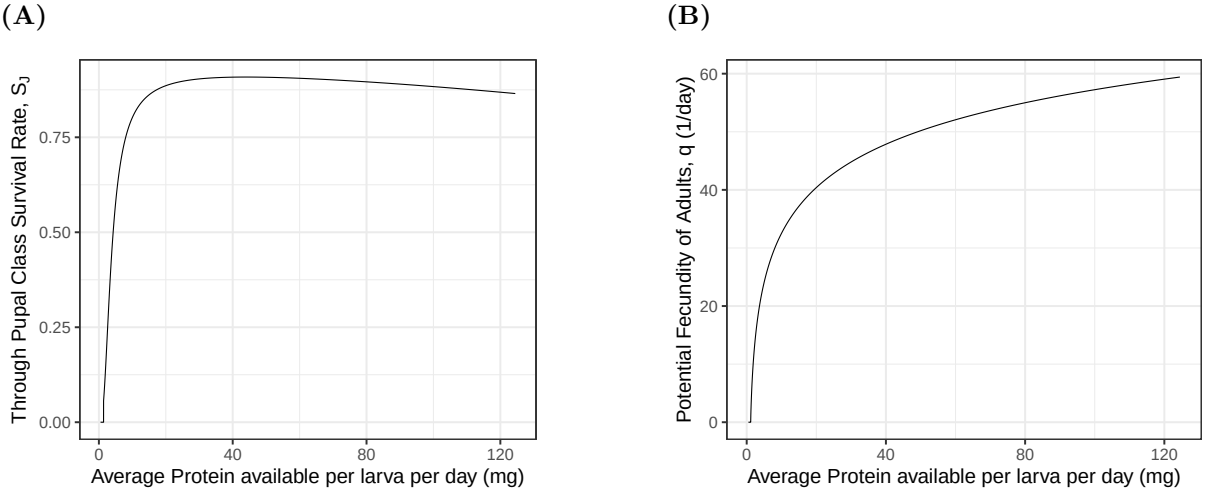

Figure 2.3: (A), The reaction norm used to determine through pupal stage survival according to the amount of protein available per larva per day as calculated by Equation (2.13) for fixed values of food per larvae per day. **(B)**, The reaction norm used to determine maximum fecundity of adults according to the amount of protein available per larva per day as calculated by Equation (2.14) for fixed values of food per larvae per day.

To complete the parametrisation of the model it is left to specify the discretisation of the environmental cue and consequently the midpoints of the intervals of the discretisation used to determine the plastic-trait values. Begin by discretising the environmental cue the average protein obtained by larvae over the course of the larval period, $\alpha(t) \in [0, \infty)$, into m intervals. The end points of the discretisation are given by $p_1 = 0$, $p_{m+1} = \infty$, and

$$p_j = \exp\left\{(j-1)\frac{4.82}{m-1}\right\}, \text{ for } j \in \{2, ..., m\}.$$

The points of the discretisation are on a logarithmic scale to capture the regions of the reaction norms that undergo the most rapid change. In Readshaw, Cuff (2006) it was found that there was no change in the traits blowflies express according to larval food after $\alpha(t) = 124$ and so $p_{m+1} = \infty$ and $p_m = 124$. This creates a catch-all environmental class for larval food conditions beyond the maximum. The midpoints of these intervals are defined

$$\alpha^k = \frac{p_{k+1} + p_k}{2} \quad \text{for } k \in \{1, ..., m\}.$$

Thus, the parameters for each environmental class are defined, $S_{J_j} = S_J(\alpha^j)$ and $q_j = q(\alpha^j)$. The definitions of the other non-plastic traits and parameter values can be found in Table 1.

Parameter	**Interpretation**	**Values**	**Parameter Source**
q_{max}	Maximum fecundity of adult blowflies $(\text{day})^{-1}$	59	Webber et al. (1995)
q_{min}	Minimum fecundity of adult blowflies $(\text{day})^{-1}$	0	Selected
τ_E	Duration of egg stage (days)	0.6	Gurney et al. (1983)
τ_L	Duration of larval stage (days)	5	Gurney et al. (1983)
τ_P	Duration of pupal and juvenile stages (days)	10	Gurney et al. (1983)
δ_L	Per capita mortality rate of larvae $(\text{day})^{-1}$	0.004	Gurney et al. (1983)
δ_A	Per capita mortality rate of adults $(\text{day})^{-1}$	0.27	Gurney et al. (1983)
S_E	Through stage survival probability of eggs $(\text{day})^{-1}$	0.959	Gurney et al. (1983)
S_L	Through stage survival probability of larvae $(\text{day})^{-1}$	0.980	Gurney et al. (1983)
K_A	Daily supply of adult food (mg)	$1,200,\ 2,000$	Nicholson (1957)
K_L	Daily supply of larval food (mg)	50000	Nicholson (1957)
v_1	Constant in functional response for S_J	-4.00	Moe et al. (2002)
v_2	Constant in functional response for S_J	3.36	Moe et al. (2002)
v_3	Constant in functional response for S_J	-0.44	Moe et al. (2002)
h_1	Constant in functional response for q	3.95	Webber (1954)
h_2	Constant in functional response for q	6.90	Webber (1954)
h_3	Constant in functional response for q	0.97	Webber (1954)
h_4	Constant in functional response for q	0.78	Webber (1954)
α_f	Lower threshold on environmental cue	1.4	Readshaw and Cuff (1980)
α_c	Upper threshold on environmental cue	124	Readshaw and Cuff (1980)
C	Initial condition	1000	Selected

Table 2.1: Table of parameters used in the phenotypically plastic blowfly model simulated in Figure 2.4A.

2.4.4 Simulating population dynamics in the Nicholson blowfly culture under experimental conditions

The model simulated under replica experimental conditions shows good qualitative and quantitative resemblance to experimental data from Nicholson's blowfly culture (Figure 2.4A), capturing the culture's dynamical behaviour before and after food limitation. Initially, when the adult food supplied was unlimited, the model predicts the regular population cycles observed in Nicholson's data. After the food was restricted to 1000mg at 610 days, the oscillations dampen, and the average population density substantially increases capturing the change in dynamical behaviour observed in Nicholson's culture. Although the population density of the simulated blowflies matches the experimental data the amplitude of the oscillations does not match. This mismatch can be explained by the high sensitivity of the model to food supply, a discussion of which, accompanied by food supplies which correctly predict both amplitudes, is provided in Appendix D.

Initially, the population exhibits temporal cycles in the dominant phenotypes (Figure 2.4B and Figure 2.4C). In the time periods where no new adults are being recruited, the phenotypic composition of the pupal and adult population does not change, resulting in the flat regions of Figures 2.4B and 2.4C. After food restriction, the range of phenotypes expressed within the population is greatly reduced. Pupae and adults in this period belong to a group of closely related environmental classes of individuals with relatively low trait values. As there is no difference between the distributions of maximum fecundity and through pupal stage survival, hereafter only fecundity is discussed.

As the model extends a previously derived non-plastic blowfly population model by Gurney et al. it is natural to question whether the population dynamics observed in Figure 2.4A can be attributed to the non-plastic population model. To test this, the non-plastic blowfly model (described in Appendix B) is simulated under Nicholson's experimental conditions. The non-plastic model overestimates the average adult density in both food conditions, predicts a decrease in

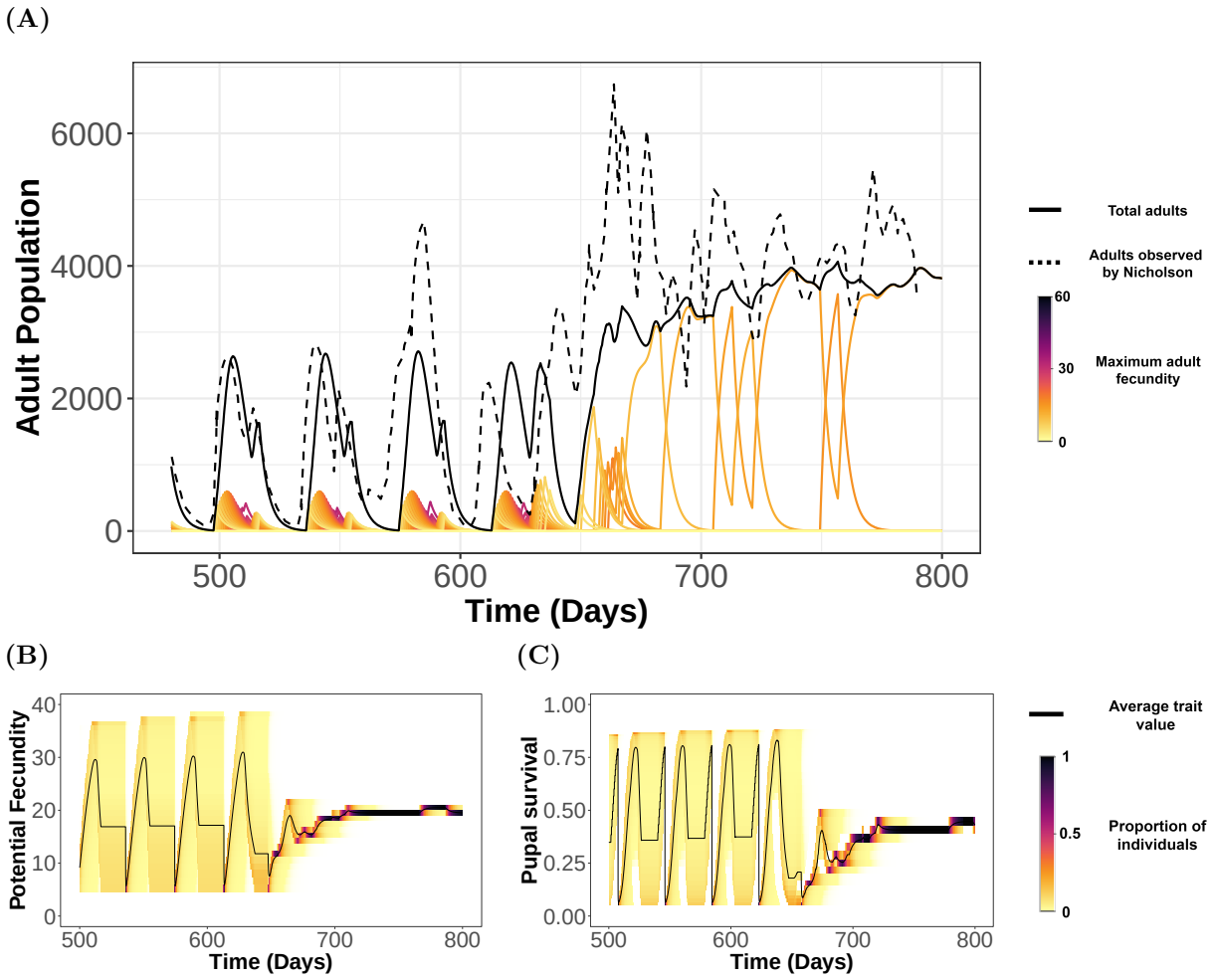

Figure 2.4: Simulation of the Nicholson blowfly culture data using the novel framework to represent phenotypic plasticity. In the culture adults blowflies were given unlimited food for 610 days, represented by $K_A = 2,000$mg, which converts to 1800mg of food supplied. After day 610 the amount of adult food supplied, K_A, was then reduced to $K_A = 1,200$mg, which converts to $1,000$mg of food supplied daily. **(A)**, Simulation of the new model which incorporates phenotypic plasticity. The number of environmental classes is $n = 64$ and each of the coloured lines represents the number of adults in an environmental class. In **(A)** the solid black line indicates the total number of adults over all environmental classes, while the dashed black line is the original data from Nicholson's culture. **(B-C)**, Change in the average value and distribution of the plastic-traits: potential fecundity and through pupal stage survival of the population simulated in Figure 2.4A.

adult density when resource availability decreases, and maintains the same population dynamics before and after the resource change as can be observed in Figure 2.5.

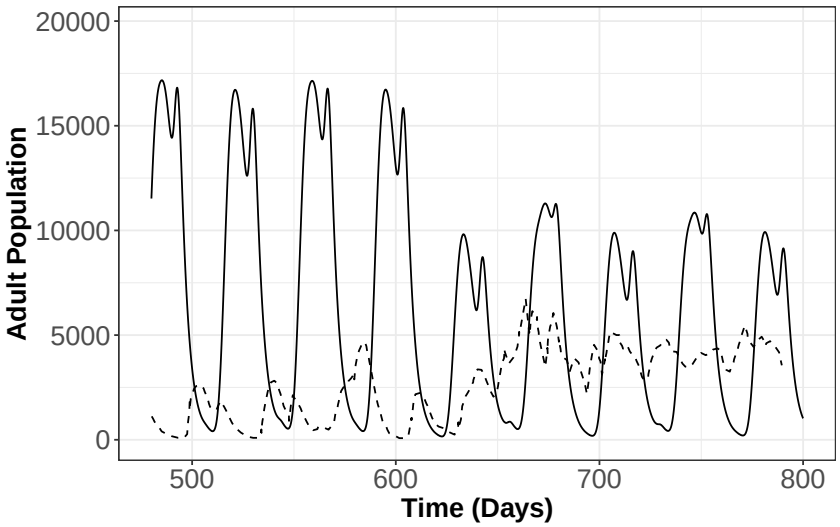

Figure 2.5: Simulations of a previously derived non-plastic blowfly model from Gurney et al. (1983) under experimental conditions with adult blowflies initially supplied with $K_A = 2,000$mg, which after day 610 is reduced to $K_A = 1,200$mg. The solid black line indicates the total number of adults, while the dashed black line is the original data from Nicholson's culture.

However, to fully determine how much of the behaviour observed in the phenotypically plastic model can be attributed to the behaviour of the non-plastic Gurney et al. (1983) model it is necessary to consider the behaviour of the non-plastic model over a wider range of food conditions. If the competitive release effect or shift in dynamical behaviour can be explained using the non-plastic model, this would indicate that phenotypic plasticity was not responsible for generating this effect. To test this the parameters, q and S_J in the Gurney model are varied. These parameters are the plastic-traits varied in the phenotypically plastic model and so by varying the values of these parameters in the non-plastic model insight is gained into how plasticity is altering the system's dynamics. I simulate the Gurney model both in the case $K_A = 1,200$mg, and the case $K_A = 2,000$mg. If for any values of q and S_J the maximum population density of the food unlimited population is less than the population density of the food limited population this would indicate the increase in population density observed in the

Nicholson blowfly culture can be explained using the non-plastic Gurney et al. formulation of the model. As can be seen in Figure 2.6, for no parameter values did the non-plastic model predict the food limited population being larger in size than the population with excess food. This suggests that the competitive release effect observed in the new phenotypically explicit model is generated by the inclusion of phenotypic plasticity.

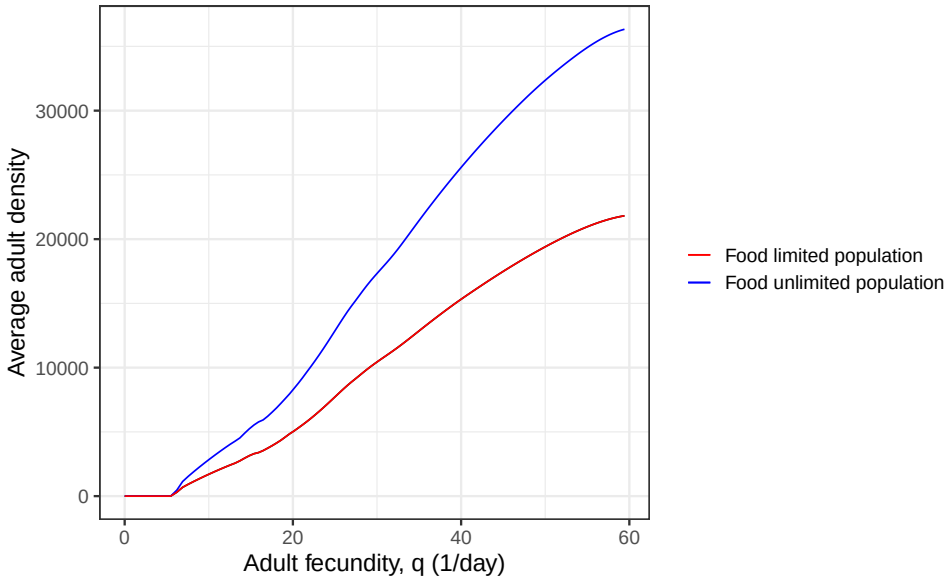

Figure 2.6: Comparison of the average adult densities observed in the Gurney et al. model in the case $K_A = 1,200$mg, and $K_A = 2,000$mg. Note that for no value of q does the average adult population density in the case $K_A = 1,200$mg exceed the average adult population density when $K_A = 2,000$mg.

2.4.5 Understanding the wider effects of phenotypic plasticity and population dynamic interactions

To explore how robust the population dynamics observed in the blowfly system are to conditions beyond those in Nicholson's experiment, the population trajectories are simulated for a wide range of possible combinations of adult and larval food supplies. For each food supply I calculate the average adult population density (Figure 2.7A), the average potential fecundity (maximum number of eggs an individual could produce in conditions of excess adult food, Figure 2.7B), the

average observed fecundity (the number of eggs an individual actually produces in the context of competitive pressures within the population, Figure 2.7C), and the difference between the average potential and observed fecundities (Figure 2.7D).

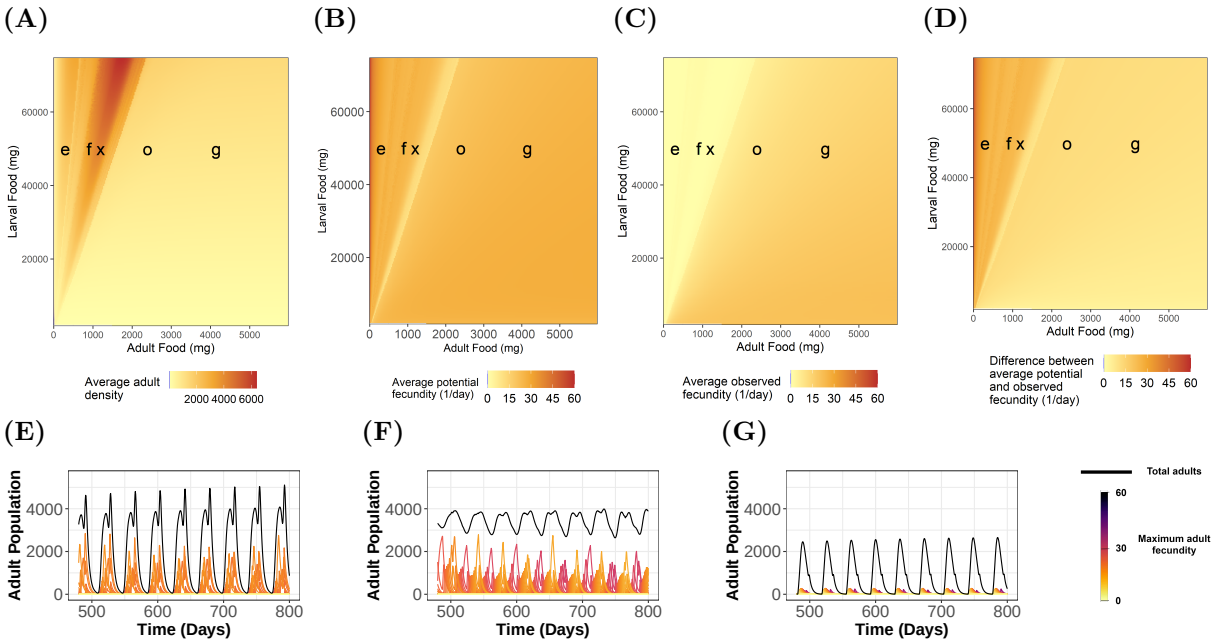

Figure 2.7: **(A-D)**, Results of varying the adult and larval food supplied to a blowfly culture. The parameter values for the limited food scenario $K_A = 1,200$mg are indicated by the black **x** and those for the unlimited food scenario, $K_A = 2,000$mg are indicated by the black **o**. **(A)**, Average adult density for different amounts of larval and adult food supplied. **(B)**, The average potential adult fecundity (the maximum number of eggs an individual produces on average in conditions of excess adult food) for different amount of larval and adult food supplied. **(C)**, The average observed fecundity (the average number of eggs an individual actually produces in the context of competitive pressures within the population, Figure 2.7C) of adults for different amounts of larval and adult food supplied. **(D)**, The difference between the maximum and observed fecundity of adults. **(E-G)**, Examples of simulations of the blowfly model. The larval food provided is $K_L = 50000$mg in each simulation and the adult food has been selected such that the average potential fecundity trait is 25, $K_A = 351$mg, $K_A = 901$mg and $K_A = 4151$mg, respectively.

The model predicts that the blowfly population exhibits one of three dynamical behaviours. In the leftmost region of Figures 2.7A-2.7D, increases in larval food supply do not change the abundance or fecundity (potential or observed) of adults. This suggests that in this region the population is limited most by the amount of adult food available. The population in this region

consists of a small number of phenotypes with similar trait values (c.f. the small range of colours in the lines representing the abundance of individuals in each environmental class in Figure 2.7E and point (e) in Figures 2.7A-2.7D). In the rightmost region of Figures 2.7A-2.7D, increases in adult food supply do not change the abundance or fecundity of adults, suggesting that availability of larval food is a limiting factor. The phenotypes expressed within the population are more diverse and the population's phenotypic composition changes during the course of a population cycle (c.f. the larger range of coloured lines in Figure 2.7G and point (g)). In the central region (the dark segment in Figure 2.7A), increases in either adult or larval food supply change the abundance and fecundity of adults. The adult population exhibits dampened oscillations and a small number of phenotypes with low trait values (Figure 2.7F and point (f)). This suggests that in this region the population is limited by the availability of both larval food and adult food. This shows that the balance of resource availability between adult and larval blowflies governs the dynamical behaviour of the blowfly population. The population dynamics are therefore characterised by the interaction between the two sources of density dependence: the instantaneous effects of adult competition and the delayed effects of larval competition through developmental plasticity.

Nicholson observed that when a culture initially supplied with 50g of larval food was supplied with 1g of adult food that "the oscillation [of the blowfly population] was comparatively slight and had lost almost all evidence of periodicity, whereas any appreciable departure from the rate of one gram of ground liver per day in either direction resulted in the increase in the amplitude of oscillation." The model predicts that when a population with a low adult food supply is supplied with increasingly more adult food that there is a sharp rise and then fall in average adult density as observed in Figure 2.7A. Similarly, when a population with a relatively low larval food supply is provided with increasingly more larval food, a similar sharp rise and fall in average adult density occurs. The behaviour Nicholson describes is precisely the behaviour that this model predicts, demonstrating that phenotypic plasticity is a mechanism by which the paradox of enrichment can be reconciled.

The predictions the model makes about the link between traits expressed by individuals and population responses are somewhat counter-intuitive and would be difficult to anticipate from reaction norms alone. From consideration of only reaction norms it would be reasonable to predict that individuals are most reproductively successful when potential fecundity is high. However, in Figures 2.7B-2.7D it is seen that the food conditions that produce individuals with the highest average potential fecundity are also those that prevent this from being exploited and are associated with low average observed fecundity and consequently low reproductive success. By comparison, conditions that produce individuals with low average potential fecundity allow those individuals to achieve this potential, meaning that individuals in these conditions are on average more reproductively successful despite their lower trait value. Therefore, the relative contribution of high and low trait-valued individuals to the intensity of future larvae competition changes dynamically according to the environmental conditions the population is subject to. This demonstrates that the seemingly reasonable assumption made from the reaction norm alone, that high trait value corresponds to high reproductive success, does not hold (Reed et al., 2013).

Individuals with traits that are indicative of high individual performance, such as average potential fecundity and average observed fecundity, arise from environmental conditions where the population is least abundant and most unstable. When average observed fecundity is highest (rightmost regions of Figures 2.7A-2.7D) population density is lowest. Conversely, when the population density is highest, and the oscillations are damped (central regions of Figures 2.7A-2.7D), the average observed fecundity is low, and the average potential fecundity is at a minimum. This shows that over most food conditions average potential fecundity and average observed fecundity are poor predictors of individual and population success. Even when average trait value is a good predictor of observed fecundity (rightmost region of Figures 2.7A-2.7D) the population's dynamics are regulated by phenotypic plasticity and so would be misrepresented by an approach that uses averaged trait values. Conversely, when average trait value is a bad predictor of fecundity (leftmost regions of Figures 2.7A-2.7D) an averaged trait approach correctly predicts the

population dynamics (as can be observed by comparing Figure 2.5 to Figure 2.7E).

The food amounts supplied in the simulations shown in Figures 2.7E-2.7G were selected to produce populations with the same average potential adult fecundity. Despite each population sharing the same average trait value, each population exhibits distinct dynamics and trait distributions which would be overlooked by an approach using averaged trait values. Only by accounting for trait variation between individuals arising from the cumulative effect of each individual's experience is it possible to capture the population level effects of these three scenarios. This highlights the need to consider the individual and population level consequences of phenotypic plasticity in a unified framework akin to what is derived here.

2.5 Discussion

I demonstrate that the interaction between phenotypic plasticity in individuals and population level effects can be a source of rich population dynamical phenomena. The disconnect between individual and population performance demonstrated in the example of Nicholson's blowflies, although certainly not universal, provides a mechanistic explanation of how pressures that are maladaptive for individuals can be beneficial for populations and *vice versa* (Reed et al., 2013; Edelaar, Bolnick, 2019; Weiner et al., 2017; Louthan et al., 2013). By representing the mechanisms by which individual variation and population level processes interact, insight is generated into how populations adapt to changing environments, which is crucial for understanding phenomena such as ecological tipping points (Dakos et al., 2019). Further, these findings support numerous previous studies proposing that failure to represent the effects of individual variation on populations is more consequential than simply mis-estimating demography (Bolnick et al., 2011; Violle et al., 2012; Sgrò et al., 2016; Lloyd-Smith et al., 2005), as it is demonstrated that patterns in individual variation can drive complete changes in the dynamical behaviour of the system being considered. This is corroborated by observational studies where it has been found that the response of populations to interventions was influenced by individual variation

(Cameron, Benton, 2004; Cameron et al., 2013). The framework is broadly applicable to systems where interaction between population dynamics and trait is important in determining the outcome of a process of interest. For example, when considering insect vectors of diseases or crop pests (e.g. mosquitoes or locusts) both abundance and trait to interact to determine the health or economic risk posed (Chandrasegaran et al., 2020; Sword et al., 2010).

Developing the model for Nicholson's blowflies was considerably simplified as I consider a well-studied model organism under controlled laboratory conditions. Although reaction norms are widely available across a broad range of taxa, outside of laboratory settings additional sources of environmental variation require the inclusion of reaction norms of higher dimension (i.e. a reaction norm considering the effect of temperature and con-specific density on development rate). However, the framework is designed to represent complex systems and so this should not pose an obstacle to implementation (see Appendix E for examples of how to represent other forms of phenotypic plasticity). For species where particular environment-trait relationships are not fully quantified or are missing entirely, due diligence must be observed in determining how sensitive the dynamics are to these uncertainties. For example, reaction norms are often most uncertain at environmental extremes (Brady et al., 2013) and so this uncertainty would need careful consideration when using the framework to predict dynamics at population range limits.

Individual variation is shown to change and be changed by population processes, but it is not predicted when trait variation alters the outcome of these processes. In invasion biology, metrics derived from reaction norms are often used to predict the competitive viability of native and invasive species (Richards et al., 2006a). Although the approach of using reaction norms directly accurately predicts the success of some invasive species (Luo et al., 2019; Knop, Reusser, 2012), it fails to explain the success of others (Muth, Pigliucci, 2007). This inconsistency limits the usefulness of reaction norms as a general predictor of a species invasiveness (Hulme, 2008; Palacio-López, Gianoli, 2011). Here, it is demonstrated that if one directly compares reaction norms without also considering a greater ecological context, one may arrive at erroneous conclusions. Therefore, it is important to determine more generally when reaction norms alone

are sufficient to predict population dynamics and in doing so reconcile the role of phenotypic plasticity in biological invasions and population biology.

Chapter 3

Predicting the population and trait dynamics of *Ae. albopictus* over a global range

3.1 Abstract

The current rapid increase in the incidence of vector-borne disease, driven by anthropogenic factors, is a growing threat to global public health. A thorough understanding of vector ecology will be critical for implementing successful control and surveillance campaigns. However, in current models the response of transmission critical vector traits to environmental variation is simplified, and this may lead to mis-estimation of the risk posed by vector-borne disease. Here, I develop a population model for the invasive dengue vector *Aedes albopictus* that uses mechanisms of individual variation to predict how transmission critical traits will respond to environmental variation. This model is validated against data from field populations across the global range of the species and demonstrates excellent predictive ability across broad environmental gradients. Mean-field models are shown to lack this generalisability, demonstrating the need to reconsider how trait variation is accounted for in predictions of vector population dynamics.

3.2 Introduction

The rapid global invasion of *Ae. albopictus* has been facilitated by the extraordinary ecological plasticity displayed the species across its geographical distribution (Paupy et al., 2009). Between climates the population dynamics expressed by *Ae. albopictus* change substantially, and this alters the ability of these populations to vector disease. In temperate regions populations display strong seasonality in adult abundance, and consequently there is only a short period of time over which disease can be vectored (Carrieri et al., 2011). By contrast in tropical regions adult activity can be maintained all year round, and variation in abundance appears to vary primarily with precipitation (Haramboure et al., 2020; Rozilawati et al., 2007). In between these two extremes are a diverse range of intermediary dynamical behaviours that even in the same location can vary substantially between years (Willis, Nasci, 1994; Xia et al., 2018). To understand the current risk posed by populations of *Ae. albopictus* across its global range it will be necessary to identify the mechanisms that drive this variability.

Niche-based distribution models have found that the niche occupied by *Ae. albopictus* in its invaded range appears to have shifted from the niche it occupies in the native range in Southeast Asia (Medley, 2010). One explanation proposed for this shift in niche is that different vector populations have different genetic structures, a factor that is known to change the vectoriality of tick populations, and of *Anopheline* mosquito species (McCoy, 2008; Fontenille, Simard, 2004). However, investigations into the genetic structure of *Ae. albopictus* populations around the globe have found an apparent lack of structure between vector populations across the species range, attributing much of the variation observed to human-mediated introductions rather than adaptation (Latreille et al., 2019).

Environmental variation has a complex and multi-faceted effect on the population dynamical processes of mosquito species, and these cannot be captured solely through association (Purse, Golding, 2015). However, despite the theorised importance of interactions between environmental variables, trait expression, and population dynamics, explicit mechanisms of individual

variation are generally omitted in the current models predicting transmission risk (Cator et al., 2020). It is common to implicitly make broad simplifying assumptions about how environment acts on trait expression, representing mechanisms of trait variation either through instantaneous responses to the current climate or omitting them wholly. For example, although variation in adult longevity is incorporated into predictions of the risk posed by mosquito populations, it is assumed that this trait varies only in response to the current environmental conditions experienced by adult mosquitoes (Metelmann et al., 2021; Mordecai et al., 2017). This implicitly assumes that all individuals have experienced the same historical environmental conditions regardless of their actual experience of the environment through development and therefore the effect of intraspecific variation is overlooked (Violle et al., 2012). For mosquito populations this reduces the dynamic trait structures that are observed in the field to a single population average that cannot account for the population's historic environmental experience nor how this experience alters the ability of populations to vector disease (Willis, Nasci, 1994). When tailored for populations in specific environments mean-field approaches have proven successful and allow the attribution of environmental processes to population level responses (Ewing et al., 2016; Ewing, 2017; Ewing et al., 2021). However, mechanistic models are often applied over broad environmental gradients over which these assumptions are less appropriate and this may lead to a mis-estimation of disease risk.

The modelling framework developed in Chapter 2 and Brass et al. (2021) is designed to track the interaction between population and trait dynamics in response to environmental variation across developmental stages and between generations. This approach allows the attribution of population responses to specific mechanisms of individual variation, and therefore is ideal for determining how the trait dynamics of vector populations contribute to outbreak risk. Here, this approach is used to develop a stage-phenotypically structured population model for *Ae. albopictus*, an invasive mosquito species and major vector of dengue (Zhang et al., 2019). This species is an ideal and important candidate for understanding the effect of environmentally induced trait variation on disease risk since its wide global range means that its populations are

subject to a diverse range of environmental conditions. The dynamics exhibited by populations of *Ae. albopictus* across its range are very different, with populations in temperate locations exhibiting strong seasonality but those in more tropical climates active all year round (Carrieri et al., 2012; Haramboure et al., 2020). In field populations environmental variation shapes trait distributions and it is theorised that these differences alter the ability of these populations to transmit disease (Willis, Nasci, 1994; Suzuki et al., 1993). Despite predictions of broad suitability for the transmission of dengue by *Ae. albopictus* in much of the invasive range, outbreaks have so far been limited in size and distribution (Liu-Helmersson et al., 2016; Brady et al., 2012). It is my hypothesis that by accounting for the effect of environmental variation on the trait structure and population dynamics of *Ae. albopictus* both the population dynamics of the species across its range and the current patterns of disease incidence around the globe can be understood.

3.3 Methods

3.3.1 Model overview

The general framework developed in Chapter 2 is used to derive a model for *Ae. albopictus* to derive a model that represents the effect of developmental plasticity in adult trait in response to the environmental experiences of juveniles (Brass et al., 2021). Within the model individuals with different experiences of the past environment are grouped into different environmental classes which describe how this experience alters the traits they express now. By linking individual-level variation to population response the model predicts not only the population's dynamics but also the population's trait structure. As was demonstrated in Chapter 2 this approach is flexible and able to incorporate the effect, both instantaneous and delayed, of environmental stressors on multiple traits making it ideal for accounting for the complex life-history of *Ae. albopictus*.

The model considers the dynamics of a population of mosquitoes arising from a single waterbody of fixed dimension, taking as inputs only environmental variables from the location being

simulated and outputting predictions of population and trait (Figure 3.1). It is assumed that the water body only varies in response to changes in temperature, the accumulation of precipitation, and through evaporation of standing water and is otherwise identical in every respect between locations. Adult mosquitoes oviposit eggs either onto the surface of the water or around the sides of the habitat, with the proportion of eggs being placed around the habitat's sides increasing as water level decreases (Rey, O'Connell, 2014). The eggs placed into or around the water body express either a diapausing or non-diapausing phenotype which is determined by a maternal effect in response to falling temperatures and decreasing photoperiod (Lacour et al., 2015). The survival of eggs through the egg stage is assumed to be determined solely by temperature (Delatte et al., 2009). Initially all eggs develop at a temperature-dependent rate and are referred to as active eggs regardless of location in the habitat or phenotype expressed. Once development is complete, only eggs on the water's surface expressing the non-diapausing phenotype hatch into larvae with all other eggs transitioning into one of two dormancy classes. When eggs placed around the sides of the habitat finish development they enter egg quiescence, a form of irregular dormancy that allows persistence through dry periods (Diniz et al., 2017). Quiescence continues until the dormant egg is inundated by precipitation after which it immediately hatches if expressing the non-diapausing phenotype and transitions to the diapausing egg class otherwise. Egg diapause is a form of regular dormancy that allows eggs to withstand cold temperatures, and is the primary mechanism by which *Ae. albopictus* populations persist overwinter in temperate climates (Armbruster, 2016). Once development is complete, provided an inundation event has occurred if the diapausing egg is also quiescent, diapause eggs remain dormant until a critical temperature and photoperiod is reached after which they immediately hatch (Lacour et al., 2015).

Larval mosquitoes compete for available resources in the aquatic habitat and are assumed to develop at a rate determined by both the current temperature and the intensity of larval competition (Ezeakacha, Yee, 2019). The ecology of larval mosquitoes is complex, and to produce a coherent model with the data currently available it is necessary to make broad simplifying

assumptions about the life-history of larvae. I assume that all larvae are functionally identical regardless of larval instar or previous experience of dormancy during the egg stage and so consider only a single larval class (Poelchau et al., 2013). It is assumed that there is no interspecific competition either for resource or through predation and that the only intraspecific competition is from competition for resource and space (Marini et al., 2017; Mastrantonio et al., 2018). Available resource is assumed to be consumed in its entirety and to be replenished daily, representing the product of temperature-dependent metabolic processes in the larval environment. Once larval development is complete pupation begins with the development of pupae assumed to depend solely on temperature (Delatte et al., 2009). The container habitats that *Ae. albopictus* prefers are generally small and vulnerable to flushing, a process whereby the body of water overflows and individuals are swept away, and drying out (Dieng et al., 2012). To represent flushing whenever the height of the water in the habitat exceeds the height of the container and rainfall is sufficiently intense an increase in the mortality of larvae and pupae occurs, and when the container dries out all non-quiescent juveniles die out.

Adult mosquitoes experience developmental plasticity in response to their experience of temperature and intraspecific competition as larvae (Yoshioka et al., 2012). This is represented by tracking each individual's experience of the environment through development and using this to determine the traits that individuals express as adults. Specifically, each individual's experience of the average temperature and the average food available per larvae per day over the course of the larval period is used to predict that individual's wing length, which is then used to determine the fecundity and longevity of that individual as an adult (Blackmore, Lord, 2000). Both fecundity and longevity are then further modified by the current temperature (Delatte et al., 2009; Brady et al., 2014). The adult resources necessary to survive and complete the reproductive cycle, such as sugar and blood meals, are always assumed to be in excess and the model does not represent any effects of competition between adults (Bellini et al., 2014). The production of cold resistant diapausing eggs is triggered when falling temperatures and photoperiod reach a critical threshold (Lacour et al., 2015). A schematic representation of the model is shown

Figure 3.1.

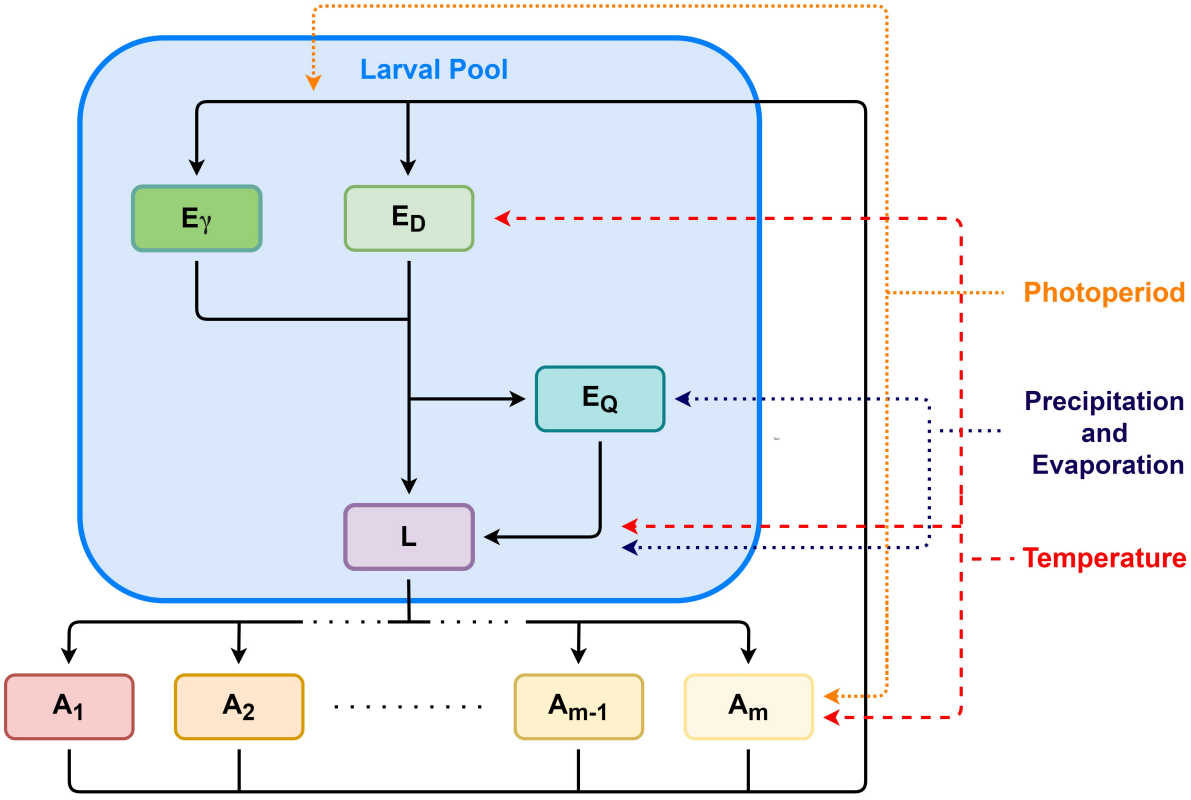

Figure 3.1: Schematic of the model used to represent the population dynamics of *Aedes albopictus*. I consider a stage structured model with three explicitly modelled life-stages, eggs, larvae, and adults with pupae only being represented implicitly. The model considers the dynamics of a population from a single water-body of fixed dimension with a water level that is dependent solely on precipitation and evaporation. Eggs are divided into three different classes, active eggs E_γ, diapausing eggs E_D, and quiescent eggs E_Q depending on the location they are placed in the pool (active/quiescent) and the phenotype they express (diapausing/non-diapausing). After hatching eggs proceed to the larval class where development depends on temperature, intraspecific density, and the food available per larvae per day which is assumed to relate to the amount of water accumulated in the habitat and the current temperature. Once larval development is complete larvae transition to the pupal class which is represented implicitly. Upon maturation to adulthood each individual's experience of its environment as a larva determines the traits that individual expresses as an adult through developmental plasticity. To represent this wing length is discretised into m environmental classes, with m sufficiently large to avoid the effects of discretisation, and assign to each a set of adult traits, with adults in the x^{th} environmental class denoted A_x.

3.3.2 Model details

The environment

Environmental variation is incorporated into the model through temperature, photoperiod, evaporation, and precipitation from the location in which the simulated population is situated. Meteorological data is sourced from the ERA5 climate reanalysis dataset (Muñoz Sabater, 2019). Climatic variables in this dataset are available at a 0.1°x0.1° resolution at an hourly time interval which is processed to represent either a daily mean temperature or the total accumulated precipitation and evaporation each day. For use in the model each environmental variable is extended to continuous time using splines, which were then tested against the climate data to ensure there were no errors in the interpolation. Splines were created using the function Spline1D from version 0.5.2 of the Dierckx package, a wrapper from the Fortran library of the same name (Dierckx, 1995).

The temperature at time t is denoted $T(t)$, and for simplicity I assume that the temperature of the larval pool and the air temperature are always the same (Paaijmans et al., 2010). Temperature is used throughout the model to instantaneously alter the traits expressed by individuals in each developmental stage. Temperature plays a further role in two more complex instances of phenotypic plasticity that are represented in the model. Specifically, an instance of developmental plasticity that uses the average temperature an individual experienced over the larval period in combination with the average amount of food available per larva per day to determine the wing lengths of emerging adults. Also included is a maternal effect where the temperature and the photoperiod at time t, denoted $\psi(t)$, determines the proportion of produced eggs that express diapausing phenotype. A combination of temperature and photoperiod subsequently determines when diapausing eggs are released from dormancy.

The total precipitation and evaporation each day, denoted $\rho(t)$ and $\epsilon(t)$ respectively are used to simulate the dynamics of the aquatic developmental habitat. The model simulates the dynamics of a single cylindrical water body with a surface area of μmm^2 and maximum volume of Vmm^3.

Throughout the subsequent analysis these parameters are kept constant across the range of locations considered and have been selected to be consistent with productive habitats observed in the field (Toma et al., 1982). Water accumulates in the habitat through precipitation, denoted $\rho(t)$, and leaves through both evaporation, $\epsilon(t)$, and overspill. Overspill occurs when the amount of water in the pool would exceed the pools volume, at which point any additional precipitation is not added to the pools total volume. If an overspill event happens concurrently with an intense period of precipitation a spike in mortality of the larval and pupal classes occurs, representing individuals being flushed away (Dieng et al., 2012). The total amount of water in the habitat on day t after all precipitation and evaporation can therefore be expressed by the series

$$W_t = min\left\{W_{t-1} + \mu(\rho(t) - \epsilon(t)), V\right\} \tag{3.1}$$

with initial condition such that the habitat is full at the start of the simulation, i.e. $W_0 = V$. This series for daily water level is then extended to continuous time using a spline, such that the water level at time t is denoted $W(t)$. Whenever $W(t) = 0$ the container has dried out and all non-quiescent juvenile stages (active eggs, diapausing eggs, larvae, and pupae) die-off. This parameter also governs the proportion of eggs produced that are quiescent and when they are released from dormancy.

Eggs

The number of active, quiescent and diapausing eggs present in the population at time t are denoted by $E_\gamma(t)$, $E_Q(t)$ and $E_D(t)$ respectively. Active eggs develop at a temperature-dependent rate, immediately hatching once development is complete if they are at or below the current water level and moving into the quiescent class otherwise (Delatte et al., 2009). Quiescent eggs remain dormant until inundated by precipitation after which they immediately hatch (Diniz et al., 2017). Diapausing eggs are cold resistant and are produced in response to a maternal

effect, they remain dormant until a critical temperature and photoperiod threshold is reached after which they immediately hatch (Lacour et al., 2015). In other *Aedes* species it has been demonstrated that adult body size is related to egg size and that larger egg sizes increase desiccation resistance (Steinwascher, 1984; Faull, Williams, 2015). Although weak effects of egg size on survival have been observed in *Ae. albopictus*, there is insufficient empirical data to justify the inclusion of such a function in this model. Therefore, it is assumed that the only maternal effect is whether an egg is active or diapausing (Sota, Mogi, 1992) .

For active eggs, I define $\tau_{E_\gamma}(t)$, $\delta_{E_\gamma}(t)$, $g_{E_\gamma}(t)$, and $S_{E_\gamma}(t)$ to be the stage duration, mortality rate, development rate, and through-stage survival proportion respectively with $\tau_{E_\gamma}(t) = 1/g_{E_\gamma}(t)$ and $\delta_{E_\gamma(t)} = -log(S_{E_\gamma}(t))/\tau_{E_\gamma}(t)$. The forms of the reaction norms used for egg survival and development were selected by fitting data to functional forms that have been used in previous models, trialling quadratic and Briere functional forms for the development rates, and quadratic and Gaussian functional forms for through stage survival with each functional form being truncated at a value close to 0 (Mordecai et al., 2017). Functional forms were fit using a weighted non-linear least squares approach and AIC was used for model selection, using the nls function in R (R Core Team, 2022). Further explanation of this fitting procedure along with both the code and life-history traits used to perform the fitting can be found in a repository at `https://zenodo.org/record/7796206#.ZCslmnbMKUk`. The parameter values are reported in Appendix J, and the data used perform this parametrisation was taken from a variety of sources (Delatte et al., 2009; Li lin et al., 2015; Li et al., 2021b; Blagrove et al., 2013; Calvitti et al., 2010; Mamai et al., 2019; Maamor et al., 2019; Zhang et al., 2015; Monteiro et al., 2007). The best fitting functional form for the development rate of active eggs was a quadratic with functional form

$$g_{E_\gamma}(T) = max\left\{\sigma_{11}T^2 + \sigma_{12}T + \sigma_{13}, 0.01\right\},$$

and the best model for the through stage survival of active eggs was a Gaussian with functional

form

$$S_{E_\gamma}(T) = \frac{\sigma_{21}}{\sigma_{22}\sqrt{2\pi}} \exp\left(-\frac{1}{2}\left(\frac{T-\sigma_{23}}{\sigma_{22}}\right)^2\right).$$

The result of this fitting is provided in Figures 3.2A and 3.2B respectively.

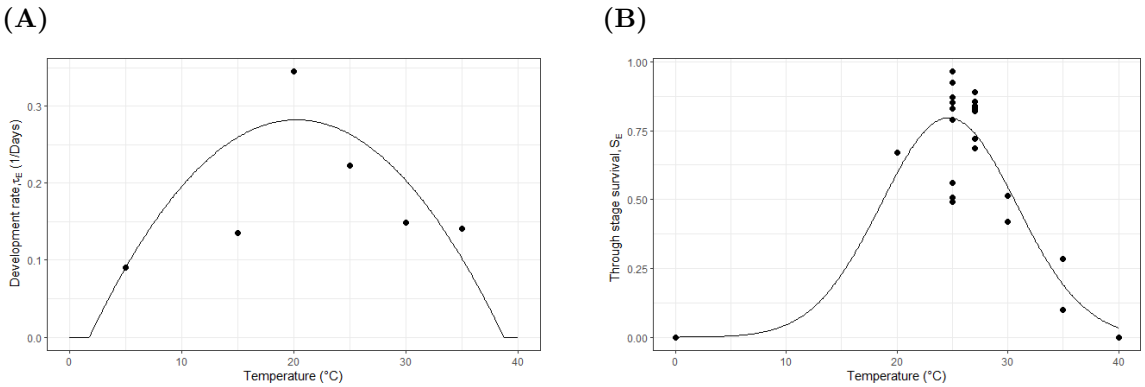

Figure 3.2: Reaction norms for active eggs, the black line is the model prediction and each point represents the data used to fit the model. **(A)** Development rate of active eggs, $g_{E_\gamma}(T)$. **(B)** Through egg-stage survival of active eggs, $S_{E_\gamma}(t)$.

Egg quiescence is a mechanism of irregular dormancy that ensures there is a reservoir of eggs able to persist through periods when the habitat has completely dried out (Diniz et al., 2017). After maturing out of the active stage a proportion of eggs are assumed to enter the quiescent egg class. The proportion of eggs that enter the quiescent class at time t is represented by the function $Q(t)$ which is defined

$$Q(t) = \begin{cases} \frac{V-W(t)}{V}, & \text{if } W(t) < W(t-1) \\ 0, & \text{otherwise.} \end{cases} \tag{3.2}$$

This function links the proportion of eggs that become quiescent to the height of the water in the container habitat. The condition $W(t) < W(t-1)$ ensures eggs only become quiescent if the

water level on day t is lower than that on day $t-1$. This choice of functional form ensures that when the habitat completely dries out, $W(t) = 0$, all eggs become quiescent upon maturation and so $Q(t) = 1$. As the water level rises a lower proportion of eggs enter the quiescent class until the habitat is completely filled, $W(t) = V$, and therefore $Q(t) = 0$. Within the quiescent egg class it is assumed that the same temperature-dependent mortality rate used for active eggs is suitable for quiescent eggs.

As egg quiescence is an irregular form of dormancy, maturation out of the quiescent class is triggered by inundation rather than the completion of development. This is represented through the function $h_Q(t)$, which describes the proportion of eggs that hatch out of the quiescent class at time t and is defined

$$h_Q(t) = \begin{cases} 1 - \frac{V - W(t)}{V} & \text{if } W(t) > W(t-1) \\ 0, & \text{otherwise.} \end{cases} \tag{3.3}$$

When the habitat is full, $W(t) = V$ and so $h_Q(t) = 1$, representing that when the habitat is completely filled all quiescent eggs are inundated and therefore should hatch immediately. The condition $W(t) > W(t-1)$ ensures that no eggs are released from quiescence when the water level at time t is lower than the water level at time $t-1$ and therefore no new eggs would become inundated.

Egg diapause is a mechanism of regular dormancy that allows the persistence of populations through cold winter months and is governed by a maternal effect (Lacour et al., 2015). The production of diapausing eggs is triggered by the exposure of adults to a critical photoperiod and temperature. This is represented in this model by the function $D(t)$, which describes the proportion of adults at time t that are producing non-diapause eggs and is defined

$$D(t) = \begin{cases} 1 - \frac{1}{1+15e^{((\psi(t,l)-\phi(l))}}, & \text{if } T(t) \leq 18, \text{ and } \phi(t) \leq \phi(t-1) \\ 1, & \text{otherwise} \end{cases} \tag{3.4}$$

with the functional form taken from Lacour et al. (2015) and where $\phi(l)$ is the critical photoperiod threshold required to induce the production of diapausing eggs in adults at latitude l defined

$$\phi(l) = 0.1|l| + 9.5$$

according to the relationship determined by Armbruster (2016). Emergence of eggs from diapause is triggered by the current environmental conditions exceeding a critical temperature and photoperiod threshold (Petrić et al., 2021). This is represented by the function $h_D(t)$ which immediately releases eggs from diapause once the environmental thresholds are reached which is defined

$$h_D(t) = \begin{cases} 1, & \text{if } T(t) \geq 12.5, \text{ and } PP(t) > \phi(l), \text{ and } \phi(t) > \phi(t-1) \\ 0, & \text{otherwise.} \end{cases} \tag{3.5}$$

The mortality rate of diapausing eggs is defined

$$\delta_{E_D}(t) = \begin{cases} 0.01, & \text{if } T(t) > -12 \\ 0.1, & \text{otherwise.} \end{cases} \tag{3.6}$$

Note in this case that when the temperature is below the thermal limit mortality is not absolute, a

decision which has been made due to evidence that diapausing eggs can withstand short intervals of low-temperature conditions (Thomas et al., 2012). This leniency ensures that a brief period of intense cold does not kill off whole populations whilst ensuring that sustained low temperatures remain unsuitable.

Larvae

Larval *Ae. albopictus* consume a range of bacteria, plants and detritus and both the time that larvae take to develop and the proportion of individuals that survive through the larval stage is assumed to depend on the intensity of intraspecific competition for resource in addition to temperature (Ezeakacha, Yee, 2019). To account for resource dynamics in the model requires the definition of how much resource is in the habitat at any time and how this is expected to vary. Accurately predicting how much resource is available for larval *Ae. albopictus* in a container habitat from climate data alone would be a significant undertaking for even a limited geographical range, but the model requires predictions that will hold globally. Resource dynamics are complex, and the amount of resource available in a container habitat varies with location, micro-climate, and community composition amongst many other factors that are not accounted for (Kulaš et al., 2021). Instead, I assume that the amount of food available in the container is temperature-dependent, proportional to the volume of water in the habitat and completely independent of location. The gross primary productivity of the larval habitat is then defined to be

$$F(t) = 10^{-6}\log_{10}(0.45 + 0.095T(t))W(t) + f_d \tag{3.7}$$

where the logarithmic term represents the products of respiration and the constant term, f_d, is a reservoir of nutrition from the decay of detritus (White et al., 1991). It is further assumed that larvae divide the available food equally and completely (i. e. scramble competition) (Gavotte

et al., 2009). The amount of food available per larvae per day, $\alpha(t)$, can therefore be expressed by

$$\alpha(t) = \frac{F(t)}{L(t)}.$$

The functions used to represent larval life-history processes are comprised of multiple components but are principally constructed from reaction norms for larval development rate, $g_L(T(t), \alpha(t))$, and through-stage survival independently of hydrological processes, $\hat{S_L}(T(t), \alpha(t))$. To fit the multi-dimensional reaction norms for larvae I use generalised additive mixed effect models (GAMMs) using the R package gamm4 version 0.2.6 and both the life-history data used to parametrise these reaction norms and the code to fit the models can be found in the repository `https://zenodo.org/record/7796206#.ZCslmnbMKUk` (R Core Team, 2022; Wood, Scheipl, 2020). I consider models that include different combinations of temperature, density, and an interaction term between the two variables. As the data used to parametrise these functions is sourced from laboratory experiments that used populations of *Ae. albopictus* from different origin locations and reared larvae on different diets these factors are included as random effects. For each life-history trait the model with the lowest AIC is selected, the result of which for larval development rate and through stage survival is shown in Figure 3.3 and the data used for this fitting was compiled from a variety of sources (Buckner et al., 2016; Calado, Navarro da Silva, 2002; Calvitti et al., 2010; Delatte et al., 2009; Giatropoulos et al., 2022b; Kamimurai et al., 2002; Li lin et al., 2015; Li et al., 2021a; Lima-Camara et al., 2022; Jong et al., 2017; Maamor et al., 2019; Mamai et al., 2019; Marini et al., 2020; Monteiro et al., 2007; Mori, 1979; Puggioli et al., 2017; Reiskind, Lounibos, 2009; Reiskind, Zarrabi, 2012; Riback et al., 2015; Russell, Cator, 2022; Sauers et al., 2022; Sultana, Tuno, 2021; Yoshioka et al., 2012; Zhang et al., 2015).

The through larval stage duration is defined, $\tau_L(T(t), \alpha(t)) = 1/g_L(T(t), \alpha(t))$, but the larval mortality term, $\delta_L(T(t), \alpha(t))$, takes a more complicated form to account for the dynamics of the container habitat and density dependence. The water level of the container habitat varies with

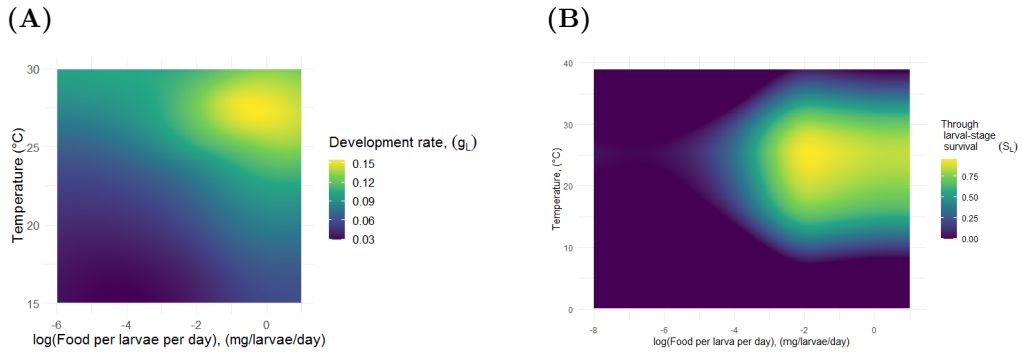

Figure 3.3: The reaction norms used to parametrise the larval stage. **(A)** The reaction norm linking larval development rate to temperature and the amount of food available per larva per day. **(B)** The reaction norm linking through larval stage survival to temperature and the amount of food available per larva per day.

evaporation and precipitation and this means spikes in larval mortality can be induced either through the habitat drying out or through the flushing of larvae when the habitat overflows. This is represented in the larval mortality rate by setting $\delta_L(t) = \delta_d$ whenever the habitat dries out, (i. e. $W(t) = 0$) and similarly setting $\delta_L(t) = \delta_f$ whenever the habitat overflows and the intensity of rainfall is sufficient to initiate flushing (i. e. $W(t) = V$ and $\mu\rho(t) > 0.5V$). The final component of the larval mortality function is an overcrowding term that increases the mortality of larvae when the larval density exceeds 3 larvae per ml according to a Gompertz function (Balestrino et al., 2014). High larval densities are unfavourable for survival, and the term is necessary in addition to the reaction norms to ensure that the fluctuating water level does not cause implausibly high larval densities (Leisnham et al., 2021). Therefore the expression for the mortality rate of larvae is defined

$$\delta_L(t) = \begin{cases} max\left\{\frac{-\log(\hat{S_L}(T(t),\alpha(t)))}{\tau_L(T(t),\alpha(t))} + \exp\left(-\exp\left(\frac{1-L(t)/3}{W(t)/1000}\right)\right), 1\right\}, & \text{if } 0 < W(t) \leq V \text{ and } \mu\rho(t) \leq 0.5V, \\ \delta_d, \text{ if } W(t) = 0, \\ \delta_f, \text{ if } W(t) = V \text{ and } \mu\rho(t) > 0.5V. \end{cases} \tag{3.8}$$

Pupae parameters

Pupal development rate and survival are assumed to depend solely on temperature as there is a lack of experimental data to quantify carry-over effects from larval stage. Denote these by $g_P(t)$ and $S_P(t)$ respectively and with the forms of the reaction norms defining these in Figure 3.4. These reaction norms are fitted using the same procedure described for the egg stage, with a Briere function best describing the relationship between pupal development rate and temperature with form

$$g_P(T) = max\left\{\sigma_{31}T(T-\sigma_{32})(\sigma_{33}-T)^{1/\sigma_{34}}, 0.01\right\}$$

and a quadratic function form for the relationship between through pupal stage survival and temperature independently of hydrological processes

$$\hat{S}_P(T) = max\left\{\sigma_{41}T^2 + \sigma_{42}T + \sigma_{43}, 0.01\right\}$$

parametrised using data from various sources (Briegel, Timmermann, 2001; Calvitti et al., 2010; Delatte et al., 2009; Jong et al., 2017; Kamimurai et al., 2002; Maamor et al., 2019; Monteiro et al., 2007; Reiskind, Zarrabi, 2013; Zhang et al., 2015).

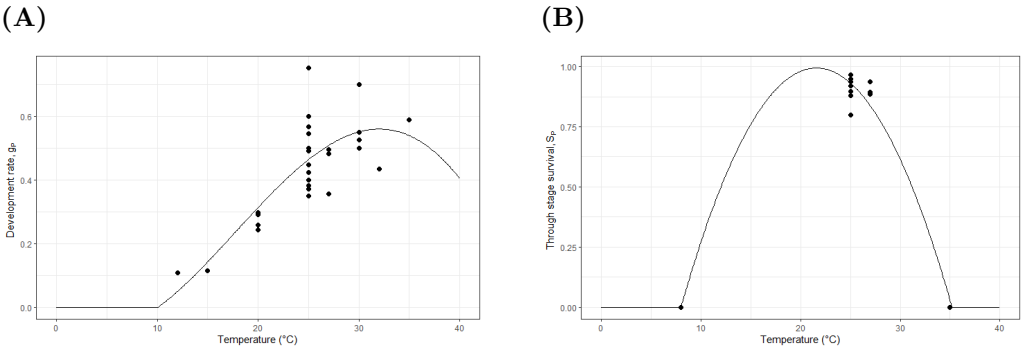

Figure 3.4: The reaction norms used to parametrise the pupal stage. **(A)** The reaction norm linking the duration of the pupal stage to temperature. **(B)** The reaction norm through pupal stage survival.

The survival and mortality parameters are modified as in the larval stage to induce mortality when $W(t) = 0$ and to account for flushing such that

$$\delta_P(t) = \begin{cases} \frac{-\log(\hat{S_P}(T(t)))}{\tau_P(T(t))}, & \text{if } 0 < W(t) \leq V \text{ and } \mu\rho(t) \leq 0.5V, \\ \delta_d, & \text{if } W(t) = 0, \\ \delta_f, & \text{if } W(t) = V \text{ and } \mu\rho(t) > 0.5V. \end{cases} \tag{3.9}$$

Adults parameters

Ae. albopictus experiences developmental plasticity in response to the temperature, food availability, and conspecific density experienced during juvenile development that contributes towards temperature-dependent mortality and fecundity of adults (Ezeakacha, Yee, 2019; Blackmore, Lord, 2000). This is included in the model by using an individual's experience of larval competition and temperature through development to predict the wing length that individual will express as an adult. This wing length is then used along with the current temperature to define the mortality rate of adults and the rate at which eggs are produced. This overlooks a known crowding effect whereby high densities of larvae inhibit development independently of competition for resource (Yoshioka et al., 2012). This assumption is necessary as much of the experimental data used to parametrise reaction norms does not control for larval density and food availability simultaneously and therefore this relationship cannot be included in the model. Also omitted are the effects of the availability of adult resource on the production of eggs, and other varied processes demonstrably important in the life-history of adults (Sultana, Tuno, 2021; Farjana et al., 2012). Using the same GAMM fitting procedure as described for larvae, I fit reaction norms for the wing length of emerging adults, as predicted by the average larval temperature and food available per larvae per day over the course of the larval period, $w_L(T_{avg}(t), \bar{\alpha}(t))$, and for the time until 50% adult mortality as predicted by wing length and

temperature, $\tau_{A_{50}}(w_L, T(t))$. The form of these functions can be seen in Figure 3.5 and are parameterised using laboratory data from a variety of sources (Alam, Tuno, 2020; Allgood, Yee, 2014; Alto, Juliano, 2001; Alto et al., 2005, 2015, 2008; Armbruster, Hutchinson, 2002; Bara et al., 2015; Black et al., 1989; Blagrove et al., 2013; Briegel, Timmermann, 2001; Calvitti et al., 2010; Costanzo et al., 2015, 2018; Deng et al., 2021; Ezeakacha, Yee, 2019; Farjana et al., 2012; Giatropoulos et al., 2022a; Jong et al., 2017; Li lin et al., 2015; Li et al., 2021b; Lima-Camara et al., 2022; Mamai et al., 2019; Marini et al., 2020; Mori, 1979; Muturi et al., 2011; Reiskind, Lounibos, 2009; Reiskind, Zarrabi, 2013; Riback et al., 2015; Russell, Cator, 2022; Sauers et al., 2022; Shahrudin et al., 2019; Sultana, Tuno, 2021; Sultana et al., 2021; Westbrook, 2010; Westbrook et al., 2010; Wiwatanaratanabutr, Kittayapong, 2006; Yee et al., 2012, 2017; Yoshioka et al., 2012; Zhang et al., 2015).

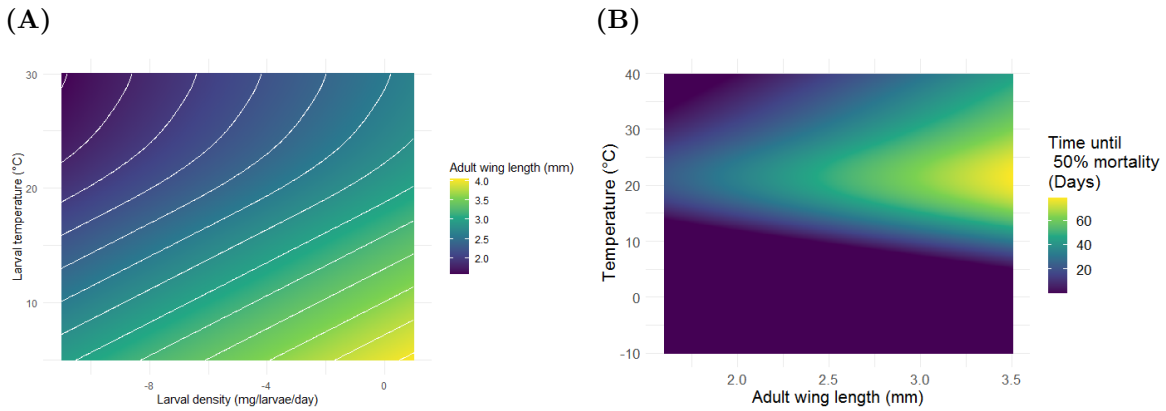

Figure 3.5: The reaction norms used to parametrise the adult stage. **(A)** The reaction surface linking historical experience of larval density and temperature to adult wing-length. **(B)**, The relationship between adult wing length the current temperature and adult longevity. This is converted into a mortality rate for use in the model.

In this framework the effects of developmental plasticity are represented by assigning each individual to an environmental class that reflects their experience of the environment through development. This is achieved by separating adults into m environmental-classes the wing length they are predicted to express based upon their experience of temperature and resource availability as larvae according to the function w_L. This is achieved by dividing the possible

wing lengths an adult could express, (w_{min}, w_{max}) into m equally spaced subintervals and denote by w_j the midpoint of the j^{th} sub-interval. Then define the function g such that $g(w) = w_j$ if $w \in \mathbb{R}$ is in the j^{th} subinterval of (w_{min}, w_{max}). To determine how much food was available for an individual maturing into adulthood at time t define

$$\bar{\alpha}(t) = \frac{\int_{t-\tau_P(t)-\tau_L(t-\tau_P(t))}^{t-\tau_P(t)} \frac{F(s)}{L(s)} ds}{\tau_L(t-\tau_P(t))}.$$

Then define the transition function, $w_j(T_{avg}(t), \bar{\alpha}(t)))$ such that

$$w_j(T_{avg}(t), \bar{\alpha}(t)) = \begin{cases} 1, & \text{if } g(w(T_{avg}(t), \bar{\alpha})(t)) = w_j \\ 0, & \text{otherwise} \end{cases}$$

for $j \in 1, ..., m$.

The fecundity of an individual expressing wing-length w is then given by

$$q(w) = 0.5 \exp^{\sigma_{51} + \sigma_{52} w}$$

noting that factor of 0.5 is required as only females produce eggs (Blackmore, Lord, 2000). The duration of a gonotrophic cycle is assumed to be temperature-dependent and to be the reciprocal of the biting rate. This is parameterised using a Briere function taken from taken from Mordecai et al. (2017) of the form

$$G(T(t)) = \frac{1}{max\{\sigma_{61} T(T - \sigma_{62})(\sigma_{63} - T)^{\frac{1}{2}}, 0.01\}}$$

from which the rate at which an individual with wing length w produces eggs at temperature $T(t)$ can be expressed. The rate at which adults in environmental class j produce eggs at time t is therefore defined

$$q_j(T(t)) = \frac{q(w_j)}{G(T(t))}.$$

Similarly, for individuals in environmental class j that express wing length w_j the mortality rate of adults is defined to be

$$\delta_{A_j}(T(t)) = \frac{-\log(0.5)}{\tau_{A_{50}}(w_j, T(t))}.$$

Population model

The model is defined

$$\frac{dE_\gamma(t)}{dt} = R_{E_\gamma}(t) - M_{E_\gamma}(t) - \delta_{E_\gamma}(t)E_\gamma(t), \tag{3.10}$$
$$\frac{dE_D(t)}{dt} = R_{E_D}(t) - M_{E_D}(t) - \delta_{E_D}(t)E_D(t), \tag{3.11}$$
$$\frac{dE_Q(t)}{dt} = R_{E_Q}(t) - M_{E_Q}(t) - \delta_{E_Q}(t)E_Q(t), \tag{3.12}$$
$$\frac{dL(t)}{dt} = R_L(t) - M_L(t) - \delta_L(t)L(t), \tag{3.13}$$
$$\frac{dA_j(t)}{dt} = R_{A_j}(t) - \delta_{A_j}(t)A_j(t), \text{ for } j \in 1, ..., m. \tag{3.14}$$

The variable delay terms are defined such that

$$\frac{d\tau_{E_\gamma}(t)}{dt} = 1 - \frac{g_{E_\gamma}(t)}{g_{E_\gamma}(t - \tau_{E_\gamma}(t))}, \tag{3.15}$$
$$\frac{d\tau_L(t)}{dt} = 1 - \frac{g_L(t)}{g_L(t - \tau_L(t))}, \tag{3.16}$$
$$\frac{d\tau_P(t)}{dt} = 1 - \frac{g_P(t)}{g_P(t - \tau_P(t))}. \tag{3.17}$$

The through stage survival terms are defined such that

$$\frac{dS_{E_\gamma}(t)}{dt} = S_{E_\gamma}(t)\left(\frac{g_{E_\gamma}(t)\delta_{E_\gamma}(t-\tau_{E_\gamma}(t))}{g_{E_\gamma}(t-\tau_{E_\gamma}(t))} - \delta_{E_\gamma}(t)\right), \tag{3.18}$$

$$\frac{dS_L(t)}{dt} = S_L(t)\left(\frac{g_L(t)\delta_L(t-\tau_L(t))}{g_L(t-\tau_L(t))} - \delta_L(t)\right), \tag{3.19}$$

$$\frac{dS_P(t)}{dt} = S_P(t)\left(\frac{g_P(t)\delta_J(t-\tau_P(t))}{g_P(t-\tau_P(t))} - \delta_P(t)\right). \tag{3.20}$$

Recruitment and maturation terms defined,

$$R_{E_\gamma}(t) = D(t)\left(\frac{\sum_{j=1}^{m} q_j A_j(t)}{G(t)}\right) + C(t), \tag{3.21}$$

$$M_{E_\gamma}(t) = \frac{g_{E_\gamma}(t)}{g_{E_\gamma}(t-\tau_E(t)}R_{E_\gamma}(t-\tau_{E_\gamma}(t))S_{E_\gamma}(t), \tag{3.22}$$

$$R_{E_D}(t) = (1-D(t))\left(\frac{\sum_{j=1}^{m} q_j A_j(t)}{G(t)}\right), \tag{3.23}$$

$$M_{E_D}(t) = h_D(t)E_D(t), \tag{3.24}$$

$$R_{E_Q}(t) = Q(t)(M_{E_\gamma}(t) + M_{E_D}(t)), \tag{3.25}$$

$$M_{E_Q}(t) = h_Q(t)E_Q(t), \tag{3.26}$$

$$R_L(t) = (1-Q(t-\tau_E(t)))(M_{E_\gamma}(t) + M_{E_D}(t)) + M_{E_Q}(t), \tag{3.27}$$

$$M_L(t) = \frac{g_L(t)}{g_L(t-\tau_L(t))}R_L(t-\tau_L(t))S_L(t), \tag{3.28}$$

$$R_{A_j}(t) = w_j(\alpha(t))\frac{g_P(t)}{g_P(t-\tau_P(t))}M_L(t-\tau_P(t))S_P(t), \text{ for } j \in 1,...,m, \tag{3.29}$$

and the transition functions defined

$$w_j(\alpha(t)) = \begin{cases} 1, & \text{if } \; g(\bar{\alpha}(t)) = \alpha^j, \; \text{ for } \; j \in 1, ..., m \\ 0, & \text{otherwise.} \end{cases} \tag{3.30}$$

The model dynamics are initiated with the initial conditions $E_D(0) = 100$, $E_\gamma(0) = E_Q(0) = L(0) = A_j(0) = 0$ for $j \in 1, ..., m$, $S_X(0) = \exp\{-\tau(T(0))\delta_X(T(0))\}$ for $X \in E, L, P$. With initial history such that for all $t \leq 0$, $R_X(t) = M_X(t) = 0$ for $X \in E, L, P, A$. The model was simulated in Julia version 1.8. using the package DifferentialEquations, and code that can be used to replicate these results can be found in the repository (Bezanson et al., 2017; Rackauckas, Nie, 2017).

3.3.3 Validations of the population dynamical model

The model is validated by comparing its predictions to the population and trait dynamics of field populations of *Ae. albopictus* from across the species range. The methodologies employed across the different field datasets used for validation are not standardised, having come from many different studies with different purposes. The studies in the validation dataset include collections of eggs from ovitraps, counts of larvae through dipping, full counts of both larvae and pupae, active and passive adult collection with a large selection of bait types including human landing collection, and wing length measurements in field and semi-field conditions. The spatial and temporal resolution of these datasets varies from observations from a single location every two months for a single year, to weekly average observations taken from large surveillance networks over many years. Between locations where field studies included in the validation set were conducted there are further differences in factors such as land-use type and the form and intensity of mosquito control programs that are not accounted for by the model. Given the great range in study designs considered I do not aim to use this field data to draw conclusions about how the model anticipates changes in absolute mosquito abundance between locations. Instead,

these datasets are used to assess how well the model predicts population dynamics and within dataset relative abundances.

In many locations it is necessary to compare the model's predictions of the number of eggs within the population to the number of eggs that have accumulated in ovitraps over a number of days. Therefore I convert the predictions of the number of eggs present in the population at time t to the number of eggs that would be collected in an ovitrap given the dynamics of the population that are predicted, a quantity which is termed oviposition activity. For a study with a sampling period of τ_{sample} the number of individuals that would collect in an ovitrap sampled at time t is given by

$$OA(t) = \begin{cases} \sum_{i=1}^{\tau_{sample}} \sum_{j=1}^{m} \frac{q_j A_j(i)}{G(i)} - \frac{q_j A_j(i-\tau_E(i))}{G(i-\tau_E(i))} \text{ if } \tau(E(i)) < \tau_{sample}, \\ \sum_{i=1}^{\tau_{sample}} \sum_{j=1}^{m} \frac{q_j A_j(i)}{G(i)} - \frac{q_j A_j(i-\tau_{sample})}{G(i-\tau_{sample})}, \text{ otherwise.} \end{cases} \tag{3.31}$$

When studies in the validation dataset did not explicitly report the number of mosquitoes collected in the field the relevant data has been extracted from graphs using WebPlotDigitizer (Rohatgi, 2022). How well the predicted dynamics correspond to those observed in the field population is quantified using R^2 as a measure of goodness of fit. As both the field studies and the model only reflect relative abundance I uniformly apply a scaling factor to the model's predictions, further, as the precise time of sampling is often ambiguous I also allow a uniform time-shift on the date of observation by up to half of the interval between samples. The scaling factor and time-shift pair are selected by trialling a range of possible values and retaining the pair that produces the maximum R^2. I specifically seek the scaling factor, $s_f \in \mathbb{R}$ and time shift $t_s \in \mathbb{I}$ such that for field observations y_i reported at time t_i and model estimates $\hat{y}_i$ made at time $t_i + \hat{t}_i$ with $i \in 1, ..., n$ and $\tau_{sample} \leq t_s \leq \tau_{sample}$ the following quantity,

$$R^2 = 1 - \frac{\sum_{i=1}^{n}(y_i - s_f \hat{y}_i(t_i + \hat{t}_s))^2}{\sum_{i=1}^{n}(y_i - \bar{y})^2}.$$

is maximised. For datasets with multiple years of observations a single scaling factor and time shift is used for the entire dataset, preserving comparisons of relative density and fit between years. For each validation both the scaling factor and the time shift are reported in addition to the value of R^2.

3.4 Results

3.4.1 Global validation against field data

The model's predictions are validated against field populations across the species global range, with the validation dataset encompassing populations from 41 locations, from 14 countries and territories, across 4 continents. In Figure 3.6 it can be observed that the model achieves excellent predictions of the population and trait dynamics of *Ae. albopictus* across the species' global range. The model accurately predicts detailed within season dynamics, the start and end of the mosquito season, and captures the observed between year variability across a broad range of locations (see adult numbers in Guangzhou, China (2006-2015), $R^2 = 0.58$, and Rimini, Italy (2008), $R^2 = 0.94$) (Lacour et al., 2015; Carrieri et al., 2012). When data pertaining to multiple life-stages is available the model successfully predicts the dynamics of each life-stage (see adult wing length and adult numbers in Lake Charles, USA (1990), $R^2 = 995$ and Nagasaki, Japan, $R^2 = 0.87$) (Willis, Nasci, 1994; Suzuki et al., 1993). Good quantitative correspondence with multi-year data sets, predicting inter-annual variation in abundance and dynamics (see oviposition activity in Trento, Italy (2010-2020), $R^2 = 0.68$, and adult numbers in Suffolk, USA (2009-2018), $R^2 = 0.65$) (Museo delle Sceinze, 2021; Xu et al., 2017). The model's predictions hold over a broad range of environments and reflect the differences in population dynamics observed between temperate and tropical environments (see Monmouth, New Jersey,

USA (2009), $R^2 = 0.51$, and St. Paul, La Réunion (2013), $R^2 = 0.54$) (Fonseca et al., 2013; Haramboure et al., 2020). These validations demonstrate that, through the careful consideration of the mechanisms by which environmental variation acts on the life-history of a species, broadly generalisable predictions of population dynamics can be achieved. The full set of validations is presented in Appendix G, with full detail of model fit and scaling factors for each location considered and a detailed example of the model's outputs from a single location is provided in Appendix F.

3.4.2 Understand the effects of phenotypic structure using non-plastic and unstructured models

To demonstrate how these predictions compare to those made by models that omit the interaction between vector population trait dynamics and environmental variation I develop a suite of model variants that make common simplifying assumptions about how vector trait responds to environment. For example, a version of the model is derived that assumes all adults share the same invariant wing length. Under this assumption the only variation in adult trait occurs due to changes in instantaneous environmental conditions, and so the effects of previous environments on the expression of trait are ignored. This assumption is common in derivatives of the classical Ross-MacDonald transmission model and consequently is currently widely made when predicting disease risk (Cator et al., 2020). Also considered are a model where adult wing length varies instantaneously with the environment adults experience (an assumption similar to that used in the widely used DENSiM model) and a model that considers the effect of past environments on the population's average wing length but does not include an explicit trait structure (Focks et al., 1995). By comparing the predictions made by these model variants to those made by the trait-structured model the role of phenotypic plasticity in generating predictions of population dynamics can be discerned.

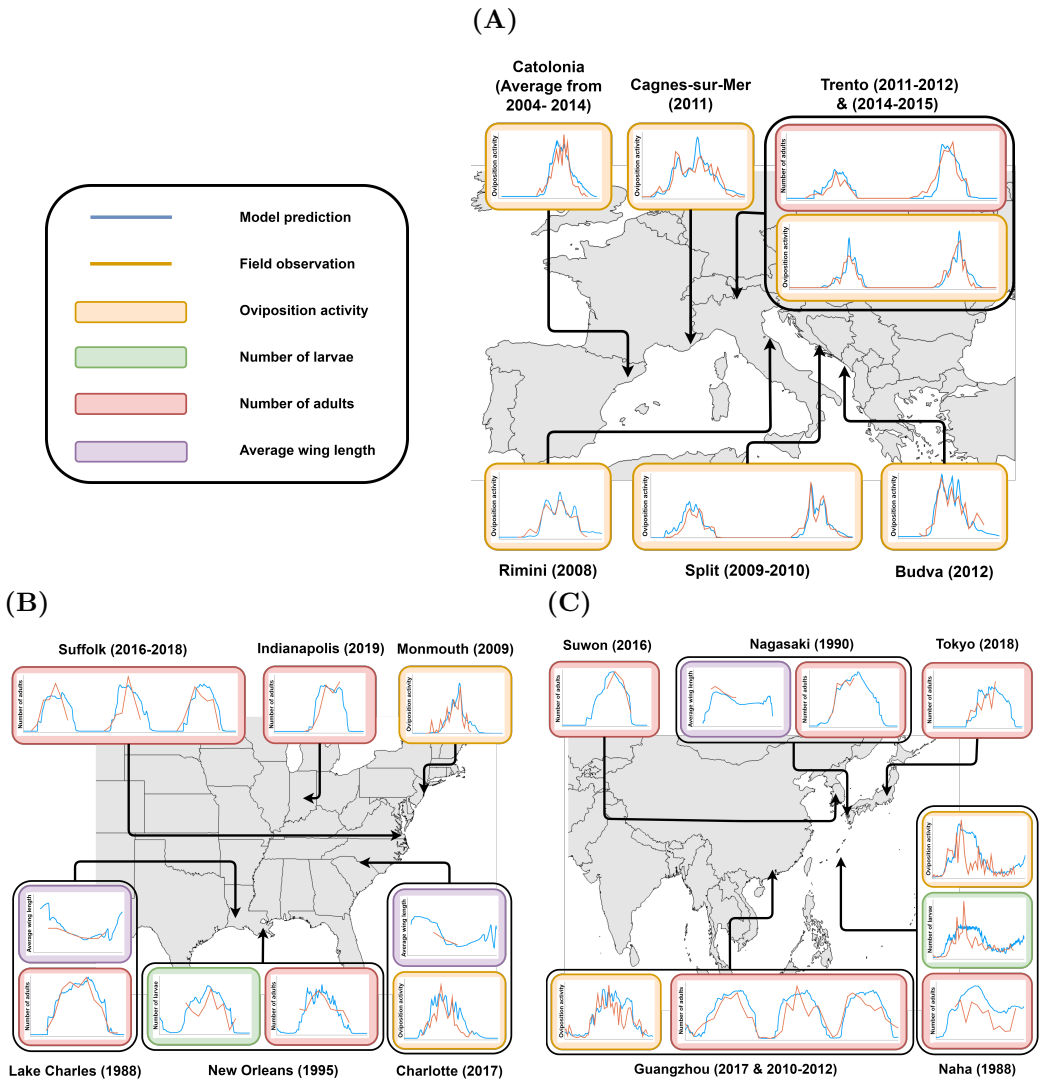

Figure 3.6: Validations of the model's scaled predictions against field data for locations around the world. In each case the x-axis is time, and the y-axis is either the scaled abundance of individuals in a specific life-stage or an average trait value. Scaling of the model predictions follows the methodology described in the validation section of the Methods, and further detail about each prediction can be found in Appendix G. Each blue line represents the model's prediction of the dynamics of the population at the corresponding location, the orange lines represent field observations from that same location. The colour of the outer box indicates the type of data that is being compared, yellow boxes are for oviposition activity, which is the number of eggs predicted to present in an ovitrap, green boxes indicate larval numbers, red boxes indicate adult numbers, and purple for average wing length. The location and year of each comparison are indicated below each graph. **(A)** Comparisons for Europe. **(B)** Comparisons for North America. **(C)** Comparisons for Asia.

3.4.3 Constant wing length models

The first variant considered is a model that assumes that all adults express the same constant wing-length. Under this assumption adult trait still varies, but only in response to the current temperature, and does not vary in response to the intensity of larval competition, nor the average temperature experienced by individuals through development. This assumption is common in mechanistic models of vector and disease dynamics and is also comparable to the assumptions made by metric based R_0 models that are widely used to predict the incidence of vector-borne disease (although these metric-based R_0 models often additionally assume a constant host-to-vector ratio) (Liu-Helmersson et al., 2016; Mordecai et al., 2017). This model is derived by setting $m = 1$ in the population dynamical model and selecting a wing-length that all individuals within the single environmental class express.

To make comparisons of between the model's predictions the constant wing length model is simulated in Cagnes-sur-Mer, where the temperate environment causes the population to express a strong diapause response. In this region the trait structured model predicts that the cold winter limits the number of generations of adults produced per season and this produces simple trait structures as shown in Figure 3.7A. It can be observed in Figure 3.7B that not all constant wing lengths models predict that this location is suitable for populations of *Ae. albopictus*, and that between the constant wing length models there is generally disagreement on the timing end of the active season and the abundance of adults. In general the larger the constant wing-length selected the fewer adults are produced, which occurs due to the omission of the instance of developmental plasticity that would reduce adult quality in response to high larval densities. This results in a small number of large individuals being able to maintain high larval densities unfavourable for development, which in the full model would be mitigated by a reduction in adult quality. The exception to this trend are the models for constant wing lengths 1.8 and $2.2mm$, where the stressful environmental conditions in combination with the increased mortality associated with low wing lengths cause the populations to die out. However, besides

these differences in this location the population dynamics predicted by the constant wing-length models and the plastic model that includes a full trait structure are generally similar.

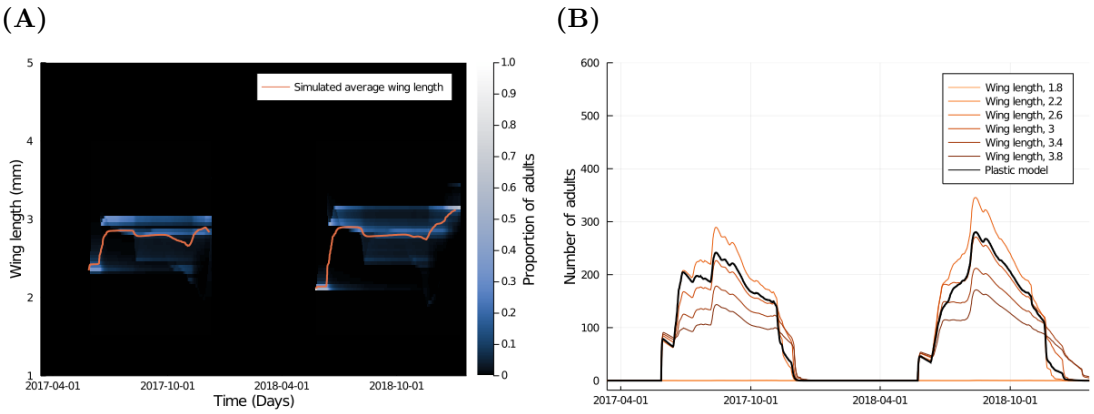

Figure 3.7: (A) The trait dynamics of the full model in Cagnes-sur-Mer. **(B)** A comparison of the number of adults predicted by the plastic model and the non-plastic model simulated at various wing-lengths in Cagnes-sur-Mer.

Consider now the dynamics of both models in Guangzhou where the trait structured model predicts a more complex trait structure (Figure 3.8A). Although aspects of constant wing-length models can still be observed within the dynamics of the full model (In Figure 3.8B), the predictions made by both are evidently more distinct than is the case in Cagnes-sur-Mer. The constant wing length models disagree with each other on the ability of adults to persist through the winter, with models with low wing lengths predicting strong seasonality in abundance, whereas models with high wing lengths predict little inter-annual variation in adult numbers. The dynamics predicted by the plastic model are distinct from any predicted by the constant wing length models, with a clear peak in adult numbers towards the end of the season and variability in the ability of adults to survive through the winter.

Finally, consider the dynamics of the non-plastic model Tokyo. The temperature in Tokyo is generally favourable in the summer months for the development of *Ae. albopictus* but the population experiences regular periods without precipitation inducing intense larval competition. In Figure 3.9B it can be observed that the different constant wing length models predict distinct

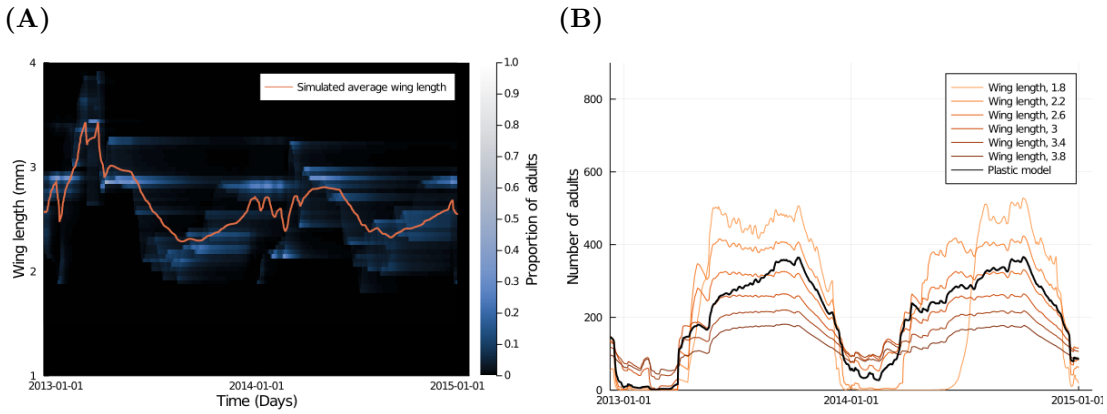

Figure 3.8: **(A)** The trait dynamics of the full model in Guangzhou. **(B)** A comparison of the number of adults predicted by the plastic model and the non-plastic model simulated at various wing-lengths in Guangzhou.

population dynamics despite the strong seasonality observed in this location. Between models the time of peak abundance, and number of peaks observed per season varies.

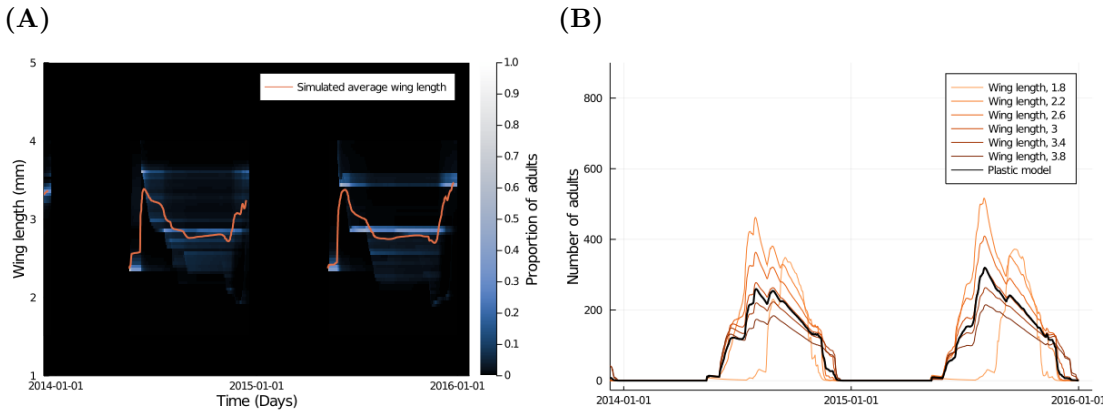

Figure 3.9: **(A)** The trait dynamics of the full model in Tokyo. **(B)** A comparison of the number of adults predicted by the plastic model and the non-plastic model simulated at various wing-lengths in Tokyo.

3.4.4 Models with instantaneously varying wing length

Although it has been demonstrated that the inclusion of mechanisms of trait variation change the model's predictions, there are many simpler ways that trait variation could be represented. The

simplest possible way that trait variation could be represented is by assuming that wing length varies instantaneously with the developmental experience of adults as they are recruited. Under this assumption although adult wing length does change in response to developmental conditions, the population average trait value does not in any way reflect the population's environmental history or trait structure. To derive a model of this type the constant wing length model is adapted such that the wing length of the single environmental class varies according to the function that relates average larval temperature and food available per larvae per day to predict the wing length of emerging adults (Figure 3.5A).

When this model is simulated it can be observed that the similarity between the instantaneous model and the plastic model varies between locations (see Figure 3.10). In Cagnes-sur-Mer the instantaneous model predicts similar adult dynamics and abundance to that of the plastic model despite predicting different trait dynamics (Figures 3.10A and 3.10B). However, towards the end of the season the sharp decrease in adult trait predicted by the instantaneous model, which is induced by a brief cold spell, causes the end of the active season sooner than is predicted by the full model. In Guangzhou the highly variable wing length predicted by the instantaneous model causes sudden drops in adult abundance throughout the year that are not predicted by the plastic model (Figures 3.10C and 3.10D). To see that this behaviour is undesirable consider a population currently held under favourable conditions such that all adults are large. If the environment was to suddenly become unfavourable, perhaps because of a lack of precipitation inducing high larval densities, under the instantaneously varying formulation all of the large adults would shrink, as if they too had developed under these conditions. This would then cause a corresponding increase in adult mortality and individuals would begin to die off due to a spike in larval density they never experienced during development. By contrast, in the plastic model this period of high larval competition does not in any way alter the longevity of adults currently in the population and so the population persists. This could be somewhat mitigated by assuming adults express a trait determined by the average developmental conditions over a suitable interval of time, which would smooth the sharp variation in trait that is currently

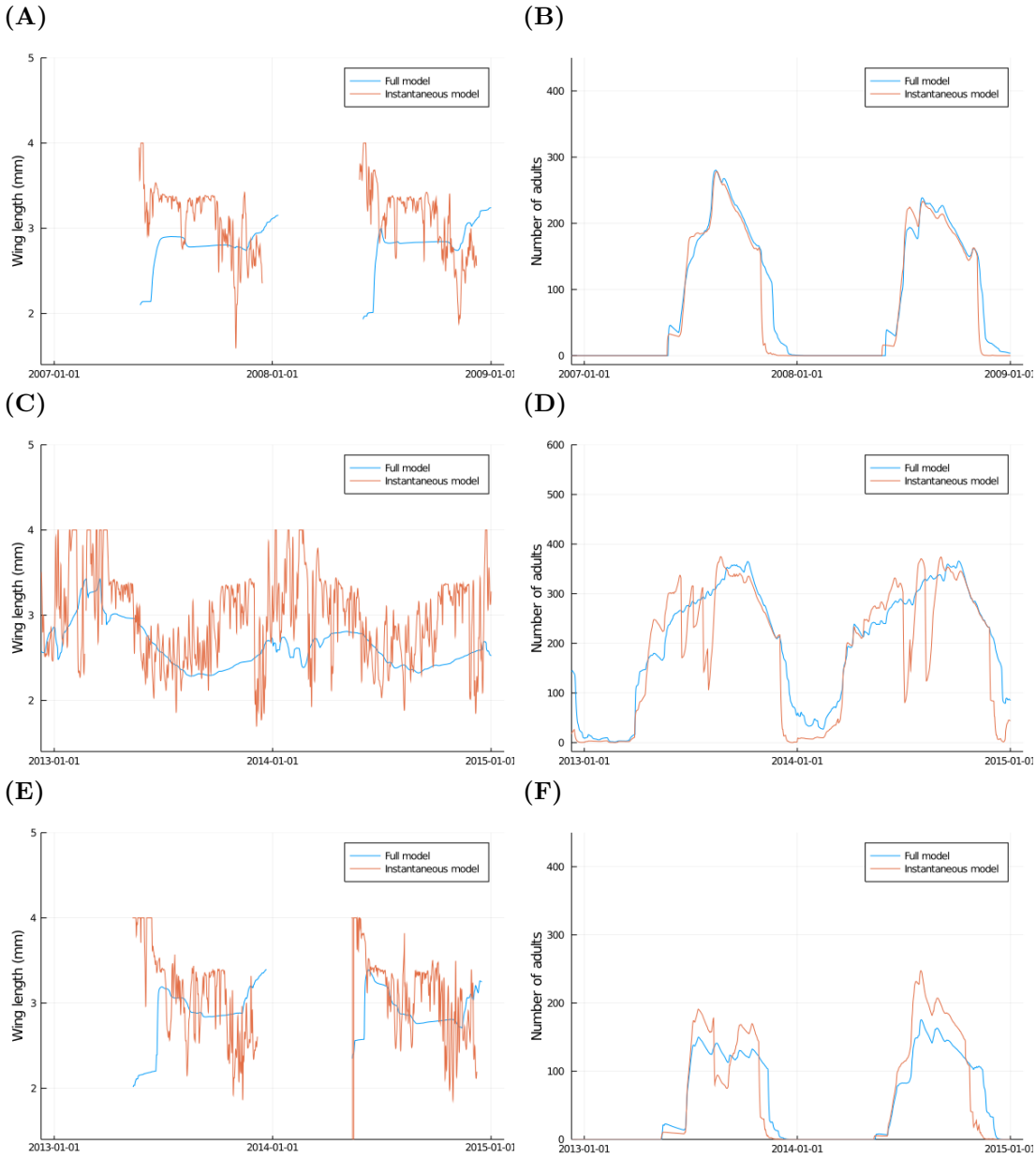

Figure 3.10: A comparison of the predictions made by the full model and the model with instantaneously varying wing length model for **(A)** Wing length in Cagnes-sur-Mer. **(B)** Number of adults in Cagnes-sur-Mer. **(C)** Wing length in Guangzhou. **(D)** Number of adults in Guangzhou. **(E)** Wing length in Tokyo. **(F)** Number of adults Tokyo.

predicted but would not address the underlying issue which is that the effect of environmental history on population trait structure is not being adequately represented.

3.4.5 Models with variable average wing length but without population structure

Finally, consider a model that includes all of the same mechanisms of trait variation that are considered in the plastic model but that forgoes a trait structure in favour of a population average that varies proportionally with the wing length of adults entering and leaving the population. The average wing length, denoted $w_{avg}(t)$, varies as individuals mature into the adult stage, expressing a wing-length representing their larval experience, and as adults expressing the old population average die. To track this I define a differential equation that describes how the populations total wing-length varies, defined

$$\frac{dw_T}{dt} = R_A(t)w_l(T_{avg}(t), \bar{\alpha}(t)) - A(t)\delta_A(T(t), \frac{w_T(t)}{A(t)}).$$

This can then be converted to a population average wing length, $w_{avg}(t) = \frac{w_T(t)}{A(t)}$. This population average wing-length is used along with temperature in the reaction norms to allow adult traits to vary according to the current average. As for the previous variants this model is simulated in Cagnes-sur-Mer, Guangzhou, and Tokyo. This model variant broadly predicts the same population dynamics and average trait value as the model with full trait structure (Figure 3.11). However, although at the start of each year the population's average wing length and abundance tend to be very similar, as the year continues both average wing length and adult numbers begin to deviate from each other. In each case by the end of the active season the average wing length of the full model is higher than is predicted by the constant wing length model, and the adult density lower. By examining the trait structures in Figure 3.7A, 3.8A, and 3.9A in each location large individuals produced at the start of the active season are still present in the population by the end of the active season. Although the plastic model can track these individuals the unstructured model can only track the population's average trait value

and so "forgets" these individuals and this causes the small discrepancy in population dynamics between the two models.

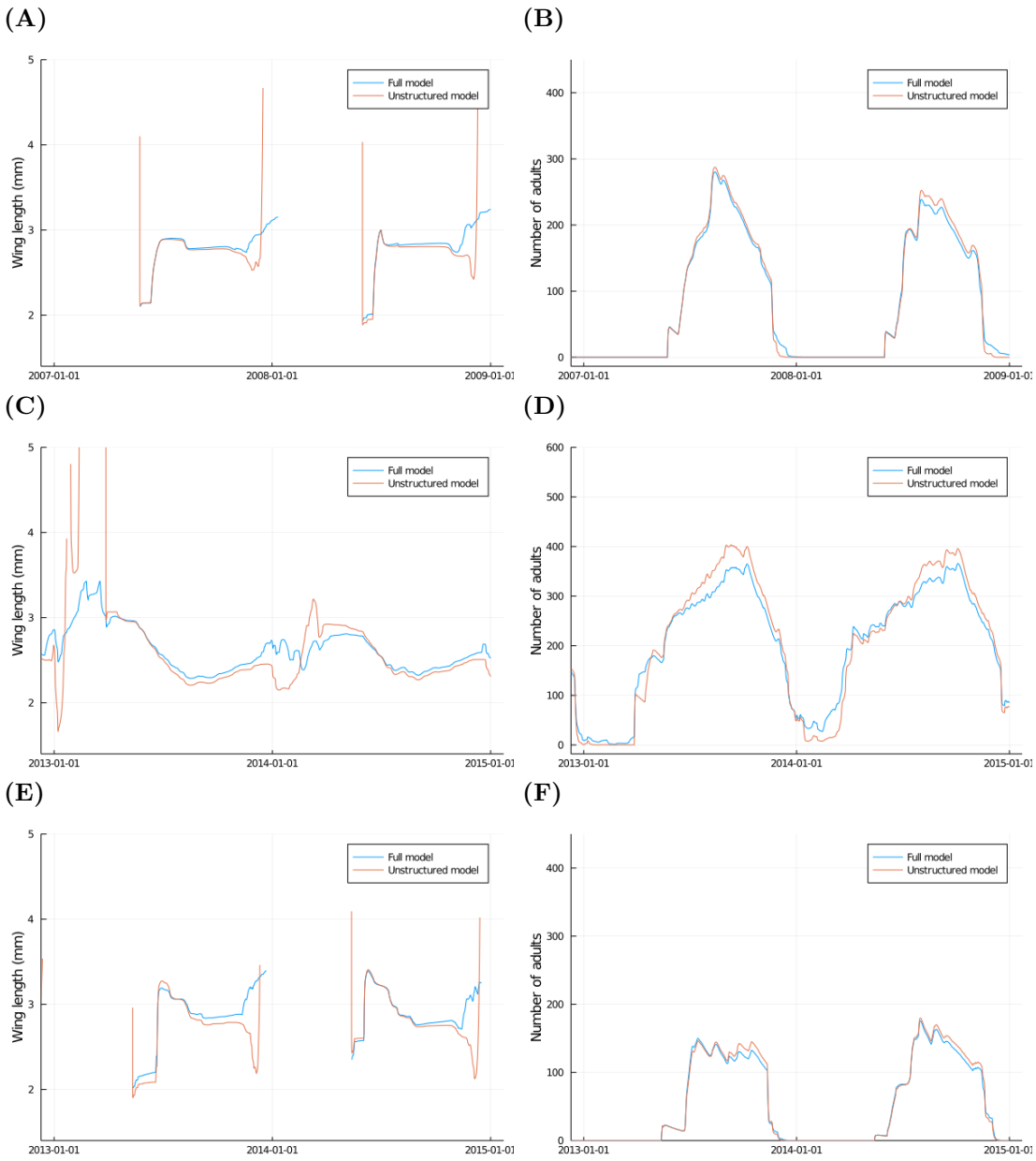

Figure 3.11: A comparison of the predictions made by the plastic model and the unstructured model for **(A)** Wing length in Cagnes-sur-Mer. **(B)** Adults in Cagnes-sur-Mer. **(C)** Wing length in Guangzhou. **(D)** Adults in Guangzhou. **(E)** Wing length in Tokyo. **(F)** Adults in Tokyo

The similarity between the predictions made by model variants and those made by the model with full trait structure depends on the environmental conditions the population being considered is subject to. In environments where populations exhibit simple trait structures, either due to short active seasons or little environmental variation (for example, Cagnes-sur-Mer or La Rèunion respectively) constant wing length models can reproduce the dynamics of the trait structured model provided the constant wing length has been selected to approximate the population's average wing length. However, as population average wing length varies between environments this shows that models omitting mechanisms of variation entirely are not generalisable. Similar differences between population dynamics across environments are observed in the two more sophisticated model variants considered to lesser degrees, with the most epidemiollogically significant departure between the full model and these variants being differences in the ability of adults to persist overwinter.

3.4.6 Climatic suitability for *Ae. albopictus*

I use the model to predict the population dynamics of *Ae. albopictus* for regions where model validations were performed, outputting parameters of interest. These predictions should be interpreted with care as there are factors such as habitat availability, land-use type, or competitor species that are not accounted for. It is assumed that there is always a suitable water body and sufficient adult resource, factors that are unlikely to be true in arid environments even if there is sufficient rainfall to allow a population to persist. Humidity is important in determining adult mortality rates, and regions of low humidity are unlikely to be able to support populations of the species regardless of other environmental dynamics. For this reason a requirement is added that within the active season, as predicted by the model, the average relative humidity should be above 55%. This means that the maps that follow are more akin to environmental suitability indices than a true distribution model.

In Figure 3.12 the average abundance of adults as predicted by this model is displayed over the

regions of Europe, Asia, and North America for which there were validation data sets between the years $2015 - 2020$. The average adult density follows a clear latitudinal gradient, with populations closer to the equator being more abundant. However, as the species undergoes a strong diapause response in temperate regions this increased abundance does not necessarily translate to higher transmission risk, as during the winter months populations temperatures are not favourable for dengue transmission even in parts of the range where there is still adult activity. To account for this I also consider the average abundance of adult mosquitoes during the active season. The active season in this case is defined to be the time between the emergence of the first adult of the year and the death of the final adult, and so this metric describes the relative abundance of adult mosquitoes during period there is an active vector population. In Figure 3.12 it can be observed that during the period when adult mosquitoes are active, the average abundance of adult mosquitoes is comparable between climatic zones. Given that the abundance of adults is a critical determining factor in the ability of populations to vector disease this suggests that differences in the abundance of mosquitoes alone are not sufficient to explain observed differences in outbreak size between regions. For example, the average abundance of adults predicted in Guangzhou, China, the location of the largest *Ae. albopictus* vectored outbreak of dengue to date, is similar to that predicted in Cagnes-sur-Mer, France, a location that infrequently experiences isolated instances of autochthonous transmission.

Environmental suitability for *Ae. albopictus* is predicted throughout the majority of coastal southern Europe, and the model's predictions align well with the current known distribution of the species in this region (ECDC, 2022b). Areas of unsuitability in this region often coincide with mountain ranges, for example the large patch of unsuitability predicted in Northern Italy and throughout Switzerland and Austria coincides with the Alps. The Pyrenees, Massif Central, Apennines, Dinaric Alps, and the Carpathian mountains are similarly outlined. The exception to this is central Spain, which is predicted to be mostly unsuitable due to low humidity and a lack of precipitation. Britain and the Brittany and Normandy regions of France are predicted to have limited suitability for the species which matches the current northern limit of the species

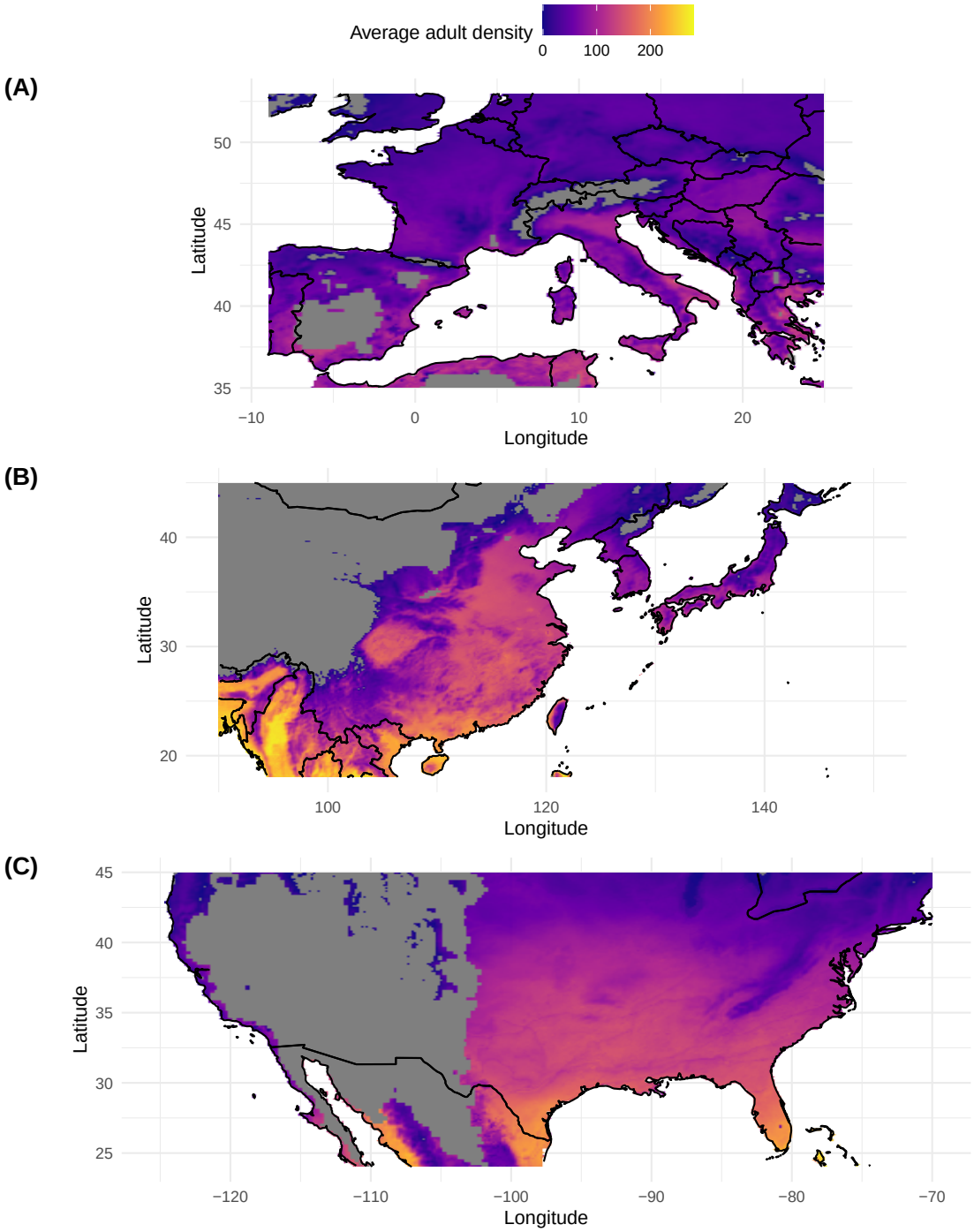

Figure 3.12: The model's prediction of the average adult density over the year in **(A)** North America, **(B)** Europe, and **(C)** Asia.

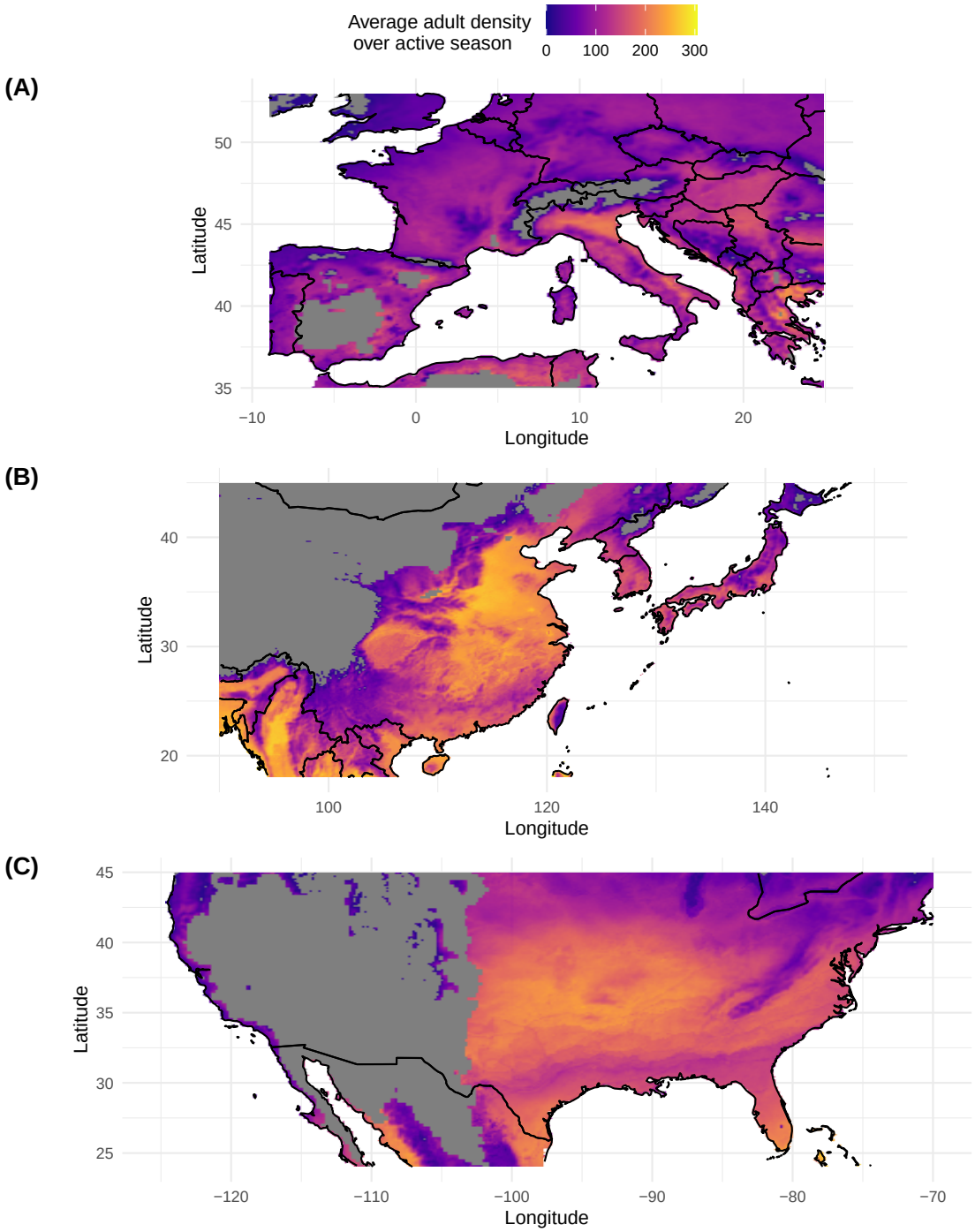

Figure 3.13: The model's prediction of the average adult density over the active season in **(A)** North America, **(B)** Europe, and **(C)** Asia.

distribution.

Oliveira et al. (2021) analysed previous distribution model's predictions of the current climatic suitability of Europe for *Ae. albopictus* and produced a consensus map, identifying regions of agreement and disagreement between these models. The predictions made by the model derived here generally agree with the current consensus in eastern and central Europe, predicting high suitability in Italy, the coastal Balkans and Greece and high unsuitability in the Alps (Figure 3.14A). In western Europe there is more uncertainty in the consensus model and the model derived here disagrees with some aspects of previous predictions. In south-eastern Spain, a region with established populations of *Ae. albopictus*, this model predicts high suitability for populations of *Ae. albopictus* but the consensus model predicts that this region is generally unsuitable (ECDC, 2022b). Central Spain is a region of general disagreement between previous models with some models predicting broad suitability and others predicting unsuitability. The predictions made here agree with the models that predict limited suitability in this region. Much of the south of Britain is predicted to be suitable by consensus but is predicted here to be relatively unfavourable for the establishment of populations, in agreement with previous mechanistic models for the region (Metelmann et al., 2019).

The model's predictions over the range considered in Asia also appear to match the species known distribution throughout the region (Echeverry-Cárdenas et al., 2021; Metelmann et al., 2021). These predictions also align with the predictions made by species distribution models that considered this region, with the greatest deviation being the limited suitability that is predicted here in northern Japan but which is not anticipated by previous models (Zheng et al., 2019; Kraemer et al., 2015; Benedict et al., 2007; Ding et al., 2017). In Japan, suitability is predicted throughout the islands of Honshu, Shikoku, and Kyushu, with limited suitability predicted in southern Hokkaido, matching occurrence records (Kobayashi et al., 2002). In China, the model's predictions align well with the species current extent, predicting the distribution limits in the north and west (Zheng et al., 2019).

Throughout the majority of the eastern USA I predict broad suitability for *Ae. albopictus* with more limited suitability the west coast limited to coastal areas (Figure 3.14C). These predictions align with predictions made by distribution models over this region, which predict similar suitability (Kramer, Ciota, 2015; Kamal et al., 2018; Johnson et al., 2017; Richards et al., 2019; Ding et al., 2017; Ogden et al., 2014). In the western USA the general lack of suitability can be attributed to a combination of desert and mountainous regions. The limits of the species range as predicted by the model reflect the species current distribution in this region (Kamal et al., 2018). Populations of *Ae. albopictus* have been observed along the northern limit that is predicted by the model with evidence of overwintering populations in Ontario and Wisconsin (Giordano et al., 2020). However, this is a region where the presence of *Ae. aegpyti* should be considered when interpreting this model's predictions. For example, in Figure 3.12 broad suitability is predicted for *Ae. albopictus* throughout the state of Florida. However, in southern parts of the state *Ae. albopictus* is largely absent, having been displaced by *Ae. aegypti* which is more suited to the regional climatic conditions (Lounibos, Kramer, 2016). This is predicted by distribution models that consider the species joint distribution, but not by my model as the effects of interspecific competition are not accounted for in this model's predictions of suitability (Khan et al., 2020)

3.5 Discussion

To predict how vector populations and will respond to environmental change it is critical to account for the mechanisms of variation through which that change occurs, building population responses out of individual level variation rather than prescribing them through average traits. The efficacy of such an approach is demonstrated here as without any back-fitting, and despite making broad assumptions about mosquito ecology, the model accurately predicts the population and trait dynamics of field populations of *Ae. albopictus* across the species global range from meteorological data. This demonstrates that the diverse population dynamical behaviours

exhibited by the species over its range can be understood through the effect of environmental variation on life-history traits. However, vector abundance alone is not sufficient to understand global trends in dengue incidence, as high abundances are observed in regions where dengue is endemic and those where dengue is currently absent.

Despite this, the thorough understanding of vector population dynamics developed here will be invaluable for guiding control activities and interventions. Novel and existing control techniques (transgenic mosquitoes, gene-drives and sterile insect technique) require accurate models of mosquito population dynamics for risk assessment (Oliva et al., 2021; Bier, 2022). Models of vector population dynamics are also incorporated into models that guide the roll-out of vaccination campaigns (Ferguson et al., 2016). In each case, predictions of vector population dynamics that will remain robust across broad spatial and temporal gradients are integral to designing effective control efforts. Beyond predictions of vector abundance the ability of this methodology to link environmental variation to trait may allow intervention campaigns to specifically target large individuals (Lloyd-Smith et al., 2005). However, the efficacy of such an intervention as a control method is not currently clear as changing the population's trait structure may have unanticipated consequences on transmission dynamics (Cameron et al., 2013).

The ability of the model to predict population dynamics from meteorological variables does not in any way preclude the importance of local factors in the determining patterns of vector abundance and consequently the risk of vector-borne disease. The datasets used to validate the model are generally taken from established vector populations in regions where the species is a notable nuisance, introducing a site-selection bias for regions where local conditions are suitable for mosquito development. Land-use, socio-economic factors, and micro-climatic variables are demonstrably important in determining vector abundance on small geographical scales and can further be shown to be associated with disease incidence (Gao et al., 2021; Wimberly et al., 2020; Little et al., 2017; LaDeau et al., 2013). Past attempts to identify container-level variables that predict the small-scale distribution of *Ae. albopictus* could no consistent associations between years (Shragai, Harrington, 2019). To better understand the local factors that drive differences

in abundance over small scales, further exploration of the mechanisms by which micro-climate interacts with the life-histories of mosquito species will be required.

The work undertaken here relies on the extensive and thorough effort that has been expended in understanding the life-history of *Ae. albopictus*. For many vectors of neglected or emerging diseases detailed information about the interaction between trait and environment does not currently exist and would not be feasible to collect in exhaustive detail. Although concerted efforts have begun to collate such information and identify gaps in understanding, further work should also be undertaken to understand the conditions under which trait variation alters population responses to help effectively target these efforts (Amos et al., 2022). Developing this understanding is critical beyond vector-borne disease as mechanisms of individual variation are also critical in determining the outcome of biological invasions, interspecific competition, and species responses to climate change (Boutin, Lane, 2014; Hahn et al., 2012; Buskirk, McCollum, 1999). To produce predictions that are robust to challenges of a changing climate, a fundamental shift is required in the way that trait is accounted for, moving away from mean-fields and towards a more complete representation of the mechanisms by which individuals vary.

*

Chapter 4

Predicting the global transmission dynamics of dengue vectored by *Ae. albopictus*

4.1 Abstract

The current alarming increase in the prevalence of dengue is a threat to global public health, characterised by an intensification of disease burden in endemic regions and the expansion of dengue to areas it has long been absent. Despite predictions that temperate regions are suitable for sustained dengue transmission, outbreaks in these areas have so far been small and sporadic. It has been proposed that this mismatch between prediction and observation may be due to environmentally induced variation in vector trait changes the ability of vector populations to transmit disease, but this mechanism is not fully accounted for in current predictive approaches. Here, I derive a Susceptible-Infected-Resistant model for the spread of dengue by *Aedes albopictus*, an invasive mosquito species and vector of dengue, that accounts for the relationship between environment, vector trait, and disease transmission. This model is validated against historic dengue outbreaks and shows how a vector population's trait structure can change the ability of that population to maintain pathogen transmission cycles. Less risk is predicted in

temperate regions than in previous models, coinciding with the currently observed incidence of dengue throughout these regions.

4.2 Introduction

In 2014 the largest dengue outbreak vectored principally by *Ae. albopictus* occurred in Guangzhou, China, lasting for 7 months, hospitalising 14,055 people and causing a total of 37,376 suspected cases (Luo et al., 2017). Before 2014 there had been regular dengue outbreaks throughout the Guangdong region since the establishment of *Ae. albopictus* in 1978, but the 2014 outbreak caused almost 10 times more cases than the previous 13 years combined and was therefore of considerable concern to public health authorities (Zhang et al., 2019). Before 2014, outwith the Guangdong region, the role of *Ae. albopictus* as a vector of dengue had been fairly minor, and the species was considered a secondary vector capable of maintaining low levels of infection in rural areas that could be imported into urban regions infested with *Ae. aegpyti*, the primary vector of dengue (Gratz, 2004). Since 2014, outbreaks of dengue vectored by *Ae. albopictus* have continued to occur around the globe, though as of yet none have matched the 2014 outbreak in Guangzhou in magnitude (Brady, Hay, 2020). There are now yearly outbreaks of dengue in Reunion, where dengue now appears to be endemic, low level autochthonous transmission occurs regularly throughout Europe during the summer, and isolated moderately sized outbreaks in Hawai'i and Japan (European Centre for Disease Prevention and Control, 2019). Understanding why *Ae. albopictus* is capable of maintaining dengue transmission cycles in some areas and not others is critical first step in predicting when this latent vector population will become a wide-spread threat to public health.

Vectors, hosts, and diseases frequently have complex relationships with their environments which can directly influence the transmission cycle. Individual environmental variables act on components of the disease transmission cycle in generally straightforward ways but determining how these components cumulatively determine disease risk over broad spatial and temporal scales is

substantially more difficult. For ectothermic vectors, traits critical in determining vector competence are often highly sensitive to temperature, directly linking environmental variation to changes in disease risk (Deutsch et al., 2008; Gilbert et al., 2014; Samuel et al., 2016). For example, adult mosquitoes experiencing stressful temperatures often have reduced adult longevity when compared to adults subject to more favourable environmental conditions (Brady et al., 2013). Adult longevity determines how likely it is that an individual mosquito will be able to complete the pathogen transmission cycle, and as such is a trait of epidemiological interest (Bara et al., 2015). However, adult longevity is also sensitive to the temperature and intensity of competition experienced by larval mosquitoes throughout development, linking trait expression to population dynamical processes and historical abiotic environmental variables (Ezeakacha, Yee, 2019). Population dynamical processes are in turn linked to environmental variables through life-history traits such as development rates, through stage survival, and fecundity (Delatte et al., 2009). This feedback between trait and population dynamics induced by environmental variation means that to anticipate how disease incidence varies over space and through time it is necessary to first determine how a complex series of past and present environmental conditions, population states, and species-specific processes interact to determine the traits that individuals within a population express (Kramer, Ciota, 2015).

The model framework developed in Chapter 3 proved capable of predicting the population and trait dynamics of *Ae. albopictus* over its global range and therefore is an ideal basis for exploring how environmentally induced trait variation explains current differences in transmission risk. For this purpose, the population dynamical model is incorporated into an SIR model for the transmission of dengue. This is then used to predict how changes in vector population's trait dynamics alter the competence of these populations to vector disease through variation in transmission critical traits. Previous mechanistic models of this system omit this mechanism of individual variation and predict broad suitability for the transmission of dengue by *Ae. albopictus* (Mordecai et al., 2017; Ryan et al., 2018; Metelmann et al., 2021; Fan, Liu, 2019). By more completely representing vector trait variation I aim to produce predictions of dengue outbreak

size and location that better align with currently observed dengue incidence around the globe.

4.3 Methods

4.3.1 SIR Model

The model for the population and trait dynamics of *Ae. albopictus* that was derived and validated in Chapter 3 is incorporated into a susceptible-infected-resistant (SIR) model for dengue vectored by *Ae. albopictus* (Figure 4.1). This model considers the introduction of a single serotype of dengue into a completely susceptible human population. This simplified representation of the urban dengue transmission cycle is most applicable to non-endemic regions where the likelihood of multiple serotypes circulating simultaneously is reduced and therefore the human population is less likely to develop serious complications (Guzman et al., 2013). The human population consists of individuals susceptible to infection H_S, individuals that are infected H_I, and individuals resistant to infection due to having recovered H_R. It is assumed that the size of the human population is constant with the exception of the entry of infected individuals into the population. Mosquitoes are assumed to bite at a temperature-dependent rate of $b(t)$ bites per mosquito per day that is inversely proportional to the length of the gonotrophic cycle such that $b(t) = 1/G(T(t))$. The proportion of uninfected mosquitoes that become infected after biting an infected human is denoted $h_v(t)$, a function that takes the form used in Liu-Helmersson et al. (2016). After the extrinsic incubation period, $\tau_{EIP}(t)$, the proportion of bites that successfully transmit an infection from an infected mosquito to an uninfected human is denoted $v_h(t)$ (Brady et al., 2014; Liu-Helmersson et al., 2016). After the intrinsic incubation period, τ_{IIP}, the infected human is capable of transmitting the infection to new mosquitoes and recovers from the infection after the recovery period, τ_{REC}. In this model large individuals are assumed have no direct advantage in the act of transmission over small individuals and do not bite more aggressively nor transmit disease more competently. The only advantage large individuals have over small

is in their extended longevity which allows a greater proportion of individuals contracting an infection survive to pass that infection on especially under stressful environmental conditions.

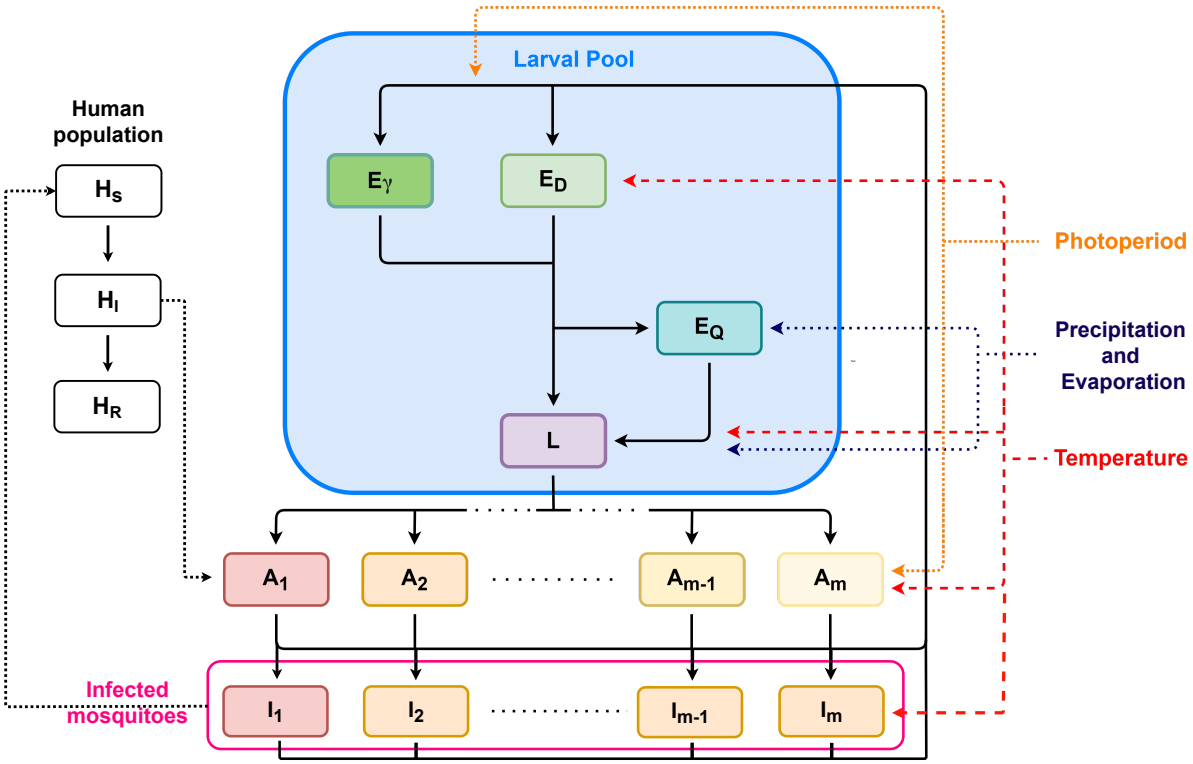

Figure 4.1: Schematic of the model used to represent the transmission of dengue by *Ae. albopictus*. The model retains many of the features of the model defined in Chapter 3. Upon infection by biting an infected human, H_I, uninfected mosquitoes in environmental class j, A_j, transition to the corresponding infected mosquito class, I_j. The infection cycle begins when a susceptible human, H_S, is bitten by an infected mosquito after which that individual has chance to become infected and move into the infected human class H_I. After the recovery period infected humans move into the resistant class, H_R, in which they cannot be infected again.

As the population model predicts the number of mosquitoes arising from a single habitat and I now wish to predict the disease transmission dynamics for a human population it is necessary to consider how to reconcile both populations to the same spatial scale. Mark and recapture studies have demonstrated that adult females can disperse up to a mile from their release site (Vavassori et al., 2019). Further, analysis of dengue epidemics has shown that disease dynamics can best be understood in $2km$x$2km$ grids (Ren et al., 2018). For these reasons the model is simulated

at a spatial scale of $4km^2$, using the number of humans per $4km^2$ for the human population in combination with an estimate of the number of larval habitats per $4km^2$ for the mosquito population. To estimate the number of productive larval habitats per $4km^2$, κ, it is assumed that the number of larval habitats is fixed between locations and within seasons and then select a number that is comparable to those observed in the field (Evans et al., 2019; Little et al., 2017; Carrieri et al., 2012; McClure et al., 2018). *Ae. albopictus* is an opportunistic feeder and in the absence of humans will bite other species, these bites cannot propagate dengue (outside of the geographically limited sylvatic transmission cycle (Gubler, 2002)) but do allow for egg production and so can maintain the mosquito population. To represent this a population of non-human food sources is included in the model, H_B, which is estimated from field observations of rates of anthropophily and mammal densities (Santini et al., 2022).

To define the SIR model the following additions and modifications are made to the population model presented in Chapter 3. The structured human population is represented with addition of the equations

$$\frac{dH_S(t)}{dt} = -R_H(t) \tag{4.1}$$

$$\frac{dH_I(t)}{dt} = R_H(t - \tau_{IIP}) - R_H(t - \tau_{IIP} - \tau_{REC}) + C(t) - C(t - \tau_{REC}) \tag{4.2}$$

$$\frac{dH_R(t)}{dt} = R_H(t - \tau_{IIP} - \tau_{REC}) + C(t - \tau_{REC}) \tag{4.3}$$

where

$$R_H(t) = v_h(t)b(t)\kappa \sum_{j=1}^{m} I_j \frac{H_S(t)}{H_T(t)} \tag{4.4}$$

and $H_T(t) = H_S(t) + H_I(t) + H_R(t) + H_B$ and $C(t)$ is an impulse defined as in the population

model that initiates the transmission cycle through the introduction of an infectious individual at time t. Note that the inclusion of non-human food sources introduces a dilution effect, as when H_B is large in relation to $H_S(t)$ the value of $R_H(t)$ will be low. This means that when the human population size is small, and therefore most bloodmeals are assumed to come from hosts that cannot become infected with dengue, the model predicts that only a low number of total bites by infected mosquitoes result in susceptible humans becoming infected.

To represent infections in the mosquito population an infectious adult classes are added, one for each environmental class, denoted $I_j(t)$. The number of mosquitoes in environmental class j that become infected at time t is denoted $R_{I_j}(t)$, and defined

$$R_{I_j}(t) = h_v(t)b(t)A_j(t)\frac{H_I(t)}{H_T(t)},$$

and the number of mosquitoes in environmental class j that become infectious at time t is denoted $M_{A_j}(t)$ and is defined

$$M_{A_j}(t) = R_{I_j}(t - \tau_{EIP}(t))S_{EIP_j}(t)$$

where $S_{EIP_j}(t)$ is the proportion of individuals in environmental class j that survive the infectious period.

The dynamics of infected mosquitoes can therefore be defined

$$\frac{dI_j(t)}{dt} = M_{A_j}(t) - \delta_{I_j}(t)I_j(t), \text{ for } j \in 1, ..., m \tag{4.5}$$

$$\frac{d\tau_{EIP}(t)}{dt} = 1 - \frac{g_{EIP}(t)}{g_{EIP}(t - \tau_{EIP}(t))} \tag{4.6}$$

$$\frac{dS_{EIP_j}(t)}{dt} = S_{EIP_j}(t)\left(\frac{g_{EIP}(t)\delta_{A_j}(t - \tau_{EIP}(t))}{\tau_{EIP}(t)} - \delta_{A_j}(t)\right), \text{ for } j \in 1, ..., m \tag{4.7}$$

$$\tag{4.8}$$

and the equation for the rate of change of adults in environmental class j is modified to include a term representing mosquitoes becoming exposed to infected humans and thus leaving the uninfected adult classes such that

$$\frac{dA_j(t)}{dt} = R_{A_j}(t) - \delta_{A_j}(t)A_j(t) - M_{A_j}(t), \text{ for } j \in 1, ..., m. \tag{4.9}$$

The full SIR model can therefore be expressed by

$$\frac{dE_\gamma(t)}{dt} = R_{E_\gamma}(t) - M_{E_\gamma}(t) - \delta_{E_\gamma}(t)E_\gamma(t), \tag{4.10}$$
$$\frac{dE_D(t)}{dt} = R_{E_D}(t) - M_{E_D}(t) - \delta_{E_D}(t)E_D(t), \tag{4.11}$$
$$\frac{dE_Q(t)}{dt} = R_{E_Q}(t) - M_{E_Q}(t) - \delta_{E_Q}(t)E_Q(t), \tag{4.12}$$
$$\frac{dL(t)}{dt} = R_L(t) - M_L(t) - \delta_L(t)L(t), \tag{4.13}$$
$$\frac{dA_j(t)}{dt} = R_{A_j}(t) - \delta_{A_j}(t)A_j(t) - M_{A_j}(t), \text{ for } j \in 1, ..., m \tag{4.14}$$
$$\frac{dI_j(t)}{dt} = M_{A_j}(t) - \delta_{I_j}(t)I_j(t), \text{ for } j \in 1, ..., m. \tag{4.15}$$
$$\tag{4.16}$$

The variable delay terms are defined such that

$$\frac{d\tau_{E_\gamma}(t)}{dt} = 1 - \frac{g_{E_\gamma}(t)}{g_{E_\gamma}(t - \tau_{E_\gamma}(t))}, \tag{4.17}$$

$$\frac{d\tau_L(t)}{dt} = 1 - \frac{g_L(t)}{g_L(t - \tau_L(t))}, \tag{4.18}$$

$$\frac{d\tau_P(t)}{dt} = 1 - \frac{g_P(t)}{g_P(t - \tau_P(t))}, \tag{4.19}$$

$$\frac{d\tau_{EIP}(t)}{dt} = 1 - \frac{g_{EIP}(t)}{g_{EIP}(t - \tau_{EIP}(t))}. \tag{4.20}$$

$$\tag{4.21}$$

The through stage survival terms are defined such that

$$\frac{dS_{E_\gamma}(t)}{dt} = S_{E_\gamma}(t)\left(\frac{g_{E_\gamma}(t)\delta_{E_\gamma}(t - \tau_{E_\gamma}(t))}{g_{E_\gamma}(t - \tau_{E_\gamma}(t))} - \delta_{E_\gamma}(t)\right), \tag{4.22}$$

$$\frac{dS_L(t)}{dt} = S_L(t)\left(\frac{g_L(t)\delta_L(t - \tau_L(t))}{g_L(t - \tau_L(t))} - \delta_L(t)\right), \tag{4.23}$$

$$\frac{dS_P(t)}{dt} = S_P(t)\left(\frac{g_P(t)\delta_P(t - \tau_P(t))}{g_P(t - \tau_P(t))} - \delta_P(t)\right), \tag{4.24}$$

$$\frac{dS_{EIP_j}(t)}{dt} = S_{EIP_j}(t)\left(\frac{g_{EIP}(t)\delta_{A_j}(t - \tau_{EIP}(t))}{\tau_{EIP}(t)} - \delta_{A_j}(t)\right), \text{ for } j \in 1, ..., m. \tag{4.25}$$

The same initial conditions as in the non-SIR model are used, with the additional history $H_I(0) = H_R(0) = 0$ with $H_S(0)$ being the human population density.

4.3.2 R_T derivation

To quantify how disease risk changes between regions I derive an expression for the reproduction number R_T for the SIR model. The reproduction number is distinct from the basic reproduction number as it reflects how transmission risk varies as the outbreak progresses, accounting for how changes in the infection structure of the population alter the potential for the outbreak

to continue as time passes (Wallinga, Teunis, 2004). Assume that a single infected human is introduced precisely at the end of the intrinsic incubation period, τ_{IIP}, and so can be bitten for the full duration of the infectious period. Let $b(t)$ be the biting rate, H_S the number of the susceptible humans, and $A_j(t)$ the number of uninfected adult mosquitoes in environmental class j present at time t. The number of bites per day which the infected individual receives can be expressed

$$\sum_{j=1}^{n} \frac{b(t)A_j(t)}{H_T}.$$

The proportion of mosquitoes that become infected after biting an infectious individual is denoted by $h_v(t)$. Mosquitoes only go on to transmit the infection if they survive through the extrinsic incubation period, $\tau_{EIP}(t)$, the proportion of such surviving mosquitoes is denoted $S_{EIP_j}(t)$. Given that an infected human remains viraemic for around 4 days, τ_{REC} (Gubler et al., 1981) the number of mosquitoes that bite the introduced infectious human, develop an infection and, survive to transmit the disease per day can be expressed by

$$\sum_{j=1}^{n} \int_{t}^{t+\tau_{REC}} \frac{b(s)A_j(s)h_v(s)S_{EIP_j}(s+\tau_{EIP}(s))}{H_T} ds.$$

The proportion of bites from infected mosquitoes that transmit the infection to a susceptible human is denoted $v_h(t)$ and the mortality rate of adult mosquitoes in environmental class j is denoted $\delta_{A_j}(t)$. The number of new infections that a mosquito infected at time t in environmental class j causes over it's lifespan can be approximated by

$$\int_{t+\tau_{EIP}(t)}^{t+1/\delta_{A_j}(t+\tau_{EIP}(t))+\tau_{EIP}(t)} \frac{b(s)v_h(s)H_S}{H_T} ds.$$

Note that this is only an approximation of this quantity as $1/\delta_{A_j}(t)$ is fixed at time t and does not account for any temperature induced changes in adult mortality that occur between times

$t + \tau_{EIP}(t)$ and $t + 1/\delta_{A_j}(t + \tau_{EIP}(t)) + \tau_{EIP}(t)$ nor how $\tau_{EIP}(t)$ varies between time t and $t + \tau_{EIP}(t)$. The number of new infections caused by the introduction of a single infectious human at time t can therefore be approximated by

$$R_T(t) = \sum_{j=1}^{n} \Bigg(\int_t^{t+\tau_{REF}} \frac{h_v(s)b(s)A_j(s)S_{EIP_j}(s+\tau_{EIP}(s))}{H_T} \Bigg(\int_{s+\tau_{EIP}(s)}^{s+\frac{1}{\delta_{A_j}(s+\tau_{EIP}(s))}+\tau_{EIP}(s)} \frac{b(u)v_h(u)H_S}{H_T} du \Bigg) ds \Bigg). \tag{4.26}$$

When interpreting the R_T of dengue in this model the length of the transmission cycles involved must be considered. When an infected individual is introduced for the infection cycle to continue mosquitoes must be infected and these mosquitoes may live for up 3 months. This means that although the value of R_T might be high, the subsequent infections may occur over an extended period of time and so does not necessarily imply the occurrence of a large outbreak. This is particularly notable in temperate regions where large long-lived individuals are regularly produced at the start of the active season. For this reason, it is common when comparing outbreak risk between regions to use the length of time for which $R_T > 1$ rather than the maximal value, an approach we follow here.

4.3.3 Model validation against dengue outbreaks

For validation the SIR model's predictions are compared to historical dengue outbreaks where the primary vector responsible was *Ae. albopictus*. In each location the number of reported instances of autochthonous dengue transmission are compared to the output of the model over the same area. The outbreaks considered are the $2013 - 2014$ outbreaks of dengue in Guangzhou, China, the 2014 outbreak in Tokyo, Japan, the $2017 - 2021$ outbreak on La Réunion, France, the $2015 - 2016$ outbreak on Hawai'i, USA, and various instances of autochthonous transmission throughout Europe (Zhang et al., 2019; Yuan et al., 2019; Vincent et al., 2019; European

Centre for Disease Prevention and Control, 2019; ECDC, 2022a). These outbreaks encompass a broad range of disease dynamics occurring over a range of spatial scales, from a few isolated instances of autochthonous transmission in temperate regions of Europe over small areas to a complex multi-year epidemic over a large portion of the island Réunion. Initiating the model's infection dynamics requires the definition of an initial infection scenario which describes how many infectious individuals are introduced into the human population and when these introductions occur. In each case reports from each outbreak are used to select a likely introduction scenario and area over which the outbreak thought to have taken place, although there is often great uncertainty in both (for each outbreak this is further outlined in Appendix H). This uncertainty means that, although unlike the outputs from the population dynamical model the predictions are not rescaled, these validations are primarily intended to demonstrate that the model can predict both sensible disease dynamics and outbreak magnitude under plausible outbreak scenarios. The code used produce the results that follow can be found in a repository at `https://zenodo.org/record/7796206#.ZCslmnbMKUk`.

The model predicts the magnitude, duration, and dynamics of dengue outbreaks across broad environmental gradients under plausible introduction scenarios (Figure 4.2). In the Alpes-Maritimes department of France, the model consistently predicts small numbers of autochthonous transmissions reflecting the limited outbreaks that have been observed in this region. In Tokyo and Guangzhou model correctly predicts the magnitudes of the medium and large outbreaks that occurred in these regions. For the complex multi-year outbreak in La Rèunion the model proves able to accurately predict inter-annual differences in the number of dengue cases across multiple years as well as the time of peak transmission each year. During each of these outbreaks there were active vector control campaigns, and this may explain the general reduced resemblance of these predictions to field data towards the latter half of each outbreak. For example, in Guangzhou in 2014 a considerable intensification of vector control activities occurred halfway through the outbreak to which previous analyses have attributed a substantial reduction in final outbreak size and duration (Lin et al., 2016b).

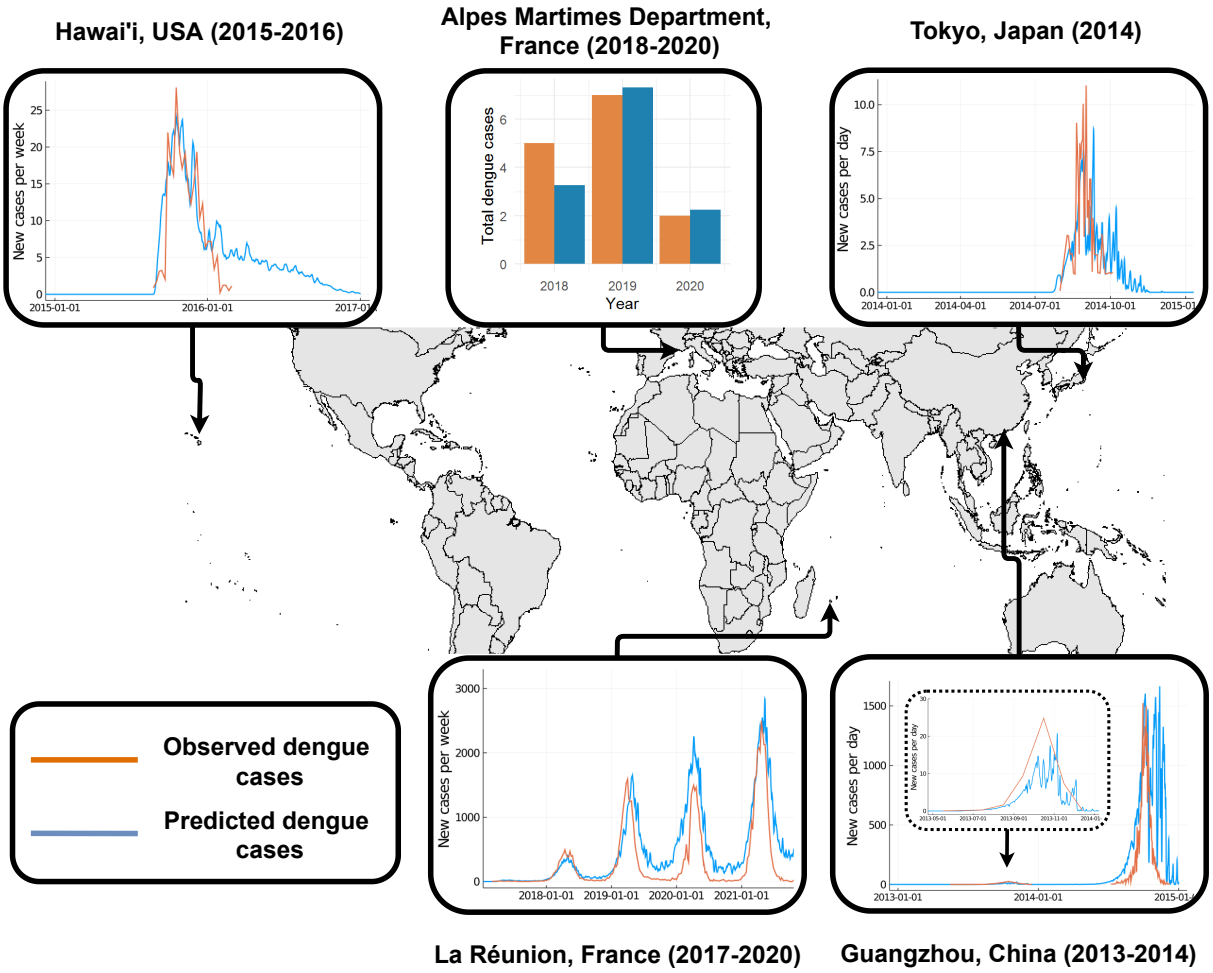

Figure 4.2: Comparisons of the number of instances of autochthonous transmission detected during historical dengue outbreaks and the model's predictions. For each outbreak the x-axis is time and the y-axis is the number of instances of autochthonous transmission, with the blue lines representing model predictions and the orange lines field observations from that same location. Note that due to differences in the way dengue cases were reported for different outbreaks the y-axes may change. The scenarios under which the model was simulated for each scenario are discussed in detail in Appendix H.

4.4 Results

4.4.1 Non-plastic and unstructured models

Exhaustively representing mechanisms of individual variation as in the model developed here is more complex than standard approaches that make simplifying assumptions about the interaction between trait and environment. To justify this additional complexity I must demonstrate that by fully representing mechanisms of phenotypic plasticity different predictions of disease dynamics are produced than would be made by simpler approaches. For this purpose, I consider the model variants derived in Chapter 3 that make common simplifying assumptions about how trait interacts with environment. The predictions made by these variant models are compared to those made by the trait structured model over three of the outbreak locations considered in Figure 4.2 that encompass a range of outbreak sizes and climates. These are a small outbreak in Cagnes-sur-Mer, France of around 5 of dengue cases, an outbreak in Tokyo, Japan of around 100 cases, and a large outbreak in Guangzhou, China of $36,342$ cases. In each of these locations the model was able to predict both the disease and population dynamics observed in the field under a plausible introduction scenario and so any substantial deviation from the model's predictions will indicate a worsening of model performance.

To compare the plastic SIR model and the constant wing length SIR models R_T is computed from equation 4.26 with $m = 1$ and used to compare the number of dengue cases produced per day under the same introduction scenarios used in Figure 4.2. In Figure 4.3 it can be observed that that although the behaviour observed in the expression for the reproduction number, R_T, is comparable to that in adult numbers, outbreak size can be highly variable by wing-length. In Cagnes-sur-Mer, France, the constant wing length models all produce similar predictions of R_T and disease dynamics. However, in Guangzhou outbreak size is highly sensitive to wing-length with the peak of the largest outbreak 20 times higher than that of the smallest outbreak (Figure 4.3D). When comparing the plastic model's predictions of adult dynamics to those

made by the constant wing-length models it could be observed that the population's average trait value was often a good indicator of which constant wing length model was most similar to the plastic model (for example see Figure 3.7A. Here, this is no longer the case and that the constant wing-length model that produces the most similar dengue dynamics often has a wing length higher than the population average. For example, in Figures 4.3E and 4.3F the closest constant wing length model is the model with wing length $3.8mm$, considerably higher than the population average wing length during this period (see Figure 3.9A). This disparity demonstrates that the mechanisms of variation included in the plastic model produce quantitatively different predictions of outbreaks size than would be predicted by average trait alone.

These examples demonstrate that the effect of phenotypic plasticity on disease dynamics varies from location to location and through time. Although the dynamics of the model with trait structure can sometimes be well represented by a non-plastic model, anticipating when this is the case requires an understanding of the population's trait dynamics. Given that even relatively small differences in population dynamics can then result in substantive differences in disease dynamics this justifies representing mechanisms of individual variation in predictions of disease risk.

The small differences between the population and trait dynamics of the plastic model and the unstructured model does not seem to justify the inclusion of a trait structure in the model. However, I now consider the extension of the unstructured model with variable average wing-length to disease dynamics. I then simulate this model for the $2013 - 2014$ outbreak in Guangzhou, under two different introduction scenarios. The first is under the same introduction scenario as is used in Figure 4.2 which was selected to match the introductions observed in the outbreak. Under these conditions the unstructured model predicts more dengue transmission than the plastic model (Figure 4.4A). In the second introduction scenario a small number of cases are introduced at the start of 2013 and then do not introduce any further cases. Under these conditions the plastic model predicts an outbreak in 2014 larger than was observed in 2013 and

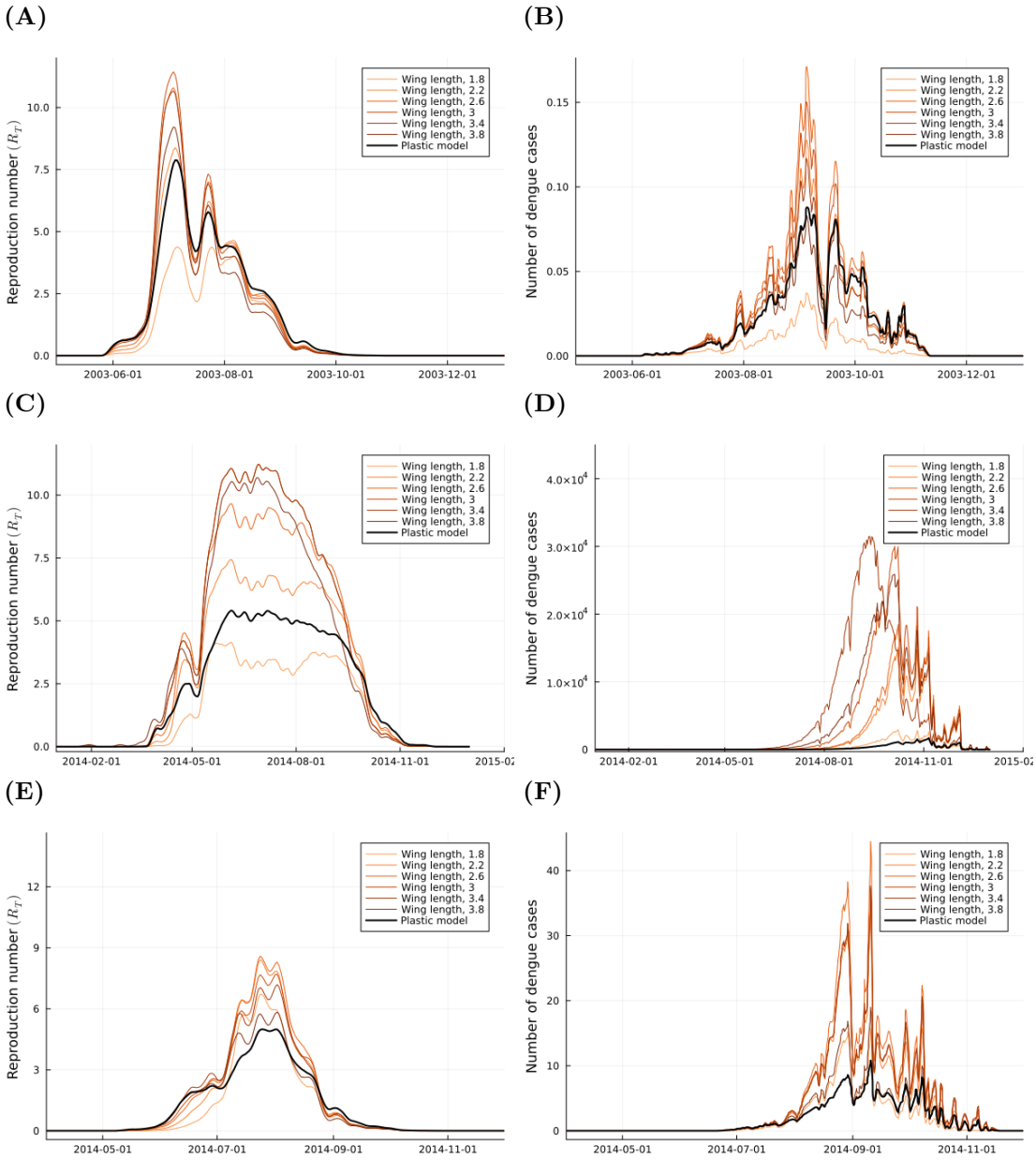

Figure 4.3: A comparison of the predictions made by the full model and the constant wing length model for **(A)** R_T in Cagnes-sur-Mer. **(B)** Number of dengue cases in Cagnes-sur-Mer. **(C)** R_T in Guangzhou. **(D)** Number of dengue cases in Guangzhou. **(E)** R_T in Tokyo. **(F)** Number of dengue cases in Tokyo.

the unstructured model predicts very little transmission in 2014, despite predicting more dengue cases in 2013 (Figure 4.4B). If the simulation is continued the plastic model continues to predict larger and larger outbreaks, whereas the unstructured model does not predict any transmission beyond 2014. Despite their similar population and trait dynamics these two models produce different predictions of disease dynamics that have different implications for vector control. The plastic model with full trait structure predicts that dengue is now endemic to Guangzhou, but the unstructured model suggests that Guangzhou is still a dengue sink. As the only difference between the plastic model and the unstructured model is the presence of a trait structure this demonstrates that the inclusion of a full trait structure in the model produces quantitatively different predictions of disease dynamics.

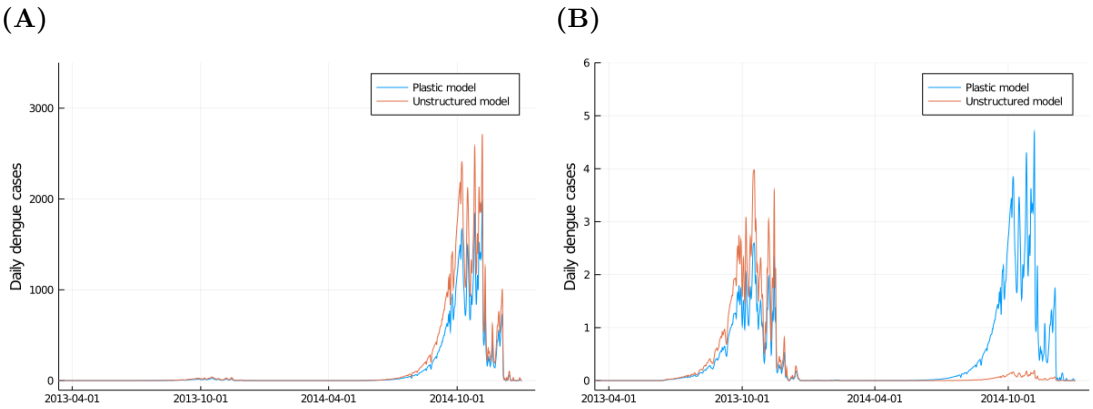

Figure 4.4: A comparison of the number of dengue cases predicted in the Guangzhou 2013 – 2014 outbreak between the plastic model and the unstructured model under different introduction scenarios. **(A)** Under an introduction scenario informed by that observed during the outbreak. **(B)** Under an introduction scenario where cases are only imported during 2013.

4.4.2 The role of trait variation in producing disease outbreaks

To understand how environmental history and population trait structure contribute to the predictions of disease dynamics I consider four of the outbreak locations previously considered (Figure 4.2) which represent a range of different climate types and outbreak sizes. In each location the distribution of adult wing lengths is compared to the distribution of the wing length

of mosquitoes responsible for each transmission event. In the Alpes-Maritimes Department of France during the period when infections are increasing (between July and September) the 75^{th} percentile of the wing length distribution roughly coincides with the 50^{th} percentile of the infection distribution (Figure 4.5A). This shows that a small number of large individuals, produced long before dengue transmission begins, are responsible for the majority of transmission events. This can be demonstrated quantitatively as over the whole outbreak individuals with wing lengths above the population average of $3mm$ make up 17% of the population but account for 78% of all transmission events. In this location the extended longevity associated with developing under favourable conditions confers a transmission advantage over small individuals that are less able to survive through the period of time between contracting an infection and becoming infective. This is a factor that would be overlooked if the model had assumed that all individuals shared the same average wing length, as is common in previous approaches. However, the role of trait variation in determining the ability of vector populations to maintain disease outbreaks changes across environments as the population's underlying trait structure varies. For example, consider the outbreak on La Réunion where little variance in adult wing length occurs during periods of peak infection and so there is no substantial deviation between the wing length of adults and the wing length of infecting adults (Figure 4.5B).

As a population's trait structure becomes more complex the role of trait in determining transmission dynamics can no longer be captured by simple summary statistics. For example, in Hawai'i individuals with wing lengths over $2.7mm$ make up 18% of the total population but account for 46% of all transmission over the course of the outbreak, but in Guangzhou, individuals with wing length over $2.7mm$ account for 38% of all individuals but are responsible for only 12% of all transmission. This result can be understood by considering the trait dynamics exhibited by these populations and the underlying environmental variation that gives rise to them. In both locations each population's average wing length oscillates between a maximum in the winter, when larval densities are low, and a minimum in the summer when larval densities are high. Large individuals produced in the spring persist throughout the summer creating a dynamic wing

length distribution that evolves seasonally (see Figure 4.5C and 4.5D). On Hawai'i individuals substantially larger than the population average are responsible for the majority of transmission throughout the year. Despite large individuals not being abundant during the summer months when the temperature is optimal for disease transmission small individuals do not survive long enough to sustain the dengue transmission cycle. This observation explains the disproportionate number of transmission events attributable to large individuals and also explains the contrary result obtained in Guangzhou. In Guangzhou, the environmental conditions are such that the small individuals that are most abundant in the summer are competent vectors of dengue and so are responsible for more transmission than large individuals that are most abundant during the winter, a period that was not favourable for transmission. However, in Guangzhou trait structure still plays in important role in disease transmission dynamics and large individuals are responsible for maintaining the transmission cycle through cold winter months, allowing the infection to be maintained in the population between years (Figure 4.5D). Further, at the start of the outbreak in 2014 these same large individuals are more capable of transmitting dengue than small individuals, accelerating the spread of dengue at the start of the outbreak and extending the transmission period.

4.4.3 Global risk predictions of transmission risk

To predict transmission risk over the species global range I apply the novel expression for the reproduction number, R_T, defined in Equation 4.26. This formulation of R_T accounts for the effect of the vector population's trait structure on the ability of that population to transmit disease and so produces predictions that reflect how variation in a population's trait structure alters the ability of that population to vector disease between climates. R_T is computed across the species global range and the average length of time the environmental conditions were suitable for the transmission of dengue between $2017 - 2020$ is reported (Figure 4.6). It is predicted that areas of risk are generally restricted to areas of high human population density. This is a consequence of the dilution effect caused by the population of dead-end non-human

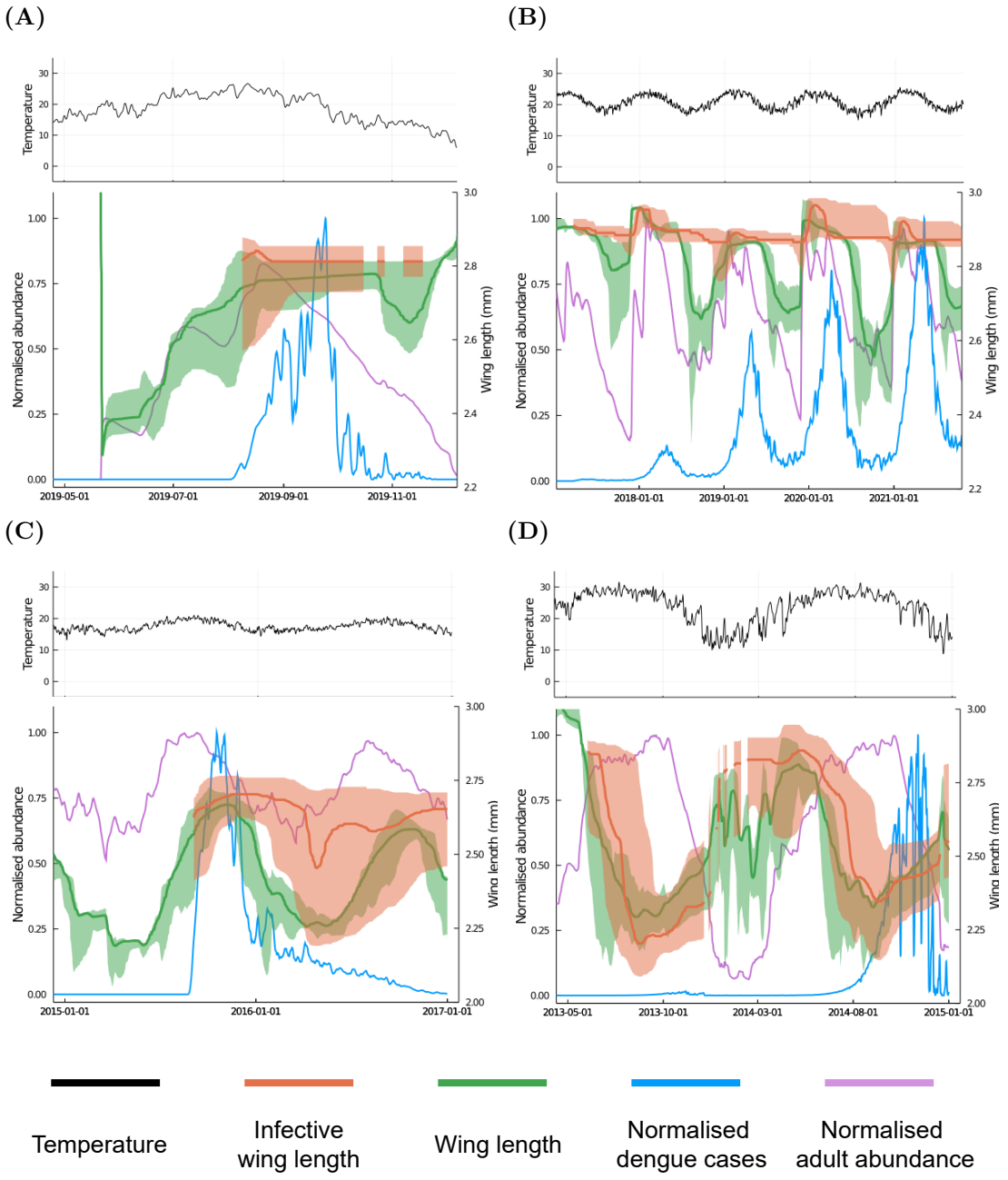

Figure 4.5: A comparison of the distributions of adult wing length and infections attributable to adults of a specific wing length for four historic dengue outbreaks. In each case the green line indicates the population's average wing length at a given time with the bars indicating the 25^{th} and 75^{th} percentiles of the wing length distribution. The orange line indicates the 50^{th} percentile of the distribution of infections by wing length with the bars indicating the 25^{th} and 75^{th} percentiles of this distribution. The blue and purple lines indicate the normalised number of dengue cases and adults respectively. Comparison for outbreaks in: **(A)** Cagnes-sur-Mer, France (2020); **(B)** Réunion (2017 – 2021); **(C)** Hawai'i (2015 – 2017); **(D)** Guangzhou in (2013 – 2014).

hosts incorporated in the SIR model that are used only for blood meals and do not contribute to the dengue transmission cycle. Further, the presence of a substantial vector populations is not predicted to be a sufficient condition to maintain the dengue transmission cycle (compare these predictions to the predictions of suitability for the establishment of populations of *Ae. albopictus* in Figure 3.12).

Europe currently experiences limited autochthonous transmission of dengue by *Ae. albopictus*, and each of the locations in which dengue transmission has been observed is predicted by the model (with the exception of an outbreak in Croatia that occurred outside of the period of time considered) (ECDC, 2022b). In this region only short periods are predicted to be suitable for transmission which reflects the observed magnitude of these outbreaks. In China, where dengue outbreaks vectored by *Ae. albopictus* frequent, I predict longer transmission periods over a wider area than in Europe. These predictions align with the observed location and magnitude of historical dengue outbreaks in the region, and the Guangdong region in particular is a clear hotspot (Yue et al., 2022). Transmission risk is predicted to be low throughout northern China and is comparable to that observed in southern areas of Europe where outbreaks usually only consist of a small number of detected cases. In America it is predicted that there are isolated areas of risk throughout the eastern USA with little suitability for transmission in the west. The region with highest predicted risk is Miami, Florida, where there have been confirmed instances of autochthonous transmission vectored *Ae. aegpyti* which out-competes *Ae. albopictus* in this region. The locations of historic outbreaks in Texas are predicted to be able to sustain transmission, though again the presence of *Ae. aegpyti* in this region is not accounted for in our predictions (Brunkard et al., 2007).

Compared to previous statistical models of dengue incidence the predicted area at risk aligns most closely with that predicted by Messina et al. (2019), though this model additionally considers *Ae. aegpyti*. Less suitability for transmission is predicted than in the model by Rogers et al. (2014), especially in northern latitudes. Compared to previous mechanistic models that do not account for interactions between population, environment, and trait it is predicted that

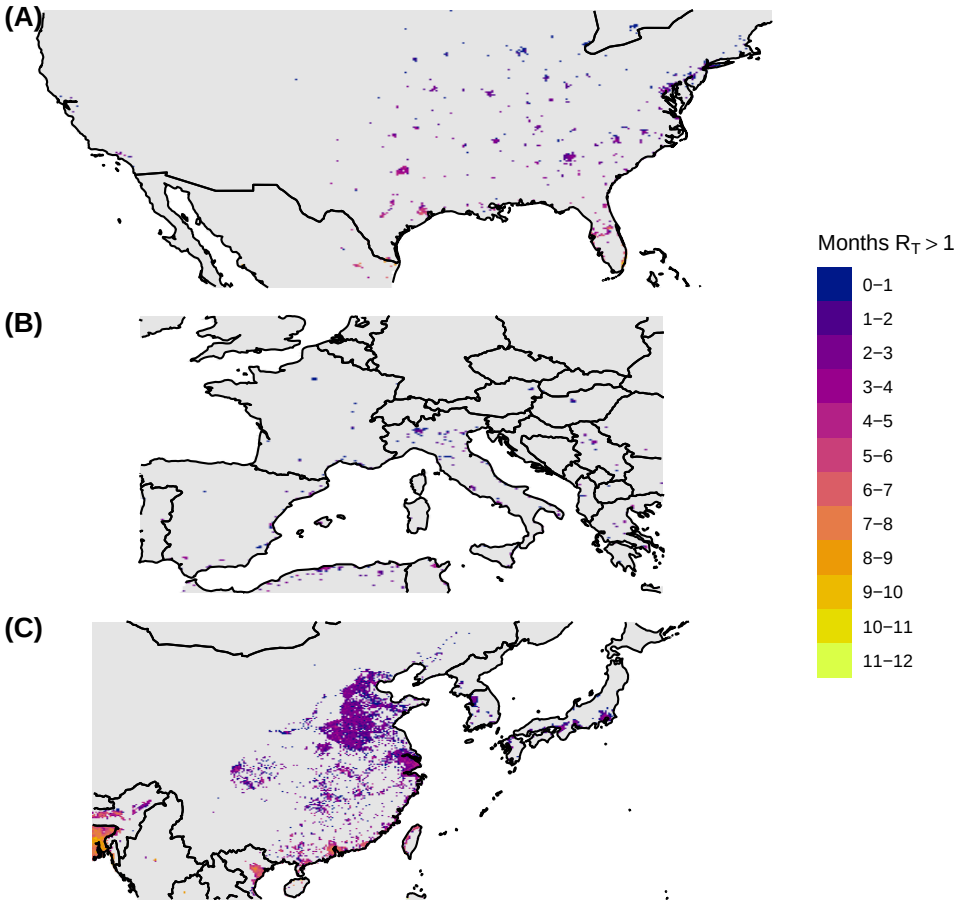

Figure 4.6: The length of time for which the model predicts that the reproduction number will be greater than one ($R_T > 1$) and that predicted by a standard metric-based approach that does not consider population dynamics or trait variation. Each cell represents the 4 year average for that location. **(A,B,C)** The model's predictions of the duration of time for which $R_T > 1$ in North America, Europe, and Asia respectively.

a smaller geographical area is at risk for a shorter period of time (Mordecai et al., 2017; Metelmann et al., 2021; Ryan et al., 2018). This is demonstrated in Appendix I where a standard R_0 approach is compared to the model's predictions. To demonstrate that the approximation used to estimate the value of R_T is valid I compare the regions where transmission risk is predicted to those where the SIR model predicts that the total number of dengue cases is greater than the number of cases introduced. As the predicted number of dengue cases is not subject to the approximation needed to compute R_T, close correspondence between regions of predicted risk and regions where the total cases are above the number introduced will demonstrate the validity of the approximation. To test this correspondence I compute the average total annual number of dengue cases predicted per grid cell and check if the number of cases predicted by the model exceeds the sum of the number of cases introduced through the introduction scenario and the total amount of autochthonous transmission that would occur for over the period of time $R_T > 1$ if instead $R_T = 1$ over the full period. I find that this never occurs and therefore the use of an approximation has not erroneously predicted an outbreak where the SIR model predicts that an outbreak could not occur.

4.5 Discussion

I demonstrate how variation in a vector population's trait structure, as determined by the environmental conditions that it experiences, alters the ability of that population to transmit disease. During the large outbreaks that occurred in Guangzhou and La Réunion the majority of vectors present in the population are predicted to be competent to transmit dengue during the periods when temperatures are optimal. By contrast in temperate regions, such as Cagnes-sur-Mer, this is predicted not to be the case and instead only a small proportion of the total vector population is capable of maintaining the transmission cycle. As mean-field models are often parametrised under the assumption that all individuals develop under favourable conditions this may explain the current apparent overestimation of the risk that *Ae. albopictus* poses (Brady,

Hay, 2020; Lambrechts et al., 2010). This suggests that although mean-field approaches may perform well when parametrised for specific environmental conditions in locations where trait structures are simple, the predictions made by a model tailored for one climate do not necessarily generalise between climates and so should be interpreted with caution (Cator et al., 2020).

By considering mechanisms of individual variation novel insights are generated pertaining to systems of biological interest, and the work undertaken here could be extended to other *Aedes*-borne diseases and other vectors of epidemiological significance. The obvious candidate for such an effort is the primary vector of dengue *Ae. aegypti* which is better adapted to warmer climates than *Ae. albopictus* (Kraemer et al., 2019). The life-history of this vector is well studied and so a similarly detailed modelling approach is both possible and appropriate. Over much of the range of *Ae. aegypti* temperature is less variable, and this lack of strong seasonality means that detecting environmentally induced changes in population and trait dynamics in the field will be substantially more difficult than for *Ae. albopictus*. However, this demonstration of the importance of trait in producing disease dynamics, even in climates with little temperature variation (see the discussion of the role trait in producing disease dynamics in Hawai'i), motivates further exploration to better understand the changing global incidence of dengue.

The current risk posed by *Ae. albopictus* over the majority of the range that has been considered is predicted here to currently be low, which is in line with both disease incidence data and analyses of the species vector competence. Even so, the large outbreaks that now regularly occur on Guangzhou and La Réunion are worrying exceptions and given the current general trend of increase in the incidence of vector-borne disease careful surveillance and control is remains critical. Even over the last 20 years the model predicts that developmental habitats have become more productive, and the length of the transmission season has extended. Warm summers would allow more vectors to be competent, and this in turn would bring predictions of risk back in line with previous models. Given that this trend is unlikely to reverse it is only a matter of time before larger outbreaks vectored by *Ae. albopictus* begin to occur outside the limited geographical range they are currently observed. In many regions this could quickly

change the current status of *Ae. albopictus* as a nuisance biter into a serious public health risk.

Chapter 5

Discussion

In the following discussion I recapitulate the work's principal findings, discussing the content and drawing conclusions.

5.1 Recapitulation

Chapter 2 pertained to the development of a novel modelling framework to represent the effect of phenotypic plasticity on population and trait dynamics. A flexible modelling framework was derived, capable of representing the effect of multiple instances of phenotypic plasticity in response to multiple environmental drivers. The framework was applied to Nicholson's classical blowfly experiments and shown to provide novel insights into a well-studied system. Previously unexplained cryptic population dynamical behaviour naturally emerged from the system, and this was demonstrated to be a consequence of the model's explicit representation of mechanisms of individual variation.

Chapter 3 applied the framework derived in Chapter 2 to the invasive mosquito species *Ae. albopictus*, a vector of dengue. By representing the delayed effects of phenotypic plasticity on the traits expressed by adult mosquitoes the model is able to predict the population and trait

dynamics of field populations from meteorological data. The role of trait variation in facilitating the model's high generalisability was demonstrated by considering model variants that made common simplifying assumptions about the relationship between environmental variation and trait expression. When model was applied over the species' global range, the predicted distribution is shown to broadly agree with both the species currently observed range and the predictions made by species distribution models.

In Chapter 4 the model derived in Chapter 3 that was used to predict the population and trait dynamics of *Ae. albopictus* is incorporated into an SIR model for the transmission of dengue. This model is validated against historic dengue outbreaks and is able to predict observed transmission dynamics and anticipate differences in outbreak magnitude between locations. When extended over the species global range the model predicts a shorter time over which the dengue transmission cycle can be sustained than previous mean-field approaches. The predicted area of risk is also smaller than that predicted by previous mechanistic models and aligns well with current disease incidence. Vector trait is shown to be the determining factor in these predictions of reduced risk, and it is demonstrated that in many temperate environments a large proportion of vectors within the population are not competent to maintain the pathogen transmission cycle.

5.2 Main findings

This thesis aimed to explore the role of vector trait variation in determining current global patterns in the incidence of vector-borne diseases. Current models of disease incidence make simplifying assumptions about how transmission critical traits respond to environmental variation (Cator et al., 2020). These assumptions produce easily interpretable predictions of disease risk over broad areas but overlook mechanisms that are known to drive population response to environmental change (Violle et al., 2012). Improving on previous predictions required an approach that explicitly accounted for mechanisms of individual variation, which was developed and shown to provide new insights into complex biological systems. Models derived using this

framework were able to explain cryptic population dynamical behaviours, such as the paradox of enrichment which had previouslly been observed experimentally by Nicholson, and were shown to predict observed differences in population-level processes across broad environmental gradients (Nicholson, 1957).

By explicitly representing the effects of a delayed instance of phenotypic plasticity on a transmission critical trait I demonstrate how a vector population's environmentally induced trait structure drives disease dynamics. In regions where low levels of transmission occur, only a small subset of large, long-lived mosquitoes were capable of maintaining the transmission cycle. By contrast in regions where large dengue outbreaks occurred the majority of individuals within the vector population were competent to transmit dengue regardless of trait. Between regions where large outbreaks of dengue occur and those where small outbreaks occur it was demonstrated that there is little difference in the productivity of developmental habitats at time of peak transmission. This shows that vector abundance alone is not sufficient to predict disease incidence across environmental gradients, just as in the experimental blowfly culture patterns of individual variation did not translate to population-level responses. Only when trait and population dynamics are considered in concert, in a system that allows the interaction between the two, were generalisable predictions produced.

More broadly this is part of the growing body of evidence that the way that mechanisms of individual variation are incorporated into predictions of how population's will respond to environmental change needs to be rethought to further our understanding of population ecology (Bolnick et al., 2011; Hendry, 2016; Johnston et al., 2019; Lion, 2018; Lipowsky et al., 2015; Lloyd-Smith et al., 2005; Sgrò et al., 2016; Turcotte, Levine, 2016). Mean-field assumptions are often made implicitly, without consideration for the complex biological processes through which an individual's environmental experiences determine its life-history. The increasing availability of trait data and developments in theory means that now is an ideal time to start directly accounting for mechanisms of variation in predictions of population processes rather than using implicitly assumed averaged trait approaches (Violle et al., 2012). Trait-based approaches have

been long advocated for as a way of producing generalisable predictions but despite this there has only been a limited application of theory to generate predictions on a global scale such as achieved here (Green et al., 2022). The work undertaken in this thesis demonstrates that these generalisable predictions are not only attainable but can provide insights into important biological systems.

5.3 Future directions

The modelling framework developed here has broad applicability beyond the transmission of dengue by *Ae. albopictus* and there is scope for substantial building from this body of work.

5.3.1 Improving on model assumptions

The assumptions that were made to derive, parameterise and implement the model to predict the population dynamics of *Ae. albopictus* in Chapter 3 were broad and far-reaching. Generally, these assumptions were made due to gaps in the current understanding of how the life-history of *Ae. albopictus* interacts with environmental variables. To substantially improve of on any of these assumptions would represent a significant amount of experimental work. Yet, exploring how these factors affect the mechanisms by which the species varies on a more local scale would provide a deeper understanding into how the incidence of vector-borne will change in the future.

The model for the population dynamics of *Ae. albopictus* derived in Chapter 3 and used in Chapter 4 assumes that the quantity and physical characteristics of aquatic developmental habitats remain constant through space and time. This greatly simplifies the model but omits processes that are demonstrably important in determining the abundance of *Ae. albopictus*. A field survey by Evans et al. (2019) has shown that the number of larval habitats fluctuates throughout the year and that this is associated with changes in adult density. However, predicting how the availability of larval habitats changes is challenging, due to the cryptic nature of these habitats

and presence of precipitation independent standing water due to human activity (Nguyen et al., 2011; Unlu et al., 2014). To scale up surveillance, citizen science projects have proven an effective solution, but even when the distribution of developmental habitats becomes better understood, using this knowledge to improve predictions of disease risk will be challenging (Jordan et al., 2017; Low et al., 2021). The size of larval habitats has been shown to vary with land-use type and socio-economic variables and this changes the intensity of density dependent competition (Reiskind, Zarrabi, 2012; Parker et al., 2018). The physical chemical properties of the water in developmental habitats can change oviposition preferences and has been implicated as a cause of increased vectorial capacity (Gunathilaka et al., 2018b; Ramasamy et al., 2011; Medeiros-Sousa et al., 2020). The presence of predatory or competitor species can also change oviposition preferences, mortality rates, and development rates in a way that changes on a species-to-species basis and that has been shown to interact with other container-level variables such as food availability, and habitat complexity (Juliano et al., 2019; Wasserberg et al., 2013; Costanzo et al., 2005; Silberbush, Resetarits, 2017; Cuthbert et al., 2019). To better understand how the characteristics of developmental habitats changes disease incidence, a deeper understanding of the mechanisms by which container-level variables interact with the life-history of the species will be required.

The model derived in Chapter 3 also assumes that the temperature in the water experienced by juveniles and the temperature of the air experienced by adults are always the same. The difference between air and water temperature have been shown to vary according to a variety of micro-climatic and environmental factors, including the material the habitat is made from and the level of shade over the habitat (Kumar et al., 2015; Paaijmans et al., 2008). Improving on this assumption therefore requires a better understanding of the characteristics of larval habitats in the field, the difficulties of which have already been outlined. It is further assumed that the average daily temperature captures the effects of diurnal temperature variation on mosquito trait. Diurnal temperature variation is predicted to increase the sensitivity of vectors to climate change through changes in developmental traits (Paaijmans et al., 2013; Zapletal et al., 2018). However, the effect of diurnal variation on the temperature in the developmental habitat varies

according to the habitat's physical characteristics such as the volume of water and material the habitat is made of. Further complicating the inclusion of diurnal variation in these predictions is that diurnal variation is not considered in the data used to parametrise the model, the majority of which is sourced from constant temperature experiments. To more completely represent the effect of temperature on the life-history of *Ae. albopictus* therefore requires both a better understanding of larval habitats, and further experiments exploring the role of temperature variation on mosquito trait.

Here, it is demonstrated that accurate predictions of the longevity of adult mosquitoes are critical in determining the ability of vector populations to transmit pathogens. However, there are multiple factors known to alter the longevity of adult mosquitoes that are not accounted in the models due to a lack of data regarding their interaction with wing length and temperature. This lack of data is a known problem and a systematic literature by Schmidt et al. (2018) into the relationship between humidity, longevity and temperature could not identity a statistically significant relationship which was attributed to a lack of experimental data over a sufficient range of conditions. To go a step further than this and define a relationship between, temperature, wing length, humidity, and longevity is therefore currently impracticable without further extensive experimental work. Omitted for similar reasons is the demonstrably independent relationship between larval food availability, larval density, and temperature on adult wing length and age-specific mortality rates (Yoshioka et al., 2012). The same carry-over effect that alters adult longevity also has implications for the ability of vectors to transmit disease and there is evidence that larvae developing under stressful environmental conditions have thinner midguts as adults, allowing infections to become disseminated faster (Herd et al., 2021). However, the precise nature of this mechanism is currently unknown and there is also evidence for the opposite relationship with experiments run at different temperatures and densities reaching the conclusion that low densities and temperatures accelerated the dissemination of infection (Westbrook et al., 2010; Nasci, Mitchell, 1994).

5.3.2 Further applications of the model

Ae. albopictus is an invasive species and each year more regions report the first occurrence of the species. Considering the dynamics that occur when small numbers of vectors are introduced into the system at different times of the year would potentially produce useful indices for predicting invasion risk. Additionally, environmental suitability for vector populations and dengue transmission is predicted here only for regions where there is data from field populations. Given the close correspondence between the distribution of vector occurrence and model predictions over the range considered it would be useful to extend this model to the rest of the globe to predict the limits of species current environmental niche. A similar approach could be extended to the SIR model, pairing the dynamical disease model with predictions of dengue importation such as predicted in the model by Liebig et al. (2019) to convert estimates of how long dengue transmission is possible to predictions of how likely autochthonous transmission is in a given region.

The models produce predictions of vector population dynamics that hold across the species global range, validated against 34 years of data from field populations. This generality should hold into the future and so using this framework to predict how the distribution of vector populations and incidence of dengue will evolve in response to future climate change is a natural next step. Even over the relatively short period considered here the model predicts that larval habitats are becoming more productive over most of the range considered year on year, and the suitability for dengue is increasing. Previous mechanistic predictions of the future distribution of dengue generally predict higher incidence in latitudes already at risk and a northward expansion of both vector population and dengue incidence. Compared to previous predictions this model starts from a lower baseline, predicting less suitability for dengue transmission for less time over a smaller geographical range (Ryan et al., 2018). It is therefore unclear how the model will predict regions at risk of dengue transmission will change and therefore this promises to be a productive avenue for future research.

A final and important direction for further work with this model is to predict the efficacy of vector control campaigns. There is only limited evidence that current vector control efforts targeting *Aedes* species are effective (Roiz et al., 2022). Population models are frequently used to guide interventions and given this models excellent resemblance to field data it's predictions could be invaluable for assessing how to optimally control vector populations. Current control techniques target different life-stages and determining what combination of control techniques to apply to efficiently reduce biting adult numbers will be a complex problem due to the delayed and non-linear effects of density and environment on mosquito life-history. However, an effective model to evaluate control strategies will likely also require a spatial element to account for local variables important in determining small-scale mosquito abundance (Falcón-Lezama et al., 2016). Additionally, human mediated dispersal has implicated in undermining historic control efforts through regular reintroductions from infested areas (Lee et al., 2021; Goiri et al., 2020). Once again, a deeper understanding of the distribution and properties of developmental habitats will be an important first step in being able to predict the outcome of control.

5.3.3 Adaptation of the model

The model derived in Chapter 4 to predict dengue transmission could readily be adapted to predict the transmission one of the more than 25 other viruses for which *Ae. albopictus* is a competent vector (Amraoui et al., 2019). Of these, the three most well-studied and epidemiologically relevant are Chikungunya (CHIKV), Zika (ZIKV), and yellow fever (YFV). Chikungunya is a growing global threat and *Ae. albopictus* is the primary vector implicated in recent outbreaks, which now occur across the mosquitoes native and invasive range (Silva, Dermody, 2017). A capacity for both horizontal and vertical transmission of ZIKA by *Ae. albopictus* has been demonstrated, which is of growing concern to global public health since the outbreak throughout the Americas in 2015 (Lai et al., 2020). *Ae. albopictus* has also been shown to be a competent vector of yellow fever, though little is currently known about its role in maintaining outbreaks of the disease (Amraoui et al., 2016). To adapt the model to predict the risk of

transmission associated with each of these viruses presents different challenges that would need addressing before specific predictions could be made. However, in each case the primary barrier to achieving model specificity is the lack of knowledge about how traits such as EIP change with temperature within *Ae. albopictus*. Experimental work continues to explore the relationship between temperature and vectorial capacity for each virus, which will be required to understand the risk they pose to public health (Mercier et al., 2022).

The population model developed in Chapter 3 could also be used to predict the populations dynamics of other *Aedes* species over their ranges and as was briefly discussed in Chapter 4. *Ae. aegypti* the primary vector dengue is the obvious candidate. However, although the extension of the population dynamical model may be fairly straightforward, an extension of the SIR model to predict the dynamics of dengue outbreaks vectored by *Ae. aegypti* would require a substantial amount of further work. The lack of strong seasonality throughout the locations over which the transmission of dengue by *Ae. aegpyti* is observed means that outbreaks are often multi-strain, with multiple serotypes co-circulating simultaneously. This complicates the mosquito transmission cycle, as mosquitoes can potentially be simultaneously infected with different DENV serotypes (Pérez-Castro et al., 2016). Different strains of dengue also present different severities of clinical manifestation and there is evidence of strain-specific differences in transmission traits (Andrade et al., 2016; Ekwudu et al., 2020). Long-lasting resistance to further infection in the host population presents a further modelling challenge, as after being infected by a serotype, life-time immunity is incurred to subsequent infection by viruses of the same serotype (Gibbons et al., 2007). Further, infection by one serotype induces a period of cross-immunity against all other serotypes of dengue that can last between $1 - 3$ years (Reich et al., 2013). Tracking the host populations immune status will be critical to understand disease dynamics but also health risk, as individuals that have experienced infection by one serotype have a higher change of developing severe complications upon infection by other serotypes (Woodall, Adams, 2014; Narayan, Tripathi, 2020).

An additional complication in producing accurate predictions of the dengue risk posed by *Ae.*

aegpyti is the presence of *Ae. albopictus* throughout much of its range (Kraemer et al., 2015). In many locations where *Ae. aegpyti* is the primary vector dengue *Ae. albopictus* often also occurs, and it has been suggested that each vector species plays a different role in the maintenance of dengue outbreaks (Lin et al., 2016a). The outcome of competition between these two species is complex and has been shown to depend on local environmental conditions (Juliano et al., 2004; Murrell, Juliano, 2008; Lizuain et al., 2022; Lounibos, Kramer, 2016). These same experiments demonstrate that the relationship between adult wing length temperature, larval density, and food availability is altered by the degree of interspecific that individuals experience, and so the ability of *Ae. aegypti* to maintain dengue outbreaks depends not only on the abundance of *Ae. albopictus* but also the degree they overlap in developmental habitats. Incorporating this into a model would once again require a deeper understanding of the distribution and properties of larval habitats and further experimental work quantifying the effect of interspecific competition on developmental plasticity in both species.

Other mosquito vectors would also be amenable to this approach and both the life-history of West Nile Virus vector *Culex pipiens* and malarial *Anopheles* mosquitoes have previously predicted through delay differential equations (Ewing et al., 2016; Beck-Johnson et al., 2013). The feasibility of extending these models to incorporate developmental plasticity in response to larval competition will depend on the availability of experimental data exploring these relationships, and special care would need to be taken to capture species-specific life-history processes. As these mosquito species inhabitant larger and less temporary habitats than *Ae. albopictus* it will be necessary to start considering the effect of interspecific competition from predators which is known to greatly affect the dynamics and traits of mosquito species. This could be an important avenue of future research as the role of reduced adult trait in response to high larval densities in suppressing malaria outbreaks appears to be complex and evolving (Ijumba, Lindsay, 2001; Chan et al., 2021).

5.3.4 The role of phenotypic plasticity

The general modelling framework is a first step in reconciling theory with empirical evidence regarding the role of phenotypic plasticity in determining population responses to environmental change. In both systems considered here, complex dynamical behaviours that occurred in response to changes in environmental conditions emerged naturally as a consequence of mechanisms of individual variation. Given the uncertainty in the role of phenotypic plasticity in mediating population responses ecological disturbances, this approach represents a promising first step toward a more predictive ecological theory (Hulme, 2008; Violle et al., 2012).

Although the effects of passive developmental plasticity are explored thoroughly here, other forms of phenotypic plasticity are also likely to have complex effects on population dynamics. Maternal effects are an inter-generational form of plasticity that can be anticipatory, whereby the traits expressed by juveniles are determined by adult's predictions of future environmental conditions (Bernardo, 1996). When this form of plasticity is active rather than passive it is prone to cue-anticipation mismatch, where the environmental conditions anticipated by adults and those experienced by juveniles do not match and so an unfavourable trait is expressed (Kuijper, Hoyle, 2015). Maternal effects have been found in ecologically important species, for example both passive and active maternal effects have been observed in desert locusts which are an invasive crop pest, and species of bee which are currently in broad decline (Preston et al., 2019; Maeno et al., 2013). Exploring whether the differential action of active and passive maternal effects on the life-history of these ecologically important species can explain their different responses to the changing climate could be an important avenue of future research with implications for food security (Soroye et al., 2020; Meynard et al., 2020).

Models parametrised using this approach are data-hungry and parametrising multi-dimensional reaction norms requires a substantial amount of life-history data. For vectors of neglected or emerging tropical disease, this does knowledge base does not yet exist and though data collection efforts are ongoing understanding which traits to target will require a greater understanding

of when phenotypic plasticity matters in determining population responses to environmental change. To facilitate this the phenomenological relationships that were used here to describe how the traits expressed by *Ae. albopictus* vary response to the historic environment should also be informed by rigorous theory, such as is proposed in the metabolic theory of ecology (Brown et al., 2004). This would for a more complete description of the mechanisms that are so important in determining population response and this deeper understanding of trait-environment interactions will be necessary to apply this theory to more complex systems with species interactions over multiple trophic levels (Wong et al., 2019).

5.4 Summary

In this thesis I have explored the role of trait variation in determining the risk of vector-borne disease. I derived a novel framework able to represent the effect of environment-trait feedbacks on population dynamics. This model was validated on Nicholson's blowflies and then applied to the invasive mosquito species *Ae. albopictus*. By parametrising experimentally derived multi-dimensional reaction norms I represented the effect of developmental plasticity on the longevity of adult mosquitoes and demonstrate that this approach is able to replicate the population dynamics of field populations of vectors across the species global range as well as predict the timing and magnitude of dengue outbreaks. I demonstrate how the role of trait in determining disease dynamics changes between climates, and how in many of the historic outbreaks considered a small number of large individuals accounted for a majority of transmission events. I further predict, there is currently less risk of dengue transmission in the invaded range than previous approaches but that this risk is increasing.

Appendices

A Model derivation from first principles

To demonstrate that the modelling framework is rigorous it must be derived from first principles, and to do this the derivation of the Gurney et al. (1983) model is extended to include phenotypic plasticity. This demonstrates that this extension of the Gurney et al. stage-structured delay differential equation framework (described in Chapter 1) to represent phenotypic plasticity does not violate the assumptions made in the Gurney et al. framework and so is mathematically rigorous. I begin with the continuous Von Foerster equation, a partial differential equation describing how individuals age, and convert it into a system of coupled delay differential equations (Kermack, McKendrick, 1927).

Consider a single species with constant sex ratio that expresses phenotypic plasticity in d plastic traits in response to a set of z environmental cues. Let all individuals with age a, in environmental class j at time t have the same per capita reproduction and death rates, $\beta_j(a,t)$, and $\delta_j(a,t)$ respectively. Note that these per capita rates are age dependent and so functional forms that reflect demographic processes can be freely chosen. For example, in a species where sexual maturity is reached at age a_m the per capita reproduction rate may be chosen such that $\beta_j(a,t) = 0$ for $a < a_m$. Denote the number of individuals with age in the interval $a \to a + da$ in environmental class j at time t by $f_j(a,t)$. Assuming the system is closed (i.e. no immigration or emigration) describe the change in population due to ageing and death by the Von Foerster

equation (Kermack, McKendrick, 1927)

$$\frac{\partial f_j(a,t)}{\partial t} = \underbrace{-\frac{\partial f_j(a,t)}{\partial a}}_{\text{ageing}} \underbrace{-\delta_j(a,t) f_j(a,t)}_{\text{death}} \qquad a > 0. \tag{1}$$

The rate at which the population produces offspring at time t into environmental class j is described by the renewal condition

$$B_j(t) = f_j(0,t) = \sum_{l=1}^{m} w_{l,j}(\boldsymbol{\alpha}(t)) \int_0^\infty f_l(a,t)\beta_l(a,t)\, da \tag{2}$$

where the function $w_{kj}(\boldsymbol{\alpha}(t))$ determines the fraction of individuals born at time t that acquire life-history parameters associated with environmental class j. As was stated in the overview it is required that $0 \leq w_{kj}(\boldsymbol{\alpha}(t)) \leq 1,\ \forall j,k \in 1,...,m$ and that $\sum_{j=1}^{m} w_{kj}(\boldsymbol{\alpha}(t)) = 1$.

The total birth rate of individuals across all phenotypes is then given by

$$B(t) = \sum_{j=1}^{m} B_j(t) = \sum_{j=1}^{m}\sum_{l=1}^{m} w_{l,j}(\boldsymbol{\alpha}(t)) \int_0^\infty f_l(a,t)\beta_l(a,t)\, da \tag{3}$$

$$= \int_0^\infty \sum_{j=1}^{m}\sum_{l=1}^{m} w_{l,j}(\boldsymbol{\alpha}(t)) f_l(a,t)\beta_l(a,t)\, da. \tag{4}$$

Equation 1 can be solved using the method of characteristics (Kot, 2001) to find $f_j(a,t)$, giving

$$f_i(a,t) = f_i(0,t-a)\exp\left(-\int_{t-a}^{t} \delta_i(t')dt'\right) \tag{5a}$$

$$= B_i(t-a)P_i(t-a,a) \tag{5b}$$

where $P_i(t,a)$ is the cumulative survival probability that an individual born at time t expressing phenotype i survives until at least stage a.

Assume stage transitions occur at fixed time intervals, and that the population has n life-stages. Denote the number of individuals in life-stage i and environmental class j by $N_{i,j}(t)$. Assume that all individuals in life-stage i and environmental class j are functionally identical, such that

$$\delta_j(a,t) = \delta_{i,j}(t), \quad \forall\, a_{i,j} \le a \le a_{i+1,j} \tag{6}$$

$$\beta_j(a,t) = \beta_{i,j}(t), \quad \forall\, a_{i,j} \le a \le a_{i+1,j} \tag{7}$$

where $a_{i,j}$ is the age at which an individual enters life-stage i and environmental class j, and $a_{i+1,j}$ the age when that individual matures to life stage $i+1$. Then divide the population into stages as follows

$$N_{i,j}(t) = \int_{a_{i,j}}^{a_{i+1,j}} f_j(a,t)\, da. \tag{8}$$

Furthermore, define $R_{i,j}(t)$ as the rate of recruitment from stage $i-1$ into age class i for individuals maturing into environmental class j at time t. Similarly, define $M_{i,j}(t)$ as the rate of maturation from life-stage i into the life-stage $i+1$ for individuals in environmental class j at time t. Finally, define $D_{i,j}(t)$ as the rate of death of individuals in life-stage i and environmental class j. Then,

$$\frac{dN_{i,j}(t)}{dt} = R_{i,j}(t) - M_{i,j}(t) - D_{i,j}(t). \tag{9}$$

Integrating Equation (1) over the interval $a_{i,j} \le a \le a_{i+1,j}$ and then comparing to (9) yields the

relationship

$$R_{i,j}(t) = f_i(a_{i,j}, t) \tag{10a}$$

$$M_{i,j}(t) = f_i(a_{i+1,j}, t). \tag{10b}$$

Furthermore, as newborns enter at life-stage $i = 1$,

$$R_{1,j}(t) = f_j(0,t) = \sum_{k=1}^{m} w_{kj}(\boldsymbol{\alpha}(t)) \sum_{v=1}^{n} \beta_{vk}(t) N_{vk}(t) \qquad j \in 1, ..., m. \tag{11}$$

Substitution of the solution (5b) into Equations (10a) and (10b) yields

$$R_{i,j}(t) = B(t - a_{i,j}) P(t - a_{i,j}, a_{i,j}), \qquad i \in 2, ..., n, \;\; j \in 1, ..., m \tag{12a}$$

$$M_{i,j}(t) = B(t - a_{i+1,j}) P(t - a_{i+1,j}, a_{i+1,j}), \;\; i \in 1, ..., n-1, \;\; j \in 1, ..., m. \tag{12b}$$

Define the following quantities,

$$\tau_{i,j} \equiv a_{i+1,j} - a_{i,j} \tag{13}$$

as the duration of stage i for individuals in environmental class j.

Define

$$S_{i,j}(t) = \frac{P_j(t - a_{i+1,j}, a_{i+1,j})}{P_j(t - a_{i+1,j}, a_{i,j})} \tag{14}$$

to represent the fraction of individuals recruited into stage i, and environmental class j at time $t - \tau_{i,j}$ that survive to be recruited into stage $i + 1$ at time t. Note that

$$M_{i,j}(t) = R_{i,j}(t - \tau_{i,j})S_{i,j}(t) \tag{15}$$

and thus

$$R_{i+1,j}(t) = M_{i,j}(t). \tag{16}$$

Hence, the extension of the Gurney et al. modelling framework to phenotypic plasticity is mathematically rigorous.

B The Gurney, Nisbet and Lawton blowfly model

The phenotypically plastic blowfly model is an extension of the non-plastic blowfly model developed by Gurney et al. (1983). The model is a stage-structured delay-differential equation model that considers five life-stages, eggs, larvae, pupae, juvenile adults, and reproductive adults. Denote the number of eggs at time t by $E(t)$, similarly denote the number of larvae by $L(t)$, pupae by $P(t)$, juvenile adults by $J(t)$, and mature adults by $A(t)$. Denote by τ_E, τ_L, τ_P, and τ_J the duration of the egg, larval, pupal, and juvenile developmental stages respectively. Denote by $\delta_E, \delta_L, \delta_P, \delta_J$ the mortality rate of the egg, larval, pupal, and juvenile developmental stages respectively. Define $S_E = e^{-\delta_E \tau_E}$ to be the probability of surviving the duration of the egg developmental stage and similarly define S_L, S_P, and S_J for the larval, pupal, and juvenile stages respectively. Let q be the fecundity of adult blowflies and K_A the amount of adult food supplied daily.

The model takes the form

$$\dot{E(t)} = R_E(t) - R_E(t-\tau_E)S_E - \delta_E E(t) \tag{17a}$$

$$\dot{L(t)} = R_L(t) - R_L(t-\tau_L)S_L - \delta_L L(t) \tag{17b}$$

$$\dot{P(t)} = R_P(t) - R_P(t-\tau_P)S_P - \delta_P P(t) \tag{17c}$$

$$\dot{J(t)} = R_J(t) - R_J(t-\tau_J)S_J - \delta_J J(t) \tag{17d}$$

$$\dot{A(t)} = R_A(t) - \delta_A A(t) \tag{17e}$$

where

$$R_E(t) = qA(t)\exp\{-A(t)/K_A\} + I(t) \tag{18}$$

$$R_L(t) = R_E(t-\tau_E)S_E \tag{19}$$

$$R_P(t) = R_P(t-\tau_L)S_L \tag{20}$$

$$R_J(t) = R_P(t-\tau_P)S_P \tag{21}$$

$$R_A(t) = R_J(t-\tau_J)S_J \tag{22}$$

and the inoculation term, $I(t)$, is a function to initiate the dynamics, akin to an initial condition (Kot, 2001).

Equation 17 can be collapsed down into a single equation for adults given by

$$\frac{dA(t)}{dt} = qSA(t-\tau)\exp\{-A(t-\tau)/K_A\} - \delta_A A(t) + SI(t-\tau) \tag{23}$$

where $S = S_E S_L S_P S_J$, and $\tau = \tau_E + \tau_L + \tau_P + \tau_J$.

The Gurney et al. model describes adult competition, with the assumption that larvae always acquire sufficient food. Adult blowflies that do not get sufficient protein from food must resorb oocytes to complete egg maturation, directly reducing fecundity (Vogt et al., 1985), which is represented by a direct reduction of fecundity when adult density is high. Competition for adult resources produces was found to explain the population cycles, matching the period of the oscillations observed by Nicholson (Nicholson, 1957), but underestimated the population peaks.

C Steady-state analysis

To determine the long-term behaviour of the phenotypically plastic blowfly model stability analysis is performed, beginning with an analysis of the non-plastic model described in Appendix A.

C.1 Identification of steady-states of the Gurney et al. blowfly model

The blowfly model presented in Gurney et al. (1983) and described in Equations (17) can be reduced to

$$\frac{dL}{dt} = R_L(t) - R_L(t-\tau_L)S_L - \delta_L L(t) \tag{24}$$

$$\frac{dA}{dt} = R_A(t) - \delta_A A(t) \tag{25}$$

where

$$R_L(t) = qA(t-\tau_E)\exp^{\frac{-A(t-\tau_E)}{K_A}} S_E \tag{26}$$

$$R_A(t) = R_L(t-\tau_J)S_J. \tag{27}$$

This system has a trivial steady state $(0,0)$, and a single non-trivial steady state given by

$$L^* = \frac{-\delta_A K_A S_E(1-S_L)}{\delta_L S_E S_L S_J}\ln\left(\frac{\delta_A}{qS_E S_L S_J}\right) \tag{28}$$

$$A^* = -K_A \ln\left(\frac{\delta_A}{qS_E S_L S_J}\right). \tag{29}$$

To determine the stability of these steady-states consider a linearisation of the system about each steady state. For a generic steady-state located at (L_{Eq}, A_{Eq}), for $\bar{L} = L - L_{Eq}$, and $\bar{A} = A - A_{Eq}$ the linearisation then takes the form,

$$\begin{pmatrix} \frac{d\bar{L}}{dt} \\ \frac{d\bar{A}}{dt} \end{pmatrix} = V_0 \begin{pmatrix} \bar{L}(t) \\ \bar{A}(t) \end{pmatrix} + V_1 \begin{pmatrix} \bar{L}(t-\tau_E) \\ \bar{A}(t-\tau_E) \end{pmatrix} + V_2 \begin{pmatrix} \bar{L}(t-\tau_E-\tau_L) \\ \bar{A}(t-\tau_E-\tau_L) \end{pmatrix} + V_3 \begin{pmatrix} \bar{L}(t-\tau_E-\tau_L-\tau_J) \\ \bar{A}(t-\tau_E-\tau_L-\tau_J) \end{pmatrix} \tag{30}$$

where

$$V_0 = \begin{pmatrix} -\delta_L & 0 \\ 0 & -\delta_A \end{pmatrix} \tag{31}$$

$$V_1 = \begin{pmatrix} 0 & qe^{\frac{-A^{Eq}}{K_A}}(1 - \frac{A^{Eq}}{K_A})S_E \\ 0 & 0 \end{pmatrix} \tag{32}$$

$$V_2 = \begin{pmatrix} 0 & -qe^{\frac{-A^{Eq}}{K_A}}(1 - \frac{A^{Eq}}{K_A})S_E S_L \\ 0 & 0 \end{pmatrix} \tag{33}$$

$$V_3 = \begin{pmatrix} 0 & 0 \\ 0 & qe^{\frac{-A^{Eq}}{K_A}}(1 - \frac{A^{Eq}}{K_A})S_E S_L S_J \end{pmatrix}. \tag{34}$$

C.2 The stability of the trivial steady-state

I begin by determining the stability of the trivial steady state for different values of the plastic traits S_J and q. Fix all the remaining parameters at the values given in Gurney et al. model. When all the delays are infinite, i.e. $\tau_E = \tau_L = \tau_J = \infty$, the trivial steady-state is stable unconditionally. When all the delays are 0, i.e. $\tau_E = \tau_L = \tau_J = 0$, the trivial steady-state

is stable provided $\delta_A > qS_ES_LS_J$. It can be shown that for the chosen reaction norms this condition holds provided $S_J = 0$.

C.3 The stability of the non-trivial steady-state

To determine the stability of the non-trivial steady-state the value of all non-plastic parameters are fixed to determine what conditions on S_J and q give stability. As in the trivial steady state it can readily be shown that after linearisation that the non-trivial steady state is unconditionally stable when the delays are infinite. When the delays are 0 a necessary condition on the stability of the non-trivial steady-state is, $\delta_A > qe^{-\frac{A^*}{K_A}}S_ES_LS_J(1-\frac{A^*}{K_A})$. In subsequent analysis the value of K_A is varied, with this in mind note that the substitution of the expression for A^* into the condition demonstrates it is independent of the value of K_A for fixed q and S_J. The necessary condition on stability for the non-trivial steady state is satisfied provided, $q \geq 4.853\,\text{day}^{-1}$ and $S_J \geq 0.056\ \forall\, K_A$.

Supposing that the condition on stability holds, I now aim to demonstrate that the system is asymptotically stable independent of the delay. To do this consider Proposition 1 taken from (Kruthika et al., 2017).

Proposition 1. *The time-delay system is asymptotically stable if there exist matrices $X > 0$, $H_1 > 0$, $H_2 > 0$, and $H_3 > 0$, such that,*

$$Q = \begin{bmatrix} XV_0 + V_0^T G + \sum_{i=1}^{3} H_i & XV_1 & XV_2 & XV_3 \\ V_1^T X & -H_1 & 0 & 0 \\ V_2^T X & 0 & -H_2 & 0 \\ V_3^T X & 0 & 0 & -H_3 \end{bmatrix} < 0 \tag{35}$$

then the system is asymptomatically stable, independent of the delay.

The condition in Proposition 1 is a linear matrix inequality (LMI), and in this context $Q < 0$ indicates that the matrix Q should be negative-definite. This condition is evaluated here using

the YALMIP toolbox (Löfberg, 2004) in MatLab (MATLAB, 2019). Proposition 1 can be used to estimate the region of stability of the non-trivial steady state finding that the non-trivial steady-state is stable in the region of $q \in [5.386, 12.423]$ and $S_J \in [0.0594, 0.169]$.

C.4 Steady-states of the phenotypically plastic blowfly model

Now consider the steady-states of the phenotypically plastic blowfly model created using the novel framework. At steady-state the larval density is constant, and so only one $w_j(\alpha(t))$ is non-zero when the system is at steady-state. This means that at any given time all larvae maturing into adults are in the same environmental class and so share the same life-history parameters as adults. Thus, the number of non-trivial steady states is at maximum m the number of environmental classes in the discretisation. To represent both food scenarios used in the Nicholson culture in the subsequent analysis K_A takes one of two values, $K_A = 1,200$mg when food is limited and $K_A = 2,000$mg when food is unlimited.

The system has the trivial steady state and up to m potential non-trivial steady states located at

$$L_j^* = \frac{-\delta_A K_A S_E (1 - S_L)}{\delta_L S_E S_L S_{J_j}} \ln\left(\frac{\delta_A}{q_j S_E S_L S_{J_j}}\right) \tag{36}$$

$$A_j^* = -K_A \ln\left(\frac{\delta_A}{q_j S_E S_L S_{J_j}}\right) \qquad \text{for } j \in 1, ..., m. \tag{37}$$

Not all of these potential steady-states are truly steady-states as the level of competition associated with L_j^* may result in adults being recruited in A_p^* where $p \neq j$. If this is the case the system is still in flux and so these are not true steady states. The number of steady states is therefore equal to the number of times the L^* larval steady state intersects the discretisation of the environmental cue $\alpha(t)$. In Figure C.1 I show that for both values of K_A there is only one point of intersection. This means that for each value of K_A the system only has one non-trivial

steady-state which is now sought.

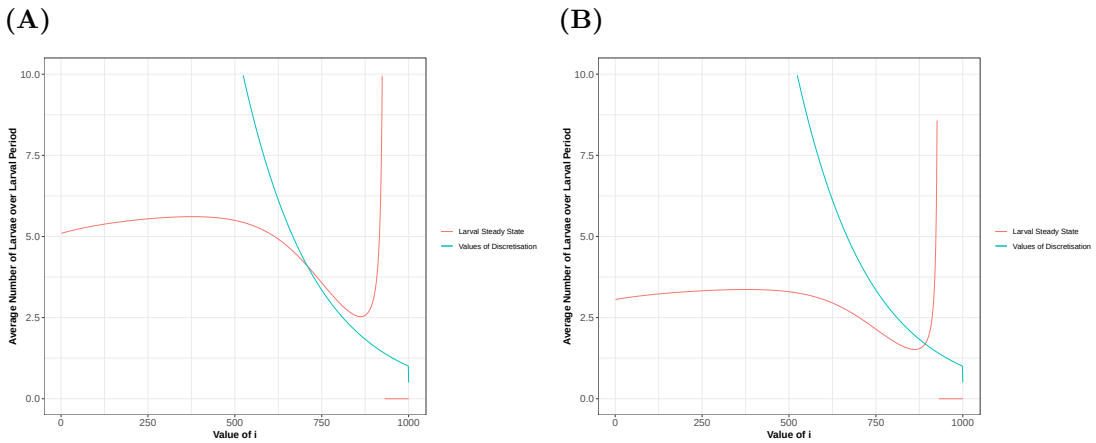

Figure C.1: Comparison of the values of the larval steady state and the discretisation of larval competition take with **(A),** $K_A = 1,200$mg, and **(B),** $K_A = 2,000$mg. In both cases the models were parametrised with $m = 900$, the trait class is indicated by j.

It can be shown that when $K_A = 1,200$mg these conditions are approximately met when $q = 21\,\text{day}^{-1}, S_{J_i} = 0.4823$. Based on previous analysis for the Gurney et al. (1983) model the trivial steady-state is unstable for this parameter combination. Similarly, using Proposition 1 the non-trivial steady state is unstable for this food condition. When $K_A = 2,000$mg using the necessary condition on stability I find that the both the trivial and non-trivial steady states do not meet the conditions for stability. Simulations of the model demonstrate oscillatory solutions for each adult food value, consistent with this result.

D Improved fit to the Nicholson culture data

Qualitatively the simulation of the blowfly model under replica experimental conditions in Figure 2a matches the experimental data for early time points but fails to produce oscillations of the correct amplitude after the amount of adult food supplied is restricted. I hypothesise that the reason for this is the high sensitivity of the model to small changes in food supply in the region of parameter space around Nicholson's experimental conditions as can be observed in Figure 4. By increasing the larval food supplied throughout the culture by 30%, increasing the initial adult supply by 20% and decreasing it by 16% after the reduction the dynamical behaviour exhibited in the Nicholson blowfly culture are better captured as shown in Figure D.1. The simulation with altered food supplies now exhibits oscillatory behaviour of the correct amplitude and the models predictions qualitatively match the data from the culture.

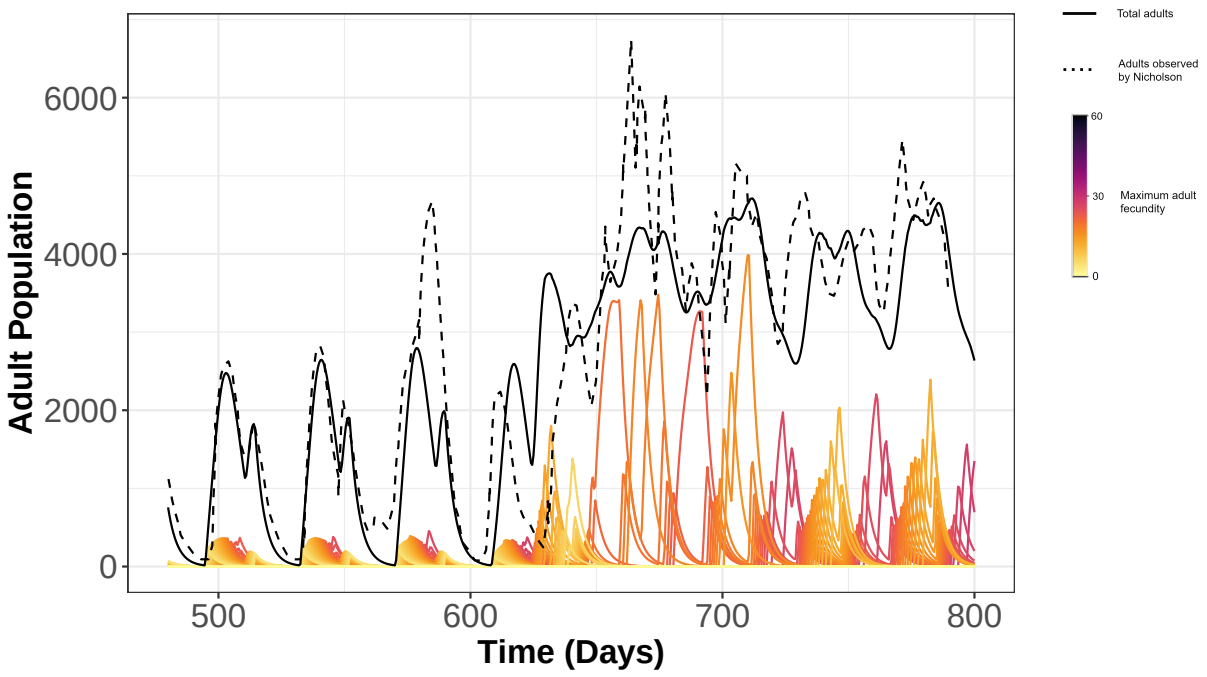

Figure D.1: Simulations of blowfly model with the unlimited food condition, represented by $K_A = 2400$ which is switched at 607 days to $K_A = 1000$mg, with $K_L = 65000$mg in both periods. The system is initiated with 48500 larvae when the culture starts when $t = 0$ days.

E Worked examples of models made using the framework

E.1 A model for a species that expresses phenotypic plasticity in response to the cumulative effect of multiple environmental cues across multiple life-stages

Consider a population with $i = 3$ life-stages N_1, N_2, and N_3 that are each subject to an environmental cue specific to that stage. Define $\alpha_{N_1}(t)$ and $\alpha_{N_2}(t)$ to be the average exposure to the environmental cues specific to life stages N_1 and N_2 respectively that an individual maturing out of that life-stage at time t experienced. Also define $\alpha_{N_3}(t)$ to be the state of the environmental cue specific to life-stage N_3 at time t. Therefore, define the vector of environmental cues to be

$$\boldsymbol{\alpha(t)} = (\alpha_{N_1}(t), \alpha_{N_2}(t), \alpha_{N_3}(t))$$

and so in this example $z = 3$. Each $\alpha_{N_i}(t)$ is discretised into m_{N_i} subintervals where the p^{th} subinterval of $\alpha_{N_i}(t)$ is denoted $\alpha_{N_i p}$. Note that these cues are not precluded from depending on one another and that such a dependency could be used to represent that an unfavourable experience in life-stage N_1 causes deleterious effects in life-stage N_2 and so on. Similarly these three environmental cues could represent the value of a single environmental variable at three developmentally important times.

An environmental class in this case is a vector of the form

$$(\alpha_{N_1 l_1}, \alpha_{N_2 l_2}, \alpha_{N_3 l_3})$$

where $l_1 \in 1, ..., m_{N_1}$, $l_2 \in 1, ..., m_{N_2}$, and $l_3 \in 1, ..., m_{N_3}$. Define the function g as in the main text and assign a lexicographical ordering to the set of environmental classes Ω_α which has $m = m_{N_1} m_{N_2} m_{N_3}$ elements. Let $\boldsymbol{\alpha}^k$ denote the k^{th} element of Ω_α. This equips us with notation necessary to refer to any combination of the three environmental cues using a single index. For example, suppose $m_{N_1} = m_{N_2} = m_{N_3} = 4$ then define an lexicographical ordering to the set

of environmental classes such that $\boldsymbol{\alpha^1} = (\alpha_{N_1 1}, \alpha_{N_2 1}, \alpha_{N_3 1})$, $\boldsymbol{\alpha^2} = (\alpha_{N_1 1}, \alpha_{N_2 1}, \alpha_{N_3 2})$, $\boldsymbol{\alpha^3} = (\alpha_{N_1 1}, \alpha_{N_2 1}, \alpha_{N_3 3})$, $\boldsymbol{\alpha^4} = (\alpha_{N_1 1}, \alpha_{N_2 1}, \alpha_{N_3 4})$, $\boldsymbol{\alpha^5} = (\alpha_{N_1 1}, \alpha_{N_2 2}, \alpha_{N_3 1})$ and so on.

Assume that the transition function that governs movement through the phenotypic structure $w_{kj}(\boldsymbol{\alpha}(t))$ is defined as in the main text. The transition function describes the proportion of individuals currently in environmental class k that transition to environmental class j at time t and is not explicitly stage-dependent. Although this may initially seem like this causes all individuals at across all life-stages to transition between classes in the same way, this is not the case as the environmental vector $\boldsymbol{\alpha(t)}$, that the transition function w_{kj} acts upon, can be (and often is) stage-dependent. This ensures that stage-specific environmental experiences can be accounted for and that a cohorts environmental history can be tracked. Indeed, at this point these is freedom to determine how the cumulative consequences of environmental conditions in previous life-stages is represented through the form of the transition functions which will be largely determined by the empirical evidence.

For example, I could instead consider a form of $w_{kj}(\boldsymbol{\alpha}(t))$ where an individual's transition to the subsequent environmental class is restricted to closely related environmental classes e.g. an individual currently in environmental class j can only transition to environmental classes within $j \pm 4$. Alternatively, I may assign individuals to environmental classes based on a distribution with skew based on the environmental history of that individual. This would represent some sort of irreversible effect of previous environmental experiences on subsequent fitness. It may also be desirable to change the form of the transition functions across different life-stages, and this is not prohibited.

Define the stage durations $\tau_{i,j}$ and $S_{i,j}(t)$ as in the main text and assume that individuals in life-stage N_3 produce offspring at a rate β. I now need to specify how the environment determines the life-history traits of individuals within the model, and this is where specific forms of phenotypic plasticity are considered. An individual's mother's exposure to α_{N_3} in life-stage N_3 determines the mortality rate of individuals in life-stage N_1 through a maternal effect.

An individual's exposure to α_{N_1} in life-stage N_1 has no effect. In life-stage N_2 an individual's previous experience of the environmental cue $\alpha_{N_1}(t)$ in life-stage N_1 in combination with the maternal effect from life-stage N_3 is assumed to alter that individual's mortality rate through developmental plasticity. In life-stage N_3 assume that an individual's previous experience of $\alpha_{N_1}(t)$ in life-stage N_1, of $\alpha_{N_2}(t)$ in life-stage N_2, and the maternal effect alter the mortality rate of that individual in life-stage N_3.

The parameters in this population that are altered by the expression of phenotypic plasticity are the stage-specific mortality rates. The mortality rate of individuals in life-stage N_i is determined by the reaction norm $\delta_{N_i}(\boldsymbol{\alpha}(t))$. Define the mortality rate of an individual in life-stage N_i and environmental class j to be $\delta_{i,j} = \delta_{N_i}(\boldsymbol{\alpha^j})$. Note that because some life-stages are independent of certain environmental cues this will introduce redundant environmental classes to the model. For example, it previously was assumed that the mortality rate of an individual in life-stage N_1 is dependent solely upon the experience of the environmental cue $\alpha_{N_3}(t)$ by that individual's mother in life-stage N_3. This means that for environmental classes $\boldsymbol{\alpha^v} = (\alpha_{N_1 v_1}, \alpha_{N_2 v_2}, \alpha_{N_3 l})$, and $\boldsymbol{\alpha^b} = (\alpha_{N_1 b_1}, \alpha_{N_2 b_2}, \alpha_{N_3 l})$ with $v, b \in 1, ..., m, \quad b_1, v_1 \in 1, ..., m_{N_1},\ b_2, v_2 \in 1, ..., m_{N_2}$, and $l \in 1, ..., m_{N_3}$ and $\delta_{N_1 v} = \delta_{N_1}(\boldsymbol{\alpha^v}) = \delta_{N_1}(\boldsymbol{\alpha^b}) = \delta_{N_1 b}\ \forall v_1, v_2, b_1, b_2$. Although this is inelegant this does not hinder the function of the model and if desired these redundant environmental classes can be addressed by utilising the simplifications Section 2.3.4.

The model then has the following form

$$\frac{dN_{1,j}}{dt} = R_{N_{1,j}}(t) - M_{N_{1,j}}(t) - \delta_{N_1,j} N_1(t) \tag{38a}$$

$$\frac{dN_{2,j}}{dt} = R_{N_{2,j}}(t) - M_{N_{2,j}}(t) - \delta_{N_2,j} N_2(t) \tag{38b}$$

$$\frac{dN_{3,j}}{dt} = R_{N_{3,j}}(t) - \delta_{N_3,j} N_3(t) \tag{38c}$$

with

$$R_{N_1,j}(t) = \sum_{k=1}^{m} w_{kj}(\boldsymbol{\alpha}(t))\beta N_{3,k}(t) \tag{39}$$

$$R_{N_2,j}(t) = \sum_{k=1}^{m} w_{kj}((\alpha_{N_1}(t), \alpha_{N_2}(t), \alpha_{N_3}(t-\tau_{N_1}))R_{1,k}(t-\tau_{1,k})S_{1,k}(t) \tag{40}$$

$$R_{N_3,j}(t) = \sum_{k=1}^{m} w_{kj}((\alpha_{N_1}(t-\tau_{N_2}), \alpha_{N_2}(t), \alpha_{N_3}(t-\tau_{N_1}-\tau_{N_2}))R_{2,k}(t-\tau_{1,k})S_{2,k}(t) \tag{41}$$

$$M_{i,j}(t) = R_{i,j}(t-\tau_{i,j})S_{i,j}(t) \tag{42}$$

for $j \in 1, ..., m$. Note that delays in the transition functions ensure that ensure that the environmental states in previous life-stages correspond to the expression of the trait in the current life-stage. Observe that despite a complicated life-history, the process of model formulation has not become substantially more complicated than the blowfly model presented here.

E.2 Example of a model with maternal effects and size based competition

In this example I adapt the blowfly model to also include a maternal effect in response an abiotic environmental cue that modifies the strength of competitive interactions between larvae. This is purely a theoretical exercise to demonstrate and is not intended to represent a specific aspect of blowfly population dynamics.

Consider a population such as described in the blowfly model, with two explicitly represented life-stages each of which compete for a separate amount of resource that is replenished daily. In addition to the developmental plasticity previously represented, assume that there is a maternal effect in response to an abiotic environmental cue experienced in the adult stage that determines the size of larvae produced by each adult. Further assume that larval size determines the ability of larva to compete for the shared larval resource, a relatively common form of phenotypic plasticity (Burgess, Marshall, 2011). The resulting model has a structure similar to that depicted in Figure 2b.

Denote the number of larvae with mothers that experienced environmental conditions associated with environmental class j present in the population at time t by $L_j(t)$, and define $L_{Tot}(t) = \sum_{j=1}^{m} L_j(t)$. Order the environmental classes such that larvae in environmental class 1 are the smallest and least competitively viable and those in m are largest and most competitively viable and assume that increased exposure to the abiotic environmental cue increases the size of larvae. To represent the differing relative strength of interaction between larvae in different classes define interaction terms γ_j that describe the rate at which individuals in environmental class j acquire juvenile resources relative to the other larvae. In this case assume that $\gamma_j = \frac{j}{m}$, and additionally assume that each day all larval resource is completely consumed and there is no reduction in the rate of resource acquisition due to satiation. Then define the average amount of food consumed by a larva in environmental class j per day as

$$\alpha_j(t) = \frac{K_L \tau_L^2 \gamma_j}{\int_{t-\tau_L}^{t} \sum_{r=1}^{m} \gamma_r L_r(s) ds} \quad \text{for } j \in 1, ..., m. \tag{43}$$

Once again this can be converted to a derivative for ease of computation

$$\frac{d\alpha_j(t)}{dt} = \frac{-\alpha_j^2(t)(\sum_{r=1}^{m} \gamma_r L_r(t) - \sum_{r=1}^{m} \gamma_r L_r(t-\tau))}{K_L \tau_L^2 \gamma_j} \quad \text{for } j \in 1, ..., m \tag{44}$$

Denote the abiotic environmental cue $\chi(t)$, and assume that it oscillates with period ζ. The corresponding transitions function for this cue are denoted $\eta_j(t)$.

The model then takes the form

$$\frac{dL_j(t)}{dt} = R_{L_j}(t) - R_{L_j}(t-\tau_L)S_L - \delta_L L_j(t) \tag{45a}$$

$$\frac{dA_j(t)}{dt} = R_{A_j}(t) - \delta_A A_j(t) \tag{45b}$$

$$\frac{d\alpha_j(t)}{dt} = \frac{-\alpha_j^2(t)(\sum_{r=1}^{m}\gamma_r L_r(t) - \sum_{r=1}^{m}\gamma_r L_r(t-\tau))}{K_L \tau_L^2 \gamma_j} \tag{45c}$$

$$\frac{d\chi(t)}{dt} = \frac{2\pi}{\zeta}\cos\left(\frac{2\pi t}{\zeta}\right) \tag{45d}$$

for $j \in 1, ..., m$. The recruitment terms are given by

$$R_{L_j}(t) = \eta(\chi_j(t-\tau_E))\left[\sum_{j=1}^{m} q_j A_j(t-\tau_E)e^{-A_{\mathrm{Tot}}(t-\tau_E)/K_A} + I(t-\tau_E)\right]S_E \tag{46}$$

$$R_{A_j}(t) = \sum_{j=1}^{m} w_j(\alpha_j(t-\tau_P-\tau_J))R_L(t-\tau_L-\tau_P-\tau_J)S_L S_{J_j} \tag{47}$$

for $j \in 1, ..., m$ where $I(t-\tau_E)$ is an inoculation term that begins the dynamics (Kot, 2001), and represents the introduction of larvae into the system at $t = 0$, and q_j and S_{J_j} are determined by the reaction norms. The general approach taken here to represent differences in intraspecific competitive ability between phenotypes could easily be extended to interspecific interactions, with the addition extra sets of equations to represent different species and appropriately defined interaction terms. An example of a simulation of this model is provided in Figure E.1.

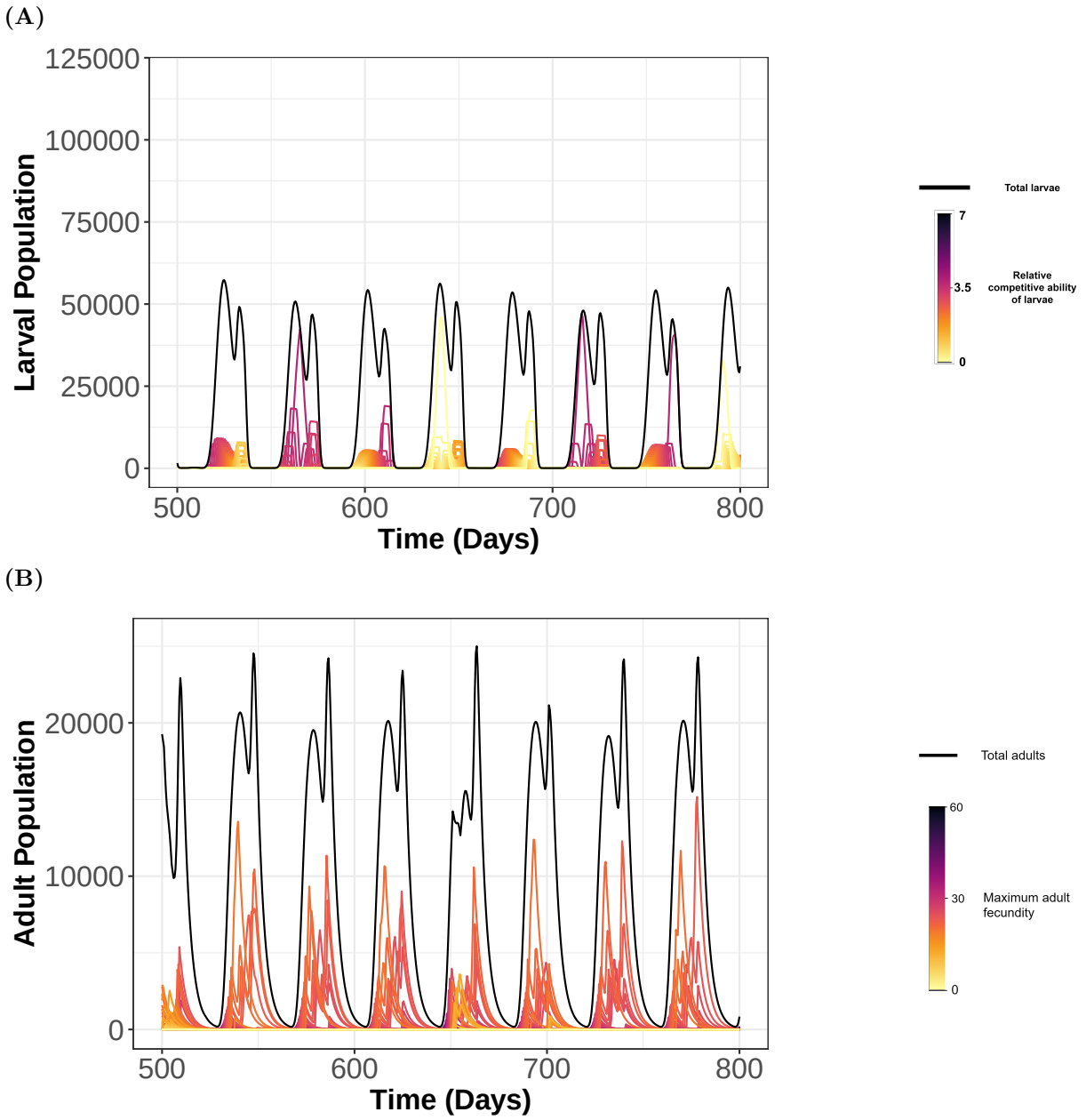

Figure E.1: Example simulation of the maternal effects model with $K_L = 50000$ and $K_A = 1,200$. **(A)** The dynamics of the larval population. The solid black line is the total number of larvae across all phenotypes and the coloured lines each represent the number of larvae in an environmental class. **(B)** The dynamics of the adult population, with the black line representing the total number of adults across all environmental classes and the coloured lines representing the number of adults in each environmental class.

F Example of model predictions

To demonstrate how model functions before presenting the global validation I begin by considering the population dynamics predicted by the model in a single location, in this case Rimini, Italy. This is a temperate location in the species invaded range where in 2007 the population of *Ae. albopictus* established in this region facilitated an outbreak of Chikungunya (Carrieri et al., 2011). In subsequent years a network of ovitraps was set-up throughout the Emilio-Romagna region, and it is to these observations I compare the models predictions (Carrieri et al., 2012).

F.1 Environment

To simulate the model in this region I input the observed temperature, precipitation, as well as the latitude of Rimini (Figure F.1). Using these quantities I simulate the model, initiating the dynamics in the year 2006 to allow a burn-in period for the population dynamics, preventing the chosen initial conditions from altering the dynamics in the prediction year. Through equation 3.7 these environmental variables are used to determine how the food available to larvae varies seasonally, as shown in Figure F.1D.

F.2 Eggs

In Figure F.2A the dynamics of the various egg classes as predicted by the model in Rimini are shown. Active eggs are produced throughout the summer and autumn, before falling temperatures and photoperiod trigger the production of diapausing eggs. As the temperature warms the duration of time taken for active eggs to develop decreases and a greater proportion survive through to the larval stage (Figures F.2B and F.2C). Diapause eggs are produced in a short period of time before cold temperatures cause any remaining adults to die off, and these dormant eggs persist throughout the winter months experiencing a constant low level of mortality. In this region the temperatures never drop low enough to reach the lower thermal limit on diapause egg

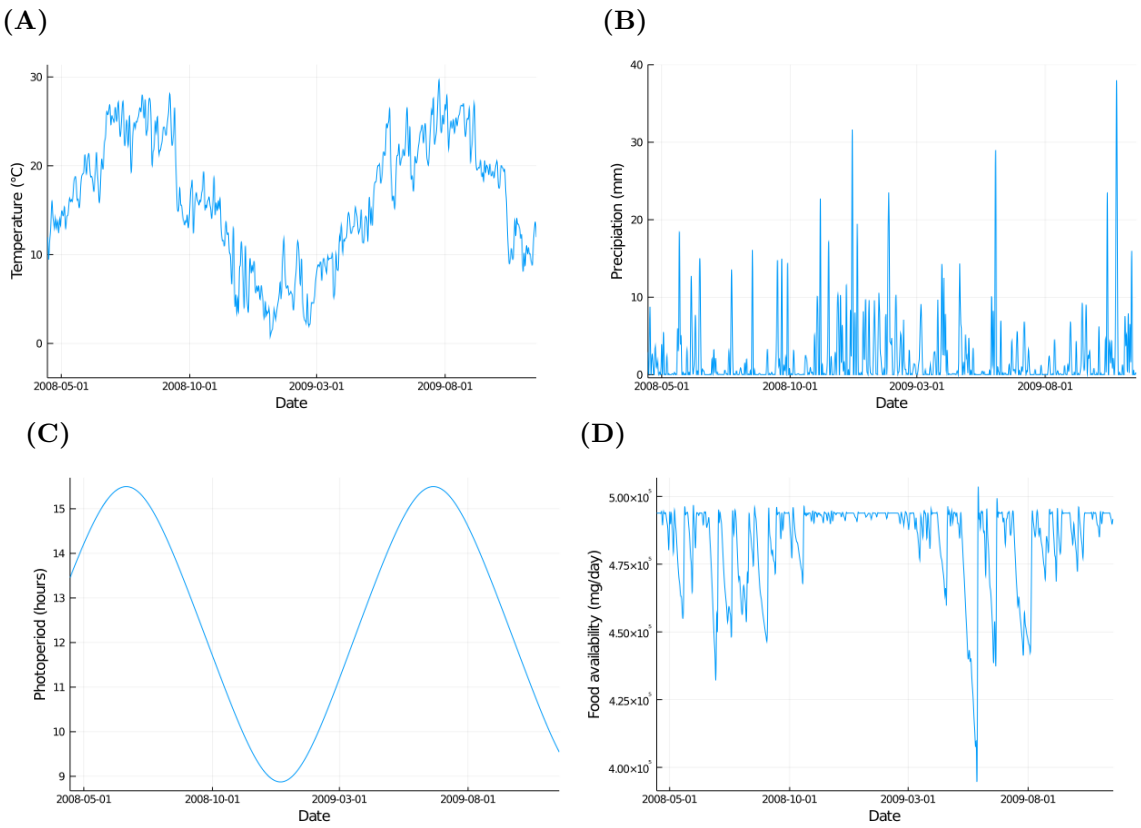

Figure F.1: The environmental variables used to simulate the model in Rimini. (A) Temperature. (B) Precipitation.(C) Photoperiod. (D) Total food produced in the developmental habitat per day.

survival described in Equation 3.6, allowing a sufficient number of eggs to survive through the winter to allow the population to persist in this region between years. When the critical photoperiod and temperature are reached these diapause eggs hatch into larvae and allow the life-cycle to continue. Quiescent eggs are produced in low-levels throughout the year whenever the water level of the container habitat begins to decrease, immediately hatching when inundated.

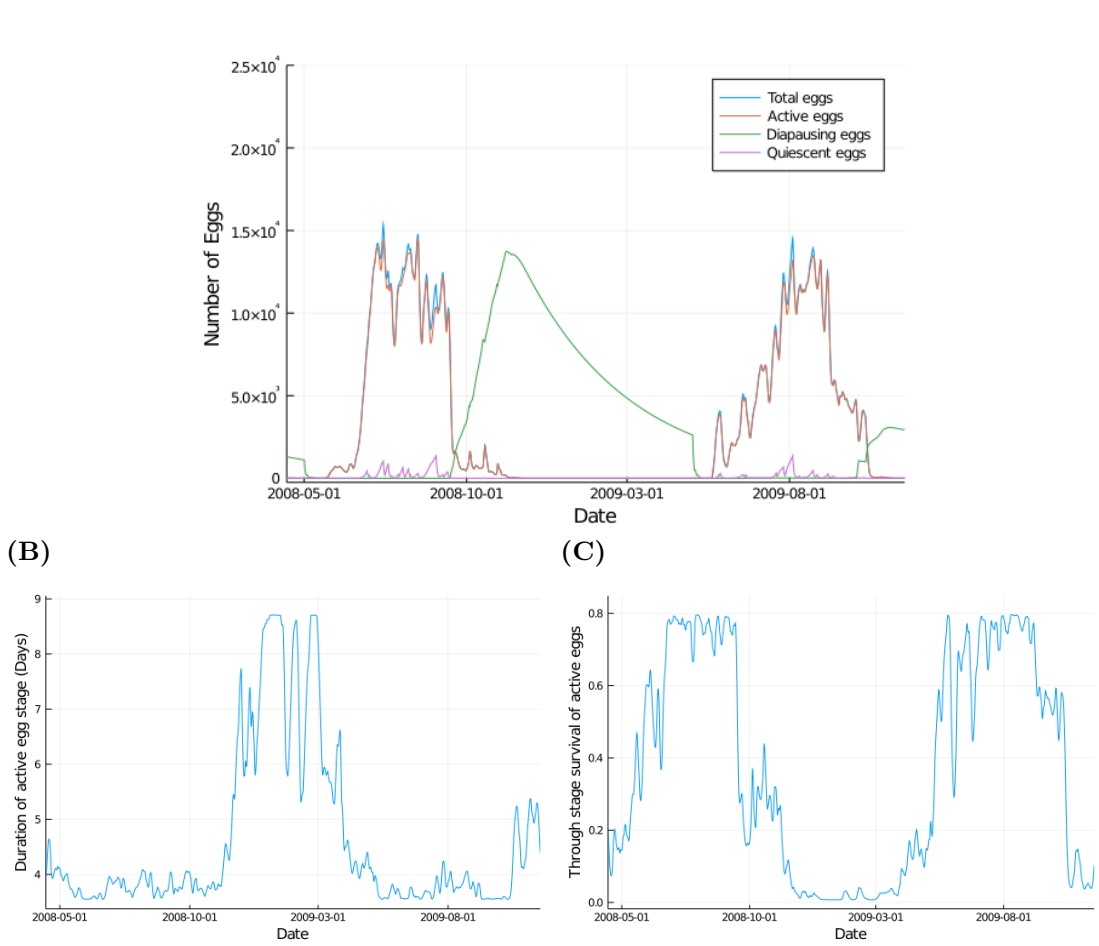

Figure F.2: Outputs from the model when simulated in Rimini, Italy for the egg stages. (A) The number of eggs predicted by the model. The blue line is the total number of eggs across all classes, the orange line is the number of active eggs, the green line represents the number of diapausing eggs, and the purple line the number of quiescent eggs. (B) How the duration of the active eggs, τ_{E_γ}, stage varies throughout the period considered.(C) How the proportion of eggs that survive through the egg class, S_{E_γ}, varies.

To compare the number of eggs predicted by the model to the number of eggs collected in

ovitraps in Rimini I apply equation 3.31 to the predicted population dynamics to produce a prediction of oviposition activity (Figure G.1A). The models predictions of total egg number and the calculated oviposition activity display different dynamics. This occurs due to the varying duration of the egg stage, temperature induced fluctuations in the length of the gonotrophic cycle, and variation in adult trait, leading to different numbers of eggs accumulating in the habitat than are detected in the regularly sampled ovitrap. To make the comparison between the models prediction and field observation I apply a scaling factor and time-shift to maximize R^2. The scaling factor applied is, $sf = 0.007$, and I find that no time-shift is required. Under these transformations the model predicts the observed oviposition activity in Rimini in 2008 accurately with $R^2 = 0.92$.

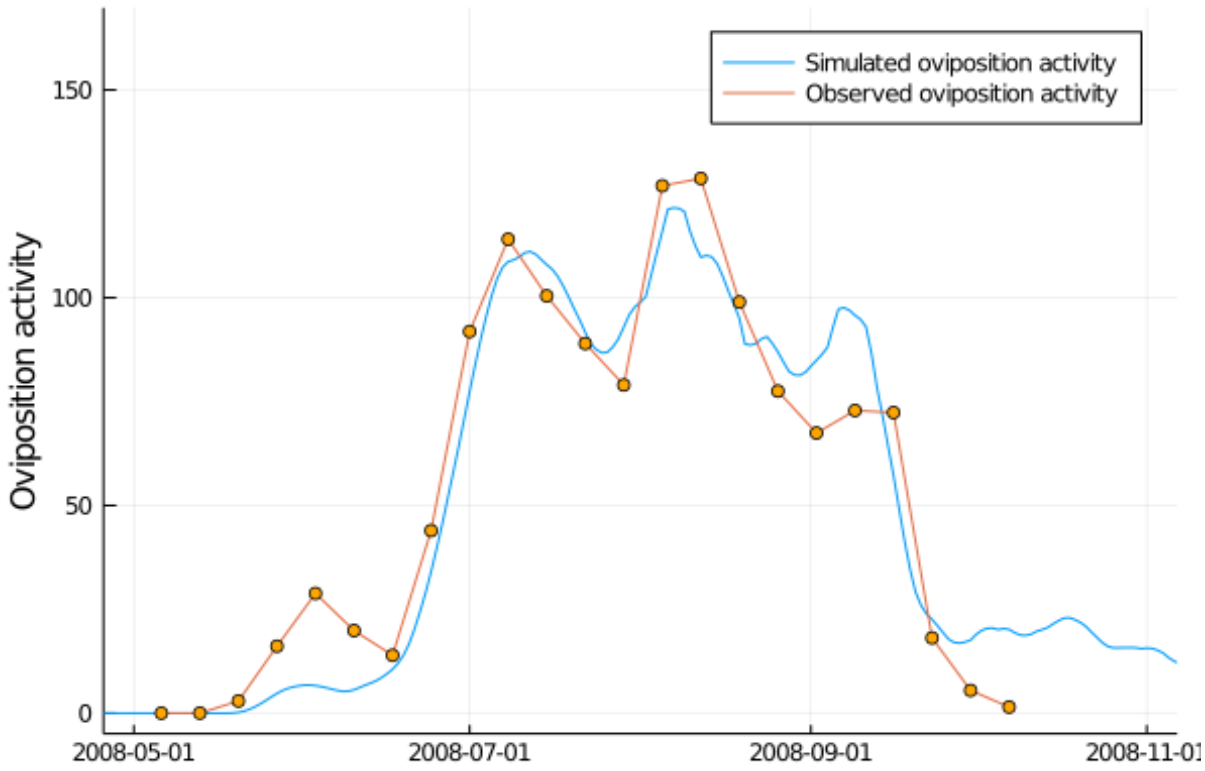

Figure F.3: A comparison of the predictions of the model (blue line) and field data (orange points and line) in the Emilio-Romagna region in the year 2008

F.3 Larvae

In Figure F.4 the abundance and traits that are predicted for larval mosquitoes are shown. The initial generation of larvae emerges due to the release of dormant eggs from diapause resulting in the synchronised spike in larval density observed at the start of the active season (Figure F.4A). After this initial generation of pharate larvae, larval numbers increase over the course of the year, eventually reaching densities unfavourable for successful development. This leads to low through stage-survivals towards the latter half of the year, which is compounded by the decrease in temperature that occurs over the same period.

F.4 Adults

The model's predictions of adult abundance follow the same seasonal trends exhibited by eggs and larvae. The wing length of adults varies through the season and between years but generally in this region the first generation of adults produced from pharate larvae have low wing lengths due to developing under unfavourable temperatures. Wing length then increases as temperatures increase towards the end of summer and then subsequently decrease as larval competition intensifies. Between years there is variation in the time of peak adult population, the start and end of the active season, and in the population's trait distribution.

(A)

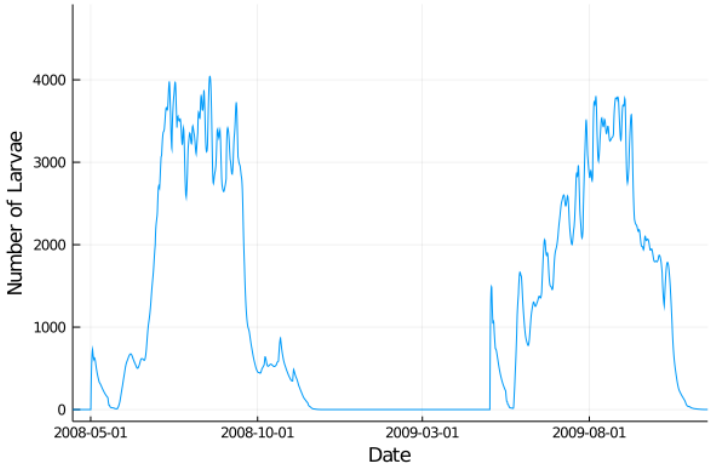

(B)

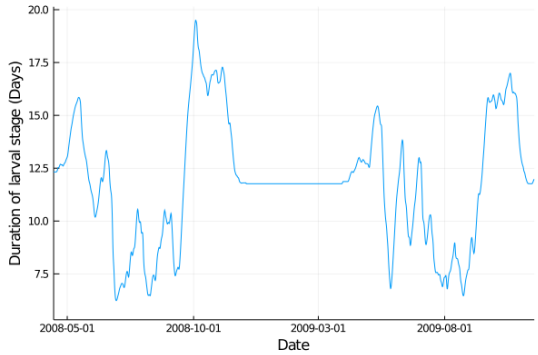

(C)

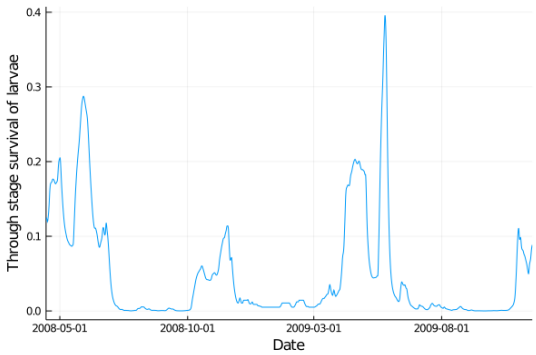

Figure F.4: Outputs from the model when simulated in Rimini, Italy for the larval stage. (A) The number of larvae predicted by the model. (B) How the duration of the larval stage, τ_L, varies throughout the period considered.(C) How the proportion of eggs that survive through the larval stage, S_L, varies.

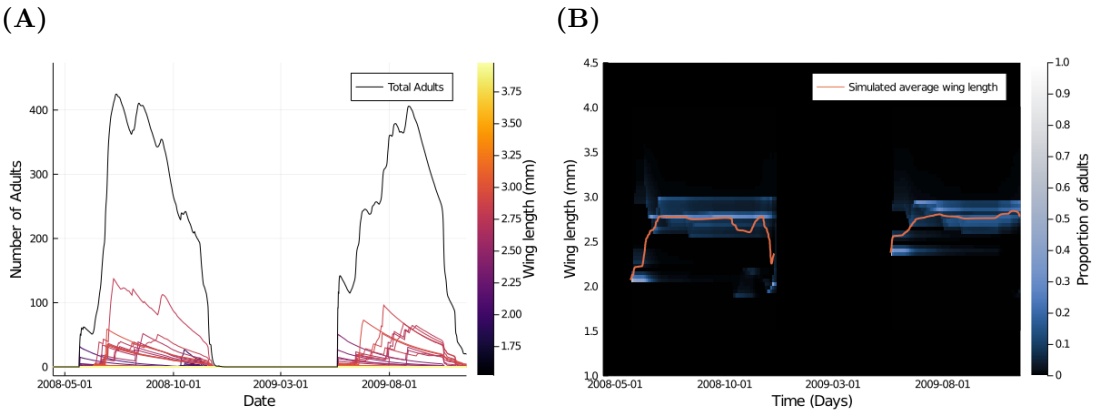

Figure F.5: Outputs from the model when simulated in Rimini, Italy for the adult stage. (A) How the number of adults varies through the year. Each coloured line represents the number of adults in an environmental class with a specific wing length, and the black line is the total number of adults across all environmental classes. (B) The model's prediction of the wing lengths expressed by adults in Rimini, the orange line is the population average trait and each blue line represents the proportion of adults within the population that express the corresponding wing length.

G Validations of the population dynamical model

Here the model derived in Chapter 3 is validated by comparing the predictions the model makes about the population and trait dynamics of *Ae. albopictus* to data observed in field studies. To compare the predicted dynamics to those observed in the field population goodness of fit is quantified using R^2. As both the field studies and the model's predictions only reflect relative abundance a scaling factor is uniformly applied to the predictions. The precise time of sampling is often ambiguous and so a uniform time-shift of observations by up to half of the interval between samples is also permitted. The scaling factor and time-shift pair is selecting by trialling a range of possible values and retaining the pair that produces the maximum R^2 value. For datasets with multiple years of observations a single scaling factor and time shift is used for the entire dataset, preserving comparisons of relative density and fit between years. For each validation both the scaling factor and the time shift are reported in addition to the value of R^2.

G.1 Europe

Emilio-Romagna, Italy

A network of ovitraps is maintained throughout the Emilio-Romagna region of Italy and the observations from these traps have been published in the years 2008, 2014, and 2015 (Carrieri et al., 2012, 2017). The sampling method used in 2008 was different to that used in $2014-2015$ and so although observations in 2014 and 2015 are directly comparable to each other they cannot be compared to observations from 2008. The model predicts the observed oviposition activity in 2008 accurately with $R^2 = 0.92$ (Figure G.1A) with a scaling factor of $sf = 0.007$ and adjusted time step of $ts = 0$ days. For the data for the combined years $2014-2015$ the same validation process yields $R^2 = 0.70$, $ts = 3$, $sf = 0.04$, and the model convincingly reproduces the difference in oviposition activity between the years (Figure G.1B).

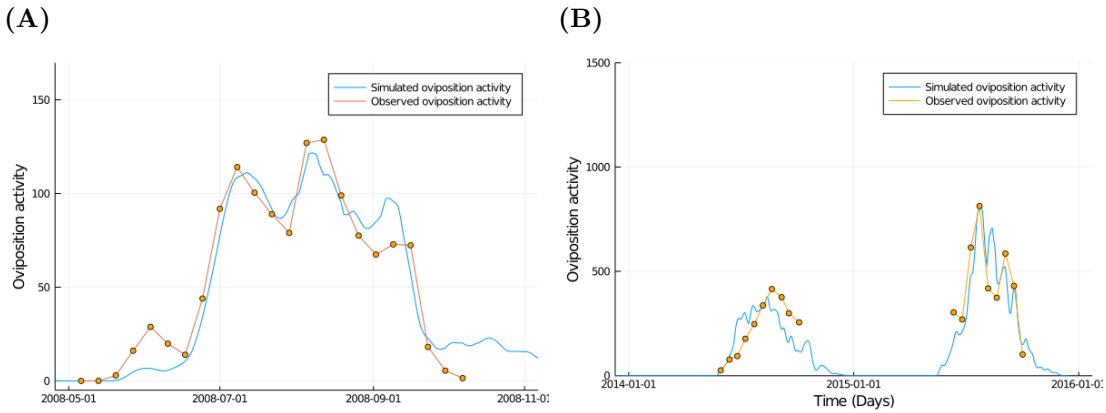

Figure G.1: A comparison of the predictions of the model (blue line) and field data (orange points and line) in the Emilio-Romagna region in the years **(A)** 2008 **(B)** 2014-2015.

In addition to oviposition activity, nuisance factor was estimated through human landing collections. To replicate this the biting rate as defined in the SIR model is used along with the predictions of adult abundance to predict the number of bites the simulated population produces per day, (i. e. $\sum_{j=1}^{m} b(t)A_j(t)$) and compare this the field observations. As can be seen in Figure G.2 the models prediction of number of bites per day sensibly follows the dynamics of

the observed nuisance factor.

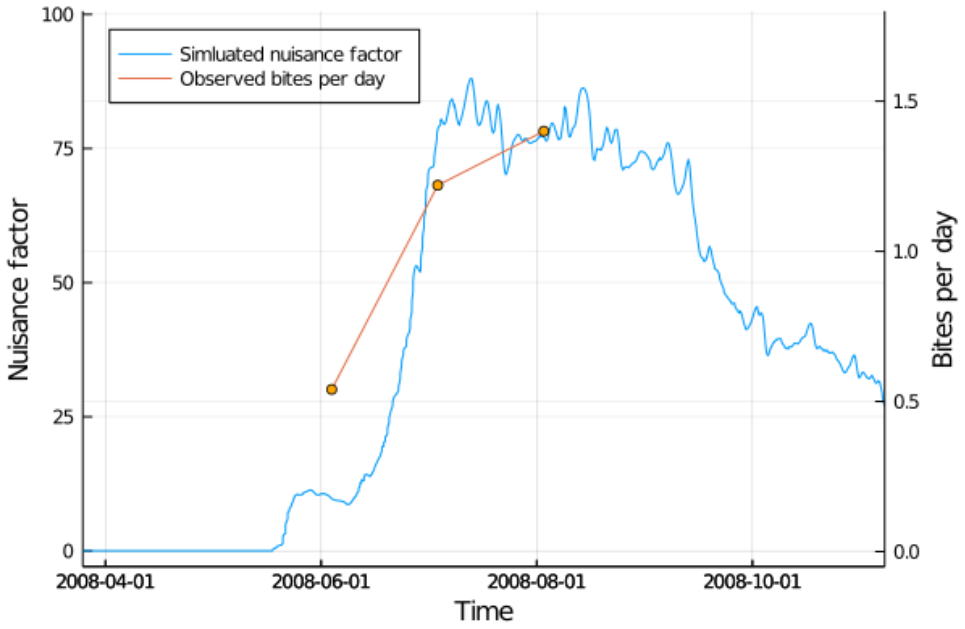

Figure G.2: A comparison of the predictions of nuisance factor from the model (blue line) and field data (orange points and line) in the Emilio-Romagna region in the year 2008.

Rome, Italy

Toma et al. (2003) monitored the oviposition activity of *Aedes albopictus* in Rome, Italy in the year 2000 (Toma et al., 2003). The model adequately predicts the dynamics of this population with a fit of $R^2 = 0.84$, $sf = 0.008$, $ts = 0$ (Figure G.3).

Como, Italy

Suter et al. (2016) monitored the oviposition activity of *Aedes albopictus* along the Swiss/Italian border in an intervention area and non-intervention area over two years (Suter et al., 2016) . The model is simulated in the non-intervention area in, Como, Italy. In Figure G.4 the comparison of model prediction to field data is $R^2 = 0.69$, $sf = 0.028$, $ts = -2$.

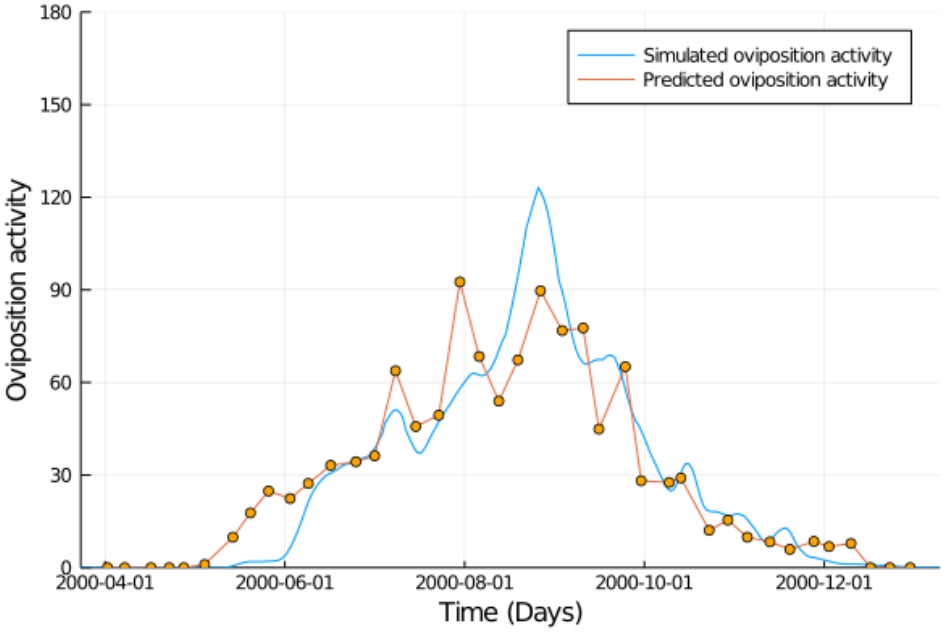

Figure G.3: A comparison of the predictions of the model (blue line) and field data (orange points and line) for Rome, Italy in the year 2000.

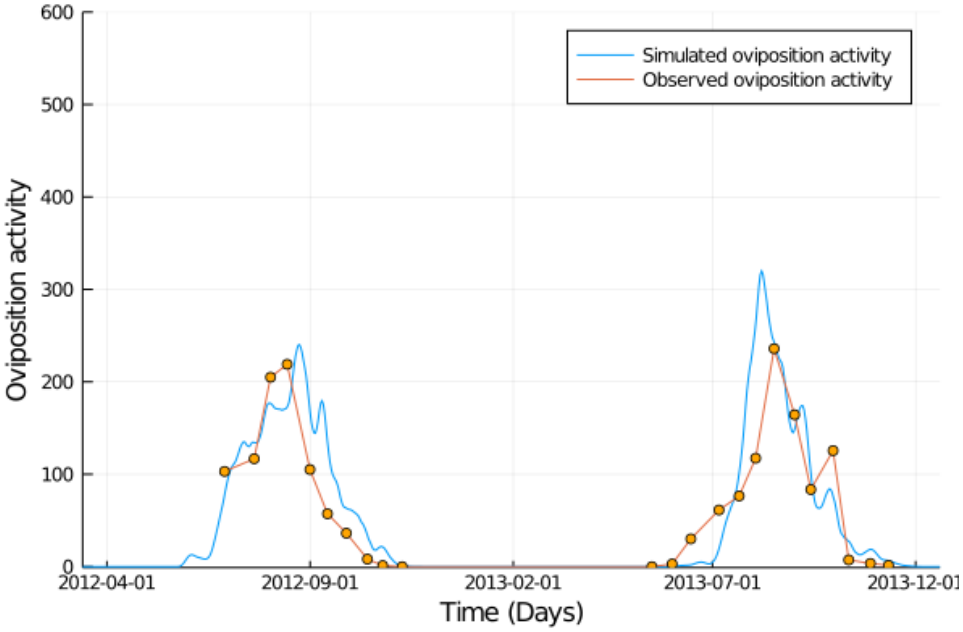

Figure G.4: A comparison of the predictions of the model (blue line) and field data (orange points and line) for Como, Italy for the years 2012 – 2013.

Catiania, Italy

Belle et al. (2018) monitored the oviposition activity in Catiania, Italy in the years 2008 and 2013 (Bella et al., 2018). The model is simulated in the citrus orchard, and in Figure G.5 it can be observed that the model performs well, $R^2 = 0.82$, $sf = 0.26$, $ts = 18$.

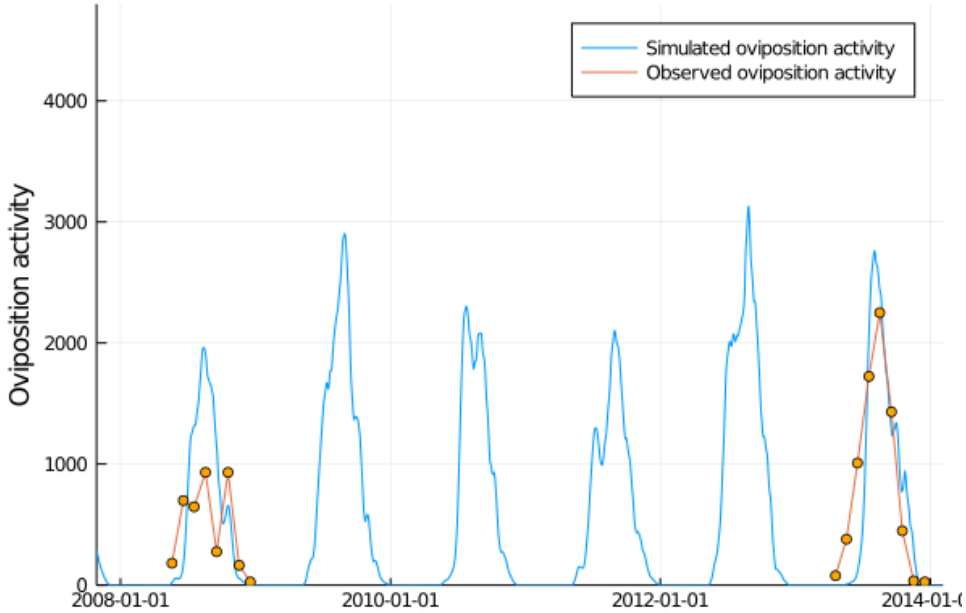

Figure G.5: A comparison of the predictions of the model (blue line) and field data (orange points and line) for Catiania, Italy for the years 2008 and 2013.

Trentino, Italy

Roiz et al. (2011) monitored the adult activity in Arco in 2008 (Roiz et al., 2011). The model achieves a fit of $R^2 = 0.84$, $sf = 0.18$,$ts = -1$, as seen in Figure G.6A. Mairini et al. (2017) monitored adult activity in a range of towns in the region for the years $2014 - 2015$ (Marini et al., 2017). To this data the model achieves a fit of $R^2 = 0.82$, $ts = -4$, $sf = 0.13$ as seen in Figure G.6B. Museo delle Scienze (MUSE) Italy monitored oviposition activity in the years $2010 - 2020$ in Trento (Museo delle Sceinze, 2021). A good fit is achieved to the multi-year data set with, $R^2 = 0.68$, $ts = -5$, $sf = 0.032$, (Figure G.6C) and the model reflects the inter-annual

differences in abundance that can be observed in this data.

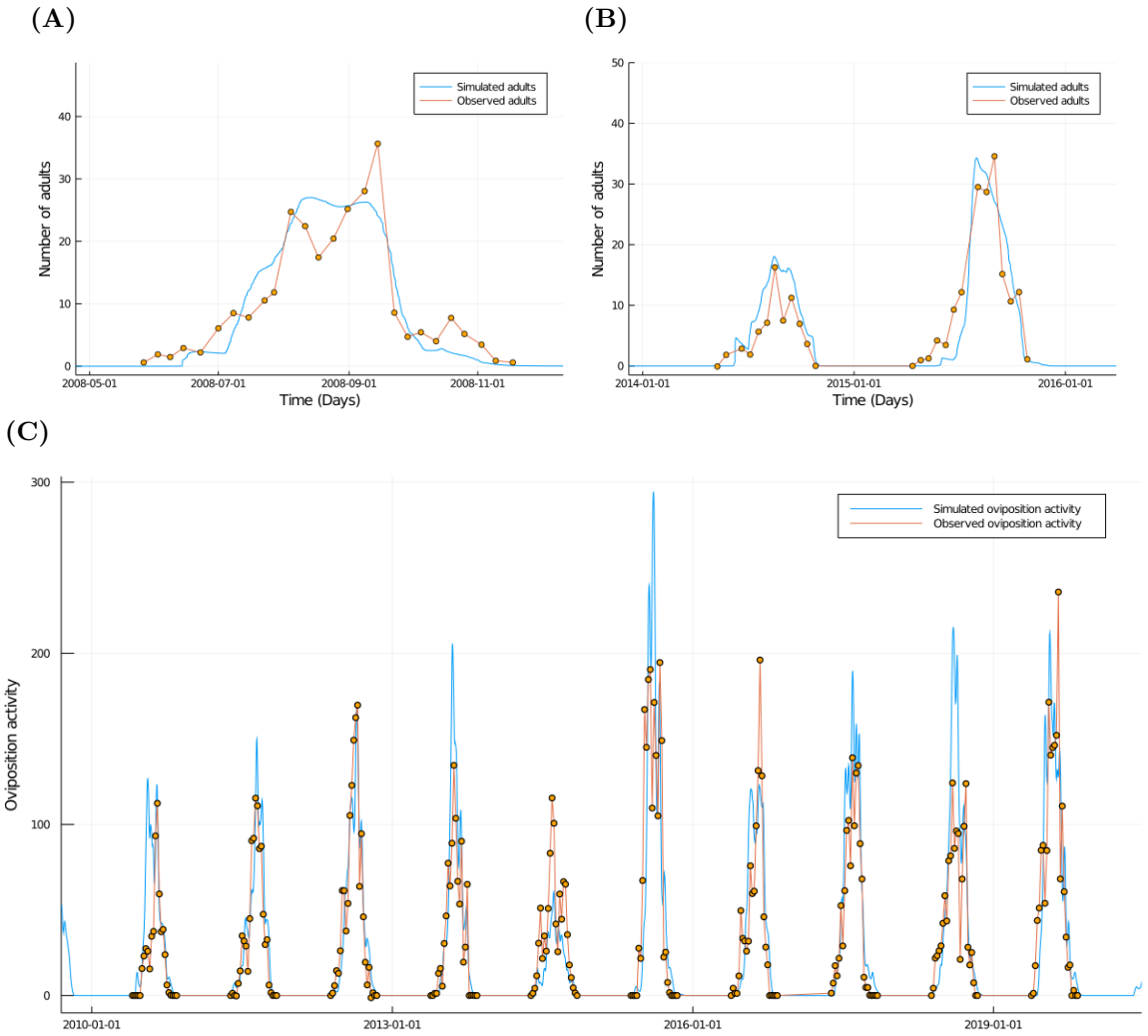

Figure G.6: A comparison of the predictions of the model (blue line) and field data (orange points and line) for data from the Trentino region. **(A)** Comparison of observed adult from Roiz et al. (2011) to model predictions in the year 2008. **(B)** Comparison of observed oviposition activity from Mairini et al. (2017) to model predictions in the years 2014−2015. **(C)** Comparison of observed oviposition activity in Trento collected by MUSE to model predictions in the years 2010 − 2020.

Cosenza, Italy

Bonnacci et al. (2015) observed the oviposition activity of *Aedes albopictus* in Cosenza, Italy in 2013 (Bonacci et al., 2015) . It is unclear when exactly the observations were made as each data point corresponds to a week of the study rather than time of the year. To compare field observations with the models predictions it is necessary to use contextual clues but this could be inaccurate by several weeks. The model fit is $R^2 = 0.50$, $sf = 0.09$, $ts = 10$ (Figure G.7).

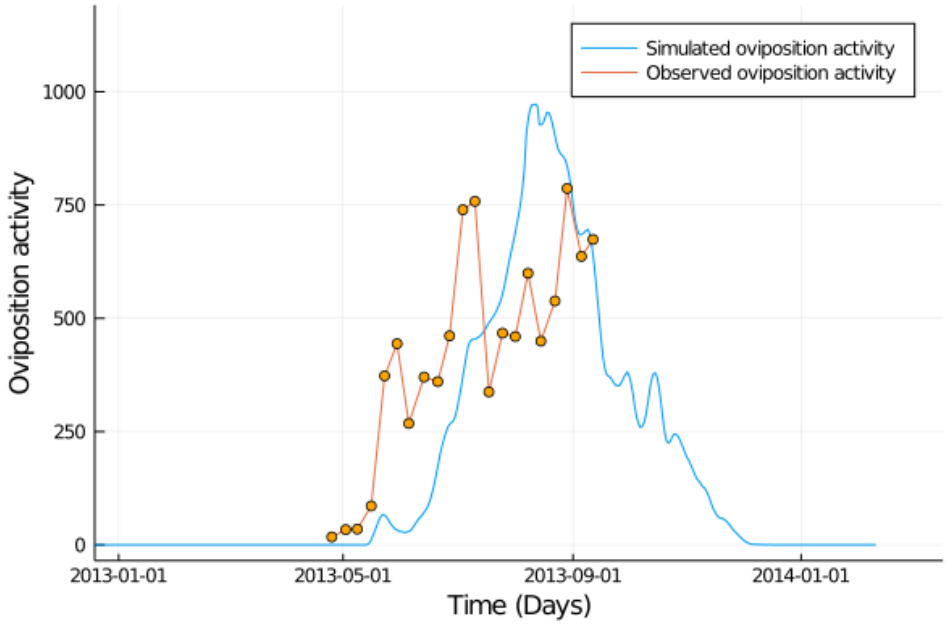

Figure G.7: The predicted oviposition activity of *Ae. albopictus* in Cosenza, Italy compared to oviposition data from Bonacci et al. (2015)

Cagnes-sur-Mer, France

Lacour et al. (2015) monitored the oviposition activity of *Aedes albopictus* in Cagnes-sur-Mer, France over the years $2011 - 2013$ (Lacour et al., 2015). The dynamics of this population are adequately predicted over multiple years with, $R^2 = 0.63$, $sf = 0.018$, $ts = 7$ (Figure G.8)

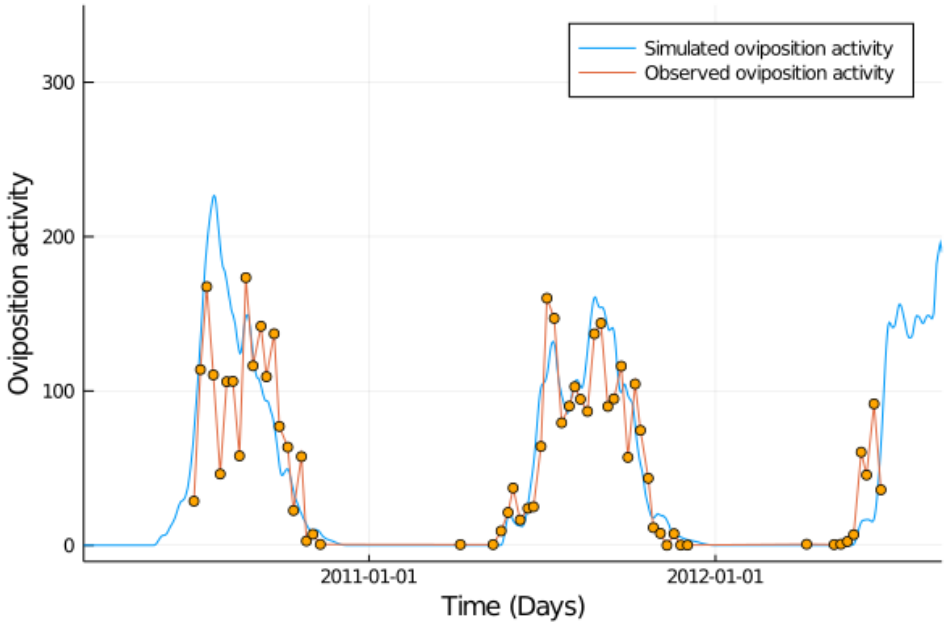

Figure G.8: A comparison of the predictions of the model (blue line) and field data (orange points and line) for Cagnes-sur-Mer, France in the years $2010 - 2012$.

Novi Sad, Serbia

In $2020 - 2021$ the oviposition activity in Novi Sad, Serbia was monitored. This data was obtained through communication with Dušan Petrić. The model achieves a fit of, $R^2 = 0.47$, $ts = 2$, $sf = 0.012$ found in Figure G.9.

Podgorica, Montenegro

Oviposition activity was monitored in Podgorica, Montenegro in 2013. This data was obtained through communication with Igor Pajović. The model achieves a fit of $R^2 = 0.57$, $ts = 7$, $sf = 0.011$ (Figure G.10).

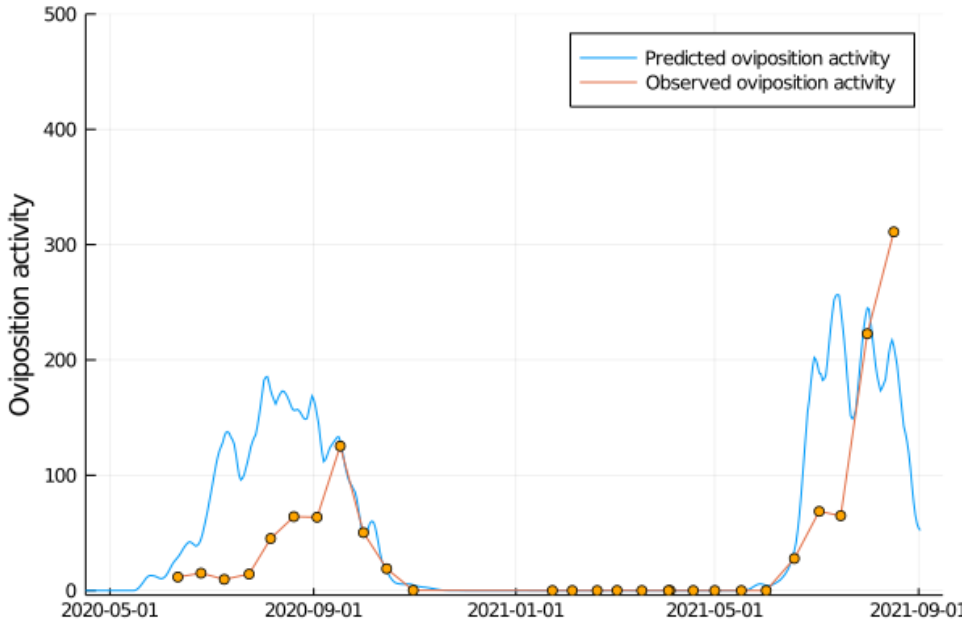

Figure G.9: A comparison of the predictions of the model (blue line) and field data (orange points and line) for Novi Sad, Serbia over the years $2020 - 2021$

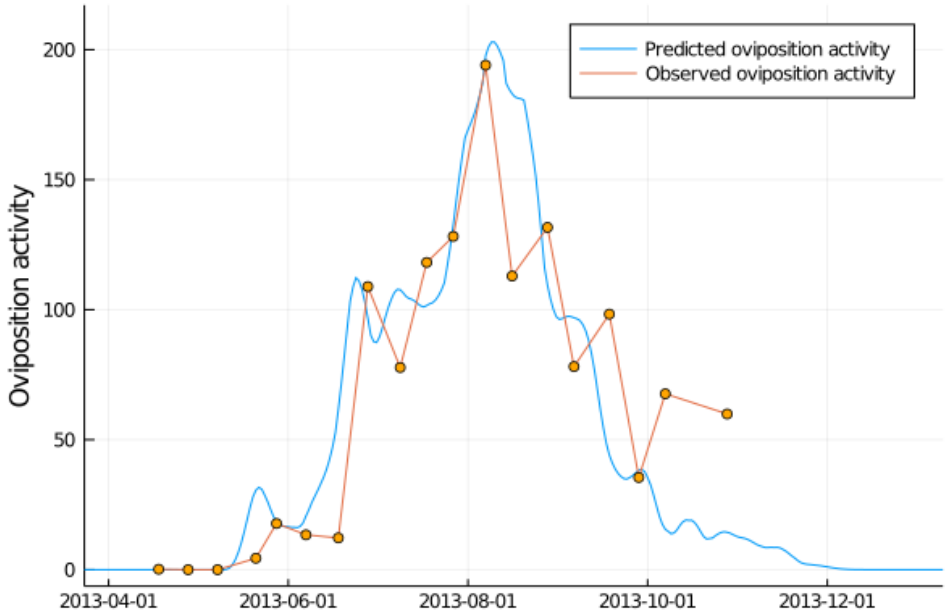

Figure G.10: A comparison of the predictions of the model (blue line) and field data (orange points and line) for Podgorica, Montenegro for the year 2013.

Zambelici, Montenegro

Oviposition activity was monitored in Zambelici, Montenegro in the years $2018 - 2019$. This data was obtained through communication with Igor Pajović. In Figure G.11 it can be observed that the model achieves a fit of $R^2 = 0.35$, $ts = 1$, $sf = 0.021$.

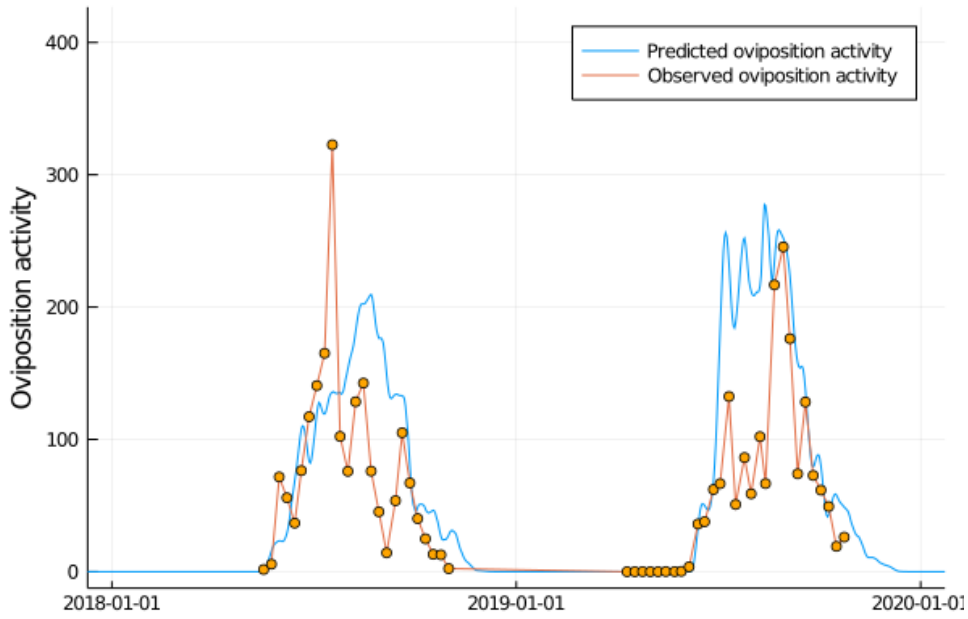

Figure G.11: A comparison of the predictions of the model (blue line) and field data (orange points and line) for Zambelici, Montenegro over the years $2018 - 2019$. The dashed purple lines indicate the times at which control efforts occurred.

Budva, Montenegro

Oviposition activity was monitored in Budva, Montenegro in 2012. This data was obtained through communication with Igor Pajović. Figure G.12 shows that the model achieves a good fit to data with $R^2 = 0.83$, $ts = -1$, $sf = 0.015$.

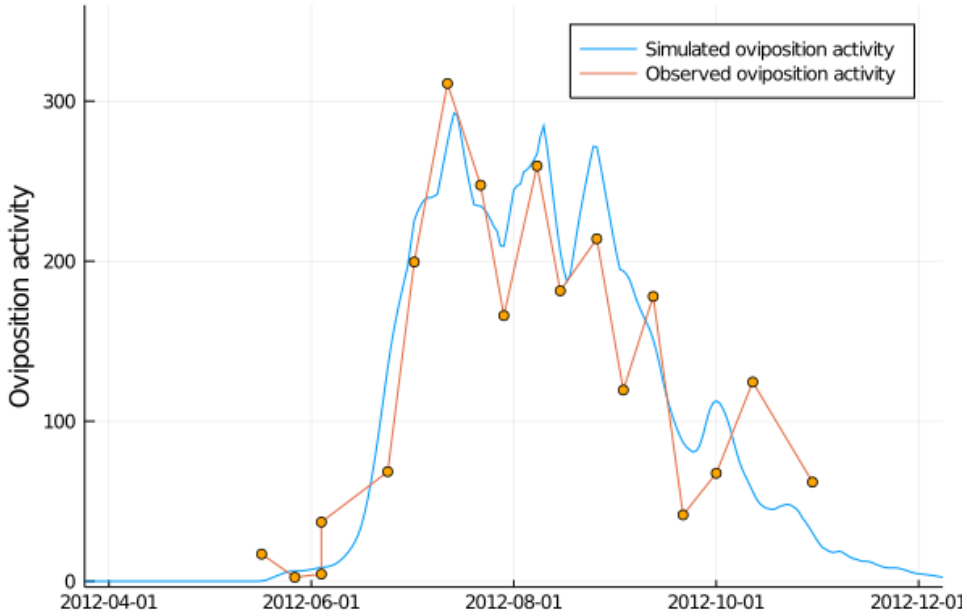

Figure G.12: A comparison of the predictions of the model (blue line) and field data (orange points and line) for Budva, Montenegro in 2012.

Ludwigshafen, Germany

Becker et al. (2022) monitored oviposition activity in Ludwigshafen in the year 2020 (Becker et al., 2022). Figure G.13 compares the model's predictions to the data find good agreement, $R^2 = 0.68$, $ts = -4$, $sf = 0.027$, however note that the model predicts oviposition activity for two months after it stopped in the field which may be attributable to the control activities in the area.

Freiburg im Breisgau, Germany

Becker et al. (2022) monitored oviposition activity in Freiburg in Breisgau in the year 2020, in an area where vector control had been implemented and in an area with no vector control. Figure G.14 compares the models predictions to the data from the non-intervention area and finds a good agreement, $R^2 = 0.98$, $ts = 2$, $sf = 0.139$.

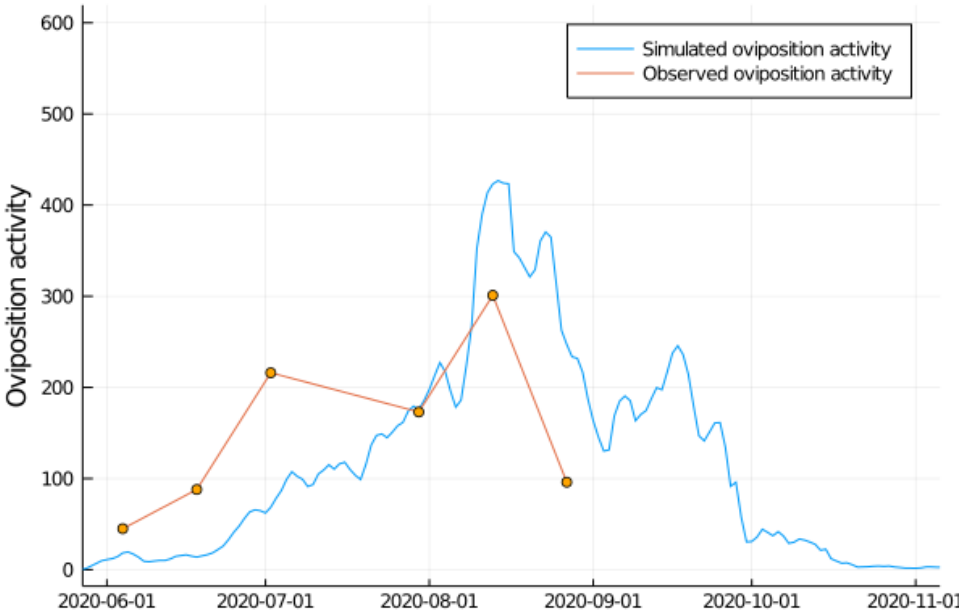

Figure G.13: A comparison of the predictions of the model (blue line) and field data (orange points and line) for Ludwigshafen, Germany, for the year 2020.

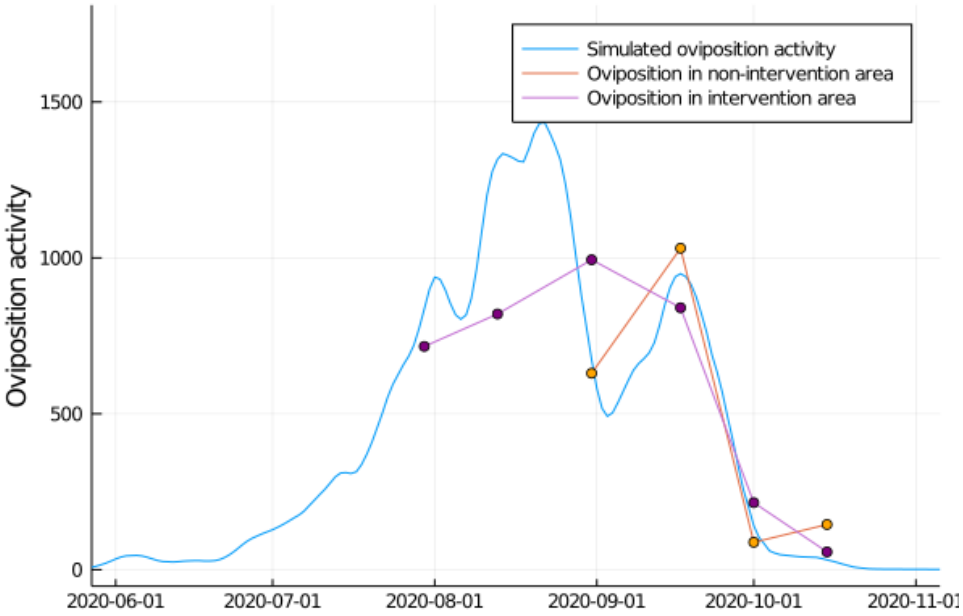

Figure G.14: A comparison of the predictions of the model (blue line) and field data (orange points and line) for Freiburg im Breisgau, Germany in 2020.

Irun, Spain

Goiri et al. (2020) monitored oviposition activity in Northern Spain over the years $2013 - 2018$, with *Ae. albopictus* being first detected in the region the simulation is based, Irun, in 2015 (Goiri et al., 2020) . This population was actively invading the region at the time of the study and there were trials of different controls methods concurrent with the sampling. These control programmes were "non-unified" and "barely effective" and it is likely the control efforts coincided with continuous introduction events occurring throughout this period (Goiri et al., 2020).Figure G.15 shows that the models predictions do not consistently match the observed field data with the model only achieving a fit of $R^2 = 0.031$, $ts = -14$, $sf = 0.01$. In Goiri et al. it is observed that *Ae. albopictus* populations often take a few years to establish and this combined with the control efforts in previous years could explain the discrepancy between observed and predicted oviposition activity. The fit for only 2018 is $R^2 = 0.50$, $sf = 0.004$,$ts = -10$.

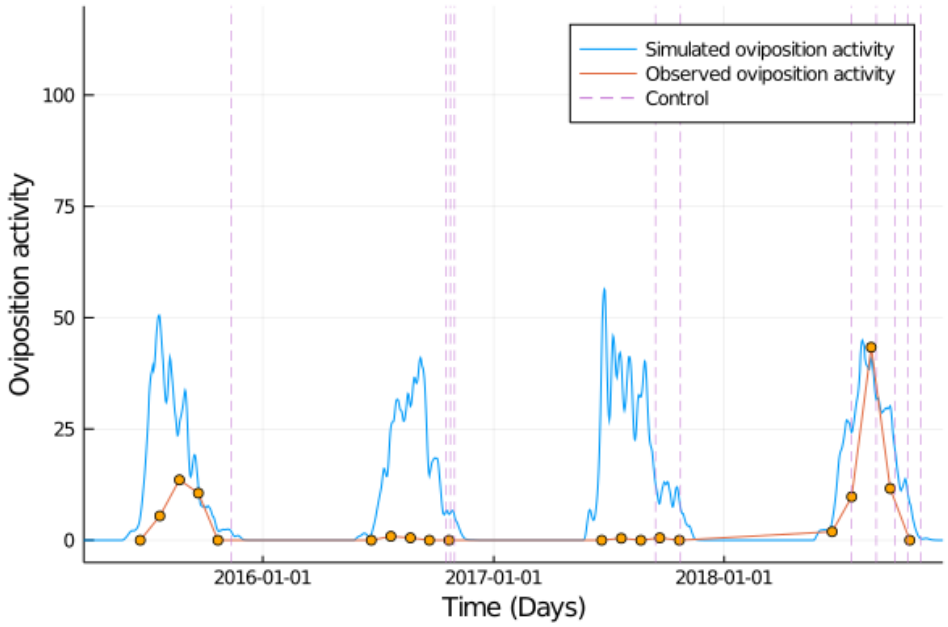

Figure G.15: A comparison of the predictions of the model (blue line) and field data (orange points and line) for Irun Spain over the years $2015 - 2018$. The dashed purple lines indicate the times at which control efforts occurred.

Baix Llobregat, Spain

Collantes et al. 2015 report the average oviposition activity observed for each week of the year in Llobregat, Spain for the years $2006 - 2014$ (Collantes et al., 2015). The model is simulated for these years and calculate the average oviposition activity. Figure G.16 shows the simulation which achieved a fit of $R^2 = 0.8$, $sf = 0.009$,$ts = 1$.

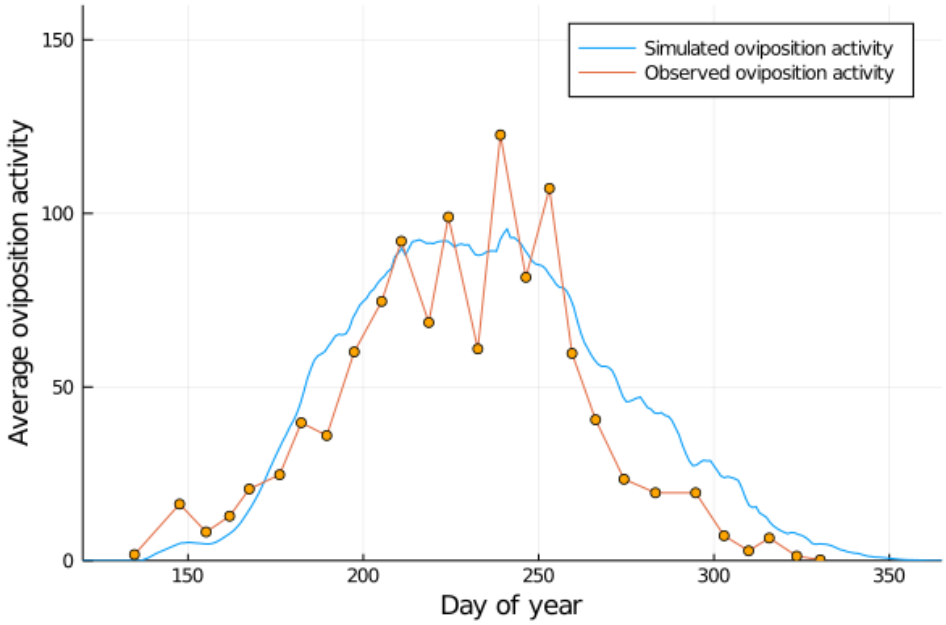

Figure G.16: A comparison of the weekly mean oviposition activity in the years $2006 - 2014$ as predicted by the model (blue line) and field data (orange points and line) for Baix Llobregat.

Split, Croatia

Zitko and Merdic report oviposition data from Split, Croatia for the years $2009 - 2010$ (Žitko, Merdić, 2014). Figure G.17 shows that the model predicts the phenology and population dynamics of both years well with $R^2 = 0.77$, $sf = 0.051$,$ts = -1$.

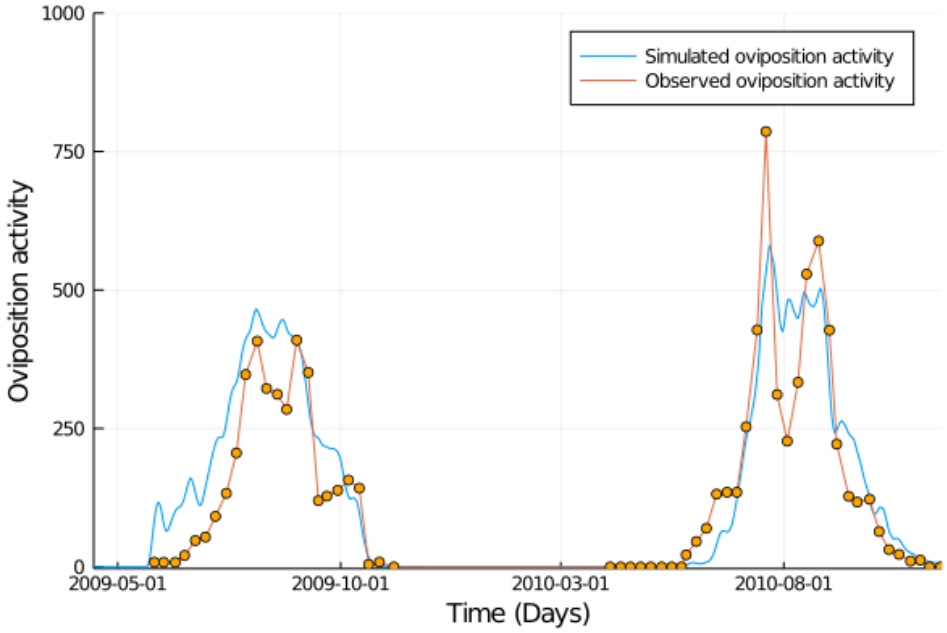

Figure G.17: A comparison of the predictions of the model (blue line) and field data (orange points and line) for Split, Croatia in the years $2009 - 2010$.

Loule, Portugal

Osorio et al. (2020), monitored the oviposition activity and number of adults in Loule, Portugal in the year 2019 (Osório et al., 2020). SDMs find this area is unsuitable for populations due to a lack of precipitation (Petrić et al., 2021), but the model predicts that a population can be maintained and achieves a good fit to the observed field data for both oviposition activity in Figure G.18A, $R^2 = 0.78$, $sf = 0.71$,$ts = -14$, and adult numbers in Figure G.18B with, $R^2 = 0.44$, $sf = 0.31$, $ts = -13$.

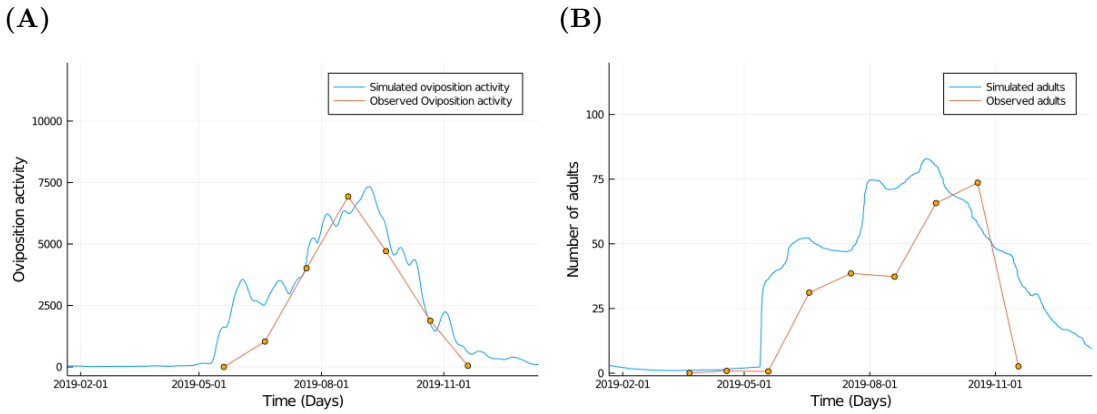

Figure G.18: A comparison of the predictions of the model (blue line) and field data (orange points and line) for Loule, Portugal in the years 2019. **(A)** Oviposition activity. **(B)** Adult numbers.

Athens, Greece

Giatropoulos al. (2012) monitored oviposition activity in Athens, Greece in the years $2009-2010$. Figure G.19 shows that the fit of the model to data is poor $R^2 = 0.12$, $sf = 0.03$,$ts = 4$. The poor fit to the data may be explained by the lack of precipitation in this region making the larval habitat unsuitable for the development of juveniles. It is likely given the urban nature of Athens that the field population observed here is at least in part reliant on sources of water that are not rain-fed.

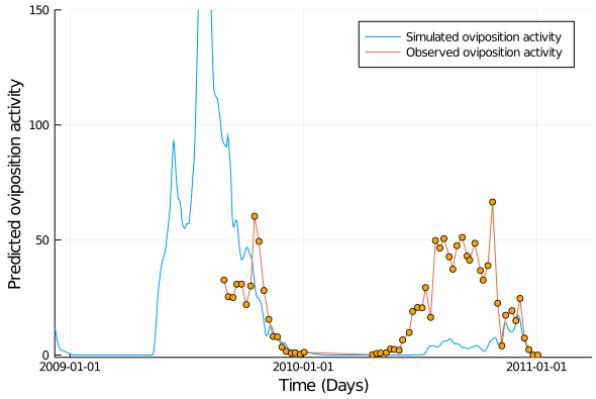

Figure G.19: A comparison of the predictions of the model (blue line) and field data (orange points and line) for Athens, Greece in the years $2009 - 2010$.

G.2 America

Lake Charles, Louisiana

Willis and Nasci (1994) measured the abundance and average wing length of adult mosquitoes in Lake Charles, Louisiana in the year 1988 (Willis, Nasci, 1994). Sampling of both host-seeking adults and of adults emerging from pupae collected from tyres was undertaken and reported separately and monthly averages are reported. It was found that the average wing-length of emerging and host-seeking adults were significantly different, indicating that population dynamical processes contribute to trait distribution. This study provides three points of comparison to the model predictions which are explored in Figure G.20. Figure G.20A shows the comparison of the model's predicted wing length to the observed average wing lengths and the average wing length of emerging adults. The model predicts both the average wing length of host seeking adults and the average wing length of emerging adults well. Additionally, in Figure G.20B it can be observed that the model also accurately predicts adult activity with $R^2 = 0.995$, $sf = 0.017$, $ts = 14$.

New Orleans, Louisiana

Comiskey et al. (1999) measured the wing length of *Aedes albopictus* in New Orleans in 1995, the method of trapping used is unknown and there was a prevalent infection throughout that altered both adult and larval mortality, reduced adult wing-length and had its own seasonal dynamics (Comiskey et al., 1999). Figure G.21A shows that the model fails to capture the average wing length of the population. However, the resemblance to the observed population dynamics is better the model comparison to the larval dynamics being, $R^2 = 0.61$, $sf = 0.01$, $ts = 11$ (Figure G.21B), and to the adult dynamics with, $R^2 = 0.37$, $sf = 0.11$, $ts = 13$ (Figure G.21C).

(A)

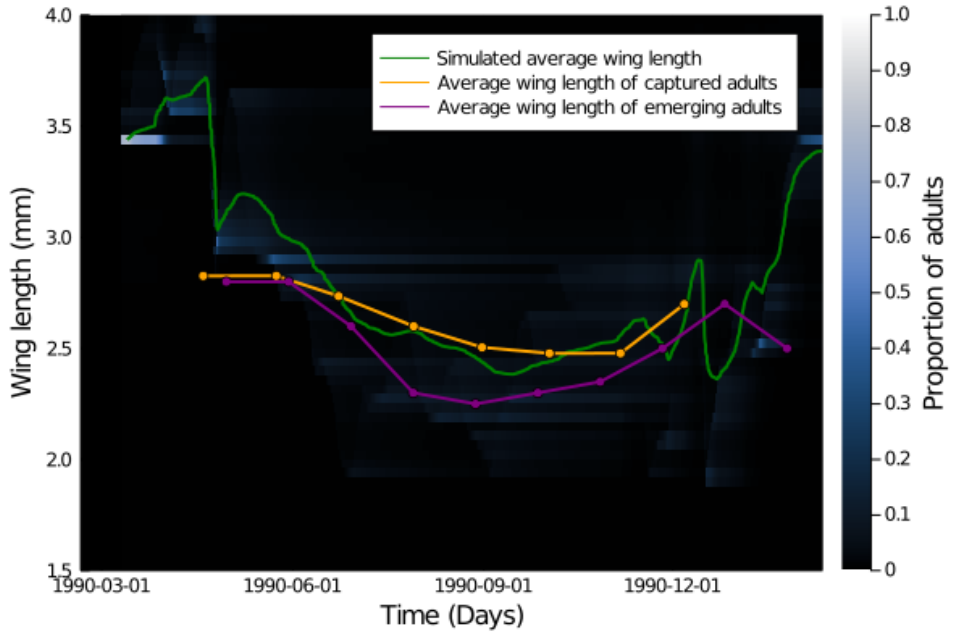

(B)

Figure G.20: Comparison of model predictions to observed field data for a population of *Aedes albopictus* in Lake Charles, Louisiana. **(A)** A comparison of the models predicted average wing length to that of adults in the field. The green line is the simulated average wing length with each blue line representing the proportion of adults within the simulated population that express a particular wing length. The orange line is the observed wing length of host seeking adults, and the purple line the average wing length of adults that emerged from pupae collected on the sampling days. **(B)** A comparison of the number of adults the model predicts are present at time t and the observed number of adults captured in the field.

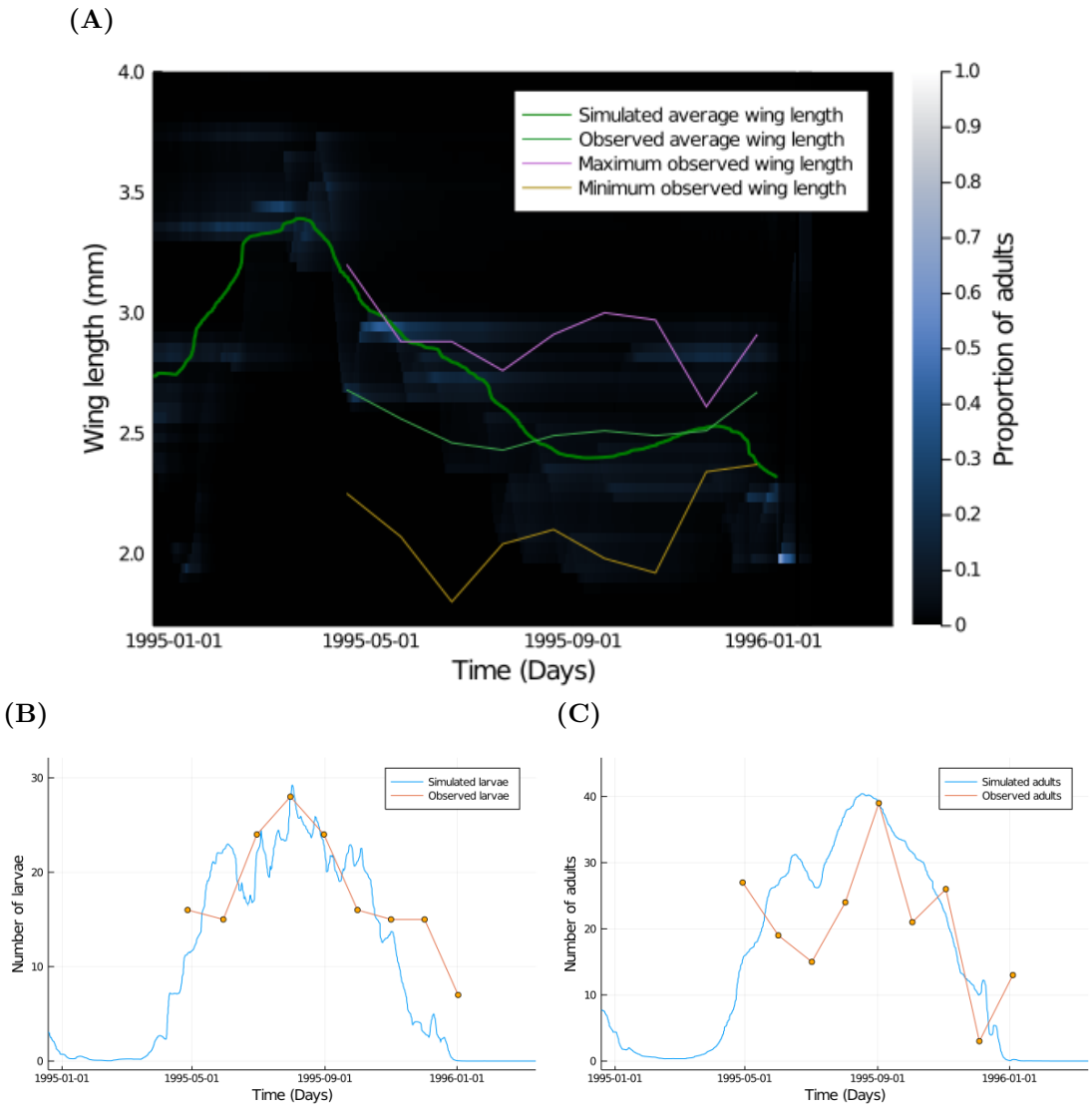

Figure G.21: Comparison of model predictions to observed field data for a population of *Aedes albopictus* in New Orleans. **(A)** A comparison of the observed and predicted trait dynamics. The green line is the simulated average wing length and each blue line represents the proportion of adults within the simulated population that express a particular wing length. The orange line is the observed wing length of host seeking adults, and the purple line the maximum wing length among adults sampled and the red line the minimum. **(B)** A comparison of observed and predicted larval dynamics. **(C)** A comparison of observed and predicted adult dynamics.

Fort Worth, Texas

We compare the models predictions to adult collections from CDC-gravid traps in Fort Worth, Texas with data sourced from Vectorbase. For each of the three years the model predicts the timing of the first population peak accurately but overestimates adult density in the later part of the year, as can be observed in Figure G.22 ($R^2 = 0.27$, $sf = 0.004$,$ts = 14$). One potential explanation for this overestimation could be the type of trap used in this collection, as gravid traps target adult mosquitoes that have successfully mated, taken a blood meal, and begun seeking an oviposition site. It has been previously demonstrated that traps targeting ovipositing mosquitoes collect larger individuals on average than passive trapping methods (Yeap et al., 2013). By only considering the abundance of adults with wing lengths greater than $2.7mm$ a more convincing fit to the data is achieved ($R^2 = 0.45$, $sf = 0.007$,$ts = -10$).

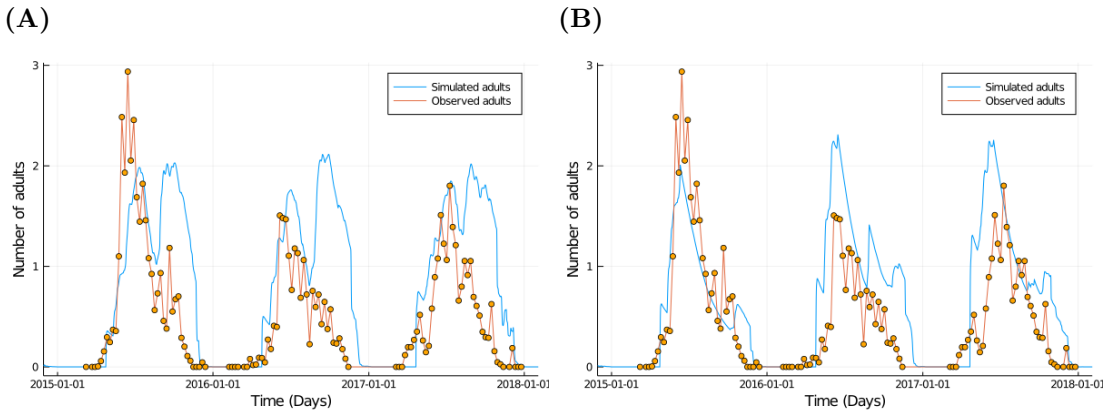

Figure G.22: Comparison of model predictions to observed field data for a population of *Aedes albopictus* in Fort Worth, Texas in the years $2015 - 2017$. **(A)** All adults. **(B)** Only adults larger than $2.7mm$.

Stratford, Connecticut

Armstrong et al. (2017) monitored the number of adults and larvae in Stratford, Connecticut in the years $2013 - 2017$ (Armstrong et al., 2017). The fit for the adult data is $R^2 = 0.06$, $ts = -7$, $sf = 0.06$ (Figure G.23A), and for the larval data the fit is $R^2 = 0.13$, $ts = -1$,

$sf = 0.024$ (Figure G.23B). The poor fit observed in the model fit to the majority of the data is potentially due to a failure to capture populations overwintering dynamics as this population regularly experiences cold winters. Cold tolerance in *Ae. albopictus* is known to be genotypically plastic and so the disparity between model predictions and field observations would likely be improved by a more specific model. This could also be attributed to the lack of life-history data at lower temperatures meaning that cold weather survival is generally overestimated. Despite this, in the years 2013 and 2016 when the population is clearly established the model adequately anticipates the observed dynamics even if failing to capture the changes in relative abundance. For just these years a fit of $R^2 = 0.08$, $ts = 1$, $sf = 0.78$ is achieved to the adult data and a fit of $R^2 = 0.39$, $ts = -1$, $sf = 0.019$ to the larval data.

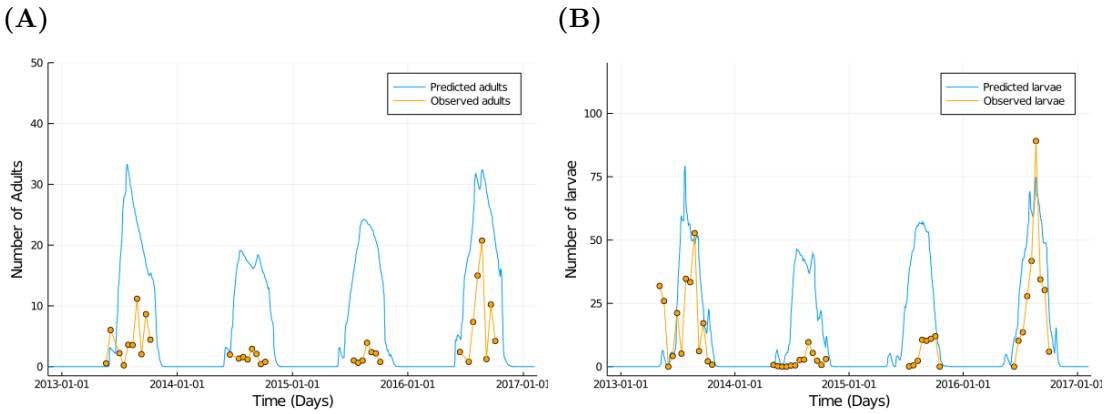

Figure G.23: A comparison of the predictions of the model (blue line) and field data (orange points and line) for Stratford, Connecticut in the years $2013 - 2017$, for **(A)** number of adults **(B)** number of larvae.

Monmouth, New Jersey

Fonesca et al. (2012) monitored adult numbers and oviposition activity in Mercer and Monmouth counties in New Jersey over the course of a year in intervention and non-intervention areas (Fonseca et al., 2013). The dynamics of a population in Monmouth county are simulated and compared to the non-intervention data. The model achieves a good fit to the observed oviposition

activity with, $R^2 = 0.51$, $sf = 0.002$,$ts = -7$ (Figure G.24A) but not the adult dynamics, $R^2 = 0.26$, $sf = 0.066$,$ts = 5$ (Figure G.24B). Note however, the similarity between the predicted adult dynamics and those observed in neighbouring Mercer county as described in Fonesca et al. .

(A) **(B)**

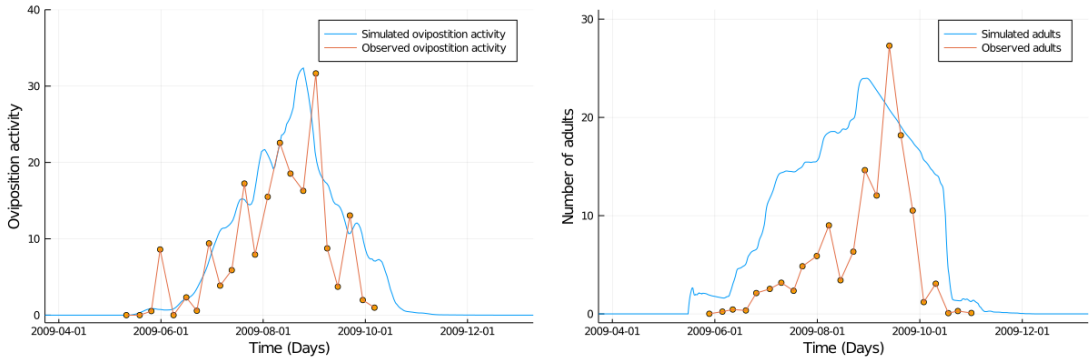

Figure G.24: A comparison of the predictions of the model (blue line) and field data (orange points and line) for Monmouth, New Jersey in the years 2009, for **(A)** oviposition activity **(B)** number of adults.

Charlotte, North Carolina

Three different studies monitored the dynamics of *Ae. albopictus* in Charlotte, North Carolina. Mundis et al. (2021) measured the average wing-length of adults captured by gravid *Aedes* traps and the model's predictions align well with the observed trait dynamics (Figure G.25A). Field data for the oviposition activity of *Ae. albopictus* in the year 2016 as used in the study Reed et al. (2018) was obtained from VectorBase (Reed et al., 2019). Figure G.25B shows that the model achieves the following fit to the oviposition activity data, $R^2 = 0.38$, $ts = 14$, $sf = 0.003$. Whiteman et al. (2018) monitored the number of gravid adults in Charlotte in 2017, the model achieves a fit of $R^2 = 0.06$, $ts = -6$, $sf = 0.024$ (Figure G.25C) (Whiteman et al., 2018).

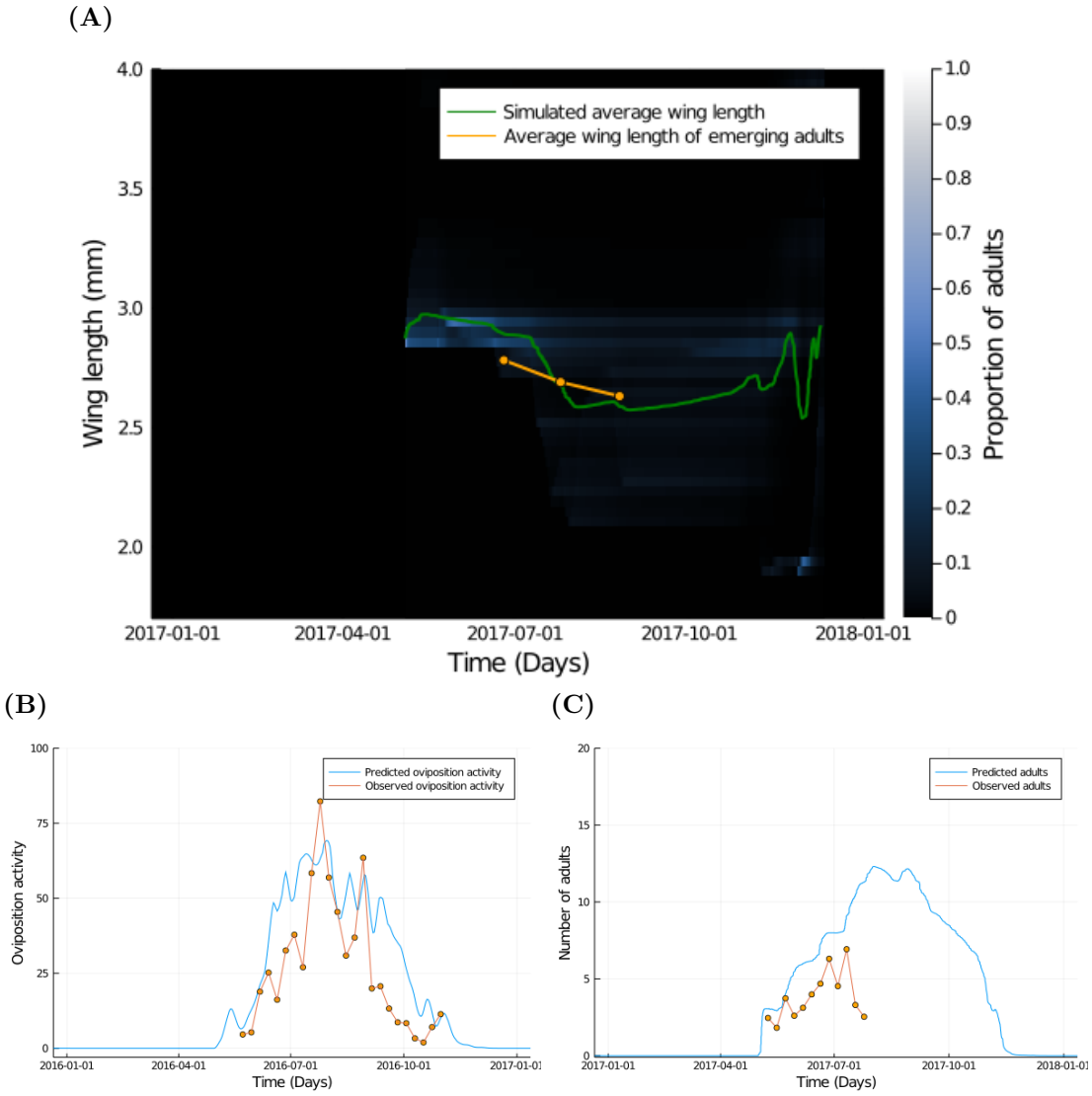

Figure G.25: A comparison of the predictions of the model (blue line) and field data (orange points and line) for Charlotte, North Carolina in the year 2016, for **(A)** Trait values, **(B)** Oviposition activity, **(C)** Adult numbers.

Raleigh, North Carolina

Reed et al. (2019) monitored the oviposition activity in Raleigh, North Carolina. Figure G.26 shows that the model predicts the observed dynamics with, $R^2 = 0.80$, $sf = 0.003$,$ts = 6$.

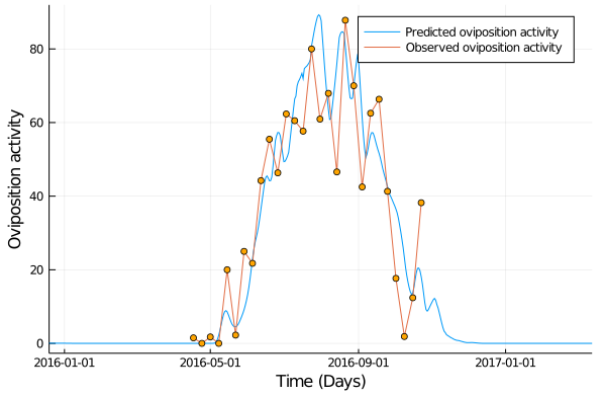

Figure G.26: A comparison of the predictions of the model (blue line) and field data (orange points and line) for Raleigh, North Carolina in the year 2016.

Asheville, North Carolina

Reed et al. (2019) monitored the oviposition activity in Asheville, North Carolina. In Figure G.27 the model predicts the observed dynamics with, $R^2 = 0.51$, $sf = 0.0018$,$ts = 3$.

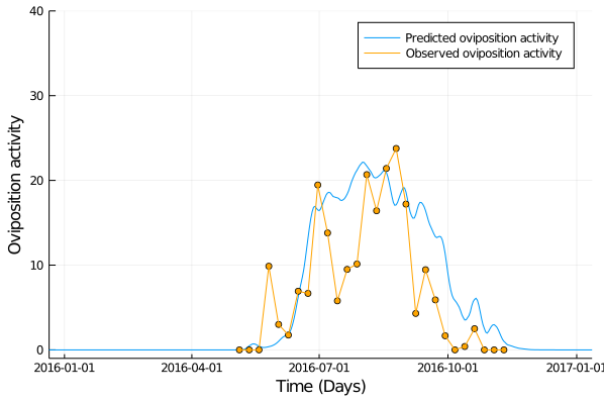

Figure G.27: A comparison of the predictions of the model (blue line) and field data (orange points and line) for Asheville, North Carolina in the year 2016.

Greenville, North Carolina

Reed et al. (2019) monitored the oviposition activity in Greenville, North Carolina. In Figure G.28 the model predicts the observed dynamics with, $R^2 = 0.40$, $sf = 0.0028$,$ts = 7$.

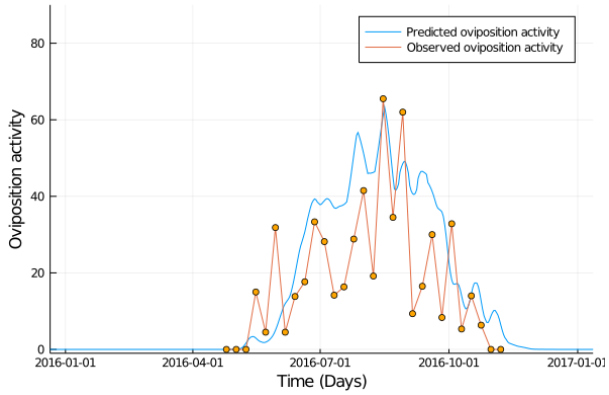

Figure G.28: A comparison of the predictions of the model (blue line) and field data (orange points and line) for Greenville, North Carolina in the year 2016.

Indianapolis, Indiana

We obtained adult data from VectorBase for Indianapolis, Indiana for the years $2018 - 2020$ to which the model achieves a fit of $R^2 = 0.69$, $sf = 0.0012$,$ts = -3$ as seen in Figure G.29.

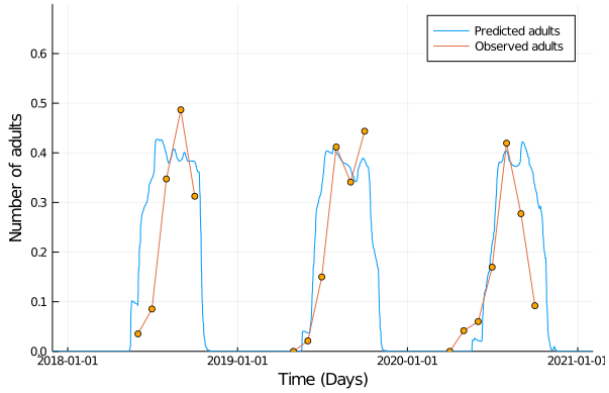

Figure G.29: A comparison of the predictions of the model (blue line) and field data (orange points and line) for Indianapolis, Indiana for the years $2019 - 2020$.

Washington, D.C.

From VectorBase adult trapping data was obtained from Washington D. C. . The provenance of this data is unclear and it features high variation in inter-year abundance and so years where observed adult densities are within the same order of magnitude are selected summarised by month, when this is done a fit of $R^2 = 0.25$, $sf = 0.12$,$ts = 2$ is achieved (Figure G.30).

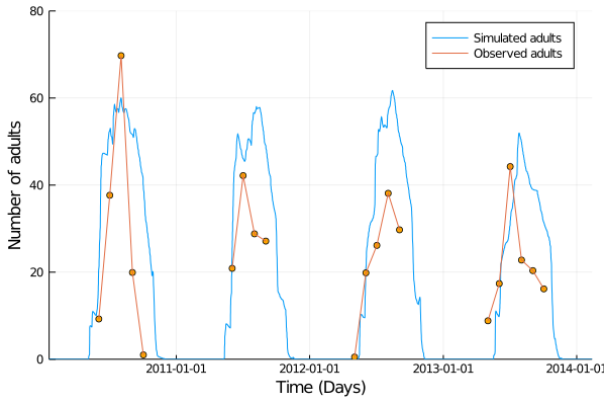

Figure G.30: A comparison of the predictions of the model (blue line) and field data (orange points and line) for Washington, D.C. for the years $2010 - 2014$.

Colombus, Ohio

From VectorBase adult data was obtained from Colombus, Ohio in 2018. A fit of $R^2 = 0.1$, $sf = 0.038$,$ts = -8$ is achieved (Figure G.31).

Suffolk, Virginia

We obtained adult data from VectorBase for Suffolk, Virginia for the years $2009 - 2018$ to which the model achieves a fit of $R^2 = 0.65$, $sf = 0.16$,$ts = 8$ as seen in Figure G.32.

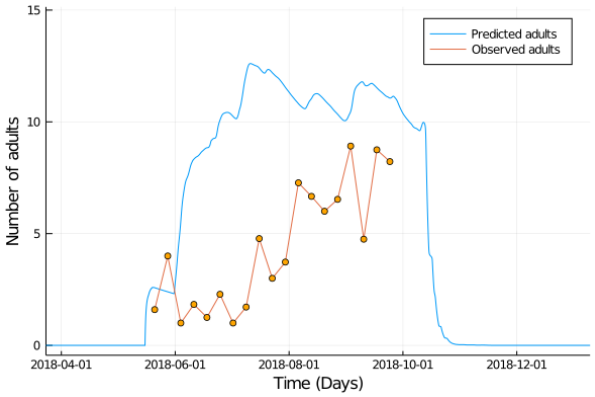

Figure G.31: A comparison of the predictions of the model (blue line) and field data (orange points and line) for Colombus, Ohio for the years 2018.

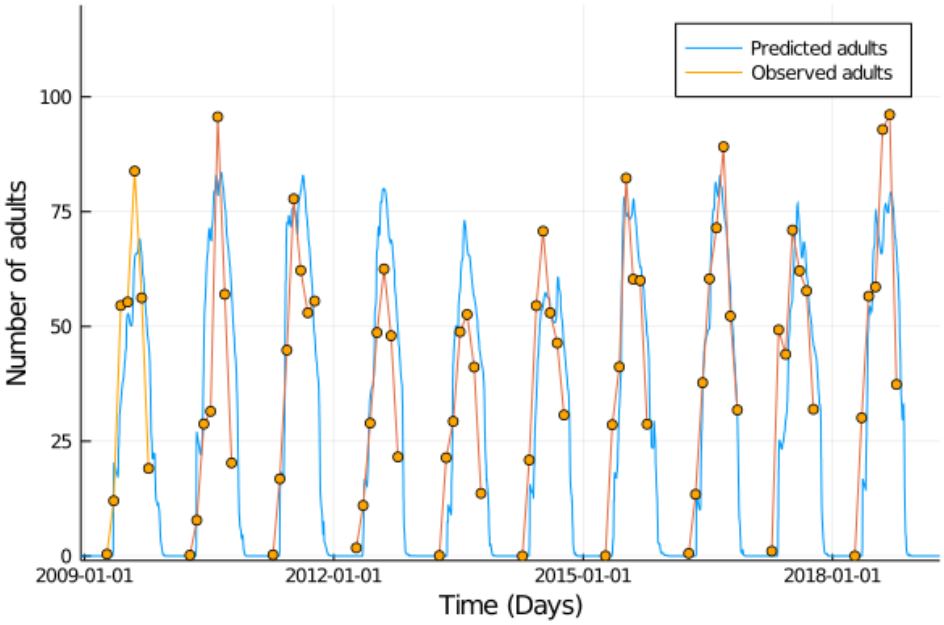

Figure G.32: A comparison of the predictions of the model (blue line) and field data (orange points and line) for Suffolk, Virginia in the years $2009 - 2018$.

Santa Rosa Beach, Florida

We obtained adult data from VectorBase for Santa Rosa Beach, Florida for the years $2014-2017$ to which the model achieves a fit of $R^2 = 0.18$, $sf = 0.006$,$ts = 7$ as seen in Figure G.33.

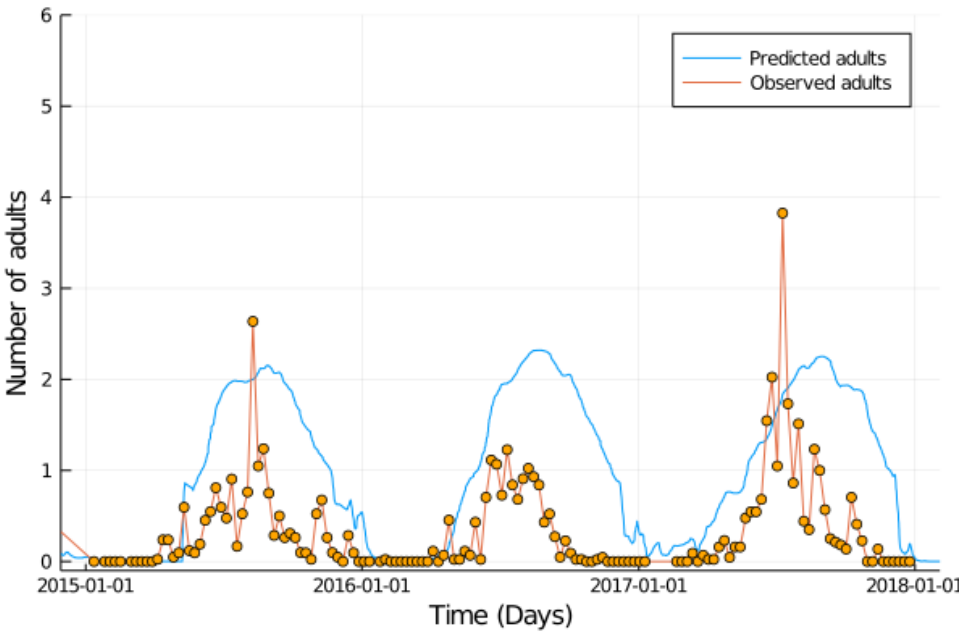

Figure G.33: A comparison of the predictions of the model (blue line) and field data (orange points and line) for Santa Rosa Beach, Florida in the years $2014 - 2017$.

G.3 Asia

Naha, Japan

Toma et al. 1982 monitored the population dynamics of *Ae. albopictus* in Naha, Japan in the years $1978 - 1979$ (Toma et al., 1982). This study is notable as the only validation set to report data from all life-stages and reports the number of eggs, larvae, pupae, and adults in the years in which the study was conducted. The model predicts the population dynamics at the start and the end of the year well for eggs and larvae (Figures G.34A and G.34B) The adult dynamics (Figure G.34C) are correctly predicted throughout the season. (A) $R^2 = 0.3$, $ts = 14$, $sf = 0.02$ (B) $R^2 = 0.4$, $ts = 11$, $sf = 0.04$ (C) $R^2 = 0.41$, $ts = 14$, $sf = 0.04$.

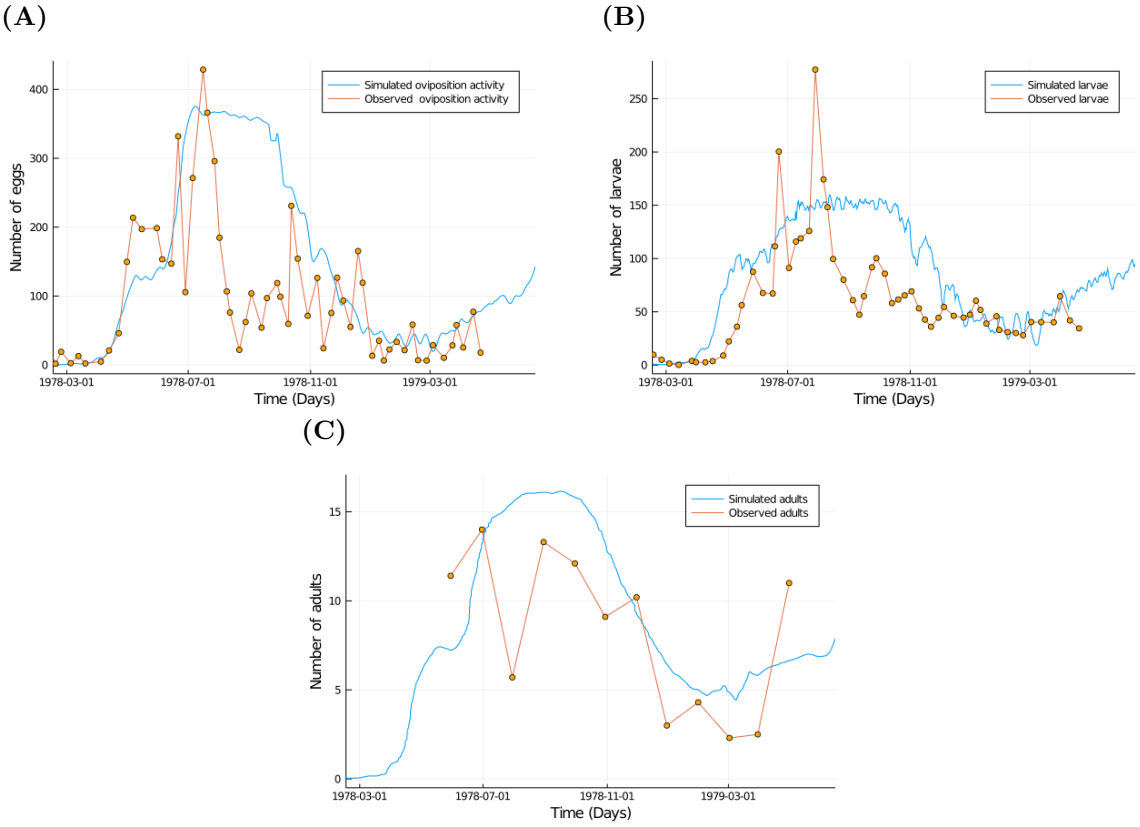

Figure G.34: A comparison of the predictions of the model (blue line) and field data (orange points and line) for Naha, Japan in the year 1978 for **(A)** Oviposition activity. **(B)** Number of larvae. **(C)** Number of adults.

Nagasaki, Japan

Suzuki et al. (1993) monitored the dynamics of a population of *Ae. albopictus* in Nagasaki, Japan in (1990) (Suzuki et al., 1993). Figure G.35A shows that to the adult data a good fit is achieved with, $R^2 = 0.87$, $ts = 2$, $sf = 0.18$. The same authors measure the average wing lengths of adults collected during this period and the model adequately predicts the observed seasonal variation as can be seen in Figure G.35B.

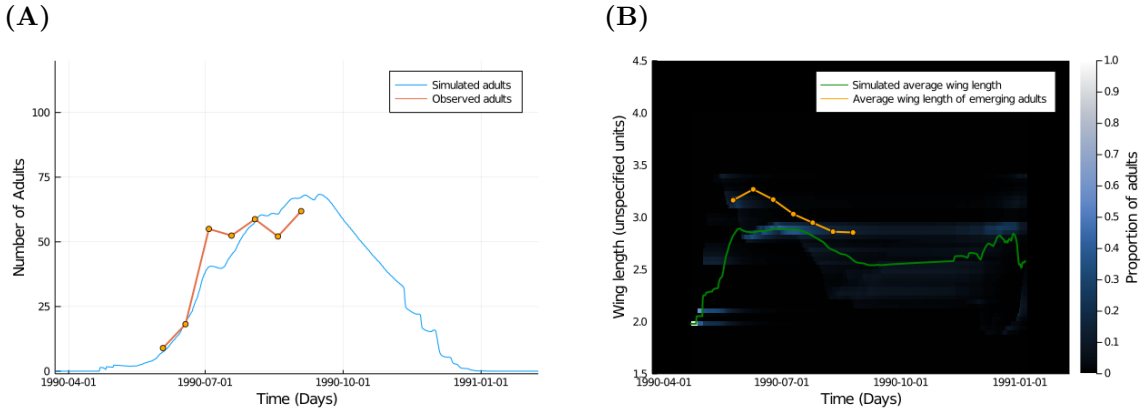

Figure G.35: A comparison of the predictions of the model (blue line) and field data (orange points and line) for Nagasaki, Japan in 1990 for **(A)** Adults numbers. **(B)** Average wing length.

Tokyo, Japan

Kori et al. (2020) monitored the number of adults parks around Tokyo in years between 2010 and 2018, and adult and larval numbers in Yoyogi park in the years $2015 - 2017$ (Kori et al., 2020). After a dengue outbreak in 2014 larval habitats were destroyed in the Tokyo metropolitan area and adulticides and larvicides are now regularly used in these areas and this may explain the general poor fit the model achieves to the majority of this data. To the adult collections from all major parks I achieve a fit of $R^2 = 0.27$, $ts = 7$, $sf = 0.023$ in Figure G.36A. To the adult collections from Yoyogi park after the intervention I achieve a fit of $R^2 = 0.13$, $ts = -6$, $sf = 0.13$ in Figure G.36B. To the larval collections from Yoyogi park I achieve a fit of $R^2 = 0.01$,

$ts = 14$, $sf = 0.028$ in Figure G.36C.

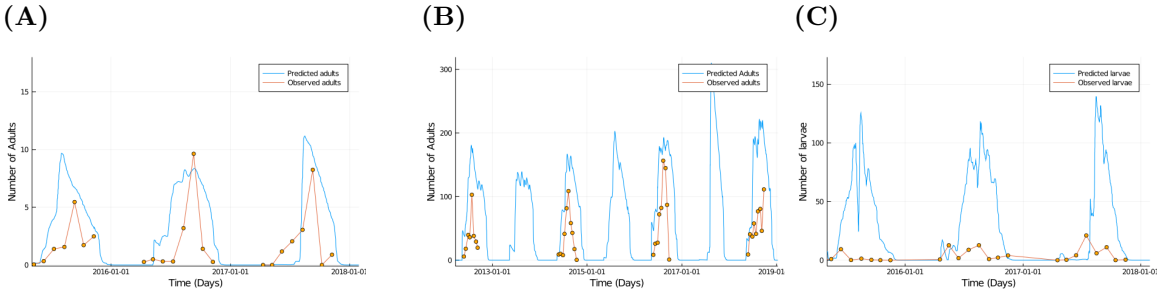

Figure G.36: A comparison of the predictions of the model (blue line) and field data (orange points and line) for Tokyo, Japan in years between 2010 and 2018 for **(A)** Adult numbers observed in major parks around Tokyo. **(B)** Adult numbers observed in Yoyogi park in the years $2015 - 2017$. **(C)** Larval numbers observed in Yoyogi park in the years $2015 - 2017$.

Guangzhao, China

In Guangzhao, Xia et al. (2018) measured oviposition activity in 2017 and Xu et al. (2017) monitored adult numbers in the years $2006 - 2015$ (Xia et al., 2018; Xu et al., 2017). In Figure G.37B it should be noted that in 2015 control activities were increased following a large dengue outbreak in 2014 explaining the low observed adults that year and so is excluded from the fitting. The model achieves a fit of, $R^2 = 0.50$, $ts = 7$, $sf = 0.027$, to the oviposition activity data (see Figure G.37A) and a fit of, $R^2 = 0.58$, $ts = 8$, $sf = 0.0045$ to the adult data (see Figure G.37B).

(A)

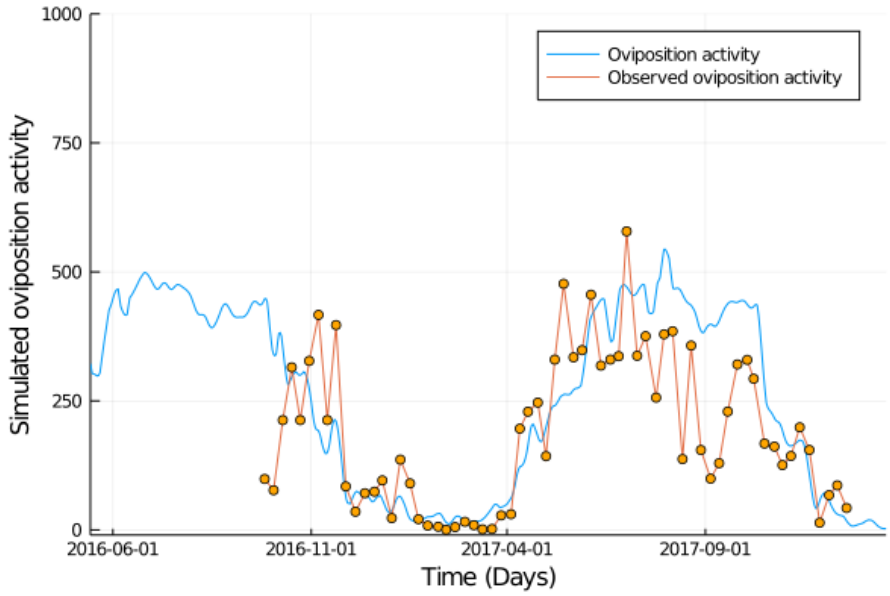

(B)

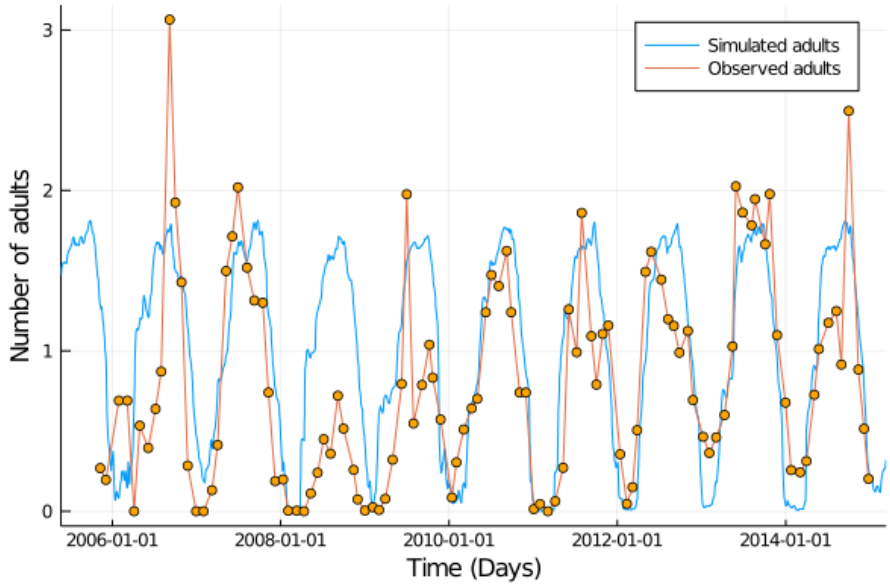

Figure G.37: A comparison of the predictions of the model (blue line) and field data (orange points and line) for Guangzhao, China over the years 2006 – 2018. **(A)** Oviposition activity for 2017 with data taken from Xia et al. (2019). **(B)** Adult abundance for the years 2006 – 2015 with data taken from Xu et al. (2017).

Suwon, South Korea

Hwang et al. (2020) (Hwang et al., 2020) monitored adult numbers in Suwon, South Korea in the year 2016. Figure G.38 shows the model predicts the observed dynamics with, $R^2 = 0.90$, $ts = 3$, $sf = 0.042$.

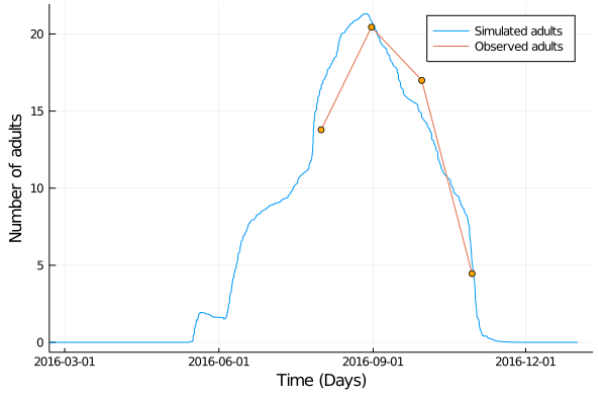

Figure G.38: A comparison of the predictions of the model (blue line) and field data (orange points and line) for Suwon, South Korea in the year 2016.

G.4 Africa

La Réunion

La Réunion has experienced regular outbreaks of dengue vectored by *Ae. albopictus* since 2015 (Vincent et al., 2019). These outbreaks are notable in the context of this work as they occur in a tropical region and are as close to endemic dengue dynamics as that are considered here.

Gougna et al. 2010 (Gouagna et al., 2020) monitored oviposition activity and observed around 200 eggs per ovitrap in each sample between October to April, which I find roughly matches the models predictions of oviposition activity. Harambourne et al. (2020) (Haramboure et al., 2020) performed larval surveys in five locations across the north of La Réunion in the years 2012 and 2013. Figure G.39 shows that the model adequately predicts observed differences in larval dynamics between locations and years. In Saint-Paul the model predicts the observed

population dynamics with, $R^2 = 0.54$, $ts = -2$, $sf = 0.027$, see Figure G.39A. In La Possession the model predicts, $R^2 = 0.51$, $ts = -1$, $sf = 0.027$, see Figure G.39B. In Saint-Bennoit I predict, $R^2 = 0.002$, $ts = -3$, $sf = 0.13$, as shown in Figure G.39C. In Saint-Marie I predict, $R^2 = 0.17$, $ts = 2$, $sf = 0.05$ as shown in Figure G.39B.

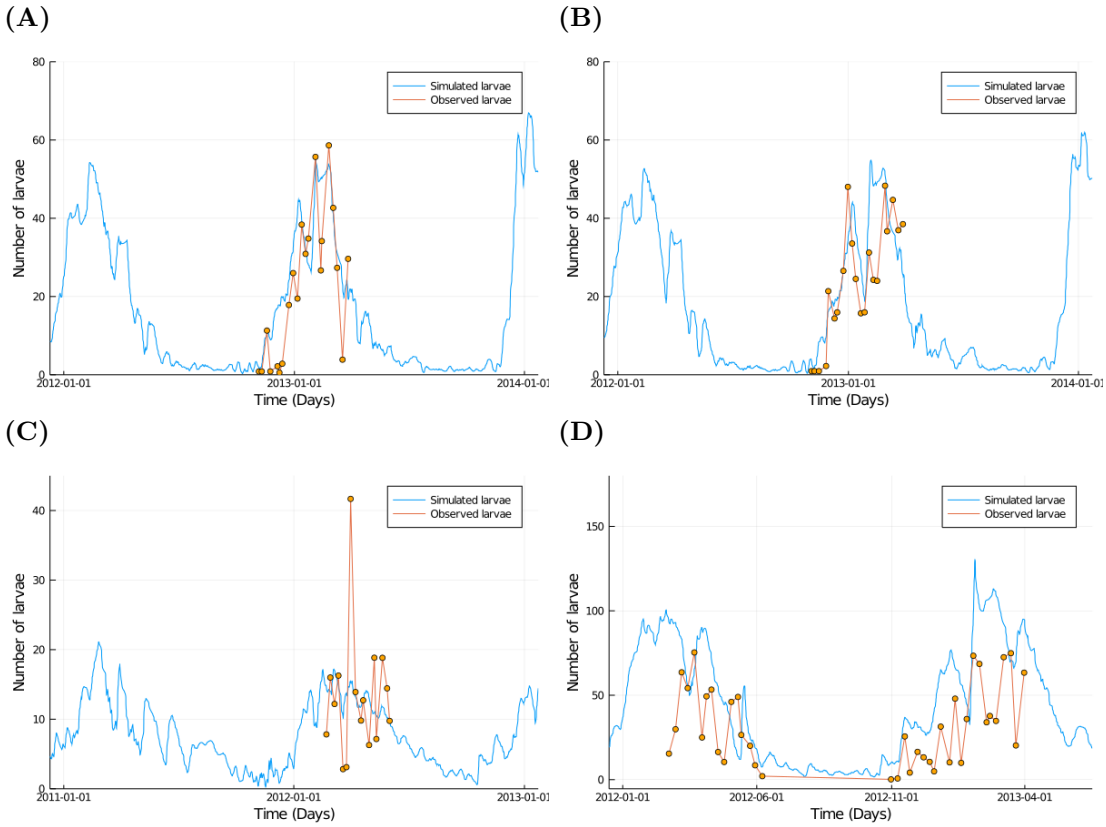

Figure G.39: A comparison of the predictions of the model (blue line) and field data (orange points and line) for larvae in sites around La Réunion. **(A)** Saint-Paul **(B)** La Possession **(C)** Saint-Bennoit **(D)** Saint-Marie.

In Saint-Marie oviposition activity data is available for the years $2013 - 2014$ to which a fit of $R^2 = 0.19$, $ts = -6$, $sf = 0.019$ is achieved as shown in Figure G.40.

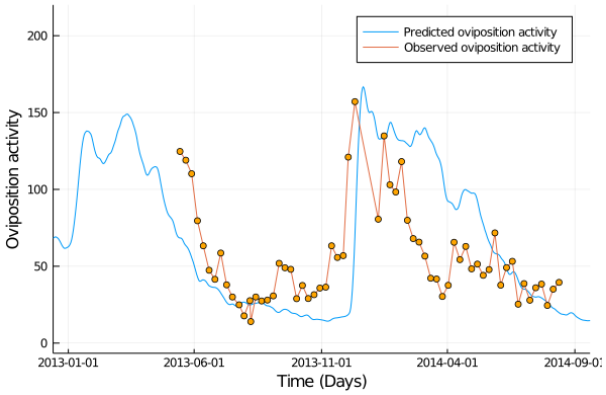

Figure G.40: A comparison of the predictions of the model (blue line) and field data (orange points and line) for oviposition activity in Saint-Marie in the years 2013 – 2014

H Validations of the SIR model

To validate the SIR model I compare the daily or weekly number of dengue cases observed over the course of real-world dengue outbreaks and compare them directly to the model output. Unlike the validations for the model of the population dynamics of *Ae. albopictus* no scaling factors are applied, although a uniform time-shift of 14 days is applied across all locations to roughly approximate the delay between when a dengue case is contracted and when it is detected (Yuan et al., 2019). In addition to the usual environmental parameters I must determine an appropriate human population density per $4km^2$, define a scenario for the introduction of dengue into the human population, and choose an area over which to simulate the model. To determine human population density the Gridded Population of the World, Version 4 (GPWv4) is used (Palisades, , SEDAC). To determine the introduction of infected humans into the population I look to contact tracing and imported case detection undertaken during the course of the outbreak. The area an outbreak has occurred over is determined by consulting maps of the spatial distribution of dengue cases.

For many of the outbreaks considered the number and timing of case introductions is not precisely known. Even for those outbreaks where considerable effort was expended on tracking introduction events the sensitivity of the model to the precise timing of these events and the

stochastic nature of the initial stages of an outbreak means that there are many reasonable introduction scenarios I might choose. At each of the outbreak locations different forms of mosquito control activity were employed and I do not account for these in any way. Control activities commonly include larval source reduction, the application of adulticides and larvicides, in combination with public health awareness campaigns and so I do not expect the effect of these control activities to be uniform across outbreak locations. This uncertainty is further exacerbated by the underlying assumptions that are made by the model for mosquito population dynamics. The aim of these validations is therefore only to demonstrate that under reasonable assumptions the model can recreate the dynamics and magnitude of dengue outbreaks. Despite this, under plausible conditions a good resemblance between observed and predicted dengue dynamics is achieved over a broad range of environments.

H.1 Cagnes-sur-Mer

In this region of France there are sporadic instances of autochthonous transmission of dengue that occur between the months of August and October (ECDC, 2022a). These outbreaks are typical of those currently experienced throughout Europe where despite the regular introduction of dengue there is little evidence of sustained cycles of disease transmission. I simulate the SIR model in this region for the years 2018, 2019, and 2020 under an introduction scenario such that a single infected individual is introduced on the first day of the first month that a dengue transmission event was reported. In Figure H.1 I see that in each year a very limited amount of dengue spread is predicted within the same order of magnitude as is observed in the field. Although the relative size of each outbreak is correctly predicted, there is substantial uncertainty in the model estimate due to the unknown amount of dengue introduced to each area, the unknown time of introduction, the role of stochasticity in the size of small outbreaks.

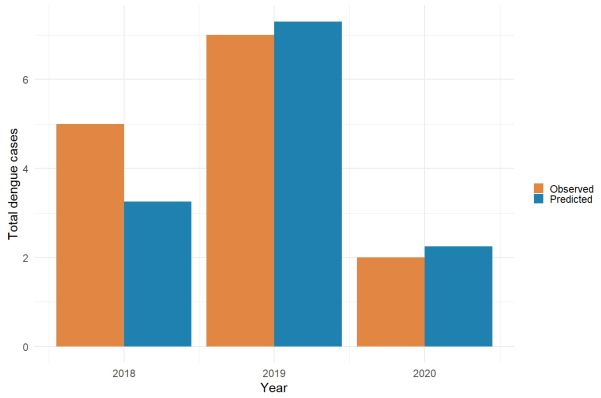

Figure H.1: A comparison of the total number of dengue cases observed in the Alpes-Maritimes department of France predicted by the model and observed in the field in the years $2018 - 2020$.

H.2 Guangzhou, China

There are regular dengue outbreaks in the Guangdong region for which *Ae. albopictus* is the primary vector, and here the SIR model is used to predict dengue dynamics in the years for which detailed dengue onset data is available. I specifically consider 2013, in which there was a relatively small outbreak, and 2014 in which there was a much larger outbreak (Xu et al., 2017). High numbers of cases were observed over an area of roughly $80km^2$ in a region in which there is on average a population density of $32,000$ people per km^2 (Yue et al., 2018). Using the SIR model the infectious individual introduction scenarios described in Luo et al. (2017) are replicated, introducing 30 infectious individuals over the region of interest through the year in 2014 with a limited initial introduction in 2013. In Figure H.2 it can be seen that under these conditions convincing dengue dynamics over the years of interest are produced, capturing the relative magnitude of the outbreaks well in addition to the initial period of infection. Although in 2013 the dynamics towards the end of the outbreak are convincingly replicated, this seems not to be the case in 2014. This mismatch likely occurs due to the substantial intervention that occurred in response to the 2014 outbreak which likely prevented the continued transmission of disease. The total number of dengue cases observed in 2014 in Guangzhou city was $36,342$

and a previous study based on time series analysis estimated that the intervention prevented an additional 23,302 cases of dengue (Lin et al., 2016b). I broadly agree with this figure and predict that the intervention prevented an additional 27,907 cases of dengue in 2014.

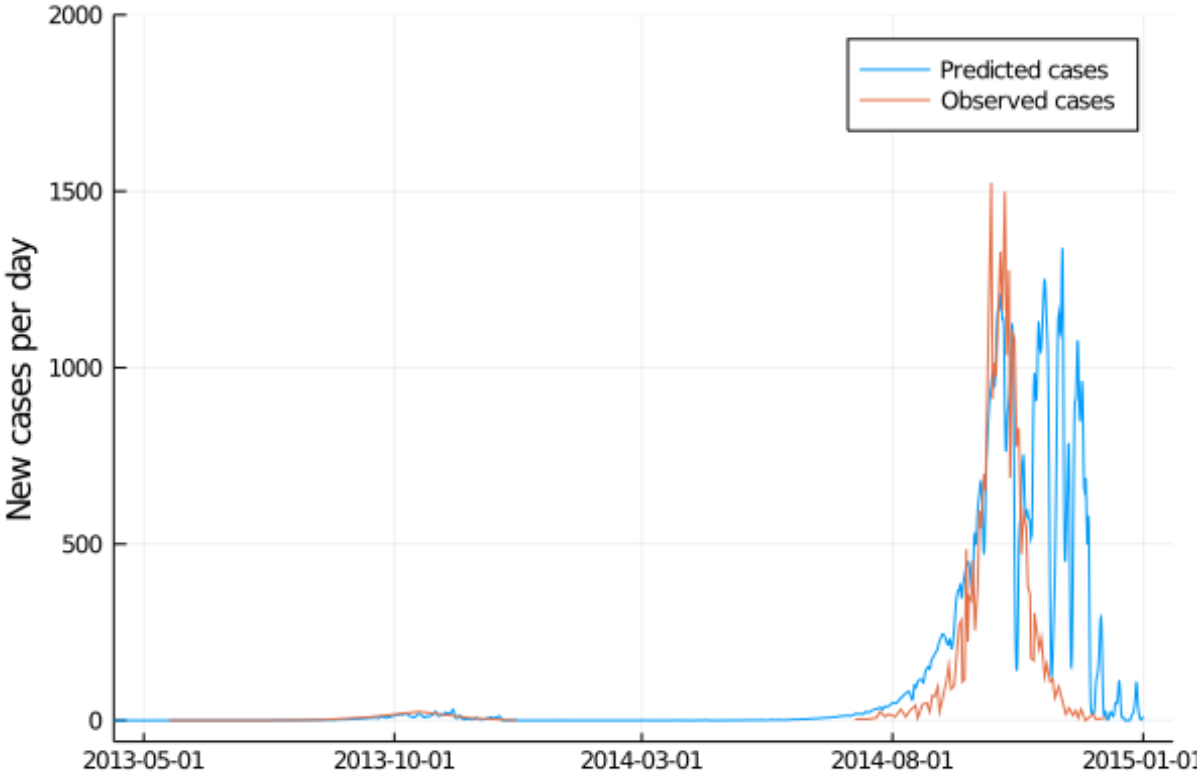

Figure H.2: A comparison of the predictions of the model (blue line) and disease incidence data (orange line) for Guangzhou, China for the years 2013 – 2014.

H.3 Tokyo, Japan

In 2014 in Tokyo there was an outbreak of dengue fever centred around Yoyogi park (Yuan et al., 2019). This outbreak coincided with an international festival that made determining the initial introduction event difficult, and so I choose an introduction scenario similar to that used in Cagnes-sur-Mer, with the first case introduced on the 1^{st} day of the first month that transmission was reported. In Figure H.3 I see that the model predicts the dengue dynamics

well, and it appears that the intervention had minimal effect on transmission dynamics.

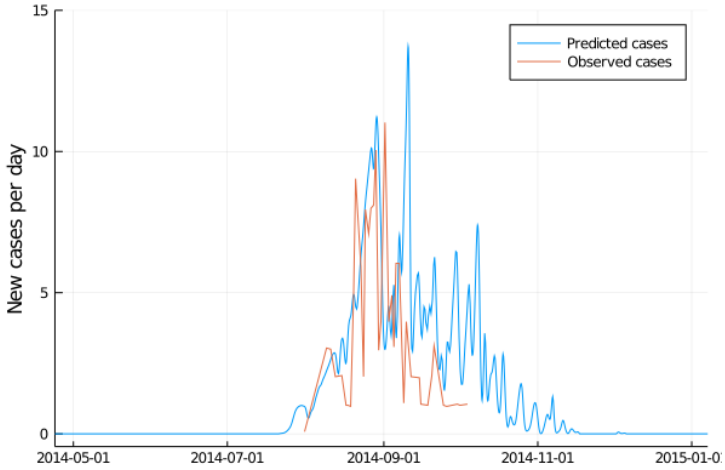

Figure H.3: A comparison of the predictions of the model (blue line) and disease incidence data (orange line) for Tokyo, Japan for the year 2014.

H.4 Réunion, France

We use the SIR model to predict the dengue dynamics of the $2017-2021$ dengue outbreak. This outbreak began in 2016 with introduction when DENV-II replaced the previously circulating DENV-I, however the first year in which DENV-II was the dominant serotype was 2017 when it circulated at low levels. After subsiding transmission was renewed in 2018 resulting in a moderate outbreak that caused $6,770$ cases of dengue over the whole year. After once again subsiding the outbreak continued in 2019 reaching a peak of cases and then being replaced by the end of the year by an outbreak of DENV-I that continued into 2021 (Hafsia S, Haramboure M, Wilkinson DA, Baldet T, Yemadje-Menudier L, Vincent M, Tran A, Atyame C, 2022). For the prediction of this outbreak I define an introduction scenario where infected individuals begin entering the population in 2017 at a level that amounts to 11 individuals each year, which is in line with the number of introduced dengue cases observed (Vincent et al., 2019). The dynamics are then simulated until the end of the outbreak in 2021 and I compare the number of cases predicted to those that were observed. In Figure H.4 it can be observed that the model predicted the relative

magnitude of outbreaks well and appears to capture the timing of the outbreaks subsidence and resurgence between years correctly. The model overestimates the amount of transmission during the winter months, and this might be attributable to control efforts reducing adult densities by the end of the year, and so reducing the number of infected adults still in the population. The switch from DENV-I to DENV-II, in 2020 has not appeared to change the similarity between the dynamics predicted to those observed, implying that the inter-annual variation observed is driven by environmental factors rather than the human population's resistance to dengue.

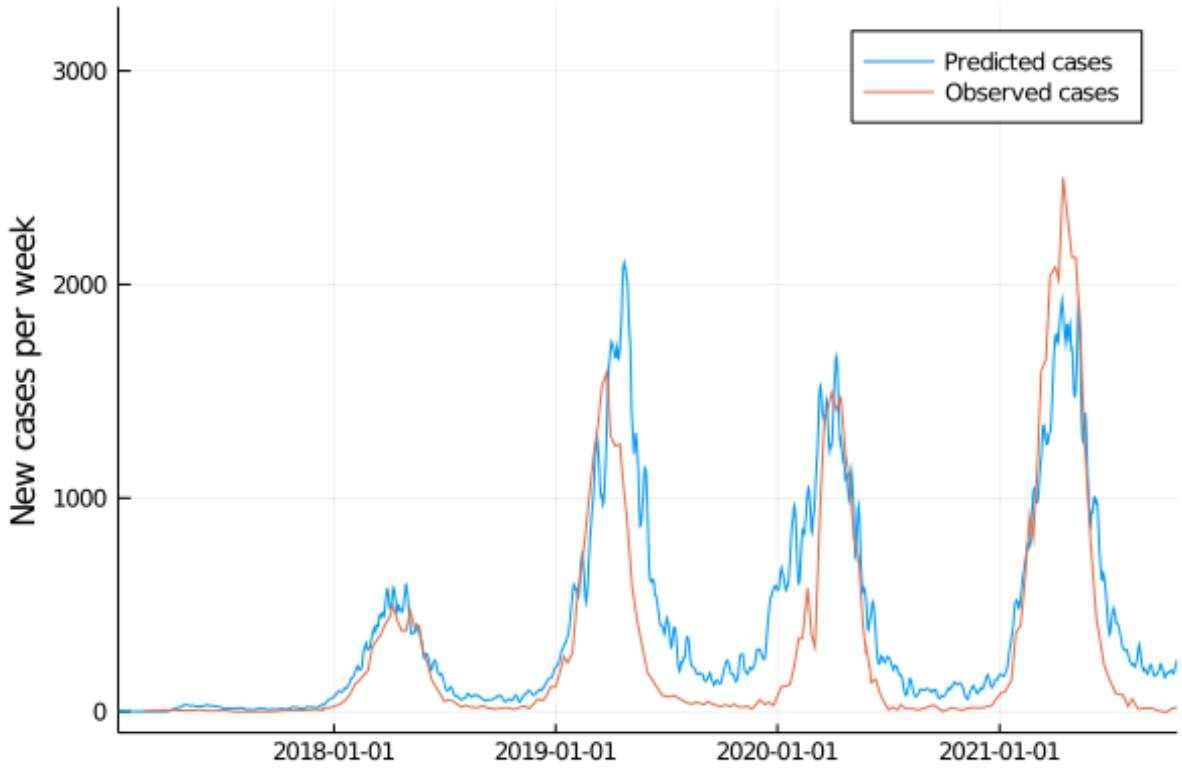

Figure H.4: A comparison of the predictions of the model (blue line) and field data (orange points and line) of the total number of dengue cases observed per week in La Réunion for the years 2017 – 2021 .

H.5 Hawai'i

There was an outbreak of dengue on the island of Hawai'i between 2015 – 2016, cases were clustered predominately in the west of the island but were observed throughout the region (Johnston et al., 2020). As of 2010 it was estimated that urban clusters in Hawai'i county covered a land area of $224.7km^2$ with an average population density of 1322.1 people per km^2, and these are the conditions under which I simulate the model (U.S. Census Bureau, 2011). As there is no information available about introduction timing I follow the introduction scenario outlined for Réunion (Figure H.5).

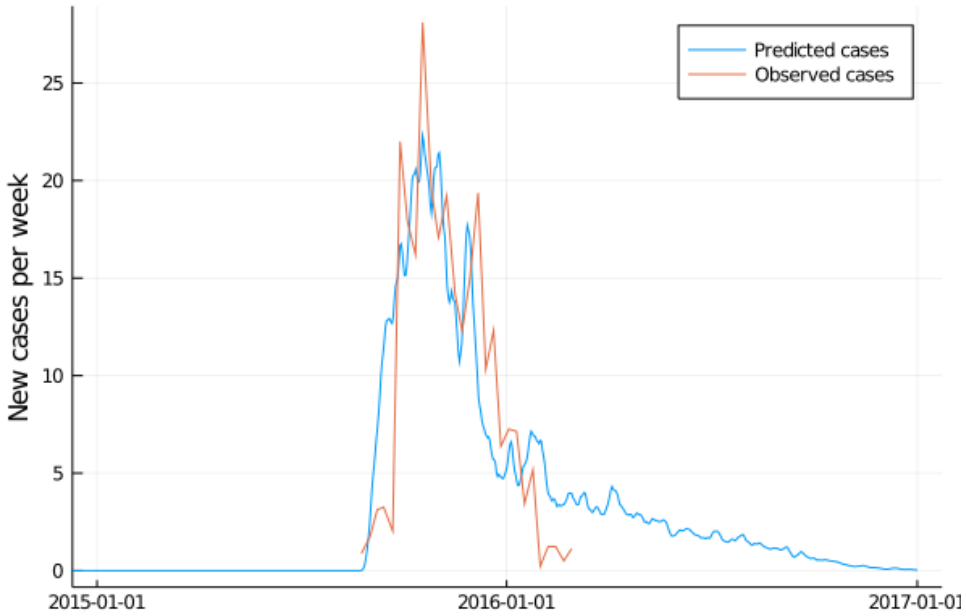

Figure H.5: A comparison of the predictions of the model (blue line) and field data (orange points and line) for the number of weekly dengue cases in Hawai'i, America.

I Non-plastic R_T

I.1 Comparison to previous R_0 equations

To contextualise the predictions of length of time for which regions are suitable for the autochthonous transmission of dengue by *Ae. albopictus* I compare my predictions to those made by a previous mechanistic model by Mordecai et al. (2017) that employed a commonly used metric to calculate a solely temperature-dependent version of R_0 for the same species (Mordecai et al., 2017). This model considers only the instantaneous response of each component of the transmission cycle to temperature and therefore can not consider the effect of population history on transmission dynamics. Consequently, rather than defining the transmission period to between the first and last time in a year that $R_0 > 1$, when using this approach instead define the transmission period to be the longest duration for which $R_0 > 1$ continuously, which is necessary due to the high variability of temperature data. In this equation $a(T)$ is the biting rate of mosquitoes, $b(T)$ is the proportion of infectious bites that successfully transmit an infection from an infected mosquito to an uninfected human, $c(T)$ is the proportion of uninfected mosquitoes that become infected upon biting an infected human. The mortality rate of adult mosquitoes is denoted $\mu(t)$, the intrinsic incubation period is $PDR(T)$, $EFD(T)$ is the number of eggs produced per female mosquito per day, $MDR(T)$ is the development rate of immature mosquitoes, N is the population density of humans, r is the rate at which humans recover from infections. The basic reproduction number $R_0(T)$ is then defined

$$R_0(T(t)) = \left(\frac{a(T)^2 b(T) c(T) \exp^{-\mu(t)/PDR(T)} EFD(T) p_{EA}(T) MDR(T)}{N r \mu(T)^3} \right)^{1/2}$$

This metric is computed over the full range considered by the trait-structured model and it can be observed that this non-plastic and non-dynamic approach predicts broad suitability for transmission of dengue over a considerably larger region (Figure I.1. Regions known to be at high risk of dengue outbreaks are often indistinct from those that experience little to no transmission.

For example, the south of Spain where little dengue transmission has occurred appears to be at similar risk to Guangzhou, the location of the largest *Ae. albopictus* vectored outbreak of dengue.

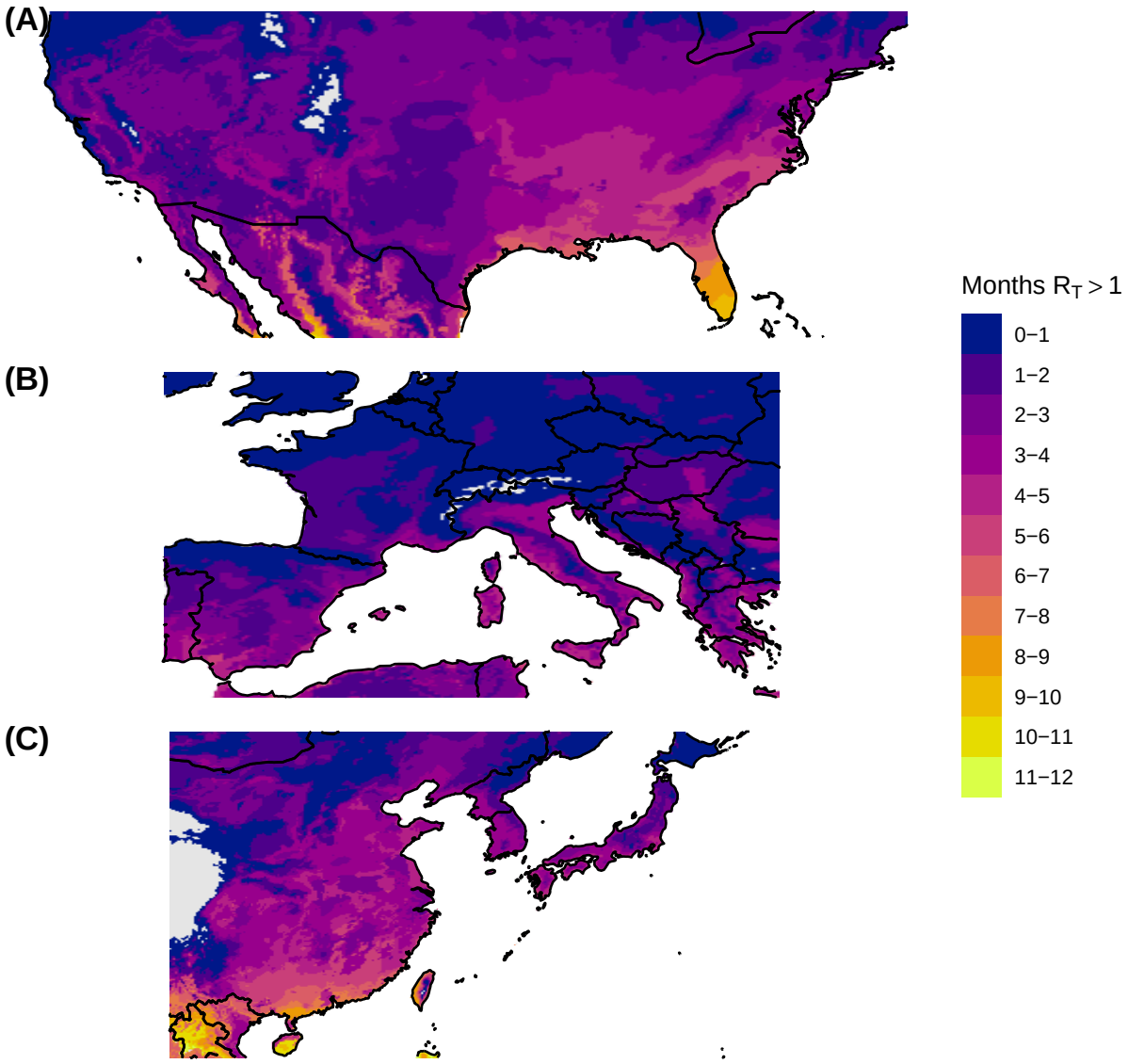

Figure I.1: The number of months for which a metric based R_0 approach predicts that the autochthonous transmission of dengue by *Ae. albopictus* is possible in **(A)** Europe. **(B)** America. **(C)** Asia. .

I.2 Non-plastic R_T with model parameters

Although for variable temperatures the integrals in Equation 4.26 do not have closed form solutions, at constant temperatures the mosquito population is at steady state and therefore R_T is constant. When this is the case the equation for R_T recovers many of the terms used in the common form of the Ross-McDonald type R_0 equation and can be expressed

$$R_T(T) = \frac{\tau_{Inf}(\frac{1}{\delta A^\star(T)} - \tau_{EIP}(T))b^2(T)h_v(T)v_h(T)A^\star(T)P_{EIP}(T)}{H_S}$$

where $A^\star(T)$ is the adult steady-state of a population held at constant temperature T, and $\delta_{A^\star}(T)$ is the associated adult mortality rate of this population.

The behaviour of Equation I.2 at different constant temperatures can be seen in Figure I.2A, and this is similar in form and optimums to previously derived equations for R_T that do not consider phenotypic plasticity or indeed trait-structure. This similarity between my approach and previous estimates at constant temperature indicates that the differences observed between the predictions of transmission duration made here and those made by previous approaches are not attributable to differences in parametrisation.

To demonstrate that this expression for R_T is accurate I can simulate the model at constant temperature without precipitation or evaporation. I select temperatures T_{Min} such that for when the model is simulated with temperature $T_{Min} - \epsilon$, $R_T < 1$ and when simulated at $T_{Min} + \epsilon$, $R_T > 1$. The infection dynamics are expected to behave such that in the case $R_T < 1$ the infection eventually dies out, for $R_T = 1$ the infection is stable, and for $R > 1$ the number of infections increases (although for sufficiently large time all infections will die out due to the lack of immigration or birth). I select $T_{Min} = 23.64$ and set $\epsilon = 0.1$ and simulate the model with a single infection introduced at $t = 1000$. Figures I.2B-I.2D show that under these conditions that the infection dynamics behave as expected.

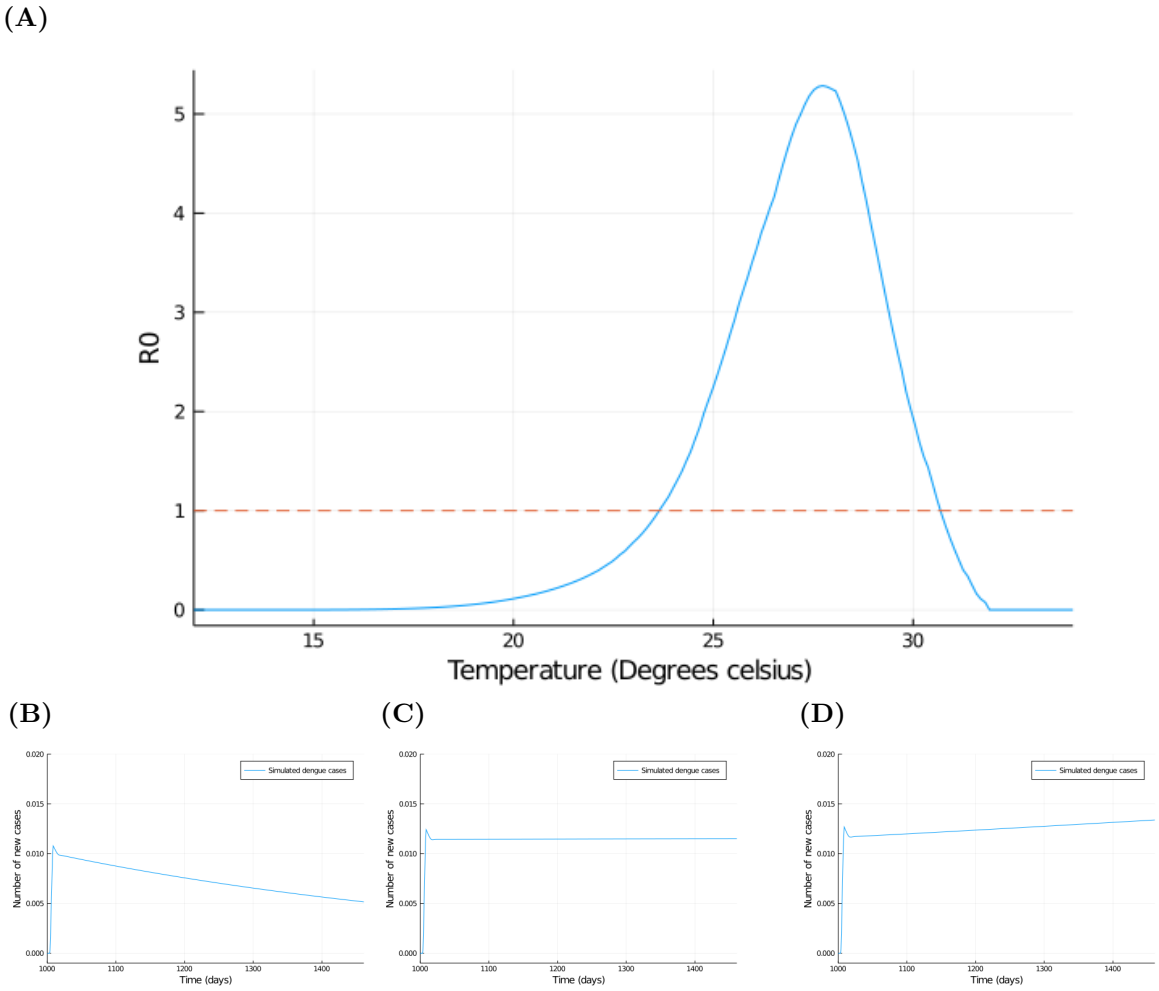

Figure I.2: (a) The value of R_T when the population is held at different constant temperatures. (b) The disease dynamics when R_T is slightly less than 1. (c) The disease dynamics when $R_T = 1$. (d) The disease dynamics when R_T is slightly above 1.

J Glossary and parameter values

Parameter	Interpretation	Values	Source
Environmental variables			
t	Time	Variable	N/A
T	Temperature	Variable	ERA5 climate reanalysis
T_{avg}	Average temperature of the larval period	Variable	ERA5 climate reanalysis
ψ	Photoperiod	Variable	N/A
ρ	Precipitation	Variable	ERA5 climate reanalysis
η	Evaporation	Variable	ERA5 climate reanalysis
μ	Surface area of developmental habitat	$130cm^2$	Tomo et al. (1982)
V	Volume of developmental habitat	500ml	Tomo et al. (1982)
W	Height of water in developmental habitat	Variable	Calculated
l	Latitude	Variable	N/A
F	Food in developmental habitat	Variable	N/A
f_d	Detritus in larval habitat	80	N/A
Eggs			
E_γ	Active eggs	Variable	N/A
E_Q	Quiescent eggs	Variable	N/A
E_D	Diapausing eggs	Variable	N/A
g_{E_γ}	Development rate of active eggs	Variable	N/A
σ_{11}	Parameter in g_{E_γ}	-0.0008256	Fitted
σ_{12}	Parameter in g_{E_γ}	0.0334072	Fitted
σ_{13}	Parameter in g_{E_γ}	-0.0557825	Fitted
τ_{E_γ}	Stage duration of active eggs	Variable	Inverse of g_{E_γ}
S_{E_γ}	Through stage survival proportion of active eggs	Variable	N/A
σ_{21}	Parameter in S_{E_γ}	12.217	Fitted
σ_{22}	Parameter in S_{E_γ}	6.115	Fitted
σ_{23}	Parameter in S_{E_γ}	24.672	Fitted
δ_{E_γ}	Mortality rate of active eggs	Variable	$-log(S_{E_\gamma})/\tau_{E_\gamma}$
Q	Proportion of eggs produced that are quiescent	Variable	N/A
h_Q	Proportion eggs of released from quiescence	Variable	N/A
D	Proportion eggs produced that are diapausing	Variable	N/A
ϕ	Critical photoperiod	Variable	Armbruster et al. (2016)
h_D	Proportion eggs of released from diapause	Variable	N/A
δ_{E_D}	Mortality rate of diapausing eggs	Variable	N/A
Larvae			
L	Larvae	Variable	N/A
α	Food per larvae per day	Variable	N/A
$\bar{\alpha}$	Average per larvae per day over developmental period	Variable	N/A
g_L	Development rate of larvae	Variable	N/A
τ_L	Stage duration of larvae	Variable	Inverse of g_L
S_L	Through stage survival proportion of larvae	Variable	N/A
$\hat{S}_L$	Through stage survival proportion of larvae independently of density and hydrological processes	Variable	N/A
δ_L	Mortality rate of larvae	Variable	N/A
δ_d	Mortality rate of juveniles when the habitat dries out	0.99	N/A
δ_f	Mortality rate of juveniles during overspill	0.2	N/A
Pupae			
P	Pupae	Variable	N/A
g_P	Development rate of pupae	Variable	N/A

σ_{31}	Parameter in g_P	$2.916e-05$	Fitted
σ_{32}	Parameter in g_P	$1.008e+01$	Fitted
σ_{33}	Parameter in g_P	$4.768e+01$	Fitted
σ_{34}	Parameter in g_P	$8.317e-01$	Fitted
τ_P	Stage duration of pupae	Variable	Inverse of g_P
S_P	Through stage survival proportion of larvae	Variable	N/A
$\hat{S}_P$	Through stage survival proportion of larvae independently of density and hydrological processes	Variable	N/A
σ_{41}	Parameter in $\hat{S}_P$	-0.0070628	Fitted
σ_{42}	Parameter in $\hat{S}_P$	0.3331028	Fitted
σ_{43}	Parameter in $\hat{S}_P$	-2.9878761	Fitted
δ_P	Mortality rate of pupae	Variable	N/A
Adults			
A_j	Adults in environmental class j	Variable	N/A
w_L	Wing length of adults	Fitted	N/A
τ_{A_50}	Time until 50% mortality of adults	Fitted	N/A
w_{min}	Minimum wing length of adults	1.5mm	N/A
w_{max}	Maximum wing length of adults	4mm	N/A
w_j	Transition function into environmental class j	4mm	N/A
q	Number of eggs produced per gonotrophic cycle	Variable	Blackmore and Lord (2000)
σ_{51}	Parameter in q	2.35	Fitted
σ_{52}	Parameter in q	0.69	Fitted
q_j	Rate at which an adults in environmental class j produce eggs	N/A	
G	Length of gonotrophic cycle	Variable	Mordecai et al. (2017)
σ_{61}	Parameter in G	$1.93e-04$	Fitted
σ_{62}	Parameter in G	10.25	Fitted
σ_{63}	Parameter in G	38.32	Fitted
δ_{A_j}	Mortality rate of adults in environmental class j	Variable	N/A
Model variables			
R_X	Recruitment of individuals into life-stage X	Variable	N/A
M_X	Maturation of individuals out of life-stage X	Variable	N/A
m	Number of environmental classes	Variable	N/A
j	Index	Variable	N/A
C	Impulse to initiate dynamics	Variable	N/A
Dengue transmission variables			
b	Biting rate	Variable	Inverse of G
h_v	Proportion of uninfected mosquitoes that become infect after biting an infected human	Variable	Liu-Helmersson et al. (2014)
v_h	Proportion of uninfected humans that become infect after being bitten by an infected mosquito	Variable	Liu-Helmersson et al. (2014)
τ_{EIP}	Length of the extrinsic incubation period (EIP)	Variable	Brady et al. (2014)
τ_{IIP}	Length of the intrinsic incubation period (IIP)	4	Chan and Johansson (2012)
τ_{rec}	Time taken for infected humans to recover from infection	4	Mordecai et al. (2017)
H_S	Number of susceptible humans	Variable	NASA SEDAC
H_I	Number of infected humans	Variable	N/A
H_R	Number of resistant humans	Variable	N/A
H_b	Size of buffer population	3750	Various
H_T	Total population	Variable	N/A
κ	Number of larval habitats per km^2	40	Various
I_j	Number of infected mosquitoes in environmental class j	Variable	N/A

P_{EIP}	Proportion of adults in environmental class j that survive through the EIP	Variable	N/A

Table J.1: Table of parameters and variables.

Bibliography

Abd Sahar. Life Cycle and Cytogenetic Study of Mosquitoes (Diptera: Culicidae) // Life Cycle and Development of Diptera. Rijeka: IntechOpen, 2020. 3.

Acasuso-Rivero Cristina, Murren Courtney J., Schlichting Carl D., Steiner Ulrich K. Adaptive phenotypic plasticity for life-history and less fitness-related traits // Proceedings of the Royal Society B: Biological Sciences. 2019. 286, 1904. 1–9.

Alam Md. Sha, Tuno Nobuko. A study comparing the growth rates of two related species, Aedes albopictus and Aedes flavopictus (Diptera: Culicidae) at different temperature regimes // Medical Entomology and Zoology. 2020. 71, 1. 25–30.

Allgood D. W., Yee D. A. Influence of resource levels, organic compounds and laboratory colonization on interspecific competition between the Asian tiger mosquito Aedes albopictus (Stegomyia albopicta) and the southern house mosquito Culex quinquefasciatus // Medical and Veterinary Entomology. 2014. 28, 3. 273–286.

Althouse Benjamin M., Hanley Kathryn A., Diallo Mawlouth, Sall Amadou A., Ba Yamar, Faye Ousmane, Diallo Diawo, Watts Douglas M., Weaver Scott C., Cummings Derek A.T. Impact of climate and mosquito vector abundance on sylvatic arbovirus circulation dynamics in senegal // American Journal of Tropical Medicine and Hygiene. 2015. 92, 1. 88–97.

Alto BW, Lounibos LP, Higgs S, Juliano SA. Larval competition differentially affects arbovirus infection in aedes mosquitoes // Ecology. 09 2005. 86, 12. 3279–3288.

Alto Barry W., Bettinardi David J., Ortiz Sara. Interspecific larval competition differentially impacts adult survival in dengue vectors // Journal of Medical Entomology. 2015. 52, 2. 163–170.

Alto Barry W., Juliano Steven A. Temperature Effects on the Dynamics of Aedes albopictus (Diptera: Culicidae) Populations in the Laboratory // Journal of Medical Entomology. 2001. 38, 4. 548–556.

Alto Barry W., Lounibos L. Philip, Mores Christopher N., Reiskind Michael H. Larval competition alters susceptibility of adult Aedes mosquitoes to dengue infection // Proceedings of the Royal Society B: Biological Sciences. 2008. 275, 1633. 463–471.

Amos Beatrice, Aurrecoechea Cristina, Barba Matthieu, Barreto Ana, Basenko Evelina Y., Bażant Wojciech, Belnap Robert, Blevins Ann S., Böhme Ulrike, Brestelli John, Brunk Brian P., Caddick Mark, Callan Danielle, Campbell Lahcen, Christensen Mikkel B.,

Christophides George K., Crouch Kathryn, Davis Kristina, Debarry Jeremy, Doherty Ryan, Duan Yikun, Dunn Michael, Falke Dave, Fisher Steve, Flicek Paul, Fox Brett, Gajria Bindu, Giraldo-Calderón Gloria I., Harb Omar S., Harper Elizabeth, Hertz-Fowler Christiane, Hickman Mark J., Howington Connor, Hu Sufen, Humphrey Jay, Iodice John, Jones Andrew, Judkins John, Kelly Sarah A., Kissinger Jessica C., Kwon Dae Kun, Lamoureux Kristopher, Lawson Daniel, Li Wei, Lies Kallie, Lodha Disha, Long Jamie, MacCallum Robert M., Maslen Gareth, McDowell Mary Ann, Nabrzyski Jaroslaw, Roos David S., Rund Samuel S.C., Schulman Stephanie Wever, Shanmugasundram Achchuthan, Sitnik Vasily, Spruill Drew, Starns David, Stoeckert Christian J., Tomko Sheena Shah, Wang Haiming, Warrenfeltz Susanne, Wieck Robert, Wilkinson Paul A., Xu Lin, Zheng Jie. VEuPathDB: The eukaryotic pathogen, vector and host bioinformatics resource center // Nucleic Acids Research. 2022. 50, D1. D898–D911.

Amraoui F, Vazeille Marie, Failloux Anna-bella. French Aedes albopictus are able to transmit yellow fever virus Experimental infection of mosquitoes // Euro Surveill. 2016. 21, 39. 1–3.

Amraoui Fadila, Ayed Wiem Ben, Madec Yoann, Faraj Chafika, Himmi Oumnia, Btissam Ameur, Sarih Mhammed, Failloux Anna Bella. Potential of aedes albopictus to cause the emergence of arboviruses in Morocco // PLoS Neglected Tropical Diseases. 2019. 13, 2. 1–12.

Anderson Jill T., Inouye David W., McKinney Amy M., Colautti Robert I., Mitchell-Olds Tom. Phenotypic plasticity and adaptive evolution contribute to advancing flowering phenology in response to climate change // Proceedings of the Royal Society B: Biological Sciences. 2012. 279, 1743. 3843–3852.

Andrade C. C., Young K. I., Johnson W. L., Villa M. E., Buraczyk C. A., Messer W. B., Hanley K. A. Rise and fall of vector infectivity during sequential strain displacements by mosquito-borne dengue virus // Journal of Evolutionary Biology. 2016. 29, 11. 2205–2218.

Armbruster Peter, Hutchinson Robert A. Pupal Mass and Wing Length as Indicators of Fecundity in Aedes albopictus and Aedes geniculatus (Diptera: Culicidae) // Journal of Medical Entomology. 2002.

Armbruster Peter A. Photoperiodic Diapause and the Establishment of Aedes albopictus (Diptera: Culicidae) in North America // Journal of Medical Entomology. 2016. 53, 5. 1013–1023.

Armstrong Philip M., Andreadis Theodore G., Shepard John J., Thomas Michael C. Northern range expansion of the Asian tiger mosquito (Aedes albopictus): Analysis of mosquito data from Connecticut, USA // PLoS Neglected Tropical Diseases. 2017. 11, 5. 1–13.

Auger Pierre, Kouokam Etienne, Sallet Gauthier, Tchuente Maurice, Tsanou Berge. The Ross-Macdonald model in a patchy environment // Mathematical Biosciences. 2008. 216, 2. 123–131.

Baker H. G., Stebbins G. I. The genetics of colonizing species. New York, 1965.

Bakker K. Backgrounds of controversies about population theories and their terminologies // Journal of Applied Entomology. 1963. 53, 1-4.

Balestrino Fabrizio, Puggioli Arianna, Gilles Jérémie R.L., Bellini Romeo. Validation of a new larval rearing unit for Aedes albopictus (Diptera: Culicidae) mass rearing // PLoS ONE. 2014. 9, 3.

Bara Jeffrey, Rapti Zoi, Cáceres Carla E., Muturi Ephantus J. Effect of larval competition on extrinsic incubation period and vectorial capacity of Aedes albopictus for dengue virus // PLoS ONE. 2015. 10, 5. 1–18.

Barbazan P., Guiserx M., Boonyuan W., Tuntparasart W., Pnotier D., Gonzalez J.-P. Modelling the effect of temperature on transmission of dengue // Medical and Veterinary Entomology. 2010. 24. 66–73.

Beck-Johnson Lindsay M., Nelson William A., Paaijmans Krijn P., Read Andrew F., Thomas Matthew B., Bjørnstad Ottar N. The effect of temperature on Anopheles mosquito population dynamics and the potential for malaria transmission // PLoS ONE. 2013.

Beck-Johnson Lindsay M., Nelson William A., Paaijmans Krijn P., Read Andrewf, Thomas Matthew B., Bjørnstad Ottar N. The importance of temperature fluctuations in understanding mosquito population dynamics and malaria risk // Royal Society Open Science. 2017.

Becker Norbert, Langentepe-Kong Sophie Min, Tokatlian Rodriguez Artin, Oo Thin Thin, Reichle Dirk, Lühken Renke, Schmidt-Chanasit Jonas, Lüthy Peter, Puggioli Arianna, Bellini Romeo. Integrated control of Aedes albopictus in Southwest Germany supported by the Sterile Insect Technique // Parasites and Vectors. 2022. 15, 1. 1–19.

Beckerman Andrew, Benton Tim G., Ranta Esa, Kaitala Veijo, Lundberg Per. Population dynamic consequences of delayed life-history effects // Trends in Ecology and Evolution. 2002. 17, 6. 263–269.

Bella Salvatore, Russo A., Suma P. Monitoring of Aedes albopictus (Skuse) (Diptera, Culicidae) in the city of Catania (Italy): Seasonal dynamics and habitat preferences // Journal of Entomological and Acarological Research. 2018. 50, 2. 25–30.

Bellini Romeo, Puggioli Arianna, Balestrino Fabrizio, Brunelli Paolo, Medici Anna, Urbanelli Sandra, Carrieri Marco. Sugar administration to newly emerged Aedes albopictus males increases their survival probability and mating performance // Acta Tropica. 2014. 132, 1. S116–S123.

Benedict Mark Q, Levine Rebecca S, Hawley William A, Lounibos L Philip. Spread of The Tiger: Global Risk of Invasion by The Mosquito *Aedes albopictus* // Vector-Borne and Zoonotic Diseases. 2007. 7, 1. 76–85.

Statistical modeling of the effect of rainfall flushing on dengue transmission in Singapore. // . 2018.

Bernardo Joseph. Maternal effects in animal ecology // American Zoologist. 1996. 36, 2. 83–105.

Bezanson Jeff, Edelman Alan, Karpinski Stefan, Shah Viral B. Julia: A fresh approach to numerical computing // SIAM review. 2017. 59, 1. 65–98.

Bhatt Samir, Gething Peter W, Brady Oliver J, Messina Jane P, Farlow Andrew W, Moyes Catherine L, Drake John M, Brownstein John S, Hoen Anne G, Sankoh Osman, Myers Monica F, George Dylan B, Jaenisch Thomas, Wint G R William, Simmons Cameron P, Scott Thomas W, Farrar Jeremy J, Hay Simon I. The global distribution and burden of dengue // Nature. 2013. 496, 7446. 504–507.

Bier Ethan. Gene drives gaining speed // Nature Reviews Genetics. 2022. 23, 1. 5–22.

Binckley Christopher A. Forest canopy, water level, and biopesticide interact to determine oviposition habitat selection in Aedes albopictus // Journal of Vector Ecology. 2017.

Black William C., Rai Karamjit S., Turco Brian J., Arroyo David C. Laboratory Study of Competition Between United States Strains of Aedes albopictus and Aedes aegypti (Diptera: Culicidae) // Journal of Medical Entomology. 1989. 26, 4. 260–271.

Blackmore Mark S, Lord Cynthia C. The relationship between size and fecundity in Aedes albopictus // Journal of Vector Ec. 2000. 25, 2. 212–217.

Blagrove Marcus S.C., Arias-Goeta Camilo, Di Genua Cristina, Failloux Anna Bella, Sinkins Steven P. A Wolbachia wMel Transinfection in Aedes albopictus Is Not Detrimental to Host Fitness and Inhibits Chikungunya Virus // PLoS Neglected Tropical Diseases. 2013. 7, 3.

Bolnick Daniel I., Amarasekare Priyanga, Araújo Márcio S., Bürger Reinhard, Levine Jonathan M., Novak Mark, Rudolf Volker H.W. W, Schreiber Sebastian J., Urban Mark C., Vasseur David A. Why intraspecific trait variation matters in community ecology // Trends in Ecology and Evolution. 2011. 26, 4. 183–192.

Bonacci Teresa, Mazzei Antonio, Hristova Vesna K, Ahmad M Ayaz. Monitoring of Aedes albopictus (Diptera, Cilicidae) in Calabria, Southern Italy // International Journal of Scientific and Engineering Research. 2015. 6, 5. 290–293.

Bosio C, Fulton R, Salasek M, Beaty B, Iv W. Dengue-2 Virus in the Mosquito Aedes aegypti // Genetics. 2000. 156, 1. 687–698.

Boutin Stan, Lane Jeffrey E. Climate change and mammals: Evolutionary versus plastic responses // Evolutionary Applications. 2014. 7, 1. 29–41.

Brady Oliver J., Gething Peter W., Bhatt Samir, Messina Jane P., Brownstein John S., Hoen Anne G., Moyes Catherine L., Farlow Andrew W., Scott Thomas W., Hay Simon I. Refining the Global Spatial Limits of Dengue Virus Transmission by Evidence-Based Consensus // PLoS Neglected Tropical Diseases. 2012. 6, 8.

Brady Oliver J., Golding Nick, Pigott David M., Kraemer Moritz U.G., Messina Jane P., Reiner Robert C., Scott Thomas W., Smith David L., Gething Peter W., Hay Simon I. Global temperature constraints on Aedes aegypti and Ae. albopictus persistence and competence for dengue virus transmission // Parasites and Vectors. 2014. 7, 1. 1–17.

Brady Oliver J., Hay Simon I. The global expansion of dengue: How aedes aegypti mosquitoes enabled the first pandemic arbovirus // Annual Review of Entomology. 2020. 65. 191–208.

Brady Oliver J, Johansson Michael a, Guerra Carlos a, Bhatt Samir, Golding Nick, Pigott David M, Delatte Hélène, Grech Marta G, Leisnham Paul T, Freitas Rafael Maciel-de, Styer Linda M, Smith David L, Scott Thomas W, Gething Peter W, Hay Simon I. Modelling adult Aedes aegypti and Aedes albBrady, O. J., Johansson, M. a, Guerra, C. a, Bhatt, S., Golding, N., Pigott, D. M., ... Hay, S. I. (2013). Modelling adult Aedes aegypti and Aedes albopictus survival at different temperatures in laboratory and fie // Parasites & vectors. 2013. 6. 351.

Brand Samuel P.C. C, Rock Kat S., Keeling Matt J. The Interaction between Vector Life History and Short Vector Life in Vector-Borne Disease Transmission and Control // PLoS Computational Biology. 2016. 12, 4. 1–21.

Brass Dominic P., Cobbold Christina A., Ewing David A., Purse Bethan V., Callaghan Amanda, White Steven M. Phenotypic plasticity as a cause and consequence of population dynamics // Ecology Letters. 2021. July. 1–12.

Briegel Hans, Timmermann Susanne E. Aedes albopictus (Diptera: Culicidae): Physiological Aspects of Development and Reproduction // Journal of Medical Entomology. 2001. 38, 4. 566–571.

Brown James H., Gillooly James F., Allen Andrew P., Savage Van M., West Geoffrey B. Toward a metabolic theory of ecology // Ecology. 2004. 85, 7. 1771–1789.

Brunkard Joan Marie, Robles López Jose Luis, Ramirez Josue, Cifuentes Enrique, Rothenberg Stephen J, Hunsperger Elizabeth A, Moore Chester G, Brussolo Regina M, Villarreal Norma A, Haddad Brent M. Dengue fever seroprevalence and risk factors, Texas-Mexico border, 2004. // Emerging infectious diseases. oct 2007. 13, 10. 1477–1483.

Buckner Eva A., Alto Barry W., Lounibos L. Philip. Larval temperature-food effects on adult mosquito infection and vertical transmission of dengue-1 virus // Journal of Medical Entomology. 2016. 53, 1. 91–98.

Burgess Scott C., Marshall Dustin J. Temperature-induced maternal effects and environmental predictability // Journal of Experimental Biology. 2011. 214, 14. 2329–2336.

Buskirk Josh Van, McCollum S. Andy. Plasticity and Selection Explain Variation in Tadpole Phenotype between Ponds with Different Predator Composition // Oikos. 1999. 85, 1. 31.

Buskirk Josh Van, Mccollum S Andy. Plasticity and Selection Explain Variation in Tadpole Phenotype between Ponds with Different Predator Composition // Oikos. 2016. 85, 1. 31–39.

Calado Daniéla Cristina, Navarro da Silva Mário Antônio. Evaluation of the temperature influence on the development of Aedes albopictus // Revista de Saude Publica. 2002. 36, 2. 173–179.

Calvitti Maurizio, Moretti Riccardo, Lampazzi Elena, Bellini Romeo, Dobson Stephen L. Characterization of a new aedes albopictus (Diptera: Culicidae)-Wolbachia pipientis (Rickettsiales: Rickettsiaceae) symbiotic association generated by artificial transfer of the wPip strain from culex pipiens (Diptera: Culicidae) // Journal of Medical Entomology. 2010. 47, 2. 179–187.

Cameron T C, Benton T G. Stage-structured harvesting and its effects : an empirical // Journal of Animal Ecology. 2004. 996–1006.

Cameron Tom C., O'Sullivan Daniel, Reynolds Alan, Piertney Stuart B., Benton Tim G. Eco-evolutionary dynamics in response to selection on life-history // Ecology Letters. 2013. 16, 6. 754–763.

Carrieri M., Angelini P., Venturelli C., Maccagnani B., Bellini R. Aedes albopictus (Diptera: Culicidae) Population Size Survey in the 2007 Chikungunya Outbreak Area in Italy. I. Characterization of Breeding Sites and Evaluation of Sampling Methodologies // Journal of Medical Entomology. 2011.

Carrieri M., Angelini P., Venturelli C., Maccagnani B., Bellini R. Aedes albopictus (Diptera: Culicidae) Population Size Survey in the 2007 Chikungunya Outbreak Area in Italy. II: Estimating Epidemic Thresholds // Journal of Medical Entomology. 2012.

Carrieri Marco, Albieri Alessandro, Urbanelli Sandra, Angelini Paola, Venturelli Claudio, Matrangolo Carmela, Bellini Romeo. Quality control and data validation procedure in large-scale quantitative monitoring of mosquito density: the case of Aedes albopictus in Emilia-Romagna region, Italy // Pathogens and Global Health. 2017. 111, 2. 83–90.

Carvajal Thaddeus M., Viacrusis Katherine M., Hernandez Lara Fides T., Ho Howell T., Amalin Divina M., Watanabe Kozo. Machine learning methods reveal the temporal pattern of dengue incidence using meteorological factors in metropolitan Manila, Philippines // BMC Infectious Diseases. 2018. 18, 1. 1–15.

Cator Lauren, Johnson Leah R, Mordecai Erin A, Moustaid Fadoua El, Smallwood Thomas, Deau Shannon La, Johansson Michael, Hudson Peter J, Boots Michael, Thomas Matthew B, Power Alison G, Pawar Samraat. More than a flying syringe: Using functional traits in vector borne disease research // bioRxiv. 2019. 501320.

Cator Lauren J., Johnson Leah R., Mordecai Erin A., El Moustaid Fadoua, Smallwood Thomas R.C., LaDeau Shannon L., Johansson Michael A., Hudson Peter J., Boots Michael, Thomas Matthew B., Power Alison G., Pawar Samraat. The Role of Vector Trait Variation in Vector-Borne Disease Dynamics // Frontiers in Ecology and Evolution. 2020. 8, July.

Chan Ta Chien, Hsu Yu Fen, Huang Shao Chun, Chen Ran Chou. Rapidly containing the first indigenous outbreak of chikungunya in taiwan—lessons learned // Tropical Medicine and Infectious Disease. 2021. 6, 3.

Chandrasegaran Karthikeyan, Lahondère Chloé, Escobar Luis E, Vinauger Clément. Linking Mosquito Ecology, Traits, Behavior, and Disease Transmission. // Trends in parasitology. apr 2020. 36, 4. 393–403.

Chevin Luis Miguel, Lande Russell, Mace Georgina M. Adaptation, plasticity, and extinction in a changing environment: Towards a predictive theory // PLoS Biology. 2010. 8, 4.

Childs Dylan Z., Rees Mark, Rose Karen E., Grubb Peter J., Ellner Stephen P. Evolution of complex flowering strategies: An age- and size-structured integral projection model // Proceedings of the Royal Society B: Biological Sciences. 2003. 270, 1526. 1829–1838.

Collantes Francisco, Delacour Sarah, Alarcón-Elbal Pedro María, Ruiz-Arrondo Ignacio, Delgado Juan Antonio, Torrell-Sorio Antonio, Bengoa Mikel, Eritja Roger, Miranda

Miguel Ángel, Molina Ricardo, Lucientes Javier. Review of ten-years presence of Aedes albopictus in Spain 2004-2014: known distribution and public health concerns // Parasites and Vectors. 2015. 8, 1.

Comiskey Nora M., Lowrie Robert C., Wesson Dawn M. Role of habitat components on the dynamics of Aedes albopictus (Diptera: Culicidae) from New Orleans // Journal of Medical Entomology. 1999. 36, 3. 313–320.

Costanzo K. S., Schelble S., Jerz K., Keenan M. The effect of photoperiod on life history and blood-feeding activity in Aedes albopictus and Aedes aegypti (Diptera: Culicidae) // Journal of Vector Ecology. 2015. 40, 1. 164–171.

Costanzo Katie S, Kesavaraju Banugopan, Juliano Steven A. Condition-specific competition in container mosquitoes: The role of noncompetiting life-history stages // Ecology. 2005. 12, 86. 3289–3295.

Costanzo Katie S., Westby Katie M., Medley Kim A. Genetic and environmental influences on the size-fecundity relationship in Aedes albopictus (Diptera: Culicidae): Impacts on population growth estimates? // PLoS ONE. 2018. 13, 8. 1–17.

Couture-Beil A., Schnute J.T., Haigh R., Wood S.N., Cairns B.J. PBSddesolve: Solver for Delay Differential Equations. 2019.

Crozier Lisa G., Hutchings Jeffrey A. Plastic and evolutionary responses to climate change in fish // Evolutionary Applications. 2014. 7, 1. 68–87.

Cuthbert Ross N., Dalu Tatenda, Wasserman Ryan J., Callaghan Amanda, Weyl Olaf L.F., Dick Jaimie T.A. Using functional responses to quantify notonectid predatory impacts across increasingly complex environments // Acta Oecologica. 2019. 95, November 2018. 116–119.

Dakos Vasilis, Matthews Blake, Hendry Andrew P., Levine Jonathan, Loeuille Nicolas, Norberg Jon, Nosil Patrik, Scheffer Marten, De Meester Luc. Ecosystem tipping points in an evolving world // Nature Ecology and Evolution. 2019. 3, 3. 355–362.

Davidson Amy Michelle, Jennions Michael, Nicotra Adrienne B. Do invasive species show higher phenotypic plasticity than native species and, if so, is it adaptive? A meta-analysis // Ecology Letters. 2011. 14, 4. 419–431.

De La Rocque S., Balenghien T., Halos L., Dietze K., Claes F., Ferrari G., Guberti V., Slingenbergh J. A review of trends in the distribution of vector-borne diseases: Is international trade contributing to their spread? // OIE Revue Scientifique et Technique. 2011. 30, 1. 119–130.

De Roos André M, Persson Lennart. Physiologically structured models – from versatile technique to ecological theory // Oikos. 2001. 94, 1. 51–71.

Delatte H., Gimonneau G., Triboire A., Fontenille D. Influence of Temperature on Immature Development, Survival, Longevity, Fecundity, and Gonotrophic Cycles of Aedes albopictus , Vector of Chikungunya and Dengue in the Indian Ocean // Journal of Medical Entomology. 2009. 46, 1. 33–41.

Deng Jielin, Guo Yijia, Su Xinghua, Liu Shuang, Yang Wenqiang, Wu Yang, Wu Kun, Yan Guiyun, Chen Xiao-Guang. Impact of deltamethrin-resistance in Aedes albopictus on its fitness cost and vector competence // PLoS neglected tropical diseases. 2021. 15, 4. e0009391.

Deutsch Curtis A., Tewksbury Joshua J., Huey Raymond B., Sheldon Kimberly S., Ghalambor Cameron K., Haak David C., Martin Paul R. Impacts of climate warming on terrestrial ectotherms across latitude // Proceedings of the National Academy of Sciences of the United States of America. 2008. 105, 18. 6668–6672.

Dieng Hamady, Rahman G. M.Saifur, Hassan A. Abu, Salmah M. R.Che, Satho Tomomitsu, Miake Fumio, Boots Michael, Sazaly Abu Bakar. The effects of simulated rainfall on immature population dynamics of Aedes albopictus and female oviposition // International Journal of Biometeorology. 2012. 56, 1. 113–120.

Dierckx P. Curve and Surface Fitting with Splines. 1995. (Monographs on numerical analysis).

Dietz K. The estimation of the basic reproduction number for infectious diseases // Statistical Methods in Medical Research. 1993. 2, 1. 23–41.

Ding Fangyu, Jiang Dong, Hao Mengmeng, Lin Gang, Fu Jingying. Mapping the spatial distribution of *Aedes aegypti* and *Aedes albopictus* // Acta Tropica. 2017. 178, August 2017. 155–162.

Diniz Diego Felipe Araujo, De Albuquerque Cleide Maria Ribeiro, Oliva Luciana Oliveira, De Melo-Santos Maria Alice Varjal, Ayres Constância Flávia Junqueira. Diapause and quiescence: Dormancy mechanisms that contribute to the geographical expansion of mosquitoes and their evolutionary success // Parasites and Vectors. 2017. 10, 1. 1–13.

Duong Veasna, Lambrechts Louis, Paul Richard E., Ly Sowath, Lay Rath Srey, Long Kanya C., Huy Rekol, Tarantola Arnaud, Scott Thomas W., Sakuntabhai Anavaj, Buchy Philippe. Asymptomatic humans transmit dengue virus to mosquitoes // Proceedings of the National Academy of Sciences of the United States of America. 2015. 112, 47. 14688–14693.

ECDC . European Centre for Disease Prevention and Control. 2022a.

ECDC . European Centre for Disease Prevention and Control and European Food Safety Authority. Mosquito maps [internet]. 2022b.

Echeverry-Cárdenas Emmanuel, López-Castañeda Carolina, Carvajal-Castro Juan D., Aguirre-Obando Oscar Alexander. Potential geographic distribution of the tiger mosquito aedes albopictus (Skuse, 1894) (diptera: Culicidae) in current and future conditions for colombia // PLoS Neglected Tropical Diseases. 2021. 15, 5. 1–20.

Edelaar Pim, Bolnick Daniel I. Appreciating the Multiple Processes Increasing Individual or Population Fitness // Trends in Ecology and Evolution. 2019. 34, 5. 435–446.

Ekwudu O'Mezie, Marquart Louise, Webb Lachlan, Lowry Kym S., Devine Gregor J., Hugo Leon E., Frentiu Francesca D. Effect of serotype and strain diversity on dengue virus replication in australian mosquito vectors // Pathogens. 2020. 9, 8. 1–14.

Erickson Richard A., Presley Steven M., Allen Linda J.S., Long Kevin R., Cox Stephen B. A stage-structured, Aedes albopictus population model // Ecological Modelling. 2010. 221, 9. 1273–1282.

Eritja Roger, Palmer John R.B., Roiz David, Sanpera-Calbet Isis, Bartumeus Frederic. Direct Evidence of Adult Aedes albopictus Dispersal by Car // Scientific Reports. 2017. 7, 1. 1–15.

European Centre for Disease Prevention and Control . Dengue outbreak in Réunion , France , and associated risk of autochthonous outbreak in the EU. 2019. 1–14.

Evans Michelle V., Hintz Carl W., Jones Lindsey, Shiau Justine, Solano Nicole, Drake John M., Murdock Courtney C. Microclimate and Larval Habitat Density Predict Adult Aedes albopictus Abundance in Urban Areas // The American Journal of Tropical Medicine and Hygiene. 2019. 101, 2. 362–370.

Ewing D. A. Modelling the phenological effects of environmental drivers on mosquito abundance: implications for West Nile virus transmission potential in the UK. 2017.

Ewing D. A., Cobbold C. A., Purse B. V., Nunn M. A., White S. M. Modelling the effect of temperature on the seasonal population dynamics of temperate mosquitoes // Journal of Theoretical Biology. 2016. 400. 65–79.

Ewing David A., Purse Bethan V., Cobbold Christina A., White Steven M. A novel approach for predicting risk of vector-borne disease establishment in marginal temperate environments under climate change: West Nile virus in the UK // Journal of the Royal Society Interface. 2021. 18, 178.

Ezeakacha Nnaemeka F., Yee Donald A. The role of temperature in affecting carry-over effects and larval competition in the globally invasive mosquito Aedes albopictus // Parasites and Vectors. 2019. 12, 1. 1–11.

Falcón-Lezama Jorge A., Martínez-Vega Ruth A., Kuri-Morales Pablo A., Ramos-Castañeda José, Adams Ben. Day-to-Day Population Movement and the Management of Dengue Epidemics // Bulletin of Mathematical Biology. 2016. 78, 10. 2011–2033.

Fan Jing Chun, Liu Qi Yong. Potential impacts of climate change on dengue fever distribution using RCP scenarios in China // Advances in Climate Change Research. 2019. 10, 1. 1–8.

Farjana T., Tuno N., Higa Y. Effects of temperature and diet on development and interspecies competition in Aedes aegypti and Aedes albopictus // Medical and Veterinary Entomology. 2012. 26, 2. 210–217.

Faull Katherine J., Williams Craig R. Intraspecific variation in desiccation survival time of Aedes aegypti (L.) mosquito eggs of Australian origin // Journal of Vector Ecology. 2015. 40, 2. 292–300.

Ferguson Neil M., Rodríguez-Barraquer Isabel, Dorigatti Ilaria, Mier-Y-Teran-Romero Luis, Laydon Daniel J., Cummings Derek A.T. Benefits and risks of the sanofi-pasteur dengue vaccine: Modeling optimal deployment // Science. 2016. 353, 6303. 1033–1036.

Focks D. A. E., Daniels E., Haile D. G., Kessling J. E. A simularion model of the epidemiology of urban dengue fever: literature analysis, model development, preliminary validation, and samples of simulation results // American Journal of Tropical Medicine and Hygiene. 1995. 5, 53. 489–506.

Fonseca Dina M., Unlu Isik, Crepeau Taryn, Farajollahi Ary, Healy Sean P., Bartlett-Healy Kristen, Strickman Daniel, Gaugler Randy, Hamilton George, Kline Daniel, Clark Gary G. Area-wide management of Aedes albopictus. Part 2: Gauging the efficacy of traditional integrated pest control measures against urban container mosquitoes // Pest Management Science. 2013. 69, 12. 1351–1361.

Fontenille Didier, Simard Frédéric. Unravelling complexities in human malaria transmission dynamics in Africa through a comprehensive knowledge of vector populations // Comparative Immunology, Microbiology and Infectious Diseases. 2004. 27, 5. 357–375.

Forsman A. Rethinking phenotypic plasticity and its consequences for individuals, populations and species // Heredity. 2015. 115, 4. 276–284.

Fox Gordon A., Kendall Bruce E. Demographic stochasticity and the variance reduction effect // Ecology. 2002. 83, 7. 1928–1934.

Fusco Giuseppe, Minelli Alessandro. Phenotypic plasticity in development and evolution: Facts and concepts // Philosophical Transactions of the Royal Society B: Biological Sciences. 2010. 365, 1540. 547–556.

Gao Panjun, Pilot Eva, Rehbock Cassandra, Gontariuk Marie, Doreleijers Simone, Wang Li, Krafft Thomas, Martens Pim, Liu Qiyong. Land use and land cover change and its impacts on dengue dynamics in China: A systematic review // PLoS Neglected Tropical Diseases. 2021. 15, 10. 1–21.

Gavotte Laurent, Mercer David R., Vandyke Rhonda, Mains James W., Dobson Stephen L. Wolbachia infection and resource competition effects on immature Aedes albopictus (Diptera: Culicidae) // Journal of Medical Entomology. 2009. 46, 3. 451–459.

Geneva: World Health Organization; . Dengue: Guidelines for Diagnosis, Treatment, Prevention and Control: New Edition. 2009. 2.

Giatropoulos Athanasios, Karamaouna Filitsa, Ampatzi Argyro, Papachristos Dimitrios, Michaelakis Antonios. Sublethal effects of oregano essential oil and its major compound carvacrol on biological parameters of Aedes albopictus (Diptera: Culicidae) // Experimental Parasitology. 10 2022a. 242. 108392.

Giatropoulos Athanasios, Papachristos Dimitrios, Michaelakis Antonios, Kapranas Apostolos, Emmanouel Nickolaos. Laboratory study on larval competition between two related mosquito species: Aedes (Stegomyia) albopictus and Aedes (Stegomyia) cretinus // Acta Tropica. 2022b. 230. 106389.

Gibbons Robert V., Kalanarooj Siripen, Jarman Richard G., Nisalak Ananda, Vaughn David W., Endy Timothy P., Mammen Mammen P., Srikiatkhachorn Anon. Analysis of repeat hospital admissions for dengue to estimate the frequency of third or fourth dengue infections resulting in admissions and dengue hemorrhagic fever, and serotype sequences // American Journal of Tropical Medicine and Hygiene. 2007. 77, 5. 910–913.

Gilbert Lucy, Aungier Jennifer, Tomkins Joseph L. Climate of origin affects tick (Ixodes ricinus) host-seeking behavior in response to temperature: Implications for resilience to climate change? // Ecology and Evolution. 2014. 4, 7. 1186–1198.

Giordano B. V., Gasparotto A., Liang P., Nelder M. P., Russell C., Hunter F. F. Discovery of an Aedes (Stegomyia) albopictus population and first records of Aedes (Stegomyia) aegypti in Canada // Medical and Veterinary Entomology. 2020. 34, 1. 10–16.

Glyzin S. D. Mathematical Model of Nicholson's Experiment // Automatic Control and Computer Sciences. 2018. 51, 7. 736–752.

Godoy Oscar, Valladares Fernando, Castro-Díez Pilar. Multispecies comparison reveals that invasive and native plants differ in their traits but not in their plasticity // Functional Ecology. 2011. 25, 6. 1248–1259.

Goiri Fátima, González Mikel Alexander, Goikolea Joseba, Oribe Madalen, Castro Visitación de, Delacour Sarah, Lucientes Javier, Ortega-araiztegi Ione, Barandika Jesús Felix, García-Pérez Ana Luisa. Progressive invasion of Aedes albopictus in Northern Spain in the period 2013–2018 and a possible association with the increase in insect bites // International Journal of Environmental Research and Public Health. 2020. 17, 5.

Gossner Céline M., Fournet Nelly, Frank Christina, Fernández-Martínez Beatriz, Del Manso Martina, Dias Joana Gomes, Valk Henriette de. Dengue virus infections among European travellers, 2015 to 2019 // Eurosurveillance. 2022. 27, 2.

Gouagna Louis Clément, Damiens David, Oliva Clélia F., Boyer Sébastien, Goff Gilbert Le, Brengues Cécile, Dehecq Jean Sébastien, Raude Jocelyn, Simard Frédéric, Fontenille Didier. Strategic approach, advances, and challenges in the development and application of the SIT for area-wide control of aedes albopictus mosquitoes in Reunion island // Insects. 2020. 11, 11. 1–24.

Gratz N. G. Critical review of the vector status of Aedes albopictus // Medical and Veterinary Entomology. 2004. 18, 3. 215–227.

Green Stephanie J., Brookson Cole B., Hardy Natasha A., Crowder Larry B. Trait-based approaches to global change ecology: Moving from description to prediction // Proceedings of the Royal Society B: Biological Sciences. 2022. 289, 1971.

Gubler D J. Resurgent vector-borne diseases as a global health problem. // Emerging infectious diseases. 1998. 4, 3. 442–450.

Gubler D. J., Suharyono W., Tan R., Abidin M., Sie A. Viraemia in patients with naturally acquired dengue infection // Bulletin of the World Health Organization. 1981. 59, 4. 623–630.

Gubler Duane J. The global emergence/resurgence of arboviral diseases as public health problems // Archives of Medical Research. 2002. 33, 4. 330–342.

Gunathilaka N, Ranathunge T, Udayanga L, Wijegunawardena A, Abeyewickreme W. Oviposition preferences of dengue vectors; Aedes aegypti and Aedes albopictus in Sri Lanka under laboratory settings // Bulletin of Entomological Research. 2018a. 108, 4. 442–450.

Gunathilaka N., Ranathunge T., Udayanga L., Wijegunawardena A., Abeyewickreme W. Oviposition preferences of dengue vectors; Aedes aegypti and Aedes albopictus in Sri Lanka under laboratory settings // Bulletin of Entomological Research. 2018b.

Gurney W. S. C., Blythe S. P., Nisbet R. M. Nicholson's blowlfies revisited // Nature. 1980. 287. 17–21.

Gurney W. S. C., Nisbet R. M., Lawton J. H. The Systematic Formulation of Tractable Single-Species Population Models Incorporating Age Structure // The Journal of Animal Ecology. 1983. 52, 2. 479.

Guzman Maria G., Alvarez Mayling, Halstead Scott B. Secondary infection as a risk factor for dengue hemorrhagic fever/dengue shock syndrome: An historical perspective and role of antibody-dependent enhancement of infection // Archives of Virology. 2013. 158, 7. 1445–1459.

Guzman Maria G., Gubler Duane J., Izquierdo Alienys, Martinez Eric, Halstead Scott B. Dengue infection // Nature Reviews Disease Primers. 2016. 2. 1–26.

Hafsia S, Haramboure M, Wilkinson DA, Baldet T, Yemadje-Menudier L, Vincent M, Tran A, Atyame C Mavingui P. Overview of dengue outbreaks in the south western Indian and analysis of factors involved in the shift towards endemicity in Reunion Island: a systematic review. // PLOS Neglected Tropical Diseases. 2022. 1–16.

Hahn Min A, Kleunen Mark van, Müller-Schärer Heinz. Increased Phenotypic Plasticity to Climate May Have Boosted the Invasion Success of Polyploid Centaurea stoebe // PLoS ONE. 2012. 7, 11.

Haramboure Marion, Labbé Pierrick, Baldet Thierry, Damiens David, Gouagna Louis Clément, Bouyer Jérémy, Tran Annelise. Modelling the control of Aedes albopictus mosquitoes based on sterile males release techniques in a tropical environment // Ecological Modelling. 2020. 424, March. 109002.

Hart Simon P., Schreiber Sebastian J., Levine Jonathan M. How variation between individuals affects species coexistence // Ecology letters. 2016. 19, 8. 825–838.

Hawley William A., Reiter Paul, Copeland Robert S., Pumpuni Charles B., Craig George B. Aedes albopictus in North America: Probable introduction in used tires from Northern Asia // Science. 1987. 236, 4805. 1114–1116.

Hendry Andrew P. Key questions on the role of phenotypic plasticity in eco-evolutionary dynamics // Journal of Heredity. 2016. 107, 1. 25–41.

Henn Jonathan J., Buzzard Vanessa, Enquist Brian J., Halbritter Aud H., Klanderud Kari, Maitner Brian S., Michaletz Sean T., Pötsch Christine, Seltzer Lorah, Telford Richard J., Yang Yan, Zhang Li, Vandvik Vigdis. Intraspecific trait variation and phenotypic plasticity mediate alpine plant species response to climate change // Frontiers in Plant Science. 2018. 871, November. 1–11.

Herd Christie S., Grant Deana G., Lin Jingyi, Franz Alexander W.E. Starvation at the larval stage increases the vector competence of Aedes aegypti females for Zika virus // PLoS Neglected Tropical Diseases. 2021. 15, 11. 1–20.

Hofhuis A, Reimerink J, Reusken C, Scholte E-J, Boer A de, Takken W, Koopmans M. The hidden passenger of lucky bamboo: do imported Aedes albopictus mosquitoes cause dengue virus transmission in the Netherlands? // Vector borne and zoonotic diseases (Larchmont, N.Y.). apr 2009. 9, 2. 217–220.

Huang Mugen, Tang Moxun, Yu Jianshe, Zheng Bo. A stage structured model of delay differential equations for Aedes mosquito population suppression // Discrete and Continuous Dynamical Systems- Series A. 2020. 40, 6. 3467–3484.

Hulme Philip E. Phenotypic plasticity and plant invasions: Is it all Jack? // Functional Ecology. 2008. 22, 1. 3–7.

Hwang Myung Jae, Kim Jong Hun, Kim Heung Chul, Kim Myung Soon, Klein Terry A., Choi Juhwa, Sim Kisung, Chung Yeonseung, Joshi Yadav Prasad, Cheong Hae Kwan. Temporal Trend of Aedes albopictus in Local Urban Parks of the Republic of Korea // Journal of Medical Entomology. 2020. 57, 4. 1082–1089.

Ijumba J. N., Lindsay S. W. Impact of irrigation on malaria in Africa: Paddies paradox // Medical and Veterinary Entomology. 2001. 15, 1. 1–11.

Jannicke Moe S., Stenseth Nils Chr, Smith Robert H. Density dependence in blowfly populations: Experimental evaluation of non-parametric time-series modelling // Oikos. 2002. 98, 3. 523–533.

Jin Xiulei, Jin Shuwan, Gao Daozhou. Mathematical Analysis of the Ross–Macdonald Model with Quarantine // Bulletin of Mathematical Biology. 2020. 82, 4. 1–26.

Johnson Tammi L, Haque Ubydul, Eisen Lars, Mutebi John-Paul, Hahn Micah B, Hayden Mary H, Savage Harry M, Eisen Rebecca J, Monaghan Andrew J, McAllister Janet. Modeling the Environmental Suitability for *Aedes* (Stegomyia) *aegypti* and *Aedes* (Stegomyia) *albopictus* (Diptera: Culicidae) in the Contiguous United States // Journal of Medical Entomology. 2017. 54, 6. 1605–1614.

Johnston A. S.A. A, Boyd R. J., Watson J. W., Paul A., Evans L. C., Gardner E. L., Boult V. L. Predicting population responses to environmental change from individual-level mechanisms: towards a standardized mechanistic approach // Proceedings. Biological sciences. 2019. 286, 1913. 20191916.

Johnston David, Viray Melissa, Ushiroda Jenny, He Hua, Whelen A., Sciulli Rebecca, Kunimoto Gail, Park Sarah. Investigation and Response to an Outbreak of Dengue: Island of Hawaii, 2015-2016 // Public Health Reports. 02 2020. 135. 003335492090406.

Jones Kate E., Patel Nikkita G., Levy Marc A., Storeygard Adam, Balk Deborah, Gittleman John L., Daszak Peter. Global trends in emerging infectious diseases // Nature. 2008. 451, 7181. 990–993.

Jong Zheng Wei, Kassim Nur Faeza A., Naziri Muhammad Aiman, Webb Cameron E. The effect of inbreeding and larval feeding regime on immature development of Aedes albopictus // Journal of Vector Ecology. 2017. 42, 1. 105–112.

Jordan Rebecca C., Sorensen Amanda E., Ladeau Shannon. Citizen Science as a Tool for Mosquito Control // Journal of the American Mosquito Control Association. 2017. 33, 3. 241–245.

Juliano Steven A., Lounibos L. Philip, O'Meara George F. A field test for competitive effects of Aedes albopictus on A. aegypti in South Florida: Differences between sites of coexistence and exclusion? // Oecologia. 2004. 139, 4. 583–593.

Juliano Steven A., Westby Katie M., Ower Geoffrey D. Know Your Enemy: Effects of a Predator on Native and Invasive Container Mosquitoes // Journal of Medical Entomology. 2019. 56, 2. 320–328.

Kamal Mahmoud, Kenawy Mohamed A, Rady Magda Hassan, Khaled Amany Soliman, Samy Abdallah M. Mapping the global potential distributions of two arboviral vectors *Aedes aegypti* and *Ae. Albopictus* under changing climate // PLoS ONE. 2018. 13, 12. 1–21.

Kamimurai Kiyoshi, Matsusei Ines Tomoco, Takahashii Hanako, Komukaii Jun, Fukudai Takayo, Suzukii Kayo. Effect of temperature on the development of Aedes aegypti and Aedes albopictus // Medical Entomology and Zoology. 2002. 53, 1. 53–58.

Kearney Michael R., Wintle Brendan A., Porter Warren P. Correlative and mechanistic models of species distribution provide congruent forecasts under climate change // Conservation Letters. 2010. 3, 3. 203–213.

Kermack W. O., McKendrick A. G. Contributions to the mathematical theory of epidemics. 1. // Proceedings of the Royal Society. 1927. 115A. 700–721.

Khan Salah Uddin, Ogden Nicholas H., Fazil Aamir A., Gachon Philippe H., Dueymes Guillaume U., Greer Amy L., Ng Victoria. Current and projected distributions of Aedes aegypti and Ae. Albopictus in Canada and the U.S. // Environmental Health Perspectives. 2020. 128, 5. 1–13.

Kilpatrick A. Marm, Randolph Sarah E. Drivers, dynamics, and control of emerging vector-borne zoonotic diseases // The Lancet. 2012. 380, 9857. 1946–1955.

Knop Eva, Reusser Nik. Jack-of-all-trades: Phenotypic plasticity facilitates the invasion of an alien slug species // Proceedings of the Royal Society B: Biological Sciences. 2012. 279, 1747. 4668–4676.

Kobayashi M., Nihei N., Kurihaha T. Analysis of northern distribution of Aedes albopictus (Diptera: Culicidae) in Japan by geographical information system // Journal of Medical Entomology. 2002. 39, 1. 4–11.

Kori Mayuko, Awano Nobuyasu, Inomata Minoru, Kuse Naoyuki, Tone Mari, Yoshimura Hanako, Jo Tatsunori, Takada Kohei, Tanaka Atsuko, Mawatari Momoko, Ueda Akihiro, Izumo Takehiro. The 2014 autochthonous dengue fever outbreak in Tokyo: A case series study and assessment of the causes and preventive measures // Respiratory Medicine Case Reports. 2020. 31. 101246.

Kot Mark. Elements of Mathematical Ecology. 2001. 393–396.

Kraemer Moritz, Reiner Robert, Brady Oliver, Messina Jane, Gilbert Marius, Pigott David, Yi Dingdong, Johnson Kimberly, Earl Lucas, Marczak Laurie, Shirude Shreya, Weaver Nicole Davis, Bisanzio Donal, Perkins T, Lai Shengjie, Lu Xin, Jones Peter, Coelho Giovanini, Carvalho Roberta, Bortel Wim Van, Marsboom Cedric, Hendrickx Guy, Schaffner Francis, Moore Chester, Nax Heinrich, Bengtsson Linus, Wetter Erik, Tatem Andrew, Brownstein John, Smith David, Lambrechts Louis, Cauchemez Simon, LINARD Catherine, Faria Nuno, Pybus Oliver, Scott Thomas, Liu Qiyong, Yu Hongjie, Wint William, Hay Simon, Golding Nick. Past and future spread of the arbovirus vectors Aedes aegypti and Aedes albopictus // Nature Microbiology. 2019. In Press.

Kraemer Moritz U G, Van Bortel Wim, Shearer Freya M, Carvalho Roberta G, Golding Nick, Mylne Adrian Q N, Wint G R William, Duda Kirsten A, Smith David L, Messina Jane P,

Teng Hwa-Jen, Pigott David M, Scott Thomas W, Moore Chester G, Schaffner Francis, Barker Christopher M, Hendrickx Guy, Brady Oliver J, Sinka Marianne E, Elyazar Iqbal R F, Hay Simon I, Coelho Giovanini E. The global distribution of the arbovirus vectors *Aedes aegypti* and *Ae. albopictus* // eLife. 2015. 4. 1–18.

Kramer Laura D., Ciota Alexander T. Dissecting vectorial capacity for mosquito-borne viruses // Current Opinion in Virology. 2015. 15. 112–118.

Kruthika H. A., Mahindrakar Arun D., Pasumarthy Ramkrishna. Stability analysis of nonlinear time-delayed systems with application to biological models // International Journal of Applied Mathematics and Computer Science. 2017. 27, 1. 91–103.

Kuijper Bram, Hoyle Rebecca B. When to rely on maternal effects and when on phenotypic plasticity? // Evolution. 2015. 69, 4. 950–968.

Kulaš Antonija, Marković Tamara, Žutinić Petar, Kajan Katarina, Karlović Igor, Orlić Sandi, Keskin Emre, Filipović Vilim, Udovič Marija Gligora. Succession of microbial community in a small water body within the alluvial aquifer of a large river // Water (Switzerland). 2021. 13, 2.

Kumar Ram, Muhid Priyanesh, Dahms Hans Uwe, Sharma Jaigopal, Hwang Jiang Shiou. Biological mosquito control is affected by alternative prey // Zoological Studies. 2015.

Kuss Patrick, Rees Mark, Ægisdóttir Hafdís Hanna, Ellner Stephen P., Jürg Stöcklin. Evolutionary demography of long-lived monocarpic perennials: a time-lagged integral projection model // Journal of Ecology. 2008. 96. 821–832.

LaDeau Shannon L., Leisnham Paul T., Biehler Dawn, Bodner Danielle. Higher mosquito production in low-income neighborhoods of baltimore and washington, DC: Understanding ecological drivers and mosquito-borne disease risk in temperate cities // International Journal of Environmental Research and Public Health. 2013. 10, 4. 1505–1526.

Lacour Guillaume, Chanaud Lionel, L'Ambert Grégory, Hance Thierry. Seasonal Synchronization of Diapause Phases in Aedes albopictus (Diptera: Culicidae) // PLoS ONE. 2015. 10, 12. 1–16.

Lai Zetian, Zhou Tengfei, Liu Shuang, Zhou Jiayong, Xu Ye, Gu Jinbao, Yan Guiyun, Chen Xiao Guang. Vertical transmission of zika virus in aedes albopictus // PLoS Neglected Tropical Diseases. 2020. 14, 10. 1–16.

Lambrechts Louis, Scott Thomas W., Gubler Duane J. Consequences of the expanding global distribution of aedes albopictus for dengue virus transmission // PLoS Neglected Tropical Diseases. 2010. 4, 5.

Latreille Anne C., Milesi Pascal, Magalon Hélène, Mavingui Patrick, Atyame Célestine M. High genetic diversity but no geographical structure of Aedes albopictus populations in Reúnion Island // Parasites and Vectors. 2019. 12, 1. 1–12.

Lee Sophie A., Jarvis Christopher I., Edmunds W. John, Economou Theodoros, Lowe Rachel. Spatial connectivity in mosquito-borne disease models: A systematic review of methods and assumptions // Journal of the Royal Society Interface. 2021. 18, 178.

Leisnham Paul T., Ladeau Shannon L., Saunders Megan E.M., Villena Oswaldo C. Condition-specific competitive effects of the invasive mosquito aedes albopictus on the resident culex pipiens among different urban container habitats may explain their coexistence in the field // Insects. 2021. 12, 11.

Li Ju lin, Zhu Guo ding, Zhou Hua yun, Tang Jian xia, Cao Jun. Effect of different temperatures on development of Aedes albopictus // Chinese journal of schistosomiasis control. 2015. 27, 1. 59–61.

Li Naizhe, Feng Yun, Vrancken Bram, Chen Yuyang, Dong Lu, Yang Qiqi, Kraemer Moritz U.G., Pybus Oliver G., Zhang Hailin, Brady Oliver J., Tian Huaiyu. Assessing the impact of COVID-19 border restrictions on dengue transmission in Yunnan Province, China: an observational epidemiological and phylogenetic analysis // The Lancet Regional Health - Western Pacific. 2021a. 14. 100259.

Li Yiji, Kamara Fatmata, Zhou Guofa, Puthiyakunnon Santhosh, Li Chunyuan, Liu Yanxia, Zhou Yanhe, Yao Lijie, Yan Guiyun, Chen Xiao Guang. Urbanization Increases *Aedes albopictus* Larval Habitats and Accelerates Mosquito Development and Survivorship // PLoS Neglected Tropical Diseases. 2014.

Li Yongjun, Zhang Meichun, Wang Xiaohua, Zheng Xiaoying, Hu Zhiyong, Xi Zhiyong. Quality control of long-term mass-reared Aedes albopictus for population suppression // Journal of Pest Science. 09 2021b. 94.

Liebig Jessica, Jansen Cassie, Paini Dean, Gardner Lauren, Jurdak Raja. A global model for predicting the arrival of imported dengue infections // PLoS ONE. 2019. 14, 12. 1–18.

Lima-Camara Tamara Nunes, Medeiros-Sousa Antônio Ralph, Coelho Ronan Rocha, Marrelli Mauro Toledo. Body size does not affect locomotor activity of Aedes aegypti and Aedes albopictus females (Diptera:Culicidae) // Acta Tropica. 2022. 231. 106430.

Lima Mauricio, Keymer Juan E., Jaksic Fabian M. El Nino-southern oscillation-driven rainfall variability and delayed density dependence cause rodent outbreaks in western South America: Linking demography and population dynamics // American Naturalist. 1999. 153, 5. 476–491.

Lin Chia Hsien, Wen Tzai Hung, Teng Hwa Jen, Chang Niann Tai. The spatio-temporal characteristics of potential dengue risk assessed by Aedes aegypti and Aedes albopictus in high-epidemic areas // Stochastic Environmental Research and Risk Assessment. 2016a. 30, 8. 2057–2066.

Lin Haixiong, Wang Xiaotong, Li Zige, Li Kangju, Lin Chunni, Yang Huijun, Yang Weiqin, Ye Xiaopeng. Epidemiological characteristics of dengue in mainland China from 1990 to 2019: A descriptive analysis // Medicine. 2020. 99, 36. e21982.

Lin Hualiang, Liu Tao, Song Tie, Lin Lifeng, Xiao Jianpeng, Lin Jinyan, He Jianfeng, Zhong Haojie, Hu Wenbiao, Deng Aiping, Peng Zhiqiang, Ma Wenjun, Zhang Yonghui. Community Involvement in Dengue Outbreak Control: An Integrated Rigorous Intervention Strategy // PLoS Neglected Tropical Diseases. 2016b. 10, 8. 1–10.

Lion Sébastien. Theoretical approaches in evolutionary ecology: Environmental feedback as a unifying perspective // American Naturalist. 2018. 191, 1. 21–44.

Lipowsky Annett, Roscher Christiane, Schumacher Jens, Michalski Stefan G., Gubsch Marlén, Buchmann Nina, Schulze Ernst Detlef, Schmid Bernhard. Plasticity of functional traits of forb species in response to biodiversity // Perspectives in Plant Ecology, Evolution and Systematics. 2015. 17, 1. 66–77.

Little Eliza, Bajwa Waheed, Shaman Jeffrey. Local environmental and meteorological conditions influencing the invasive mosquito Ae. albopictus and arbovirus transmission risk in New York City // PLoS Neglected Tropical Diseases. 2017. 11, 8. 1–19.

Liu-Helmersson Jing, Quam Mikkel, Wilder-Smith Annelies, Stenlund Hans, Ebi Kristie, Massad Eduardo, Rocklöv Joacim. Climate Change and Aedes Vectors: 21st Century Projections for Dengue Transmission in Europe // EBioMedicine. 2016. 7. 267–277.

Liu Zhuanzhuan, Zhang Zhenhong, Lai Zetian, Zhou Tengfei, Jia Zhirong, Gu Jinbao, Wu Kun, Chen Xiao Guang. Temperature increase enhances Aedes albopictus competence to transmit dengue virus // Frontiers in Microbiology. 2017. 8, DEC. 1–7.

Lizuain Arturo Andrés, Maffey Lucia, Garzón Maximiliano, Leporace Marina, Soto Danny, Diaz Paula, Salomón Oscar Daniel, Santini María Soledad, Schweigmann Nicolás. Larval Competition Between Aedes albopictus and Aedes aegypti (Diptera: Culicidae) in Argentina: Coexistence and Implications in the Distribution of the Asian Tiger Mosquito // Journal of Medical Entomology. 2022. 59, 5. 1636–1645.

Lloyd-Smith J. O., Schreiber S. J., Kopp P. E., Getz W. M. Superspreading and the effect of individual variation on disease emergence // Nature. 2005. 438, 7066. 355–359.

Löfberg J. YALMIP : A Toolbox for Modeling and Optimization in MATLAB // In Proceedings of the CACSD Conference. Taipei, Taiwan, 2004.

Lord C. C., Alto B. W., Anderson S. L., Connelly C. R., Day J. F., Richards S. L., Smartt C. T., Tabachnick W. J. Can horton hear the whos? the importance of scale in mosquito-borne disease // Journal of Medical Entomology. 2014. 51, 2. 297–313.

Lounibos Leon Philip, Kramer Laura D. Invasiveness of aedes aegypti and aedes albopictus and vectorial capacity for chikungunya virus // Journal of Infectious Diseases. 2016. 214, Suppl 5. S453–S458.

Louthan Allison M., Doak Daniel F., Goheen Jacob R., Palmer Todd M., Pringle Robert M. Climatic stress mediates the impacts of herbivory on plant population structure and components of individual fitness // Journal of Ecology. 2013. 101, 4. 1074–1083.

Low Russanne, Boger Rebecca, Nelson Peder, Kimura Matteo. GLOBE Mosquito Habitat Mapper Citizen Science Data 2017–2020 // GeoHealth. 2021. 5, 10.

Luo Lei, Jiang Li Yun, Xiao Xin Cai, Di Biao, Jing Qin Long, Wang Sheng Yong, Tang Jin Ling, Wang Ming, Tang Xiao Ping, Yang Zhi Cong. The dengue preface to endemic in mainland China: The historical largest outbreak by Aedes albopictus in Guangzhou, 2014 // Infectious Diseases of Poverty. 2017. 6, 1. 1–11.

Luo Xi, Xu Xinyu, Zheng Yi, Guo Hui, Hu Shuijin. The role of phenotypic plasticity and rapid adaptation in determining invasion success of Plantago virginica // Biological Invasions. 2019. 21, 8. 2679–2692.

Luz Paula Mendes, Codeço Cláudia Torres, Massad Eduardo, Struchiner Claudio José. Uncertainties Regarding Dengue Modeling in Rio de Janeiro, Brazil // Memorias do Instituto Oswaldo Cruz. 2003. 98, 7. 871–878.

MATLAB . 9.7.0.1190202 (R2019b). Natick, Massachusetts: The MathWorks Inc., 2019.

Maamor Wan Nurul Fatin Wn, Dom Nazri Che, Mokhtar Megat Azman Megat, Camalxaman Siti Nazrina. Effect of diet regime on the development and survival of aedes albopictus (Skuse) (diptera: Culicidae) // Pertanika Journal of Science and Technology. 2019. 27, 4. 1589–1602.

MacDonald R. G. The analysis of equilibrium in malaria // Tropical diseases bulletin. 1952. 49, 9. 813–829.

Maeno Koutaro, Piou Cyril, Ould Babah Mohamed, Nakamura Satoshi. Eggs and hatchlings variations in desert locusts: phase related characteristics and starvation tolerance // Frontiers in Physiology. 2013. 4.

Mamai Wadaka, Somda Nanwintoum Sévérin Bimbile, Maiga Hamidou, Konczal Anna, Wallner Thomas, Bakhoum Mame Thierno, Yamada Hanano, Bouyer Jérémy. Black soldier fly (Hermetia illucens) larvae powder as a larval diet ingredient for mass-rearing Aedes mosquitoes // Parasite. 2019. 26.

Marini Giovanni, Guzzetta Giorgio, Baldacchino Frederic, Arnoldi Daniele, Montarsi Fabrizio, Capelli Gioia, Rizzoli Annapaola, Merler Stefano, Rosà Roberto. The effect of interspecific competition on the temporal dynamics of Aedes albopictus and Culex pipiens // Parasites and Vectors. 2017.

Marini Giovanni, Manica Mattia, Arnoldi Daniele, Inama Enrico, Rosà Roberto, Rizzoli Annapaola. Influence of temperature on the life-cycle dynamics of aedes albopictus population established at temperate latitudes: A laboratory experiment // Insects. 2020. 11, 11. 1–17.

Mastrantonio Valentina, Crasta Graziano, Puggioli Arianna, Bellini Romeo, Urbanelli Sandra, Porretta Daniele. Cannibalism in temporary waters: Simulations and laboratory experiments revealed the role of spatial shape in the mosquito Aedes albopictus // PLoS ONE. 2018.

May Robert M. The Search for Patterns in the Balance of Nature : Advances and Retreats // Ecology. 1986. 67, 5. 1115–1126.

McClure Katherine M., Lawrence Charlotte, Kilpatrick A. Marm. Land use and larval habitat increase Aedes albopictus (Diptera: Culicidae) and Culex quinquefasciatus (Diptera: Culicidae) abundance in Lowland Hawaii // Journal of Medical Entomology. 2018. 55, 6. 1509–1516.

McCoy K. D. The population genetic structure of vectors and our understanding of disease epidemiology // Parasite. 2008. 15, August. 444–448.

McGill Brian J., Enquist Brian J., Weiher Evan, Westoby Mark. Rebuilding community ecology from functional traits // Trends in Ecology and Evolution. 2006. 21, 4. 178–185.

McManus Donald P., Dunne David W., Sacko Moussa, Utzinger Jürg, Vennervald Birgitte J., Zhou Xiao Nong. Schistosomiasis // Nature Reviews Disease Primers. 2018. 4, 1. 1–19.

Medeiros-Sousa Antônio Ralph, Oliveira-Christe Rafael de, Camargo Amanda Alves, Scinachi Claudia Araujo, Milani Gerlice Maria, Urbinatti Paulo Roberto, Natal Delsio, Ceretti-Junior Walter, Marrelli Mauro Toledo. Influence of water's physical and chemical parameters on mosquito (Diptera: Culicidae) assemblages in larval habitats in urban parks of São Paulo, Brazil // Acta Tropica. 2020. 205, July 2019. 105394.

Medley Kim A. Niche shifts during the global invasion of the Asian tiger mosquito, *Aedes albopictus* Skuse (Culicidae), revealed by reciprocal distribution models // Global Ecology and Biogeography. 2010. 19, 1. 122–133.

Mercier Aurélien, Obadia Thomas, Carraretto Davide, Velo Enkelejda, Gabiane Gaelle, Bino Silvia, Vazeille Marie, Gasperi Giuliano, Dauga Catherine, Malacrida Anna R., Reiter Paul, Failloux Anna Bella. Impact of temperature on dengue and chikungunya transmission by the mosquito Aedes albopictus // Scientific Reports. 2022. 12, 1. 1–13.

Merilä Juha, Hendry Andrew P. Climate change, adaptation, and phenotypic plasticity: The problem and the evidence // Evolutionary Applications. 2014. 7, 1. 1–14.

Merow Cory, Dahlgren Johan P., Metcalf C. Jessica E., Childs Dylan Z., Evans Margaret E.K. K, Jongejans Eelke, Record Sydne, Rees Mark, Salguero-Gómez Roberto, Mcmahon Sean M. Advancing population ecology with integral projection models: A practical guide // Methods in Ecology and Evolution. 2014. 5, 2. 99–110.

Messina Jane P., Brady Oliver J., Golding Nick, Kraemer Moritz U.G., Wint G. R.William, Ray Sarah E., Pigott David M., Shearer Freya M., Johnson Kimberly, Earl Lucas, Marczak Laurie B., Shirude Shreya, Davis Weaver Nicole, Gilbert Marius, Velayudhan Raman, Jones Peter, Jaenisch Thomas, Scott Thomas W., Reiner Robert C., Hay Simon I. The current and future global distribution and population at risk of dengue // Nature Microbiology. 2019. 4, 9. 1508–1515.

Metelmann S., Caminade C., Jones A. E., Medlock J. M., Baylis M., Morse A. P. The UK's suitability for Aedes albopictus in current and future climates // Journal of the Royal Society Interface. 2019. 16, 152.

Metelmann Soeren, Liu Xiaobo, Lu Liang, Caminade Cyril, Liu Keke, Cao Lina, Medlock Jolyon M., Baylis Matthew, Morse Andrew P., Liu Qiyong. Assessing the suitability for aedes albopictus and dengue transmission risk in china with a delay differential equation model // PLoS Neglected Tropical Diseases. 2021. 15, 3. 1–21.

Meynard Christine N., Lecoq Michel, Chapuis Marie Pierre, Piou Cyril. On the relative role of climate change and management in the current desert locust outbreak in East Africa // Global Change Biology. 2020. 26, 7. 3753–3755.

Miner Benjamin G., Sultan Sonia E., Morgan Steven G., Padilla Dianna K., Relyea Rick A. Ecological consequences of phenotypic plasticity // Trends in Ecology and Evolution. 2005. 20, 12. 685–692.

Monteiro Laura C.C., De Souza José R.B., De Albuquerque Cleide M.R. Eclosion rate, development and survivorship of Aedes albopictus (Skuse) (Diptera: Culicidae) under different water temperatures // Neotropical Entomology. 2007. 36, 6. 966–971.

Mordecai Erin A., Cohen Jeremy M., Evans Michelle V., Gudapati Prithvi, Johnson Leah R., Lippi Catherine A., Miazgowicz Kerri, Murdock Courtney C., Rohr Jason R., Ryan Sadie J., Savage Van, Shocket Marta S., Stewart Ibarra Anna, Thomas Matthew B., Weikel Daniel P. Detecting the impact of temperature on transmission of Zika, dengue, and chikungunya using mechanistic models // PLoS Neglected Tropical Diseases. 2017. 11, 4. 1–18.

Mori A. Effects of larval density and nutrition on some attributes of immature and adult Aedes albopictus // Tropical Medicine. 1979. 21, 2. 85–103.

Morin Cory W., Comrie Andrew C., Ernst Kacey. Climate and dengue transmission: Evidence and implications // Environmental Health Perspectives. 2013. 121, 11-12. 1264–1272.

Morozov Andrew, Pasternak Anna F., Arashkevich Elena G. Revisiting the Role of Individual Variability in Population Persistence and Stability // PLoS ONE. 2013. 8, 8. 1–12.

Muñoz Sabater J. ERA5-Land hourly data from 1981 to present. 2019.

Murdoch William W., Briggs Cheryl J., Roger M. Nisbet . Consumer-Resource Dynamics. 2003. 1. 31–42.

Murrell Ebony G, Juliano Steven A. Detritus type alters the outcome of interspecific competition between Aedes aegypti and Aedes albopictus (Diptera: Culicidae). // Journal of medical entomology. may 2008. 45, 3. 375–383.

Museo delle Sceinze . Museo delle Sceinze. 2021.

Muth Norris Z., Pigliucci Massimo. Implementation of a novel framework for assessing species plasticity in biological invasions: Responses of Centaurea and Crepis to phosphorus and water availability // Journal of Ecology. 2007. 95, 5. 1001–1013.

Muturi Ephantus J., Lampman Richard, Costanzo Katie, Alto Barry W. Effect of temperature and insecticide stress on life-history traits of Culex restuans and Aedes albopictus (Diptera: Culicidae) // Journal of Medical Entomology. 2011. 48, 2. 243–250.

Narayan Rohan, Tripathi Shashank. Intrinsic ADE: The Dark Side of Antibody Dependent Enhancement During Dengue Infection // Frontiers in Cellular and Infection Microbiology. 2020. 10, October. 1–6.

Nasci Roger S, Mitchell Carl J. Larval Diet, Adult Size, and Susceptibility of Aedes aegypti (Diptera: Culicidae) to Infection with Ross River Virus // Journal of Medical Entomology. jan 1994. 31, 1. 123–126.

Nguyen Le Anh P., Clements Archie C.A., Jeffery Jason A.L., Yen Nguyen Thi, Nam Vu Sinh, Vaughan Gregory, Shinkfield Ramon, Kutcher Simon C., Gatton Michelle L., Kay Brian H., Ryan Peter A. Abundance and prevalence of Aedes aegypti immatures and relationships with household water storage in rural areas in southern Viet Nam // International Health. 2011. 3, 2. 115–125.

Nicholson A. J. The self-adjustment of populations to change // Cold Spring Harbor Symposia on Quantitative Biology. 1957. 22. 154–173.

Nisbet R. M., Gurney W. S.C. C. The systematic formulation of population models for insects with dynamically varying instar duration // Theoretical Population Biology. 1983. 23, 1. 114–135.

Norris Douglas E. Mosquito-borne Diseases as a Consequence of Land Use Change // EcoHealth. 2004. 1, 1. 19–24.

Nylin S, Gotthard K. Plasticity in life-history traits // Annual Review of Entomology. 1998. 43, 125. 63–83.

Nylin S, Gotthard K. Phenotypic plasticity: linking molecular mechanisms with evolutionary outcomes // Evolutionary Ecology. 2002. 16, 3. 189–211.

Ogden Nicholas H., Milka Radojević, Caminade Cyril, Gachon Philippe. Recent and projected future climatic suitability of North America for the Asian tiger mosquito Aedes albopictus // Parasites and Vectors. 2014. 7, 1. 1–14.

Oliva Clélia, Benedict Mark, Collins Matilda, Baldet Thierry, Bellini Romeo, Bossin Hervé, Bouyer Jérémy, Corbel Vincent, Facchinelli Luca, Fouque Florence, Geier Martin, Michaelakis Antonios, Roiz David, Simard Frédéric, Tur Carlos, Gouagna Louis-Clément. Sterile Insect Technique (SIT) against Aedes Species Designing, Implementing and Evaluating Pilot Field Trials // Insects. 2021. 12. 191.

Oliveira Sandra, Rocha Jorge, Sousa Carla A., Capinha César. Wide and increasing suitability for Aedes albopictus in Europe is congruent across distribution models // Scientific Reports. 2021. 11, 1. 1–9.

Oostra Vicencio, Saastamoinen Marjo, Zwaan Bas J., Wheat Christopher W. Strong phenotypic plasticity limits potential for evolutionary responses to climate change // Nature Communications. 2018. 9, 1.

Osório Hugo C., Rocha Jorge, Roquette Rita, Guerreiro Nélia M., Zé-Zé Líbia, Amaro Fátima, Silva Manuel, Alves Maria João. Seasonal dynamics and spatial distribution of aedes albopictus (Diptera: Culicidae) in a temperate region in europe, southern portugal // International Journal of Environmental Research and Public Health. 2020. 17, 19. 1–11.

Paaijmans K. P., Takken W., Githeko A. K., Jacobs A. F.G. The effect of water turbidity on the near-surface water temperature of larval habitats of the malaria mosquito Anopheles gambiae // International Journal of Biometeorology. 2008. 52, 8. 747–753.

Paaijmans Krijn P., Heinig Rebecca L., Seliga Rebecca A., Blanford Justine I., Blanford Simon, Murdock Courtney C., Thomas Matthew B. Temperature variation makes ectotherms more sensitive to climate change // Global Change Biology. 2013. 19, 8. 2373–2380.

Paaijmans Krijn P., Imbahale Susan S., Thomas Matthew B., Takken Willem. Relevant microclimate for determining the development rate of malaria mosquitoes and possible implications of climate change // Malaria Journal. 2010. 9, 1. 1–8.

Palacio-López Kattia, Gianoli Ernesto. Invasive plants do not display greater phenotypic plasticity than their native or non-invasive counterparts: A meta-analysis // Oikos. 2011. 120, 9. 1393–1401.

Palisades New York: NASA Socioeconomic Data, (SEDAC) Applications Center. Center for International Earth Science Information Network - CIESIN - Columbia University. 2016. Gridded Population of the World, Version 4 (GPWv4): Administrative Unit Center Points with Population Estimates. Palisades, NY: NASA Socioeconomic Data and Ap. ????

Palkovacs Eric P., Post David M. Experimental evidence that phenotypic divergence in predators drives community divergence in prey // Ecology. 2009. 90, 2. 300–305.

Pandey Abhishek, Mubayi Anuj, Medlock Jan. Comparing vector-host and SIR models for dengue transmission // Mathematical Biosciences. 2013. 246, 2. 252–259.

Parham Paul Edward, Michael Edwin. Modeling the effects of weather and climate change on malaria transmission // Environmental Health Perspectives. 2010. 118, 5. 620–626.

Parker Allison T., Gardner Allison M., Perez Manuel, Allan Brian F., Muturi Ephantus J. Container Size Alters the Outcome of Interspecific Competition Between Aedes aegypti (Diptera: Culicidae) and Aedes albopictus // Journal of Medical Entomology. 2018. 56, 3. 708–715.

Pasquali S., Mariani L., Calvitti M., Moretti R., Ponti L., Chiari M., Sperandio G., Gilioli G. Development and calibration of a model for the potential establishment and impact of Aedes albopictus in Europe // Acta Tropica. 2020. 202, July 2019. 105228.

Paupy C., Delatte H., Bagny L., Corbel V., Fontenille D. Aedes albopictus, an arbovirus vector: From the darkness to the light // Microbes and Infection. 2009. 11, 14-15. 1177–1185.

Pedraza-Garcia Milton, Cubillos Luis A. Population dynamics of two small pelagic fish in the central-south area off Chile: Delayed density-dependence and biological interaction // Environmental Biology of Fishes. 2008. 82, 2. 111–122.

Pérez-Castro Rosalía, Castellanos Jaime E., Olano Víctor A., Matiz María Inés, Jaramillo Juan F., Vargas Sandra L., Sarmiento Diana M., Stenström Thor Axel, Overgaard Hans J. Detection of all four dengue serotypes in Aedes aegypti female mosquitoes collected in a rural area in Colombia // Memorias do Instituto Oswaldo Cruz. 2016. 111, 4. 233–240.

Petrić Mina, Ducheyne Els, Gossner Céline M., Marsboom Cedric, Nicolas Gaëlle, Venail Roger, Hendrickx Guy, Schaffner Francis. Seasonality and timing of peak abundance of ¡em¿Aedes albopictus¡/em¿ in Europe: Implications to public and animal health // Geospatial Health. 2021. 16, 1.

Pinto Edna, Coelho Micheline, Oliver Leuda, Massad Eduardo. The influence of climate variables on dengue in Singapore // International Journal of Environmental Health Research. 2011. 21, 6. 415–426.

Poelchau Monica F., Reynolds Julie A., Elsik Christine G., Denlinger David L., Armbruster Peter A. RNA-Seq reveals early distinctions and late convergence of gene expression between diapause and quiescence in the Asian tiger mosquito, Aedes albopictus // Journal of Experimental Biology. 2013. 216, 21. 4082–4090.

Preston Sarah R., Palmer Joseph H., Harrison James W., Carr Hanna M., Rittschof Clare C. The impacts of maternal stress on worker phenotypes in the honey bee // Apidologie. 2019. 50, 5. 704–719.

Puggioli A., Carrieri M., Dindo M. L., Medici A., Lees R. S., Gilles J. R.L., Bellini R. Development of Aedes albopictus (Diptera: Culicidae) larvae under different laboratory conditions // Journal of Medical Entomology. 2017. 54, 1. 142–149.

Purse Bethan V., Golding Nick. Tracking the distribution and impacts of diseases with biological records and distribution modelling // Biological Journal of the Linnean Society. 2015. 115, 3. 664–677.

R Core Team . R: A Language and Environment for Statistical Computing. Vienna, Austria, 2022.

Rackauckas Christopher, Nie Qing. Differentialequations.jl–a performant and feature-rich ecosystem for solving differential equations in julia // Journal of Open Research Software. 2017. 5, 1. 15.

Ramasamy Ranjan, Surendran Sinnathamby N, Jude Pavilupillai J, Dharshini Sangaralingam, Vinobaba Muthuladchumy. Larval development of *Aedes aegypti* and *Aedes albopictus* in peri-urban brackish water and its implications for transmission of arboviral diseases // PLoS Neglected Tropical Diseases. 2011. 5, 11.

Readshaw J L, Cuff W R. A Model of Nicholson's Blowfly Cycles and its Relevance to Predation Theory // The Journal of Animal Ecology. 2006. 49, 3. 1005.

Reed Emily M X, Byrd Brian D, Richards Stephanie L, Eckardt Megan, Williams Carl, Reiskind Michael H. A Statewide Survey of Container Aedes Mosquitoes (Diptera: Culicidae) in North Carolina, 2016: A Multiagency Surveillance Response to Zika Using Ovitraps // Journal of Medical Entomology. feb 2019. 56, 2. 483–490.

Reed Thomas E., Jenouvrier Stephanie, Visser Marcel E. Phenological mismatch strongly affects individual fitness but not population demography in a woodland passerine // Journal of Animal Ecology. 2013. 82, 1. 131–144.

Reich Nicholas G., Shrestha Sourya, King Aaron A., Rohani Pejman, Lessler Justin, Kalayanarooj Siripen, Yoon In Kyu, Gibbons Robert V., Burke Donald S., Cummings Derek A.T. Interactions between serotypes of dengue highlight epidemiological impact of cross-immunity // Journal of the Royal Society Interface. 2013. 10, 86.

Reinbold-Wasson Drew David, Reiskind Michael Hay. Comparative skip-oviposition behavior among container breeding aedes spp. mosquitoes (diptera: Culicidae) // Journal of Medical Entomology. 2021. 58, 6. 2091–2100.

Reiskind M. H., Lounibos L. P. Effects of intraspecific larval competition on adult longevity in the mosquitoes Aedes aegypti and Aedes albopictus // Medical and Veterinary Entomology. 2009.

Reiskind Michael H, Zarrabi Ali A. Water Surface Area and Depth Determine Oviposition Choice in *Aedes albopictus* (Diptera: Culicidae) // Journal of Medical Entomology. 2012. 49, 1. 71–76.

Reiskind Michael H., Zarrabi Ali A. Habitat quality favoured over familiarity: A rejection of natal habitat preference induction in the mosquito Aedes albopictus // Ecological Entomology. 2013. 38, 1. 96–100.

Reiter . Aedes albopictus and the world trade in used tires, 1988-1995: The shape of things to come? // Joumal of the American Mosquito Control Association. 1998. 14, 1. 83–94.

Ren Jiangping, Ling Feng, Sun Jimin, Gong Zhenyu, Liu Ying, Shi Xuguang, Zhang Rong, Zhai Yujia, Chen Enfu, Chen Zhiping. Epidemiological profile of dengue in Zhejiang Province, southeast China // PLoS ONE. 2018. 13, 12. 1–12.

Rey Jorge R., O'Connell Sheila M. Oviposition by Aedes aegypti and Aedes albopictus: Influence of congeners and of oviposition site characteristics // Journal of Vector Ecology. 2014. 39, 1. 190–196.

Riback Thais I.S., Honório Nildimar A., Pereira Renato N., Godoy Wesley A.C., Codeço Cláudia T. Better to be in bad company than to be alone? Aedes vectors respond differently to breeding site quality in the presence of others // PLoS ONE. 2015. 10, 8. 1–16.

Richards Christina L., Bossdorf Oliver, Muth Norris Z., Gurevitch Jessica, Pigliucci Massimo. Jack of all trades, master of some? On the role of phenotypic plasticity in plant invasions // Ecology Letters. 2006a. 9, 8. 981–993.

Richards Stephanie L., Ponnusamy Loganathan, Unnasch Thomas R., Hassan Hassan K., Apperson Charles S. Host-feeding patterns of Aedes albopictus (Diptera: Culicidae) in relation to availability of human and domestic animals in suburban landscapes of central North Carolina // Journal of Medical Entomology. 2006b. 43, 3. 543–551.

Richards Thomas, Tucker Bradley J., Hassan Hassan, Bron Gebbiena M., Bartholomay Lyric, Paskewitz Susan. First Detection of Aedes albopictus (Diptera: Culicidae) and Expansion of Aedes japonicus japonicus in Wisconsin, United States // Journal of Medical Entomology. 2019. 56, 1. 291–296.

Rocklöv Joacim, Dubrow Robert. Climate change: an enduring challenge for vector-borne disease prevention and control // Nature Immunology. 2020. 21, 5. 479–483.

Rogers David J., Suk Jonathan E., Semenza Jan C. Using global maps to predict the risk of dengue in Europe // Acta Tropica. 2014. 129, 1. 1–14.

Rohatgi Ankit. Webplotdigitizer: Version 4.6. 2022.

Roiz David, Neteler Markus, Castellani Cristina, Arnoldi Daniele, Rizzoli Annapaola. Climatic factors driving invasion of the tiger mosquito (Aedes albopictus) into new areas of Trentino, Northern Italy // PLoS ONE. 2011. 6, 4.

Roiz David, Wilson Anne L., Scott Thomas W., Fonseca Dina M., Jourdain Frédéric, Müller Pie, Velayudhan Raman, Corbel Vincent. Correction: Integrated Aedes management for the control of Aedes-borne diseases // PLoS Neglected Tropical Diseases. 2022. 16, 3. 1–21.

Rolff Jens, Johnston Paul R., Reynolds Stuart. Complete metamorphosis of insects // Philosophical Transactions of the Royal Society B: Biological Sciences. 2019. 374, 1783.

Roth Gregory A, Abate Degu, Abate Kalkidan Hassen, Abay Solomon M, Abbafati Cristiana, Abbasi Nooshin, Abbastabar Hedayat, Abd-Allah Foad, Abdela Jemal, Abdelalim Ahmed, Abdollahpour Ibrahim, Abdulkader Rizwan Suliankatchi, Abebe Haftom Temesgen, Abebe Molla, Abebe Zegeye, Abejie Ayenew Negesse, Abera Semaw F, Abil Olifan Zewdie,

Abraha Haftom Niguse, Abrham Aklilu Roba, Abu-Raddad Laith Jamal, Accrombessi Manfred Mario Kokou, Acharya Dilaram, Adamu Abdu A, Adebayo Oladimeji M, Adedoyin Rufus Adesoji, Adekanmbi Victor, Adetokunboh Olatunji O, Adhena Beyene Meressa, Adib Mina G, Admasie Amha, Afshin Ashkan, Agarwal Gina, Agesa Kareha M, Agrawal Anurag, Agrawal Sutapa, Ahmadi Alireza, Ahmadi Mehdi, Ahmed Muktar Beshir, Ahmed Sayem, Aichour Amani Nidhal, Aichour Ibtihel, Aichour Miloud Taki Eddine, Akbari Mohammad Esmaeil, Akinyemi Rufus Olusola, Akseer Nadia, Al-Aly Ziyad, Al-Eyadhy Ayman, Al-Raddadi Rajaa M, Alahdab Fares, Alam Khurshid, Alam Tahiya, Alebel Animut, Alene Kefyalew Addis, Alijanzadeh Mehran, Alizadeh-Navaei Reza, Aljunid Syed Mohamed, Alkerwi Ala'a, Alla François, Allebeck Peter, Alonso Jordi, Altirkawi Khalid, Alvis-Guzman Nelson, Amare Azmeraw T, Aminde Leopold N, Amini Erfan, Ammar Walid, Amoako Yaw Ampem, Anber Nahla Hamed, Andrei Catalina Liliana, Androudi Sofia, Animut Megbaru Debalkie, Anjomshoa Mina, Ansari Hossein, Ansha Mustafa Geleto, Antonio Carl Abelardo T, Anwari Palwasha, Aremu Olatunde, Ärnlöv Johan, Arora Amit, Arora Monika, Artaman Al, Aryal Krishna K, Asayesh Hamid, Asfaw Ephrem Tsegay, Ataro Zerihun, Atique Suleman, Atre Sachin R, Ausloos Marcel, Avokpaho Euripide F G A, Awasthi Ashish, Quintanilla Beatriz Paulina Ayala, Ayele Yohanes, Ayer Rakesh, Azzopardi Peter S, Babazadeh Arefeh, Bacha Umar, Badali Hamid, Badawi Alaa, Bali Ayele Geleto, Ballesteros Katherine E, Banach Maciej, Banerjee Kajori, Bannick Marlena S, Banoub Joseph Adel Mattar, Barboza Miguel A, Barker-Collo Suzanne Lyn, Bärnighausen Till Winfried, Barquera Simon, Barrero Lope H, Bassat Quique, Basu Sanjay, Baune Bernhard T, Baynes Habtamu Wondifraw, Bazargan-Hejazi Shahrzad, Bedi Neeraj, Beghi Ettore, Behzadifar Masoud, Behzadifar Meysam, Béjot Yannick, Bekele Bayu Begashaw, Belachew Abate Bekele, Belay Ezra, Belay Yihalem Abebe, Bell Michelle L, Bello Aminu K, Bennett Derrick A, Bensenor Isabela M, Berman Adam E, Bernabe Eduardo, Bernstein Robert S, Bertolacci Gregory J, Beuran Mircea, Beyranvand Tina, Bhalla Ashish, Bhattarai Suraj, Bhaumik Soumyadeeep, Bhutta Zulfiqar A, Biadgo Belete, Biehl Molly H, Bijani Ali, Bikbov Boris, Bilano Ver, Bililign Nigus, Bin Sayeed Muhammad Shahdaat, Bisanzio Donal, Biswas Tuhin, Blacker Brigette F, Basara Berrak Bora, Borschmann Rohan, Bosetti Cristina, Bozorgmehr Kayvan, Brady Oliver J, Brant Luisa C, Brayne Carol, Brazinova Alexandra, Breitborde Nicholas J K, Brenner Hermann, Briant Paul Svitil, Britton Gabrielle, Brugha Traolach, Busse Reinhard, Butt Zahid A, Callender Charlton S K H, Campos-Nonato Ismael R, Campuzano Rincon Julio Cesar, Cano Jorge, Car Mate, Cárdenas Rosario, Carreras Giulia, Carrero Juan J, Carter Austin, Carvalho Félix, Castañeda-Orjuela Carlos A, Castillo Rivas Jacqueline, Castle Chris D, Castro Clara, Castro Franz, Catalá-López Ferrán, Cerin Ester, Chaiah Yazan, Chang Jung-Chen, Charlson Fiona J, Chaturvedi Pankaj, Chiang Peggy Pei-Chia, Chimed-Ochir Odgerel, Chisumpa Vesper Hichilombwe, Chitheer Abdulaal, Chowdhury Rajiv, Christensen Hanne, Christopher Devasahayam J, Chung Sheng-Chia, Cicuttini Flavia M, Ciobanu Liliana G, Cirillo Massimo, Cohen Aaron J, Cooper Leslie Trumbull, Cortesi Paolo Angelo, Cortinovis Monica, Cousin Ewerton, Cowie Benjamin C, Criqui Michael H, Cromwell Elizabeth A, Crowe Christopher Stephen, Crump John A, Cunningham Matthew, Daba Alemneh Kabeta, Dadi Abel Fekadu, Dandona Lalit, Dandona Rakhi, Dang Anh Kim, Dargan Paul I, Daryani Ahmad, Das Siddharth K, Gupta Rajat Das, Neves José Das, Dasa Tamirat Tesfaye, Dash Aditya Prasad, Davis Adrian C, Davis Weaver Nicole, Davitoiu Dragos Virgil, Davletov Kairat, De La Hoz Fernando Pio, De Neve Jan-Walter, Degefa Meaza Girma, Degenhardt Louisa, Degfie Tizta T, Deiparine Selina, Demoz Gebre Teklemariam, Demtsu Balem Betsu, Denova-Gutiérrez Edgar, Deribe Kebede, Dervenis Nikolaos, Des Jarlais Don C, Dessie Getenet Ayalew, Dey Subhojit, Dharmaratne Samath D,

Dicker Daniel, Dinberu Mesfin Tadese, Ding Eric L, Dirac M Ashworth, Djalalinia Shirin, Dokova Klara, Doku David Teye, Donnelly Christl A, Dorsey E Ray, Doshi Pratik P, Douwes-Schultz Dirk, Doyle Kerrie E, Driscoll Tim R, Dubey Manisha, Dubljanin Eleonora, Duken Eyasu Ejeta, Duncan Bruce B, Duraes Andre R, Ebrahimi Hedyeh, Ebrahimpour Soheil, Edessa Dumessa, Edvardsson David, Eggen Anne Elise, El Bcheraoui Charbel, El Sayed Zaki Maysaa, El-Khatib Ziad, Elkout Hajer, Ellingsen Christian Lycke, Endres Matthias, Endries Aman Yesuf, Er Benjamin, Erskine Holly E, Eshrati Babak, Eskandarieh Sharareh, Esmaeili Reza, Esteghamati Alireza, Fakhar Mahdi, Fakhim Hamed, Faramarzi Mahbobeh, Fareed Mohammad, Farhadi Farzaneh, Farinha Carla Sofia E sá, Faro Andre, Farvid Maryam S, Farzadfar Farshad, Farzaei Mohammad Hosein, Feigin Valery L, Feigl Andrea B, Fentahun Netsanet, Fereshtehnejad Seyed-Mohammad, Fernandes Eduarda, Fernandes Joao C, Ferrari Alize J, Feyissa Garumma Tolu, Filip Irina, Finegold Samuel, Fischer Florian, Fitzmaurice Christina, Foigt Nataliya A, Foreman Kyle J, Fornari Carla, Frank Tahvi D, Fukumoto Takeshi, Fuller John E, Fullman Nancy, Fürst Thomas, Furtado João M, Futran Neal D, Gallus Silvano, Garcia-Basteiro Alberto L, Garcia-Gordillo Miguel A, Gardner William M, Gebre Abadi Kahsu, Gebrehiwot Tsegaye Tewelde, Gebremedhin Amanuel Tesfay, Gebremichael Bereket, Gebremichael Teklu Gebrehiwo, Gelano Tilayie Feto, Geleijnse Johanna M, Genova-Maleras Ricard, Geramo Yilma Chisha Dea, Gething Peter W, Gezae Kebede Embaye, Ghadami Mohammad Rasoul, Ghadimi Reza, Ghasemi Falavarjani Khalil, Ghasemi-Kasman Maryam, Ghimire Mamata, Gibney Katherine B, Gill Paramjit Singh, Gill Tiffany K, Gillum Richard F, Ginawi Ibrahim Abdelmageed, Giroud Maurice, Giussani Giorgia, Goenka Shifalika, Goldberg Ellen M, Goli Srinivas, Gómez-Dantés Hector, Gona Philimon N, Gopalani Sameer Vali, Gorman Taren M, Goto Atsushi, Goulart Alessandra C, Gnedovskaya Elena V, Grada Ayman, Grosso Giuseppe, Gugnani Harish Chander, Guimaraes Andre Luiz Sena, Guo Yuming, Gupta Prakash C, Gupta Rahul, Gupta Rajeev, Gupta Tanush, Gutiérrez Reyna Alma, Gyawali Bishal, Haagsma Juanita A, Hafezi-Nejad Nima, Hagos Tekleberhan B, Hailegiyorgis Tewodros Tesfa, Hailu Gessessew Bugssa, Haj-Mirzaian Arvin, Haj-Mirzaian Arya, Hamadeh Randah R, Hamidi Samer, Handal Alexis J, Hankey Graeme J, Harb Hilda L, Harikrishnan Sivadasanpillai, Haro Josep Maria, Hasan Mehedi, Hassankhani Hadi, Hassen Hamid Yimam, Havmoeller Rasmus, Hay Roderick J, Hay Simon I, He Yihua, Hedayatizadeh-Omran Akbar, Hegazy Mohamed I, Heibati Behzad, Heidari Mohsen, Hendrie Delia, Henok Andualem, Henry Nathaniel J, Herteliu Claudiu, Heydarpour Fatemeh, Heydarpour Pouria, Heydarpour Sousan, Hibstu Desalegn Tsegaw, Hoek Hans W, Hole Michael K, Homaie Rad Enayatollah, Hoogar Praveen, Hosgood H Dean, Hosseini Seyed Mostafa, Hosseinzadeh Mehdi, Hostiuc Mihaela, Hostiuc Sorin, Hotez Peter J, Hoy Damian G, Hsiao Thomas, Hu Guoqing, Huang John J, Husseini Abdullatif, Hussen Mohammedaman Mama, Hutfless Susan, Idrisov Bulat, Ilesanmi Olayinka Stephen, Iqbal Usman, Irvani Seyed Sina Naghibi, Irvine Caleb Mackay Salpeter, Islam Nazrul, Islam Sheikh Mohammed Shariful, Islami Farhad, Jacobsen Kathryn H, Jahangiry Leila, Jahanmehr Nader, Jain Sudhir Kumar, Jakovljevic Mihajlo, Jalu Moti Tolera, James Spencer L, Javanbakht Mehdi, Jayatilleke Achala Upendra, Jeemon Panniyammakal, Jenkins Kathy J, Jha Ravi Prakash, Jha Vivekanand, Johnson Catherine O, Johnson Sarah C, Jonas Jost B, Joshi Ankur, Jozwiak Jacek Jerzy, Jungari Suresh Banayya, Jürisson Mikk, Kabir Zubair, Kadel Rajendra, Kahsay Amaha, Kalani Rizwan, Karami Manoochehr, Karami Matin Behzad, Karch André, Karema Corine, Karimi-Sari Hamidreza, Kasaeian Amir, Kassa Dessalegn H, Kassa Getachew Mullu, Kassa Tesfaye Dessale, Kassebaum Nicholas J, Katikireddi Srinivasa Vittal, Kaul Anil, Kazemi Zhila, Karyani Ali Kazemi, Kazi Dhruv Satish, Kefale Adane Teshome, Keiyoro Peter Njenga, Kemp Grant Rodgers, Kengne Andre Pascal, Keren Andre, Kesavachandran Chandrasekharan Nair,

Khader Yousef Saleh, Khafaei Behzad, Khafaie Morteza Abdullatif, Khajavi Alireza, Khalid Nauman, Khalil Ibrahim A, Khan Ejaz Ahmad, Khan Muhammad Shahzeb, Khan Muhammad Ali, Khang Young-Ho, Khater Mona M, Khoja Abdullah T, Khosravi Ardeshir, Khosravi Mohammad Hossein, Khubchandani Jagdish, Kiadaliri Aliasghar A, Kibret Getiye D, Kidanemariam Zelalem Teklemariam, Kiirithio Daniel N, Kim Daniel, Kim Young-Eun, Kim Yun Jin, Kimokoti Ruth W, Kinfu Yohannes, Kisa Adnan, Kissimova-Skarbek Katarzyna, Kivimäki Mika, Knudsen Ann Kristin Skrindo, Kocarnik Jonathan M, Kochhar Sonali, Kokubo Yoshihiro, Kolola Tufa, Kopec Jacek A, Koul Parvaiz A, Koyanagi Ai, Kravchenko Michael A, Krishan Kewal, Kuate Defo Barthelemy, Kucuk Bicer Burcu, Kumar G Anil, Kumar Manasi, Kumar Pushpendra, Kutz Michael J, Kuzin Igor, Kyu Hmwe Hmwe, Lad Deepesh P, Lad Sheetal D, Lafranconi Alessandra, Lal Dharmesh Kumar, Lalloo Ratilal, Lallukka Tea, Lam Jennifer O, Lami Faris Hasan, Lansingh Van C, Lansky Sonia, Larson Heidi J, Latifi Arman, Lau Kathryn Mei-Ming, Lazarus Jeffrey V, Lebedev Georgy, Lee Paul H, Leigh James, Leili Mostafa, Leshargie Cheru Tesema, Li Shanshan, Li Yichong, Liang Juan, Lim Lee-Ling, Lim Stephen S, Limenih Miteku Andualem, Linn Shai, Liu Shiwei, Liu Yang, Lodha Rakesh, Lonsdale Chris, Lopez Alan D, Lorkowski Stefan, Lotufo Paulo A, Lozano Rafael, Lunevicius Raimundas, Ma Stefan, Macarayan Erlyn Rachelle King, Mackay Mark T, MacLachlan Jennifer H, Maddison Emilie R, Madotto Fabiana, Magdy Abd El Razek Hassan, Magdy Abd El Razek Muhammed, Maghavani Dhaval P, Majdan Marek, Majdzadeh Reza, Majeed Azeem, Malekzadeh Reza, Malta Deborah Carvalho, Manda Ana-Laura, Mandarano-Filho Luiz Garcia, Manguerra Helena, Mansournia Mohammad Ali, Mapoma Chabila Christopher, Marami Dadi, Maravilla Joemer C, Marcenes Wagner, Marczak Laurie, Marks Ashley, Marks Guy B, Martinez Gabriel, Martins-Melo Francisco Rogerlândio, Martopullo Ira, März Winfried, Marzan Melvin B, Masci Joseph R, Massenburg Benjamin Ballard, Mathur Manu Raj, Mathur Prashant, Matzopoulos Richard, Maulik Pallab K, Mazidi Mohsen, McAlinden Colm, McGrath John J, McKee Martin, McMahon Brian J, Mehata Suresh, Mehndiratta Man Mohan, Mehrotra Ravi, Mehta Kala M, Mehta Varshil, Mekonnen Tefera C, Melese Addisu, Melku Mulugeta, Memiah Peter T N, Memish Ziad A, Mendoza Walter, Mengistu Desalegn Tadese, Mengistu Getnet, Mensah George A, Mereta Seid Tiku, Meretoja Atte, Meretoja Tuomo J, Mestrovic Tomislav, Mezgebe Haftay Berhane, Miazgowski Bartosz, Miazgowski Tomasz, Millear Anoushka I, Miller Ted R, Miller-Petrie Molly Katherine, Mini G K, Mirabi Parvaneh, Mirarefin Mojde, Mirica Andreea, Mirrakhimov Erkin M, Misganaw Awoke Temesgen, Mitiku Habtamu, Moazen Babak, Mohammad Karzan Abdulmuhsin, Mohammadi Moslem, Mohammadifard Noushin, Mohammed Mohammed A, Mohammed Shafiu, Mohan Viswanathan, Mokdad Ali H, Molokhia Mariam, Monasta Lorenzo, Moradi Ghobad, Moradi-Lakeh Maziar, Moradinazar Mehdi, Moraga Paula, Morawska Lidia, Moreno Velásquez Ilais, Morgado-Da-Costa Joana, Morrison Shane Douglas, Moschos Marilita M, Mouodi Simin, Mousavi Seyyed Meysam, Muchie Kindie Fentahun, Mueller Ulrich Otto, Mukhopadhyay Satinath, Muller Kate, Mumford John Everett, Musa Jonah, Musa Kamarul Imran, Mustafa Ghulam, Muthupandian Saravanan, Nachega Jean B, Nagel Gabriele, Naheed Aliya, Nahvijou Azin, Naik Gurudatta, Nair Sanjeev, Najafi Farid, Naldi Luigi, Nam Hae Sung, Nangia Vinay, Nansseu Jobert Richie, Nascimento Bruno Ramos, Natarajan Gopalakrishnan, Neamati Nahid, Negoi Ionut, Negoi Ruxandra Irina, Neupane Subas, Newton Charles R J, Ngalesoni Frida N, Ngunjiri Josephine W, Nguyen Anh Quynh, Nguyen Grant, Nguyen Ha Thu, Nguyen Huong Thanh, Nguyen Long Hoang, Nguyen Minh, Nguyen Trang Huyen, Nichols Emma, Ningrum Dina Nur Anggraini, Nirayo Yirga Legesse, Nixon Molly R, Nolutshungu Nomonde, Nomura Shuhei, Norheim Ole F, Noroozi Mehdi, Norrving Bo, Noubiap Jean Jacques, Nouri Hamid Reza, Nourollahpour Shiadeh Malihe, Nowroozi

Mohammad Reza, Nyasulu Peter S, Odell Christopher M, Ofori-Asenso Richard, Ogbo Felix Akpojene, Oh In-Hwan, Oladimeji Olanrewaju, Olagunju Andrew T, Olivares Pedro R, Olsen Helen Elizabeth, Olusanya Bolajoko Olubukunola, Olusanya Jacob Olusegun, Ong Kanyin L, Ong Sok King Sk, Oren Eyal, Orpana Heather M, Ortiz Alberto, Ortiz Justin R, Otstavnov Stanislav S, Øverland Simon, Owolabi Mayowa Ojo, Özdemir Raziye, P A Mahesh, Pacella Rosana, Pakhale Smita, Pakhare Abhijit P, Pakpour Amir H, Pana Adrian, Panda-Jonas Songhomitra, Pandian Jeyaraj Durai, Parisi Andrea, Park Eun-Kee, Parry Charles D H, Parsian Hadi, Patel Shanti, Pati Sanghamitra, Patton George C, Paturi Vishnupriya Rao, Paulson Katherine R, Pereira Alexandre, Pereira David M, Perico Norberto, Pesudovs Konrad, Petzold Max, Phillips Michael R, Piel Frédéric B, Pigott David M, Pillay Julian David, Pirsaheb Meghdad, Pishgar Farhad, Polinder Suzanne, Postma Maarten J, Pourshams Akram, Poustchi Hossein, Pujar Ashwini, Prakash Swayam, Prasad Narayan, Purcell Caroline A, Qorbani Mostafa, Quintana Hedley, Quistberg D Alex, Rade Kirankumar Waman, Radfar Amir, Rafay Anwar, Rafiei Alireza, Rahim Fakher, Rahimi Kazem, Rahimi-Movaghar Afarin, Rahman Mahfuzar, Rahman Mohammad Hifz Ur, Rahman Muhammad Aziz, Rai Rajesh Kumar, Rajsic Sasa, Ram Usha, Ranabhat Chhabi Lal, Ranjan Prabhat, Rao Puja C, Rawaf David Laith, Rawaf Salman, Razo-García Christian, Reddy K Srinath, Reiner Robert C, Reitsma Marissa B, Remuzzi Giuseppe, Renzaho Andre M N, Resnikoff Serge, Rezaei Satar, Rezaeian Shahab, Rezai Mohammad Sadegh, Riahi Seyed Mohammad, Ribeiro Antonio Luiz P, Rios-Blancas Maria Jesus, Roba Kedir Teji, Roberts Nicholas L S, Robinson Stephen R, Roever Leonardo, Ronfani Luca, Roshandel Gholamreza, Rostami Ali, Rothenbacher Dietrich, Roy Ambuj, Rubagotti Enrico, Sachdev Perminder S, Saddik Basema, Sadeghi Ehsan, Safari Hosein, Safdarian Mahdi, Safi Sare, Safiri Saeid, Sagar Rajesh, Sahebkar Amirhossein, Sahraian Mohammad Ali, Salam Nasir, Salama Joseph S, Salamati Payman, Saldanha Raphael De Freitas, Saleem Zikria, Salimi Yahya, Salvi Sundeep Santosh, Salz Inbal, Sambala Evanson Zondani, Samy Abdallah M, Sanabria Juan, Sanchez-Niño Maria Dolores, Santomauro Damian Francesco, Santos Itamar S, Santos João Vasco, Milicevic Milena M Santric, Sao Jose Bruno Piassi, Sarker Abdur Razzaque, Sarmiento-Suárez Rodrigo, Sarrafzadegan Nizal, Sartorius Benn, Sarvi Shahabeddin, Sathian Brijesh, Satpathy Maheswar, Sawant Arundhati R, Sawhney Monika, Saxena Sonia, Sayyah Mehdi, Schaeffner Elke, Schmidt Maria Inês, Schneider Ione J C, Schöttker Ben, Schutte Aletta Elisabeth, Schwebel David C, Schwendicke Falk, Scott James G, Sekerija Mario, Sepanlou Sadaf G, Serván-Mori Edson, Seyedmousavi Seyedmojtaba, Shabaninejad Hosein, Shackelford Katya Anne, Shafieesabet Azadeh, Shahbazi Mehdi, Shaheen Amira A, Shaikh Masood Ali, Shams-Beyranvand Mehran, Shamsi Mohammadbagher, Shamsizadeh Morteza, Sharafi Kiomars, Sharif Mehdi, Sharif-Alhoseini Mahdi, Sharma Rajesh, She Jun, Sheikh Aziz, Shi Peilin, Shiferaw Mekonnen Sisay, Shigematsu Mika, Shiri Rahman, Shirkoohi Reza, Shiue Ivy, Shokraneh Farhad, Shrime Mark G, Si Si, Siabani Soraya, Siddiqi Tariq J, Sigfusdottir Inga Dora, Sigurvinsdottir Rannveig, Silberberg Donald H, Silva Diego Augusto Santos, Silva João Pedro, Silva Natacha Torres Da, Silveira Dayane Gabriele Alves, Singh Jasvinder A, Singh Narinder Pal, Singh Prashant Kumar, Singh Virendra, Sinha Dhirendra Narain, Sliwa Karen, Smith Mari, Sobaih Badr Hasan, Sobhani Soheila, Sobngwi Eugène, Soneji Samir S, Soofi Moslem, Sorensen Reed J D, Soriano Joan B, Soyiri Ireneous N, Sposato Luciano A, Sreeramareddy Chandrashekhar T, Srinivasan Vinay, Stanaway Jeffrey D, Starodubov Vladimir I, Stathopoulou Vasiliki, Stein Dan J, Steiner Caitlyn, Stewart Leo G, Stokes Mark A, Subart Michelle L, Sudaryanto Agus, Sufiyan Mu'awiyyah Babale, Sur Patrick John, Sutradhar Ipsita, Sykes Bryan L, Sylaja P N, Sylte Dillon O, Szoeke Cassandra E I, Tabarés-Seisdedos Rafael, Tabuchi Takahiro, Tadakamadla Santosh Kumar, Takahashi Ken, Tandon Nikhil, Tassew Segen Gebremeskel,

Taveira Nuno, Tehrani-Banihashemi Arash, Tekalign Tigist Gashaw, Tekle Merhawi Gebremedhin, Temsah Mohamad-Hani, Temsah Omar, Terkawi Abdullah Sulieman, Teshale Manaye Yihune, Tessema Belay, Tessema Gizachew Assefa, Thankappan Kavumpurathu Raman, Thirunavukkarasu Sathish, Thomas Nihal, Thrift Amanda G, Thurston George D, Tilahun Binyam, To Quyen G, Tobe-Gai Ruoyan, Tonelli Marcello, Topor-Madry Roman, Torre Anna E, Tortajada-Girbés Miguel, Touvier Mathilde, Tovani-Palone Marcos Roberto, Tran Bach Xuan, Tran Khanh Bao, Tripathi Suryakant, Troeger Christopher E, Truelsen Thomas Clement, Truong Nu Thi, Tsadik Afewerki Gebremeskel, Tsoi Derrick, Tudor Car Lorainne, Tuzcu E Murat, Tyrovolas Stefanos, Ukwaja Kingsley N, Ullah Irfan, Undurraga Eduardo A, Updike Rachel L, Usman Muhammad Shariq, Uthman Olalekan A, Uzun Selen Begüm, Vaduganathan Muthiah, Vaezi Afsane, Vaidya Gaurang, Valdez Pascual R, Varavikova Elena, Vasankari Tommi Juhani, Venketasubramanian Narayanaswamy, Villafaina Santos, Violante Francesco S, Vladimirov Sergey Konstantinovitch, Vlassov Vasily, Vollset Stein Emil, Vos Theo, Wagner Gregory R, Wagnew Fasil Shiferaw, Waheed Yasir, Wallin Mitchell Taylor, Walson Judd L, Wang Yanping, Wang Yuan-Pang, Wassie Molla Mesele, Weiderpass Elisabete, Weintraub Robert G, Weldegebreal Fitsum, Weldegwergs Kidu Gidey, Werdecker Andrea, Werkneh Adhena Ayaliew, West T Eoin, Westerman Ronny, Whiteford Harvey A, Widecka Justyna, Wilner Lauren B, Wilson Shadrach, Winkler Andrea Sylvia, Wiysonge Charles Shey, Wolfe Charles D A, Wu Shouling, Wu Yun-Chun, Wyper Grant M A, Xavier Denis, Xu Gelin, Yadgir Simon, Yadollahpour Ali, Yahyazadeh Jabbari Seyed Hossein, Yakob Bereket, Yan Lijing L, Yano Yuichiro, Yaseri Mehdi, Yasin Yasin Jemal, Yentür Gökalp Kadri, Yeshaneh Alex, Yimer Ebrahim M, Yip Paul, Yirsaw Biruck Desalegn, Yisma Engida, Yonemoto Naohiro, Yonga Gerald, Yoon Seok-Jun, Yotebieng Marcel, Younis Mustafa Z, Yousefifard Mahmoud, Yu Chuanhua, Zadnik Vesna, Zaidi Zoubida, Zaman Sojib Bin, Zamani Mohammad, Zare Zohreh, Zeleke Ayalew Jejaw, Zenebe Zerihun Menlkalew, Zhang Anthony Lin, Zhang Kai, Zhou Maigeng, Zodpey Sanjay, Zuhlke Liesl Joanna, Naghavi Mohsen, Murray Christopher J L. Global, regional, and national age-sex-specific mortality for 282 causes of death in 195 countries and territories, 1980–2017: a systematic analysis for the Global Burden of Disease Study 2017 // The Lancet. 2018. 392, 10159. 1736–1788.

Roy Shovonlal, Chattopadhyay J. The stability of ecosystems: A brief overview of the paradox of enrichment // Journal of Biosciences. 2007. 32, 2. 421–428.

Rozilawati H., Zairi J., Adanan C.R. Seasonal abundance of Aedes albopictus in selected urban and suburban areas in Penang , Malaysia // Tropical Biomedicine. 2007. 24, 1. 83–94.

Russell Marie C., Cator Lauren J. No Impact of Biocontrol Agent's Predation Cues on Development Time or Size of Surviving Aedes albopictus under Optimal Nutritional Availability // Insects. 2022. 13, 2.

Ryan Sadie J., Carlson Colin J., Mordecai Erin A., Johnson Leah R. Global expansion and redistribution of Aedes-borne virus transmission risk with climate change // PLoS Neglected Tropical Diseases. 2018. 13, 3. 1–20.

Sam I. Ching, Loong Shih Keng, Michael Jasmine Chandramathi, Chua Chong Long, Wan Sulaiman Wan Yusoff, Vythilingam Indra, Chan Shie Yien, Chiam Chun Wei, Yeong Yze Shiuan, AbuBakar Sazaly, Chan Yoke Fun. Genotypic and Phenotypic Characterization of Chikungunya Virus of Different Genotypes from Malaysia // PLoS ONE. 2012. 7, 11. 1–9.

Samrot Antony V., Sean Tan Chuan, Bhavya Karanam Sai, Sahithya Chamarthy Sai, Chandrasekaran Saipriya, Palanisamy Raji, Robinson Emilin Renitta, Subbiah Suresh Kumar, Mok Pooi Ling. Leptospiral infection, pathogenesis and its diagnosis—a review // Pathogens. 2021. 10, 2. 1–30.

Samuel Glady Hazitha, Adelman Zach N., Myles Kevin M. Temperature-dependent effects on the replication and transmission of arthropod-borne viruses in their insect hosts // Current Opinion in Insect Science. 2016. 16. 108–113.

Santé publique France . Surveillance de la dengue à La Réunion. 2022.

Santini Luca, Benítez-López Ana, Dormann Carsten F., Huijbregts Mark A.J. Population density estimates for terrestrial mammal species // Global Ecology and Biogeography. 2022. 31, 5. 978–994.

Sauers Logan, Hawes Kelsey, Juliano Steven. Non-linear relationships between density and demographic traits in three Aedes species // Scientific Reports. 05 2022. 12.

Schaffner Francis, Mathis Alexander. Dengue and dengue vectors in the WHO European region: Past, present, and scenarios for the future // The Lancet Infectious Diseases. 2014. 14, 12. 1271–1280.

Schmidt Chris A., Comeau Genevieve, Monaghan Andrew J., Williamson Daniel J., Ernst Kacey C. Effects of desiccation stress on adult female longevity in Aedes aegypti and Ae. albopictus (Diptera: Culicidae): results of a systematic review and pooled survival analysis // Parasites and Vectors. 2018. 11, 1. 267.

Seebacher Frank, White Craig R., Franklin Craig E. Physiological plasticity increases resilience of ectothermic animals to climate change // Nature Climate Change. 2015. 5, 1. 61–66.

Sgrò Carla M., Terblanche John S., Hoffmann Ary A. What Can Plasticity Contribute to Insect Responses to Climate Change? // Annual Review of Entomology. 2016. 61, 1. 433–451.

Shahrudin Nur Amirah, Dom Nazri Che, Ishak Ahmad Razali. Temperature stress effect on the survival of aedes albopictus (Skuse) (Diptera: Culicidae) adult mosquito: An experimental study // Malaysian Journal of Medicine and Health Sciences. 2019. 15, SP4. 106–113.

Shragai Talya, Harrington Laura, Alfonso-Parra Catalina, Avila Frank. Oviposition site attraction of Aedes albopictus to sites with conspecific and heterospecific larvae during an ongoing invasion in Medellín, Colombia // Parasites and Vectors. 2019. 12, 1. 1–10.

Shragai Talya, Harrington Laura C. Aedes albopictus (Diptera: Culicidae) on an Invasive Edge: Abundance, Spatial Distribution, and Habitat Usage of Larvae and Pupae Across Urban and Socioeconomic Environmental Gradients // Journal of Medical Entomology. 2019. 56, 2. 472–482.

Silberbush Alon, Resetarits William J. Mosquito female response to the presence of larvivorous fish does not match threat to larvae // Ecological Entomology. 2017.

Silva Laurie A., Dermody Terence S. Chikungunya virus: Epidemiology, replication, disease mechanisms, and prospective intervention strategies // Journal of Clinical Investigation. 2017. 127, 3. 737–749.

Smith David L., Battle Katherine E., Hay Simon I., Barker Christopher M., Scott Thomas W., McKenzie F. Ellis. Ross, Macdonald, and a theory for the dynamics and control of mosquito-transmitted pathogens // PLoS Pathogens. 2012. 8, 4.

Soriano-Panõs David, Arias-Castro Juddy Heliana, Reyna-Lara Adriana, Martínez Hector J., Meloni Sandro, Gómez-Gardeñes Jesús. Vector-borne epidemics driven by human mobility // Physical Review Research. 2020. 2, 1. 1–12.

Soroye Peter, Newbold Tim, Kerr Jeremy. Among Bumble Bees Across Continents // Science. 2020. 367, 6478. 685–688.

Sota T., Mogi M. Interspecific variation in desiccation survival time of Aedes (Stegomyia) mosquito eggs is correlated with habitat and egg size // Oecologia. 1992. 90, 3. 353–358.

Steinwascher Kurt. The University of Notre Dame Egg Size Variation in Aedes aegypti : Relationship to Body Size and Other Variables // The American Midland Naturalist. 1984. 112, 1. 76–84.

Stoks Robby, Geerts Aurora N., De Meester Luc. Evolutionary and plastic responses of freshwater invertebrates to climate change: Realized patterns and future potential // Evolutionary Applications. 2014. 7, 1. 42–55.

Su Glenn L Sia. Correlation of climatic factors and dengue incidence in Metro Manila, Philippines. // Ambio. jun 2008. 37, 4. 292–294.

Sultan Sonia E. Developmental plasticity: Re-conceiving the genotype // Interface Focus. 2017. 7, 5.

Sultana A, Sunahara T, Tsurukawa C, Tuno N. Reproductive interference between Aedes albopictus and Aedes flavopictus at a place of their origin // Medical and Veterinary Entomology. 2021. 35, 1. 59–67.

Effects of Temperature and Humidity on the Fecundity and Longevity of Aedes Albopictus and Aedes Flavopictus. // . 2021. October.

Suter Tobias T., Flacio Eleonora, Feijoó Fariña Begoña, Engeler Lukas, Tonolla Mauro, Regis Lêda N., de Melo Santos Maria A.V., Müller Pie. Surveillance and Control of Aedes albopictus in the Swiss-Italian Border Region: Differences in Egg Densities between Intervention and Non-intervention Areas // PLoS Neglected Tropical Diseases. 2016. 10, 1. 1–14.

Suzuki A., Tsuda Y., Takagi M., Wada Y. Seasonal observation on some population attributes of Aedes albopictus females in Nagasaki, Japan, with emphasis on the relation between the body size and the survival // Tropical Medicine. 1993. 35, 3. 91–99.

Swan Tom, Russell Tanya L., Staunton Kyran M., Field Matt A., Ritchie Scott A., Burkot Thomas R. A literature review of dispersal pathways of Aedes albopictus across different spatial scales: implications for vector surveillance // Parasites & vectors. 2022. 15, 1. 1–13.

Sword Gregory A, Lecoq Michel, Simpson Stephen J. Phase polyphenism and preventative locust management. // Journal of insect physiology. aug 2010. 56, 8. 949–957.

Szabó S., Peeters E. T.H.M. H M, Várbíró G., Borics G., Lukács B. A. Phenotypic plasticity as a clue for invasion success of the submerged aquatic plant Elodea nuttallii // Plant Biology. 2018. 21. 54–63.

Thomas Stephanie Margarete, Obermayr Ulla, Fischer Dominik, Kreyling Juergen, Beierkuhnlein Carl. Low-temperature threshold for egg survival of a post-diapause and non-diapause European aedine strain, Aedes albopictus (Diptera: Culicidae) // Parasites and Vectors. 2012. 5, 1. 1–7.

Toma Luciano, Severini Francesco, Di Luca Marco, Bella Antonino, Romi Roberto. Seasonal patterns of oviposition and egg hatching rate of Aedes albopictus in Rome. // Journal of the American Mosquito Control Association. 2003. 19, 1. 19–22.

Toma Takako, Sakamoto Shuji, Miyagi Ichiro. The seasonal appearance of aedes albopicuts in Okinawajima, the Ryukyu archipelago, Japan. 1982. 179–183.

Turcotte Martin M., Levine Jonathan M. Phenotypic Plasticity and Species Coexistence // Trends in Ecology and Evolution. 2016. 31, 10. 803–813.

U.S. Census Bureau . 2010 Census Urban and Rural Classification and Urban Area Criteria. II 2011.

Unlu Isik, Faraji Ary, Indelicato Nicholas, Fonseca Dina M. The hidden world of Asian tiger mosquitoes: Immature Aedes albopictus (Skuse) dominate in rainwater corrugated extension spouts // Transactions of the Royal Society of Tropical Medicine and Hygiene. 2014.

Urbanski Jennifer, Mogi Motoyoshi, O'Donnell Deborah, DeCotiis Mark, Toma Takako, Armbruster Peter. Rapid adaptive evolution of photoperiodic response during invasion and range expansion across a climatic gradient // American Naturalist. 2012. 179, 4. 490–500.

Valentine Matthew J., Ciraola Brenda, Jacobs Gregory R., Arnot Charlie, Kelly Patrick J., Murdock Courtney C. Effects of seasonality and land use on the diversity, relative abundance, and distribution of mosquitoes on St. Kitts, West Indies // Parasites and Vectors. 2020. 13, 1. 1–14.

Valentine Matthew John, Murdock Courtney Cuin, Kelly Patrick John. Sylvatic cycles of arboviruses in non-human primates // Parasites and Vectors. 2019. 12, 1. 1–18.

Valladares Fernando, Matesanz Silvia, Guilhaumon François, Araújo Miguel B., Balaguer Luis, Benito-Garzón Marta, Cornwell Will, Gianoli Ernesto, Kleunen Mark van, Naya Daniel E., Nicotra Adrienne B., Poorter Hendrik, Zavala Miguel A. The effects of phenotypic plasticity and local adaptation on forecasts of species range shifts under climate change // Ecology Letters. 2014. 17, 11. 1351–1364.

Valladares Fernando, Sanchez-Gomez David, Zavala Miguel A. Quantitative estimation of phenotypic plasticity: Bridging the gap between the evolutionary concept and its ecological applications // Journal of Ecology. 2006. 94, 6. 1103–1116.

Vavassori Laura, Saddler Adam, Müller Pie. Active dispersal of Aedes albopictus: A mark-release-recapture study using self-marking units // Parasites and Vectors. 2019. 12, 1. 1–14.

Vincent Muriel, Larrieu Sophie, Vilain Pascal, Etienne Aurélie, Solet Jean Louis, François Claire, Roquebert Bénédicte, Bandjee Marie Christine Jaffar, Filleul Laurent, Menudier Luce. From the threat to the large outbreak: Dengue on Reunion Island, 2015 to 2018 // Eurosurveillance. 2019. 24, 47. 1–8.

Violle Cyrille, Enquist Brian J., McGill Brian J., Jiang Lin, Albert Cécile H., Hulshof Catherine, Jung Vincent, Messier Julie. The return of the variance: Intraspecific variability in community ecology // Trends in Ecology and Evolution. 2012. 27, 4. 244–252.

Vitek Christopher J., Livdahl Artodd. Hatch plasticity in response to varied inundation frequency in Aedes albopictus // Journal of Medical Entomology. 2009. 46, 4. 766–771.

Vogt W. G., Woodburn T. L., Ellem B. A., Gerwen A. C.M. M van, Barton Browne Lindsay, Wardhaugh K. G. The relationship between dung quality and oocyte resorption in laboratory and field populations of Lucilia cuprina // Entomologia Experimentalis et Applicata. 1985. 39. 91–99.

Waldock Joanna, Proestos Yiannis, Parham Paul E., Christophides George, Chandra Nastassya L., Michael Edwin, Lelieveld Jos. The role of environmental variables on Aedes albopictus biology and chikungunya epidemiology // Pathogens and Global Health. 2013. 107, 5. 224–241.

Different Epidemic Curves for Severe Acute Respiratory Syndrome Reveal Similar Impacts of Control Measures. // . 09 2004. 160, 6. 509–516.

Wasserberg Gideon, White L., Bullard A., King J., Maxwell R. Oviposition Site Selection in Aedes albopictus (Diptera: Culicidae): Are the Effects of Predation Risk and Food Level Independent? // Journal of Medical Entomology. 2013. 50, 5. 1159–1164.

Watts Douglas M, Burke Donald S, Harrison Bruce A, Whitmire Richard E, Nisalak Ananda. Effect of Temperature on the Vector Efficiency of Aedes aegypti for Dengue 2 Virus // The American Journal of Tropical Medicine and Hygiene. 1987. 36, 1. 143–152.

Webber L. G. The relationship between larval and adult size of the Australian sheep blowfly Lucilia cuprina (Wied.) // Australian Journal of Zoology. 1954. 3, 3. 346–353.

Weiner Jacob, Du Yan Lei, Zhang Cong, Qin Xiao Liang, Li Feng Min. Evolutionary agroecology: individual fitness and population yield in wheat (Triticum aestivum) // Ecology. 2017. 98, 9. 2261–2266.

Westbrook Catherine J. Larval ecology and adult vector competence of invasive mosquitoes Aedes albopictus and Aedes aegypti for chikungunya virus. 2010.

Westbrook Catherine J., Reiskind Michael H., Pesko Kendra N., Greene Krystle E., Lounibos L. Philip. Larval environmental temperature and the susceptibility of aedes albopictus skuse (Diptera: Culicidae) to chikungunya virus // Vector-Borne and Zoonotic Diseases. 2010. 10, 3. 241–247.

White Paul A., Kalff Jacob, Rasmussen Joseph B., Gasol Josep M. The Effect of Temperature and Algal Biomass on Bacterial Production and Specific Growth Rate in Freshwater and Marine Habitats // Microbial Ecology. 1991. 21, 2. 99–118.

Whiteman Ari, Delmelle Eric, Rapp Tyler, Chen Shi, Chen Gang, Dulin Michael. A novel sampling method to measure socioeconomic drivers of Aedes albopictus distribution in Mecklenburg county, North Carolina // International Journal of Environmental Research and Public Health. 2018. 15, 10.

Willis F. S., Nasci R. S. Aedes albopictus (Diptera: Culicidae) population density and structure in southwest Louisiana // Journal of Medical Entomology. 1994. 31, 4. 594–599.

Wimberly Michael C., Davis Justin K., Evans Michelle V., Hess Andrea, Newberry Philip M., Solano-Asamoah Nicole, Murdock Courtney C. Land cover affects microclimate and temperature suitability for arbovirus transmission in an urban landscape // PLoS Neglected Tropical Diseases. 2020. 14, 9. 1–23.

Withanage Gayan P., Viswakula Sameera D., Nilmini Silva Gunawardena Y. I., Hapugoda Menaka D. A forecasting model for dengue incidence in the District of Gampaha, Sri Lanka // Parasites and Vectors. 2018. 11, 1. 1–10.

Wiwatanaratanabutr S., Kittayapong P. Effects of temephos and temperature on Wolbachia load and life history traits of Aedes albopictus // Medical and Veterinary Entomology. 2006. 20, 3. 300–307.

Wong Mark K.L., Guénard Benoit, Lewis Owen T. Trait-based ecology of terrestrial arthropods // Biological Reviews. 2019. 94, 3. 999–1022.

Wood Simon, Scheipl Fabian. gamm4: Generalized Additive Mixed Models using 'mgcv' and 'lme4'. 2020. R package version 0.2-6.

Wood Simon N. Statistical inference for noisy nonlinear ecological dynamic systems // Nature. 2010. 466, 7310. 1102–1104.

Woodall Hannah, Adams Ben. Partial cross-enhancement in models for dengue epidemiology // Journal of Theoretical Biology. 2014. 351. 67–73.

World Health Organisation . Global vector control response 2017-2030. 2017.

Xia Dan, Guo Xiang, Hu Tian, Li Li, Teng Ping Ying, Yin Qing Qing, Luo Lei, Xie Tian, Wei Yue Hong, Yang Qian, Li Shu Kai, Wang Yu Ji, Xie Yu, Li Yi Ji, Wang Chun Mei, Yang Zhi Cong, Chen Xiao Guang, Zhou Xiao Hong. Photoperiodic diapause in a subtropical population of Aedes albopictus in Guangzhou, China: Optimized field-laboratory-based study and statistical models for comprehensive characterization // Infectious Diseases of Poverty. 2018. 7, 1. 1–13.

Xiao Fang Zhen, Zhang Yi, Deng Yan Qin, He Si, Xie Han Guo, Zhou Xiao Nong, Yan Yan Sheng. The effect of temperature on the extrinsic incubation period and infection rate of dengue virus serotype 2 infection in Aedes albopictus // Archives of Virology. 2014. 159, 11. 3053–3057.

Xu Hai-Yan, Fu Xiuju, Lee Lionel, Ma Stefan, Goh Kee, Wong Jiancheng, Habibullah Mohamed, Lee Kee, Lim Tian, Tambyah Paul, Lim Chin, Ng Lee Ching. Statistical Modeling Reveals the Effect of Absolute Humidity on Dengue in Singapore // PLoS neglected tropical diseases. 05 2014. 8. e2805.

Xu Lei, Stige Leif C., Chan Kung Sik, Zhou Jie, Yang Jun, Sang Shaowei, Wang Ming, Yang Zhicong, Yan Ziqiang, Jiang Tong, Lu Liang, Yue Yujuan, Liu Xiaobo, Lin Hualiang, Xu Jianguo, Liu Qiyong, Stenseth Nils Chr. Climate variation drives dengue dynamics // Proceedings of the National Academy of Sciences of the United States of America. 2017. 114, 1. 113–118.

Yeap Heng Lin, Endersby Nancy M., Johnson Petrina H., Ritchie Scott A., Hoffmann Ary A. Body size and wing shape measurements as quality indicators of aedes aegypti mosquitoes destined for field release // American Journal of Tropical Medicine and Hygiene. 2013. 89, 1. 78–92.

Yee D. A., Allgood D., Kneitel J. M., Kuehn K. A. Constitutive Differences Between Natural and Artificial Container Mosquito Habitats: Vector Communities, Resources, Microorganisms, and Habitat Parameters // Journal of Medical Entomology. 2012. 49, 3. 482–491.

Yee Donald A., Ezeakacha Nnaemeka F., Abbott Karen C. The interactive effects of photoperiod and future climate change may have negative consequences for a wide-spread invasive insect // Oikos. 2017. 126, 1. 40–51.

Yoshioka Miho, Couret Jannelle, Kim Frances, McMillan Joseph, Burkot Thomas R., Dotson Ellen M., Kitron Uriel, Vazquez-Prokopec Gonzalo M. Diet and density dependent competition affect larval performance and oviposition site selection in the mosquito species Aedes albopictus (Diptera: Culicidae) // Parasites and Vectors. 2012. 5, 1. 1–11.

Yuan Baoyin, Lee Hyojung, Nishiura Hiroshi. Assessing dengue control in Tokyo, 2014 // PLoS Neglected Tropical Diseases. 2019. 13, 6. 1–17.

Yue Yujuan, Liu Qiyong, Liu Xiaobo, Zhao Ning, Yin Wenwu. Dengue Fever in Mainland China, 2005–2020: A Descriptive Analysis of Dengue Cases and Aedes Data // International Journal of Environmental Research and Public Health. 2022. 19, 7.

Yue Yujuan, Sun Jimin, Liu Xiaobo, Ren Dongsheng, Liu Qiyong, Xiao Xiangming, Lu Liang. Spatial analysis of dengue fever and exploration of its environmental and socio-economic risk factors using ordinary least squares: A case study in five districts of Guangzhou City, China, 2014 // International Journal of Infectious Diseases. 2018. 75. 39–48.

Zapletal Josef, Erraguntla Madhav, Adelman Zach N., Myles Kevin M., Lawley Mark A. Impacts of diurnal temperature and larval density on aquatic development of Aedes aegypti // PLoS ONE. 2018. 13, 3. 1–16.

Zeng Zhilin, Zhan Juan, Chen Liyuan, Chen Huilong, Cheng Sheng. Global, regional, and national dengue burden from 1990 to 2017: A systematic analysis based on the global burden of disease study 2017 // EClinicalMedicine. 2021. 32. 100712.

Zhang Dongjing, Zheng Xiaoying, Xi Zhiyong, Bourtzis Kostas, Gilles Jeremie R.L. Combining the sterile insect technique with the incompatible insect technique: I-impact of Wolbachia infection on the fitness of triple- and double-infected strains of Aedes albopictus // PLoS ONE. 2015. 10, 4. 1–13.

Zhang Zhoubin, Jing Qinlong, Chen Zongqiu, Li Tiegang, Jiang Liyun, Li Yilan, Luo Lei, Marshall John, Yang Zhicong. The increasing menace of dengue in Guangzhou, 2001-2016: The most important epicenter in mainland China // BMC Infectious Diseases. 2019. 19, 1. 4–11.

Zheng Xueli, Zhong Daibin, He Yulan, Zhou Guofa. Seasonality modeling of the distribution of Aedes albopictus in China based on climatic and environmental suitability // Infectious Diseases of Poverty. 2019. 8, 1. 1–9.

Žitko Toni, Merdić Enrih. Seasonal and spatial oviposition activity of aedes albopictus (Diptera: Culicidae) in Adriatic Croatia // Journal of Medical Entomology. 2014. 51, 4. 760–768.